Aalborg Universitet

AALBORG UNIVERSITY
DENMARK

UAV Connectivity over Cellular Networks

Investigation of Command and Control Link Reliability

Amorim, Rafhael Medeiros de

Publication date:
2019

Document Version
Publisher's PDF, also known as Version of record

Link to publication from Aalborg University

Citation for published version (APA):
Amorim, R. M. D. (2019). *UAV Connectivity over Cellular Networks: Investigation of Command and Control Link Reliability*. Aalborg Universitetsforlag. Ph.d.-serien for Det Tekniske Fakultet for IT og Design, Aalborg Universitet

General rights
Copyright and moral rights for the publications made accessible in the public portal are retained by the authors and/or other copyright owners and it is a condition of accessing publications that users recognise and abide by the legal requirements associated with these rights.

- Users may download and print one copy of any publication from the public portal for the purpose of private study or research.
- You may not further distribute the material or use it for any profit-making activity or commercial gain
- You may freely distribute the URL identifying the publication in the public portal -

Take down policy
If you believe that this document breaches copyright please contact us at vbn@aub.aau.dk providing details, and we will remove access to the work immediately and investigate your claim.

Downloaded from vbn.aau.dk on: May 04, 2023

UAV CONNECTIVITY OVER CELLULAR NETWORKS

INVESTIGATION OF COMMAND AND CONTROL LINK RELIABILITY

BY
RAFHAEL MEDEIROS DE AMORIM

DISSERTATION SUBMITTED 2019

AALBORG UNIVERSITY
DENMARK

UAV Connectivity over Cellular Networks

Investigation of Command and Control Link Reliability

Ph.D. Dissertation

Rafhael Medeiros de Amorim

Dissertation submitted: April 10, 2018

Dissertation submitted: April 10, 2019

PhD supervisor: Prof. Preben Mogensen
Department of Electronic Systems
Aalborg University

Assistant PhD supervisors: Dr. Jeroen Wigard
Nokia Bell Labs
Aalborg

Dr. István Z. Kovács
Nokia Bell Labs
Aalborg

PhD committee: Associate Professor Troels Pedersen (chairman)
Aalborg University

Professor David Gesbert
EURECOM

Associate Professor Rui Zhang
National University of Singapore

PhD Series: Technical Faculty of IT and Design, Aalborg University

Department: Department of Electronic Systems

ISSN (online): 2446-1628
ISBN (online): 978-87-7210-420-1

Published by:
Aalborg University Press
Langagervej 2
DK – 9220 Aalborg Ø
Phone: +45 99407140
aauf@forlag.aau.dk
forlag.aau.dk

© Copyright: Rafhael Medeiros de Amorim

Printed in Denmark by Rosendahls, 2019

Curriculum Vitae

Rafhael Medeiros de Amorim

Rafhael Medeiros de Amorim graduated as a bachelor in 2009 and was awarded his Master Degree in Electrical Engineering in 2011, both at Universidade de Brasília (University of Brasilia), Brazil. He worked for INDT (former Nokia Institute of Technology, currently Institute of Development and Technology) during 2012-2016 as a research engineer working with development of link level simulators and in support of LTE network performance evaluation and enhancement for commercial operators. Since March-2016, Rafhael is pursuing the PhD degree as a student in the Wireless Communications Networks (WCN) section at Aalborg University in close collaboration with Nokia Bell-Labs. In this period his research focus was in the challenges of providing cellular connectivity for UAVs (drones). Rafhael has joined the Nokia Bell-Labs team, in February 2019, where he continues doing research in the field of wireless communication. His main interests are performance enhancements on the PHY and MAC layers in 3GPP technologies, in special regarding the UAV connectivity and the deployment of Non-Terrestrial Networks (satellites).

Curriculum Vitae

Abstract

The establishment of a reliable command and control (C2) communication link between the Unmanned Aerial Vehicles (UAVs), also known as drones, and its pilot/command center is paramount to guarantee their safe integration into the airspace for long flight ranges. The present thesis investigate the challenges for public cellular networks, a natural main candidate, to provide this such high reliable services. In this thesis, the C2 connectivity provided is evaluated considering a target performance of 99.9 % reliability with maximum latency of 50 ms.

Field measurements demonstrated that the higher is the UAVs flight, more it is subjected to to suffer and cause interference from/to a larger number of significant radio cells of interference, even though the main signal also tends to see an increase in the received power. As a consequence, in heavily loaded simulation scenarios, the measured reliability was as low as 78 %.

Moreover, the measurements show the absence of a a clear dominant interference source. Hence, there is limited interference cancellation or suppression gains that can be achieved by some prior art features. Simulations and measurements are then used to assess other possible options to improve the reliability of the C2 link over cellular networks.

The most promising features to increase the reliability of the C2 are the usage of directional antennas at the UAV side or the connectivity diversity introduced by a multi-operator or multi-carrier hybrid connection. The reservation of spectrum resources exclusively for UAV services is also effective, but as discussion indicates, they may be economically unattractive, because of the average spectrum license prices.

The study demonstrates that up to a certain extent LTE technologies can support drone services, specially when drone-specific enhancement features are implemented. However, it is more challenging for the LTE technology to cope with the 99.9 % reliability requirements in the most stringent scenarios. The possibilities are further improved in the future 5G implementations, which brings enhancements in the air interface that help to boost the robustness of the system.

Resumé

Etableringen af en pålidelig kommando og kontrol (C2) kommunikationsforbindelse imellem et ubemandet flyvende fartøj (UAV), også kendt som droner, og dennes pilot/kommandocenter er altafgørende for at garantere en sikker integration i luftrummet for lange flyrækkevidder. Denne afhandling undersøger udfordringerne for offentlige cellulære netværk, en naturlig kandidat, i at tilbyde sådanne services med høj pålidelighed. I denne afhandling evalueres C2-forbindelsens ydeevne over LTE med et mål om 99.9 % pålidelighed med maksimalt 50 ms latenstid.

Målinger i felten demonstrerer at jo højere UAVen flyver, des højere er signalstyrken for det ønskede signal. Dog er UAVen tilsvarende mere udsat for og udsætter andre for interferens fra/til et stort antal radioceller. Som en konsekvens af dette er den målte pålidelighed, i simuleringsscenarier med høj belastning, nede på 78 %.

Endvidere viser målingerne fraværet af en klart dominerende interferenskilde. Derfor er det begrænsede forbedringer, som kan opnås ved brug af tidligere arbejder på interferensannullering eller dæmpning. Simuleringer og målinger anvendes derfor til at evaluere andre muligheder for at forbedre pålideligheden af C2-forbindelsen via cellulære netværk.

De mest lovende løsninger til at forbedre pålideligheden af C2-forbindelsen er brugen af retningsbestemte antenner på UAVen og forbindelses- forskellighed (diversitet) opnået via en hybrid forbindelse til multiple operatører eller multiple bærerfrekvenser. Reservation af spektrum udelukkende til UAV ydelser er også effektivt, men løsningen er muligvis ikke økonomisk attraktiv på grund af den gennemsnitlige pris for spektrumlicenser.

Studiet demonstrerer at LTE teknologier til en hvis grænse kan supportere C2 droneydelser og særligt når dronespecifikke forbedrende funktioner er implementeret. Det er dog mere udfordrende for LTE teknologien at håndtere pålidelighedskravet på 99.9 % i de mest krævende scenarier. Mulighederne er yderligere udbygget i fremtidige 5G opsætninger, som medfører forbedringer af radiogrænsefladen og anvender højere frekvensbånd, der øger systemets robusthed.

Contents

List of Abbreviations

3D 3-dimensional

3GPP Third Generation Partnership Project

4G 4^{th} Generation

5G 5^{th} Generation

ABS Almost Blank Subframes

ATC Air Traffic Controller

ATM Air Traffic Management

AUE airborne UE

BER Bit Error Rate

BLER Block Error Rate

BS base station

BVLOS beyond visual line-of-sight

C2 Command and Control

CAPEX Capital Expenditures

CBR Constant Bit Rate

CDF cumulative distribution function

CFI Control Format Indicator

CLPC Closed Loop Power Control

CoMP Coordinated Multipoint

CQI Channel Quality Indicator

CS/CB-CoMP Coordinated Scheduling/Coordinated Beamforming Coordinated Multipoint

DEM Digital Elevation Map

DIR Dominant Interferer Ratio

DL downlink

DRX Discontinuous Reception

DT Drive Test

e-ICIC enhanced ICIC

eICIC enhanced inter-cell interference coordination

EASA European Aviation Safety Agency

E2E end-to-end

e-PDCCH enhanced PDCCH

FAA Federal Aviation Administration

FDD Frequency Division Duplex

FTP File Transfer Protocol

GSMA GSM Association

HARQ Hybrid Automatic Repeat Request

HO Handover

IC interference cancellation

ICAO International Civil Aviation Organization

ICIC inter-cell interference coordination

IMEI International Mobile Equipment Identity

IMSI International Mobile Subscriber Identity

IoT Internet of Things

IRC Interference Rejection Combining

ISD inter-site distance

ITU International Telecommunication Union

JARUS Joint Authorities for Rulemaking on Unmanned Systems

JR-CoMP Joint Reception Coordinated Multipoint

JT-CoMP Joint Transmission Coordinated Multipoint

KPI Key Performance Indicator

LOS line-of-sight

LTE Long-Term Evolution

LTE-A LTE-Advanced

MAC Medium Access Control

MCS Modulation and Coding Scheme

MIMO Multiple Input Multiple Output

MMSE Minimum Mean Square Error

MNO Mobile Network Operator

GPS Global Positioning System

NAICS Network Assisted Interference Cancellation and Suppression

NASA National Aeronautics and Space Administration

NLOS non line-of-sight

NOMA Non-Orthogonal Multiple Access

NR New Radio

NTN Non-Terrestrial Networks

OFDM Orthogonal Frequency Division Multiplexing

OLPC Open Loop Power Control

OWD One-way Delay

PC Power Control

PCI Physical Channel Indicator

PDCCH Physical Downlink Control Channel

PDSCH Physical Downlink Shared Channel

PDP Power Delay Profile

PDU Protocol Data Unit

PPP Public-Private Partnership

PRB Physical Resource Block

PUSCH Physical Uplink Shared Channel

QCI QoS Class Identifier

QFI QoS Flow Identity

QoS Quality of Service

RAN Radio Access Network

RMa Rural Macro

RLC Radio Link Control

RLF Radio Link Failure

RSRP Reference Signal Received Power

RSRQ Reference Signal Received Quality

RSSI Received Signal Strength Indicator

Rx receiver

RTT round-trip time

SESAR Single European Sky ATM Research Programme

SIC Successive Interference Cancellation

SIR signal to interference Ratio

SINR signal to interference plus noise ratio

SNR signal to noise ratio

TDD Time Division Duplex

TTI Transmission Time Interval

TUE terrestrial UE

Tx transmit

UAV Unmanned Aerial Vehicle

UE user equipment

UDP User Datagram Protocol

UL uplink

UMTS Universal Mobile Telecommunications System

USB Universal Serial Bus

UTM Unmanned Aircraft System Traffic Management

VLL very low level

VLOS visual line of sight

VoLTE Voice over LTE

WNV Wireless Network Virtualization

Thesis Details

Thesis Title:	UAV Connectivity over Cellular Networks
Thesis Subtitle:	Investigation of Command and Control Link Reliability
PhD Candidate:	Rafhael Medeiros de Amorim
Supervisors:	Prof. Preben Mogensen - Aalborg University
	Dr. Jeroen Wigard - Nokia Bell Labs Aalborg
	Dr. István Z. Kovács - Nokia Bell Labs Aalborg

The content of this PhD thesis is a product of the research work produced between March 2016 and March 2019. The research efforts presented herein were conducted as a PhD fellow at the Wireless Communication Networks (WCN) Section, Department of Electronic Systems, Aalborg University, Denmark in close collaboration with Nokia Bell Labs in Aalborg. Within the duration of the presented research, parallel activities and mandatory courses were also carried out for fulfilling the requirements to obtain the degree of Doctor of Philosophy (PhD) from Aalborg University, Denmark. The present thesis is a

research report compiled in the format of a collection of Papers. The scientific papers that constitute the main body of this document were published in or submitted to peer-reviewed scientific periodic or conferences.

This PhD work was partially funded by Nokia Bell Labs, by the DroC2om project, which has received funds from the Single European Sky ATM Research Programme (SESAR) Joint Undertaking under the European Union's Horizon 2020 Research and Innovation Programme and by the WCN Section at Aalborg University.

The scientific articles that constitute the main body of this document consist of the following list of papers:

A. R. Amorim, P. Mogensen, T. Sorensen, I. Z. Kovacs and J. Wigard, "Pathloss Measurements and Modeling for UAVs Connected to Cellular Networks," *IEEE 85th Vehicular Technology Conference (VTC Spring)*, 2017, pp. 1-6.

B. R. Amorim, H. Nguyen, P. Mogensen, I. Z. Kovács, J. Wigard and T. B. Sørensen, "Radio Channel Modeling for UAV Communication Over Cellular Networks," in *IEEE Wireless Communications Letters*, vol. 6, no. 4, pp. 514-517, Aug. 2017.

C. R. Amorim, H. Nguyen, J. Wigard, I. Z. Kovács, T. B. Sorensen and P. Mogensen, "LTE radio measurements above urban rooftops for aerial communications," *IEEE Wireless Communications and Networking Conference (WCNC)*, 2018, pp. 1-6.

D. R. Amorim et al., "Measured Uplink Interference Caused by Aerial Vehicles in LTE Cellular Networks," in *IEEE Wireless Communications Letters*, vol. 7, no. 6, pp. 958-961, Dec. 2018.

E. I. Kovacs, R. Amorim, H. C. Nguyen, J. Wigard and P. Mogensen, "Interference Analysis for UAV Connectivity over LTE Using Aerial Radio Measurements," *IEEE 86th Vehicular Technology Conference (VTC-Fall)*, 2017, pp. 1-6.

F. H. C. Nguyen, R. Amorim, J. Wigard, I. Z. Kovacs and P. Mogensen, "Using LTE Networks for UAV Command and Control Link: A Rural-Area Coverage Analysis," *IEEE 86th Vehicular Technology Conference (VTC-Fall)*, 2017, pp. 1-6.

G. H. C. Nguyen, R. Amorim, J. Wigard, I. Z. Kovács, T. B. Sørensen and P. E. Mogensen, "How to Ensure Reliable Connectivity for Aerial Vehicles Over Cellular Networks," *IEEE Access*, vol. 6, pp. 12304-12317, 2018.

H. R. Amorim, J. Wigard, I. Z. Kovács, T. B. Sørensen, P. Mogensen, "Enabling Reliable Cellular Communication for Aerial Vehicles", *Vehicular Technology Magazine*, 2019, **Submitted 2019**.

I. R. Amorim, J. Wigard, I. Z. Kovács, T. B. Sørensen, P. Mogensen, G. Pocovi, "Improving Command and Control Reliability for Drones with Multi-Operator Connectivity", *IEEE 89th Vehicular Technology Conference (VTC Spring)*, 2019. Accepted for Publication, 2019.

J. R. Amorim, J. Wigard, I. Z. Kovács, T. B. Sørensen, P. Mogensen, "Forecasting Spectrum Demand for UAVs Served by Dedicated Allocation in Cellular Networks", *IEEE Wireless Communications and Networking Conference (WCNC)*, 2019. Accepted for Publication, 2019.

K. R. Amorim, J. Wigard, H. Nguyen, I. Z. Kovács and P. Mogensen, "Machine-Learning Identification of Airborne UAV-UEs Based on LTE Radio Measurements," *IEEE Globecom Workshops (GC Wkshps)*, 2017, pp. 1-6.

L. J. Wigard, R. Amorim, H. C. Nguyen, I. Z. Kovács and P. Mogensen, "Method for detection of airborne UEs based on LTE radio measurements," *IEEE 28th Annual International Symposium on Personal, Indoor, and Mobile Radio Communications (PIMRC)*, 2017, pp. 1-6.

According to the Ministerial Order no. 1039 of August 27, 2013, regarding the PhD Degree § 12, article 4, statements from each co-author about the PhD students contribution to the above-listed papers have been provided to the PhD school for approval prior to the submission of this thesis. These co-author statements have also been presented to the PhD committee and included as a part of their assessment.

Preface

We are moving toward a more connected world, where a multitude of devices and applications are converging to *online, smart, dynamic* solutions. This futuristic scenario poses a challenge for communication engineers, as the connectivity solutions must be able to connect a massive number of devices and be flexible enough to accommodate different requirements in diverse types of scenarios.

Among this multitude of devices, there are the UAVs, also known as drones. These devices have recently experienced a surge in the commercial market and have become a technological trend for the future, with promising potential to reduce the risk or cost of several services and human activities.

In the last three years, I have invested efforts to built the present body of work, which is focused on investigating the challenges in providing connectivity for UAVs. When I first started, I have set high goals: I had an inner desire to make a valuable contribution to the state-of-the-art, discussing possible solutions for overcome the challenges associated to the topic; whereas achieving a good level of research to be awarded the degree of Doctor of Philosophy (PhD). I hope this thesis have lived up to my initial expectations and that the reader can appreciate reading it as much as I have appreciated to write and produce it.

In truth, I could not have finished this study or achieved the current quality, without the support and guidance of numerous cast of bright people around me. First and foremost, I would like to thank my supervisors for their tireless guidance and patience to my numerous questions, each on its own way: Preben Mogensen for his sharp advices that helped me to steer my work in the right direction with his long-term sight; Jeroen Wigard for his uplifting comments and his awareness of the relevant topics trending in the state of the art; and István Z. Kovács for his thorough technical examination of my work and his attention to the detail.

Equally, I would like to thank my estimate colleagues Huan C. Nguyen and Troels B. Sørensen for their incommensurable contribution. Huan for sharing his expertise and programming skills and Troels for his enormous and valuable revision efforts and his keen eye to find flaws to be fixed in my

work. Their contribution has been significant to improve this work.

I also thank those who accepted roles as members of my PhD assessment committee, Professors Troels Pedersen, David Gesbert and Rui Zhang, for reserving their precious time and lending their expertise reading and assessing this work.

Thanks to my parents and my sister for showing me the way that brought me here and for being supportive for their son and their words of encouragement in spite of the long distance between us. To all other family members and friends, in Brazil, in Denmark and in other parts of the globe, my sincere gratitude for your support.

Thank you, also, to my colleagues at Nokia Bell Labs and Aalborg University. I really enjoyed the working environment that you helped to built in the last years and I hope we can continue to collaborate in the forthcoming years.

Last but not least, I would like to thank my family. Thank you to my wife, Patricia, who had the courage to board this adventure with me, living so far away from our home country. And for sharing, closely, with me the *ups* and *downs* of the last three years. Your supportive words and your continuous encouragement were paramount. And to the youngest and latest addition to my support crew, my sweet son, Victor, my sincere gratitude: throughout the last year, your first year, you have redefined much of my world and have gifted me with lenses that help me to put everything on a different perspective. I love you both.

Rafhael Medeiros de Amorim
Aalborg University, April 6th, 2019

Chapter 1 - Introduction

For several decades, large Unmanned Aerial Vehicles (UAVs) were used in military applications [1], without a significant effort to regulate the usage of the airspace for drones. This can be attributed to the small number of UAVs and the infrequent and special nature of their operations, usually located in remote areas [2]. However, the scenario for UAVs, also known as drones, has changed lately as a consequence of technological enhancements.

The development of lightweight materials and more efficient batteries, altogether with more affordable manufacturing costs has widened the audiences of these devices to several commercial and civilian applications [3]. The drone powered solutions are expected to become a multibillion dollar market in the near future and include applications as monitoring of properties and inspection of buildings, usage in entertainment industry (aerial imagery, special effects, etc.), delivery of goods, analysis of soil and crops in agriculture and others [4,5].

In recent years, the market for small and medium sized UAVs has experienced a rapid increase. According to the reports of Federal Aviation Administration (FAA), the number of hobbyst UAVs in the US increased from 790.000 in 2016 to 1.1 million in 2017, while the number of commercial non-hobbyist units increased from 42.000 to 110.000 registered drones. This fast growth led local airspace authorities worldwide to establish measures for a safe integration of the drones into the common airspace. In most cases, the rules initially set that the UAV remote controller (or remote pilot) should be in visual line of sight (VLOS) with the UAV in all phases of the flight and with a maximum height allowed around 120-150 m [6].

This initial set of rules aimed first at the safety of the operations and of the other airspace users. They restrained the market of commercial drone-powered solutions, by limiting their flight range. But, regarding the potential of drone applications, authorities also proposed roadmaps for the regulation of beyond visual line-of-sight (BVLOS) flight distances [2] [6]. These roadmaps include studies on technical enhancements and specifications that would allow these devices to share the airspace with legacy aerial users in a safe manner. Among such enhancements, the establishment of a reliable com-

munication link between the flying equipment and its controller available at all phases of the flight is one the key enablers for BVLOS missions.

The main focus of this thesis is the investigation of the usage of cellular networks to provide this critical communication link. The next sections will present performance requirements for this link, the advantages and challenges of using cellular networks for providing it and present the contributions and the scope of the thesis.

1.1 Communication and Control Link for UAVs

The Command and Control (C2) is the communication datalink that carries all flight related information to be exchanged between UAV and its remote pilot, or remote pilot center, in both directions [7]. According to the International Civil Aviation Organization (ICAO), it is expected that the information transmitted via C2, from the drone to the pilot, includes its telemetry (battery life, speed, height, etc.), voice and data commands from Air Traffic Controller (ATC) relayed through the drone, detection and avoidance of other UAVs and collision avoidance [7]. In the opposite direction, from the pilot to the UAV, it conveys the navigation commands and voice/data to be relayed to the ATC.

The C2 is responsible for the exchange of critical information for the flight safety, therefore it is paramount that its performance level attend a given set of performance specifications. The Joint Authorities for Rulemaking on Unmanned Systems (JARUS), a group of experts in regulatory matters, with members in 57 countries, was created with the goal to provide a single set of global recommendations for technical and operational aspects linked to the remotely piloted aircraft system services. According to JARUS recommendations, the performance of the C2 should depend on the category of the UAV, the Air Traffic Management (ATM) environment, the type of operation and the class of airspace being used [8]. It means that large UAVs flying at high altitudes will be probably subject to different performance requirements than small UAVs deployed at the very low level (VLL) airspace (up to 150 m). In the same manner, the requirements for link performance can be more relaxed for more automated devices [9].

At the time of writing, there is an ongoing global effort to establish the C2 performance requirements for a safe integration of different classes of UAVs into the airspace. The next subsection describes shortly some examples of such efforts by different authorities and groups, including the requirements proposed and studies carried out by the Third Generation Partnership Project (3GPP) for the support of C2 via cellular networks, which is the most relevant for the research presented in this thesis.

1.1.1 Review of Perfomance Specifications

International Civil Aviation Organization - 2006

In the context of the civil aviation, the assessment of the communication performance is not restricted to the wireless radio link between aircraft and ATM. It comprises all elements either airborne or ground-based involved in the exchange of information [8], including human actions.

The required communication performance concept assesses operational communication transactions in the context of an ATM function, taking into account human interactions, procedures, and environmental characteristics.

— ICAO, 2006 [10]

Following this definition, the communication performance is assessed over operational communication transactions, defined as the processes where an information is sent by an human or system and is finished when the *sender* acknowledges that the information has been correctly received at the other end [10]. The metrics proposed by ICAO for assessment of the C2 performance are a legacy from the metrics established for assessing modern systems used in *manned* civil aviation [10]. The definition of such metrics, found in [8], are repeated here for convenience:

- communication transaction time: the maximum time for completing the operational transaction, including reception acknowledgment at the transmitter end;
- continuity: the probability of completing the operational transaction within the transaction time;
- availability: the probability that the system is available for the user when a transaction has to be initiated;
- integrity: the error probability in a transaction that has been completed.

For the conventional manned aviation, the communication transaction time typically corresponds to several seconds, and mostly cover voice exchanges between pilots and ATC [10]. Even though there is no clear set of values established for UAVs, it is reasonable to consider that for some applications these values should be significantly shorter. For example, real-time navigation commands must be completed in hundreds of milliseconds to not compromise the piloting capability of the controller.

The radio technology chosen to support the C2 wireless link between UAVs and the ground infrastructure, which is the focus of the present work, is one part of a whole chain of elements that must provide a high reliable communication performance. Therefore, it must itself operate at high reliable levels.

Table 1.1: Estimated Throughput Requirements (bits/s) in [11] for the data sent to the UAV

Operational Phase	Command and Control		ATC Relay	
	Control	NavAids	Voice	Data
Pre-flight	183	0	4800	113
Departure	3286	669	4800	49
En route	1201	669	4800	23
Arrival	4606	669	4800	16
Post-Flight	1	0	4800	15

International Telecommunication Union (ITU) - 2009

In 2009, the ITU published one of the first relevant documents addressing the datalink between UAVs and the ground infrastructure [11], aiming at assessing the spectrum requirements for such service. Even though it seems to underestimate, according to current figures, the density of airborne UAVs and their applicability, it produces reference information on the amount of data to be exchanged by the drones and the ground infrastructure.

In the ITU document, the information exchanged between ground control and drone is split into communication functions, such as ATC relay, command and control, video/weather radar, etc. Then, the elements of each function are described in details to estimate the overall throughput required for each of them. For example, it is estimated that 64 bits/s are required to update the UAV's latitude information (control function) with a refresh rate of 2 Hz.

Using the detailed estimations for each element of the communication functions, it is possible to calculate the throughput requirements for a manual and automated operation of one UAV. The values for the manual operation were chosen to be shown here, as they represent the most demanding case. Table 1.1 shows the overall throughput requirements for the information transmitted from the ground infrastructure to the drone. It shows low throughput estimations for all traffic categories, with every function requiring less than 15 kbits/s.The estimations are presented in average figures, as the goal of the ITU's document was to estimate the bandwidth demand, not the instantaneous demand of a given user.

On the opposite link direction, when the UAV is transmitting to the ground station, the sense and avoid category imposes the most challenging demands, due to the video transmission (assumed to be needed intermittently), the weather radar and the tracking of other air space elements/devices (60 tracks assumed), as presented in Table 1.2.

As previosuly mentioned, though, it is not expected that all categories of communication data will be required for every kind of flight mission and for every drone class. For example, neither the weather radar nor the video

Table 1.2: Estimated Throughput Requirements (bits/s) in [11] for the data sent from the UAV

Operational Phase	Command and Control		ATC Relay		Sense and Avoid		
	Control	NavAids	Voice	Data	Target Tracks	Weather Radar	Video
Pre-flight	5	0	4800	173	9120	0	0
Departure	5715	836	4800	59	9120	27771	270000
En route	2356	836	4800	28	9120	3968	270000
Arrival	7615	1140	4800	32	9120	27771	270000
Post-Flight	2	0	4800	22	0	0	0

Table 1.3: Functions Required per UAV Class in [11]

	Function	UAV Class		
		Small	Medium	Large
Command and Control	Control	✓	✓	✓
	NavAids		✓	✓
ATC Relay	Voice		✓	✓
	Data		✓	✓
Sense and Avoid	Target Tracks		✓	✓
	Weather Radar			✓
	Video		✓	✓

streaming must be required for small drones flying at very low altitudes. Due to this different requirements, ITU has proposed one methodology where the data throughput is estimated according to to three different UAVs classes and their envisioned applications and their use of the airspace. Table 1.3 shows the functions expected to be required for each UAV class.

In Table 1.3, the small UAVs are defined as those with a total weight below 25 kg, flying at heights up to 300 m; the medium UAV to those with a total weight below 2000 kg and flying at heights up to 5500 m and the large are those UAVs exceeding those thresholds. By combining Tables 1.1 and 1.2 with Table 1.3 it is possible to see that, according to ITU early projections, drone missions carried on small heights can be served with a total throughput of less than 15 kbits/s. Regarding the reliability or latency requirements, no assumptions are made. But the document states that both should taken into consideration to support safe operations in the airspace.

National Aeronautics and Space Administration - 2017

The National Aeronautics and Space Administration (NASA) has driven efforts in developing a Unmanned Aircraft System Traffic Management (UTM) that is capable of enable safe operations in the low-altitude airspace [12]. In

Table 1.4: Categorization of Unmanned Aerial Missions [12]

Category	(R)ecreational or (C)ommercial	Take-Off Weight (kg)	BVLOS	Usage of Civilian Airports
A	R	< 25		
B	C	< 25		
C	C	25 to 600	✓	
D	C	> 600	✓	✓

the agency's vision the integrated UTM will provide efficient intercommunication network, enabled by an efficient C2 link.

As part of the roadmap to reach this goal, a collaborative research has been published with - among other specifications - the requirements for the data link, providing reference values for the ongoing development of a system architecture able to provide communication, navigation and surveillance for the UTM users [13].

Seven different performance metrics were discussed in this publication, and the specifications for each of them are related to the air space category related to the UAV's flight missions, as presented in Table 1.4. According to these definitions, categories A and B represent the small size UAVs, while category C represents medium UAVs and category D is comparable to manned aircrafts.

- Requirement 1: Range

  In [13] the range is defined as the last hop of the communication link from the ground infrastructure to the UAV. For categories A, B and C the minimum range to be supported is 5 km. For category D, the range during flight missions extends up to 1000 km (ground based transmitter) or 36000 km (satellite based transmitter in oceanic areas).

- Requirement 2: Velocity

  The speed of the UAVs, relative to the network transmitter, impacts the choice of technologies, as some standards are not suited to handle the radio challenges caused by very high speeds. For categories A,B and C the system must support speeds up to 100 km/h, whereas speeds can go up to 1000 km/h for category D.

- Requirement 3: Latecy

  In the document the maximum admissible latency is calculated based on the maximum acceptable deviation on the UAV trajectory, regarding the minimum distance to be enforced among UAVs. For all classes, the requirements of the round trip latency is defined as 350 ms.

- Requirement 4: Availability

  The availability quantifies the percentage of time the system is available for the users, as the down time compromises the safety of the missions to be deployed by the UAVs. In phone systems the availaility is assumed to be close to 99.999% [13]. Categories A and B5, which operate in VLOS ranges should be served with availability above 99.99 %. The requirement goes above 99.999 % for the categories C and D.

- Requirement 5: Integrity

  In the domain of cellular communications, the integrity is commonly referred as the Bit Error Rate (BER). The detected bit errors may be corrected and potentially fixed within the latency time, for example by requested retransmissions. The detected BER must be kept as low as 10^{-3} for all categories. The undetected bit errors are passed by as information to the upper layers of the communication protocol. They should be extremely rare, as they can result in misinterpretation of commands from the pilot and in more extreme cases cause mission failures.For all classes the undetected errors must be below as 10^{-6}.

- Requirement 6: Security

  In the document the security of all data links referred to the UAVs must be,at least, as secure as the WPA2 security protocol. The justification is that it is hard to quantitatively measure security, but the WPA2 protocol is already in use for several mission critical communications at ground level. C2

- Requirement 7: Bit rate

  The datalink bit rate requirements, as in the ITU document, is listed for different services (ATC voice and data, navigation commands, telemetry, etc.). The final values for the bit rate requirements have similar magnitude of those previously presented by the ITU document.

It is worth noting that the category D, which is comparable with the manned aviation does not belong to the scope of the present thesis. Whereas category C, which is used for commercial deployments beyond visual line-of-sight, is the one most representative for the scope of this thesis.

The Third Generation Partnership Project (3GPP) - 2017

With growing attention being driven to UAV applications, a potential market was unfolding for telecommunications service providers. This lead to field trials assessing different technologies about their capacity to provide connectivity for drones, including cellular technologies such as Long-Term

Table 1.5: 3GPP Requirements per data type [15]

Data Type	Latency	Data Rate	Reliability
C2	50 ms (one way from eNodeB to UAV)	60-100 kbps	Packet Error Loss Rate up to 0.1 %
Application	Similar to LTE terrestrial users	Up to 50 Mbps (sent from UAV)	***

Evolution (LTE) [14]. In 2017, 3GPP has responded to this demand, by addressing the support for UAV communications in LTE networks in a study item [15], whose main goal was:

Investigate the ability for aerial vehicles for LTE to be served using LTE network deployments with Base Station antennas targeting terrestrial coverage, supporting Release 14 functionality.

— 3GPP technical document RP-170779, 2017 [16]

The 3GPP activities focused on drones flying at low altitudes (up to 300 m), where several commercial activities are expected to take place, as it intended to reuse network deployments planned for terrestrial coverage. Based on the ITU document and more recent contributions from industry, the study item presented the requirements to be achieved by the service provider supporting the C2. The data connectivity was split into two different types [15]:

- C2 data: includes navigation commands and telemetry, identification, flight control authorization and requests, etc.;
- application data: includes video streaming, images, other sensors data and application specific payload.

The specific requirements for each type of application were set as showed in Table 1.5. It is possible to infer from this table that the C2 data is considered critical with stringent latency and reliability requirements, while the application data follows a performance similar to the terrestrial users in the networks, most likely to be served in a best-effort manner. It means that, likewise ITU's specifications, the video streaming transmitted from the drone is not considered a critical element of communication for drones flying at such heights. In the 3GPP scenarios, this type of transmission is regarded as application dependent.

It is also possible to see from Table 1.5 that the data rate specified for the C2 is higher than that presented by ITU and NASA, and aims at providing more capabilities to the C2 radio interface, and leave space for future technical requirements by airspace authorities. Also, the latency requirements in 3GPP are more stringent then those presented in the NASA's document.

1.2 Command and Control Data over Cellular Networks

The critical nature of C2 for the safe integration of drones into the airspace, requires that the performance requirements must be addressed ubiquitously and in all phases of the flight. These factors must be taken into account in the choice of technology/network used to provide the connectivity to the drones.

It is expected that, in the future, the certificates for BVLOS flights will be issued for the whole system, encompassing the pilot/controller, the UAV and the C2 connection [17]. Therefore, the C2 service provider will likely be object of certification under the civil aviation authority. At the time of writing, most of the commercial drones available in the market are developed for VLOS operations. These devices deploy the communication link between controller and UAV in the unlicensed spectrum of 2.4 and 5.8 GHz, using Wi-Fi 802.11 standards or a manufacturer's proprietary technology . These solutions cannot be certified as they are using unlicensed, unprotected spectrum.

From the commercial point of view, there is a demand for a certifiable service provider that can reach the C2 requirements for BVLOS. On the technical side, this can be achieved, for example, by using satellite systems [18] or by deploying a terrestrial network, either using a new dedicated spectrum and infrastructure [11] or sharing these resources with already operating networks - such as the cellular. The last option being the object of investigation of the present thesis.

Satellite systems are advantageous for operations in remote areas and over the sea connections. On the other hand, they have limited overall capacity and can present coverage issues during take-off and landing operations of small drones in dense urban deployments. Moreover, given the distance from the Earth the geostationary satellites operate, they cannot operate under stringent latency requirements with the round-trip time (RTT) being up to 270 ms [19]. For satellites operating at lower orbit altitudes, 600 to 1200 km, inter-cell mobility becomes an issue as the satellite moves at speeds as high as 7.5 km/s [19].

The latency challenges presented by satellite systems can be addressed by implementing a dedicated terrestrial network, which tends to minimize the distance between the UAV and the network access point. ITU has identified portions of the spectrum that can be allocated for future C2 implementations worldwide: from 960-977 MHz and 5030-5091 MHz [17]. However, differently from airplanes and very large drone operations, applications of small and medium sized UAVs may require very high flexibility of take-off and landing spots, therefore requiring a very dense network implementation. Given the current market size for UAV applications and the number of devices expected in operation, the costs for operating and installing such network may be very

high for the users sharing its services.

The 3GPP study on supporting the air interface part of the whole C2 channel through LTE networks is advocating in favor of reusing cellular networks as an alternative solution to overcome the costs and challenges of maintaining a network dedicated for UAVs.

1.2.1 Advantages of Cellular Networks

The usage of cellular networks for supporting the C2 present some economical advantages, when compared to satellite systems or to a dedicated terrestrial networks [20]. First of all, in most cases their operating infrastructure has been implemented over several years, and offer a ready-to-market solution, minimizing the time required for having an operational solution. They are also present in most inhabited areas, providing an almost ubiquitous coverage. Moreover, they have a solid base of terrestrial subscribers who share the operation costs and minimize the underutilization of spectrum in certain areas.

The GSM Association (GSMA), a worldwide consortium of more than 800 operators, in a response to a consultation from European Aviation Safety Agency (EASA) on the "Introduction of a regulatory framework for the operation of drones" has also pointed out some additional benefits of using cellular connectivity for drones [21]:

- Cellular networks are a global interoperable platform, providing an ubiquitous digital ecosystem that works beyond regional/country level.
- The most modern cellular technologies are designed to meet high bandwidth and low latency on a scalable design, giving support for the development of innovative services by the drone industry.
- They can provide support for identification and registration services for the drone industry with years of experience in managing such kind of information. Throughout the years they have been using the International Mobile Equipment Identity (IMEI) number to uniquely identify the hardware in use, whereas subscribers are identified via the SIM card by the unique International Mobile Subscriber Identity (IMSI). These secure standards can be applied for identifying the drones and their operators, respectively.

Besides those advantages, which are particular to the domain of cellular networks, these networks also provide other characteristics that favor the deployment of C2 links [21,22]:

- Throughout the last decades cellular networks have developed solutions for enforcing security and secrecy of the communication of its

users. The standards for ciphering, encryption and anonymization of the transactions are kept at a high level, which minimizes the likelihood of interception or break of privacy.

- The public mobile networks also operate in licensed spectrum in the vast majority of places. This protects the signal from interference from other systems and facilitates the management of the air resources.
- From the perspective of authorities, cellular networks are also attractive by providing solutions for lawful interception, which can help national security and law enforcement agencies when strictly required.

These other characteristics are not necessarily found only in cellular deployments and could be developed also for other technological solutions. But, besides the experience accumulated by professionals in the market throughout the decades of operational services, cellular technologies also offer readiness for implementation with an available infrastructure already in place.

Additionally, it is likely that many UAVs will be prepared for connecting to cellular networks anyway, as they offer a high bandwidth option for exchanging the application payload data.

Challenges

In order to exploit the advantages that cellular networks offer, it is important to investigate how well they cope with the requirements set for C2 link and which factors can impact the system performance for other subscribers in these networks.

Cellular networks have been developed and optimized for coverage of terrestrial users, therefore their settings are designed to favor mostly the coverage at ground level. As an example, the base station antennas are commonly down tilted to direct the main part of the radiated energy to a specific area on the ground and limit interference outside this area. The inter site distance and the base station heights are also planned accordingly to the density of subscribers and buildings in a given geographical area. Because of this, the network performance observed at ground level cannot be straightforward extended for airborne drones [23], and a performance assessment is required.

The radio channel models typically used for network planning and simulations of performance were also refined for terrestrial users [24]. However, airborne UAVs are flying above trees, cars, rooftops and other obstacles for the propagation of the radio wave. In other words, they are surrounded by much less scattering elements and are subject to a different propagation environment [25]. For assessing the network performance from the perspective

of UAVs requires the development of channel models suitable for their use case.

The fact that the cellular spectrum has to be shared between terrestrial users and UAVs also imposes some coexistence challenges [26,27]. The density of terrestrial users is expected to be much higher than the density of UAVs and they can consume significant part of the network resources by assessing broadband services. Moreover, the load generated by one class of users creates undesired interference for the other class. Because the C2 performance is critical, it is important to design resource allocation policies and interference management techniques that ensure reliable performance of the C2.

1.2.2 Hybrid Solutions

Throughout this section, the main potential solutions for C2 connectivity have been discussed and, as it was shown, they have their own pros and cons. Hybrid solutions, where two or more solutions are combined to provide the service, opens up possibilities to exploit the advantages provided by each of them in certain scenarios, while mitigating the drawbacks in unfavorable conditions.

One example of hybrid solution is the combination between satellite and cellular networks. The satellite system can be used to provide coverage in very remote areas, where the latency criteria can be potentially relaxed - assuming a minor risk of collision in these environments. On the other hand, when flying above dense urban areas, the C2 could be switched to the cellular connection. At the time of writing, an integrated satellite-cellular system architecture is being evaluated by the DroC2om project [28], which has received funds from the Single European Sky ATM Research Programme (SESAR) Joint Undertaking under the European Union's Horizon 2020 Research and Innovation Programme.

The hybrid solution can also be a combination of multiple cellular networks or operators, aiming at improving the overall reliability and availability of the connection.

1.3 Research Methodology

The development of the studies encompassed in this thesis are oriented by a research methodology whose phases are described as follows.

1. **Identification of the research questions:** A review on the performance requirements being discussed and proposed by the industry for UAV connectivity is performed to set the basis for the study. Then, a literature review is performed to understand the knowns and unknowns

related to the coverage of airborne devices in cellular networks, and how they mutually impact the coexistent terrestrial users. The research questions are posed based on the analysis of the challenges identified in using cellular networks for that goal.

2. **Formulation of Hypothesis:** A set of hypothesis are made to address the problems disclosed by the research questions on the light of what has already being established in the literature.

3. **Empirical Analysis:** The classical method of empirical examination of the hypothesis are adopted throughout this study is adopted whenever it is possible. In this study, field measurements were performed over real cellular networks at different times along the research, including the investigation of the propagation model, the analysis of the interference and performance of the connection and an evaluation of typical latencies observed. The choice of scenarios, heights and distances took into account the constraints imposed by regulation and safety measurements associated with flying a drone at the time of writing.

4. **Design of Solutions:** Some of the empirical findings are fed back into the set of hypothesis unveiling problems associated with the performance of cellular networks in providing service to UAVs. Some solutions are proposed to tackle these problems and help to enhance the overall link performance. Examples of such solutions include the adoption of interference mitigation techniques available in cellular networks, the usage of beam forming on the UAV, multi operator hybrid access, etc.

5. **Evaluation of hypothesis and solutions:** The hypothesis and the solutions proposed are analyzed and evaluated regarding their validity for the problems formulated by the research questions. This analysis was performed either via analytical treatment (for example to obtain a modeling for the propagation model) or via Monte Carlo simulations, using a LTE system level simulator. The simulations enable the evaluation of several features under similar assumptions, that would be difficult or untreatable to formulate in mathematical terms.

6. **Dissemination of Knowledge:** The scientific findings obtained in this investigation are disseminated by means of scientific publications, while some contributions also made to relevant fora, such as the 3GPP study item on enhanced support for UAV and the DroC2om project. Some of the novel work associated with this research were also disclosed in the form of patent applications.

1.4 Scope and Objective of the Thesis

The state-of-the-art suggests that cellular networks provide several advantages and a great potential to support C2 connectivity, albeit they indicate some challenges to be overcome. The main goal of this thesis is to evaluate, through experimental investigations and simulations, their suitability to serving critical communication to UAVs, weighing in the pros and cons of this choice. A second goal aims at set the basis for an evaluation of the features and technical enhancements required for obtaining a satisfactory performance. Additionally, the thesis wants to evaluate costs and benefits of allocating dedicated cellular spectrum resources for C2 users and of resource sharing with terrestrial users, regarding the projected demand for commercial UAV applications.

The LTE-Advanced (LTE-A), widely available in operators networks at the time of writing, is the technology chosen for most of the analysis performed in this thesis, but some considerations are also made about the by the 5^{th} Generation (5G) New Radio (NR) and how their enhancements can favor the support of C2.

As required by the goals set for this work, a suitable channel model is required for enabling a reasonable evaluation of cellular-to-UAV applications. In order to accomplish that, path loss measurements acquired from airborne devices connected over real LTE networks are provided in this work. These measurements are used to characterize a macro channel model that accounts for different UAV heights. Given the legislation constraints at the time of writing, the field experiments with airborne UAVs were limited to heights up to 120 m, thus the work presented hereafter is focused on airborne devices flying at up to such heights. Nevertheless, this shall not be a limitation for the validity of the work, as this range comprehends most of the applications to be deployed by commercial drones in VLL space.

System level simulations were performed with the path loss model obtained from the field measurements to evaluate the C2 performance under different network loads. The clearance of scattering elements in the base station-to-drone path mitigates the attenuation of the received signal from the preferred source, in spite of the down tilt of the base station antennas. However, it does not help to restrain the interference radiated by or to the neighbors whatsoever. The simulations will be used as mean to evaluate the overall implications of these contradicting effects for different network traffic loads.

Additionally, field tests in live LTE-A networks are also performed to obtain reference values for the typical latencies expected by UAVs in LTE-A networks. These tests will also provide insights of strategies to improve the reliability of C2 under latency constraints.

The assessment of the interference impact on the link performance shows

there is a challenging scenario to reliably accommodate the support for C2 in current cellular technology. A list of interference mitigation techniques were evaluated accordingly to their capacity of providing performance enhancement. These techniques include inter-cell interference coordination (ICIC), Coordinated Multipoint (CoMP) beamforming and others. Although these techniques have been widely evaluated for terrestrial communications, they may not have the same effect in this scenario. The difference lies in the fact that for terrestrial links there are typically one, or a few, sources of strong interference, whereas multiple significant sources of interference can be available for a flying device.

Hereafter in this thesis the term C2 will be used to designate the wireless radio link supporting the UAV critical communication, which is the main focus of this thesis, and not the whole end-to-end communication as in the ICAO concept.

1.4.1 Terminology and Definitions

Without further clarification, some important concepts used throughout this thesis could elicit some confusion, because the terminology accepts different (or broader) meaning in diverse contexts or fields of research. To avoid such misinterpretations these terms are defined here.

Downlink vs Uplink

Henceforth in this thesis the terms downlink (DL) and UL will be used as typically done in the telecommunication industry, which differs from the reference adopted in the aviation industry. It means that the DL represents the link transmitted from the cellular ground infrastructure to the mobile device and the uplink (UL) represents the link in the opposite direction.

Altitude vs. Height

In this thesis, simulations and measurements are performed for UAVs flying at *heights* up to 120 meters. The term height, is used in its most common definition, representing the vertical distance between the UAV and the local ground at a given time. This term is preferred over the usage of *altitude* in this thesis, as the later can refer to different reference points: the local ground (*absolute altitude*), the mean sea level (*true altitude*), pressure altitude, etc.

VLOS vs LOS

The terms VLOS and line-of-sight (LOS) represent similar concepts: the existence of an unobstructed path between one point to an object located at a given distance. The distinction is made on the applicability of each term.

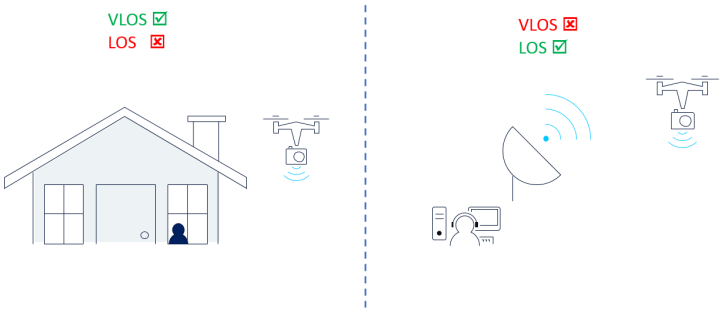

Fig. 1.1: Illustration of the difference between VLOS and LOS as used in this thesis.

The first refers to the *visual* line-of-sight or, in other words, to the distance from what a human observer can see a target object; whereas the expression line-of-sight (LOS) represents the radio line-of-sight, or the existence of an unobstructed direct radio path between transmitter and receiver. These concepts are illustrated in Fig. 1.1.

As for the opposite concepts - the negation of VLOS and LOS - the terms respectively used will be BVLOS and non line-of-sight (NLOS).

FDD vs TDD

All the analysis performed in LTE systems in this research, either simulations or measurements, were done for Frequency Division Duplex (FDD) systems, chosen because it is the most common deployment in European networks - which comprehends the scenario used for testing. Although some of the results may be straightforward extended to Time Division Duplex (TDD) systems, it is possible that some of the performance results differ from when considering TDD deployments.

1.4.2 Relevant Topics Out of the Scope of the Thesis

At the early days of this research project, the usage of UAVs as users in the cellular networks was attraction attention of the research community, but was still an incipient topic. A handful of other topics in the field of wireless communications regarding the UAVs were trending [29]. One topic that have also been of relevant interest since then was the usage of UAVs as base stations (or relay nodes) providing connectivity for terrestrial users [30,31], either by offloading a terrestrial setup in congested times [32] or for disaster relief [33].

This topic is similarly complex in terms of challenges and potentials offered, and it has its own subset of problems to be explored [34–36].

Because this scenario has been the most popular in recent years, it has been a common source of misunderstanding assuming this scenario must comprehended in a investigation about UAV's connectivity. For this reason, it is important to remark that this scenarios are out of the scope of the present work. It is the author understanding that such topics could entail one thesis on their own.

1.5 Research Questions

The goals of this thesis and their main body of research can be summarized into key research questions (Q) and hypothesis (H).

Q1 What is a good path loss model for describing the radio attenuation observed between the cellular base stations and flying devices at heights up to 120 m?

H1 The higher the UAV flying height the more likely it will experience LOS with surrounding base stations. At some point, the radio path losses approximate the attenuation in free space. The propagation coefficient must therefore be height dependent, transitioning from high values (3.7 to 4.0) at ground level to values closer to free space (2.0) at 120 m.

Q2 How this potentially height dependent path loss model impacts the network interference levels?

H2 In DL, terrestrial users usually face bad interference conditions when close to cell edge, caused by one or a few major interfering sources. As cell edges become "blurred" at higher levels [23,37], UAVs may expect significant interference level received from several different sources and more spatially widespread. The more dense the network and the higher the traffic load, the higher is the degradation expected in the signal to interference plus noise ratio (SINR). In the most stringent scenarios, the link may drop if its SINR falls below the minimum required level [38]. On the UL, a UAV is expected to cause interference to several base stations and larger area.

Q3 Can cellular networks cope with the requirements for C2 links over a LTE network?

H3 In certain environments, UAVs are expected to experience very severe interference conditions. These circumstances can compromise the reliability levels to fall below the strict requirements imposed to C2. But, looking forward to future applications, the implementation of UAV-specific interference mitigation techniques can help to enhance the link performance.

Q4 Which techniques can best enhance C2 performance?

H4 Assuming a multitude of interference sources, there are challenges to find efficient mechanisms to improve the DL and UL SINR. The performance of the techniques deployed for terrestrial users may differ from the gains observed by the C2 link.

Q5 What are the costs and benefits in a dedicated resource allocation policy associated to the C2?

H5 The projected number of UAV devices is much smaller than terrestrial subscribers. Even though, dedicating some spectrum resources for C2 users can isolate them from significant interference, it can be economically unattractive for operators due to the high cost of licensed spectrum.

1.6 Literature Review

1.6.1 Prior Art

Channel Model for UAVs

In the telecommunications industry, channel models are used to evaluate the performance of network features in simulations or to plan future network deployments. They provide an expectation of the attenuation suffered by the radio signal transmitted by a source when received by the other end of the communication link. For an accurate modeling, the choice of the model has to suit the environment of the application (e.g. indoor, rural, urban macro), the frequency used and the heights of the communicating nodes.

As mentioned in Section 1.2, most well known models used for cellular communications were refined for terrestrial users, for example the representative channel modeling used by 3GPP [24]. At the same time, among the models commonly used in the aviation industry there was a lack of validated accurated wideband models that extends for the frequency bands usually deployed in cellular networks [39,40].

In the early days, though, some reference could be found using a UAV transmitting toward measurement equipments on the ground, for example in [41,42] where an airship was transmitting a signal in the 2 GHz band, flying at heights between 100 and 300 m. In [41] a statistical analysis of the losses on the radio channel is made using a Rician model, while in [42] the excess losses on the radio path are examined through knife-edge diffraction models taking into account the surrounding scenario. But these investigations are fundamentally different from the problem being investigated in these thesis, as they measure the propagation channel between a terrestrial receiver

and the airborne transmitter, whereas this research is focused on the aerial-to-infrastructure transmission, which is likely to result in different (lower) propagation losses.

Because of the lack of such comprehensive models for, the research community has driven some attention to create channel models for UAVs applications. Among such efforts, NASA has dedicated an extensive series of studies to investigate the radio propagation channel for airborne UAVs in different environments. This series was initiated with the characterization of the suburban and near urban [43]. After the present PhD studies have started, the NASA's series continued to contribute to the state of the art characterizing the hilly and mountainous [44] and above the water [45] scenarios. The measurements were performed in the frequency bands envisioned by ITU for future C2 deployments, in the C-Band and L-Band, which are relatively close to the typical cellular frequency bands.

The measurements results indicate a strong LOS component extending for several km, where most of the received power was contained in the first few channel taps and a small delay spread was observed. In most cases, the path loss exponent varied between 1.5 and 2.2 and the shadowing standard deviation between 2.5 and 3.5 dB, both below typical terrestrial channel values. However, the experiments focused on medium to large UAVs applications, flying at heights more than 500 m above the ground transmitter, which is higher than the ceiling for low level airspace used for small UAVs (up to 300 m). Although the results offer a reference for what happens at high heights, they do not show what happens at intermediate levels, nor closer to ground level. Moreover, no current cellular network deployments were used in this reference.

1.6.2 Literature Contemporary to this Research

Within the duration of the PhD studies the topic has drawn attention from the academia and several studies have been published in parallel to this research, such as part as the NASA's series. Part of this contemporary references have mutually impacted and being impacted by the contributions of our investigation.

Channel Model for UAVs

Some of these studies have addressed the use of cellular networks for connectivity at low altitudes [46]. The authors of [47] performed measurements over cellular GSM (at 900 MHz) and UMTS (at 1.9 - 2.2 GHz) by embedding the measurement equipment to a small fixed-wing UAV. The received signal power is measured and used for fitting a model of radio attenuation that accounts for the UAV heights. However, this is not a path loss model, and

the received signal is modeled independent of the distance to transmitters, which is not applicable for long flight ranges and does not generalize well outside the field of measurements.

In [37], tests are performed in LTE networks (at 700, 1700 and 1900 MHz) using an airborne UAV at different heights (30, 60, 90 and 120 m) and several link Key Performance Indicator (KPI) are analyzed. Results are compared against free space model (path loss exponent of 2.0) and a typical log-distance propagation model [48] (exponent of 4.0), indicating that the path losses observed by an airborne UAV approximates more to the free space assumption. The work presented in [49] used a small UAV carrying a LTE mobile phone connected to a single base station at 850 MHz to perform measurements at five different heights (15, 30, 60, 90 and 120 m) in a suburban environment. Based on the field measurements, the authors provide a model that includes an extra term, the "excess path loss", in the log-distance model used for the terrestrial channel, that accounts for the angle between ground base station and UAV. The closed expression provided for the excess path loss takes into account the clearance of the radio path, but it also implicitly takes into the model the vertical gains of the antennas used in the LTE phone and in the ground transmitter during the measurements. Because of this, the model cannot be straightforward generalized for different antenna deployments.

In part due to the contributions of the results found in this thesis, the 3GPP channel model has also being updated for including user heights above 20 m [24], in order to enable the analysis of the radio link peformance for UAV [15].

Interference Mitigation for UAVs

There are two opposing effects, one favorable and the other adverse, in what concerns the cellular coverage for UAVs: the orientation of the antennas and the clearance of the radio path [49]. The antennas in the ground base stations are often down tilted, directing the main part of the transmitted power to the ground. At the same time, airborne devices experience better radio clearance, with the LOS likelihood increasing with height [50], which is reflected in some of the first path loss models made available for UAVs.

Previous works have showed that the gain obtained in the path loss attenuation of the signal tends to overcome the losses introduced by antenna side lobe attenuation [38]. UAVs flying right above the base stations will probably be subjected to very high side lobe attenuations on the vertical domain, but they can benefit from the improved path losses to connect to a further distant base station. Observe that the angle between the ground base station and UAV tend to zero as their difference of heights gets much smaller than the horizontal distance between them.

However, challenges arise because the density of sites in cellular networks

were originally designed for providing coverage to terrestrial users. The obstacles present at ground level help to contain the transmit power within the intended radius of a given cell. Without this help from the environment the transmitted power will be received with very low attenuation for users connected to different cells. Airborne UAVs therefore tend to perceive a higher number of neighboring cells in the network [37] with a higher average power level [23]. In spite of the better radio signal received from the cell the user is connected to, the overall signal-to-interference ratio decreases, degrading the quality of the radio link [23].

Because of this, aerial UEs is susceptible to severe interference from multiple sources [20] and that can compromise the performance. A theoretical analysis has demonstrated that although the coverage probability at very low heights is at reasonable levels, it degrades significantly for high heights UAVs [51].

One interesting strategy to circumvent the problems caused by the increased interference is the usage of very directional antenna transmissions in the base station, for example through Massive Multiple Input Multiple Output (MIMO) deployments [52]. The reference in [52] demonstrates how the performance of the UAVs can be enhanced by focusing the desired transmitted signal in the direction of the target user, while minimizing - positioning nulls - of the other base stations in that same direction.

On the other direction, the UL, the interference is caused by the UAVs to several base stations in a large area, because of the higher LOS likelihood. Some references have instigated different solutions to this problem, some in line of the work produced in this research. In [53], a cooperative interference cancellation is proposed for maximizing the throughput of the users in a multi-beam UAV system. The study in [54], UL Non-Orthogonal Multiple Access (NOMA) is used to minimize the interference caused by the UAVs, whereas a similar approach is attempted in [55,56] by means of adjusting the power control settings.

As it will become evident in this thesis, the UL problem is considered of lower impact, because of the lower density of UAVs compared to the terrestrial users and the data rate required by them in most cases. The power control, then, becomes the preferred approach in this thesis, because it is a rather simple solution that is easily adaptable for today's networks, and provide sufficient gains.

A comprehensive review for the interference mitigation techniques is presented in [57], which is focused on the maximization of the user throughput. Similar investigations are proposed in this paper through simulations and measurements, but more focused on the maximization of the reliability of the C2 link.

1.7 Contributions

Contributions to the state-of-the-art

The key contributions provided by this research for the state-of-the-art in this topic are listed below:

1. **A height dependent propagation model.**

   The results obtained through field measurements collected by devices attached to a real UAV suggest different propagation attenuation observed at different heights. As presented in the state of the art review, there was a lack of models for airborne devices connected to ground base stations in cellular frequencies accounting for this factor. In order to capture this effect into path loss estimations, a modification on the classical log-distance model is suggested to take into account the height of the user. The height-dependent path loss model provide a single expression that can be used by simulation environments to evaluate the link performance.

2. **Characterization of the patterns of the interference caused and received by UAVs.**

   Throughout this thesis a series of assessments are made about the interference in the C2 channel measured in real network deployments. The observations point out that there the C2 scenario is different from that observed at ground level. In the DL the link is subject to several sources of significant interference, from multiple neighbor cells and not just that in the vicinity of the serving base stations, which can cause a rapid degradation of the link by increasing the overall load in the network. In the UL, the flying device transmission power is causing high interference level even to base stations located tens of kilometers away from the transmitting spot. The characterization of the interference is important to define which interference mitigation techniques have the potential to enhance link performance.

3. **Performance evaluation and interference mitigation techniques for UAVs through simulations.** Because of the unique distribution of the interfering sources in the power domain, some of the typical mitigation techniques commonly exploited in cellular networks do not provide significant gain for the link performance. This is demonstrated in this thesis by a series of simulations. The study shows that, for different network load conditions, ICIC would lead to high inefficiency and high complexity, requiring in some cases more than 10 cells to be muted per instant of transmission to alleviate the DL interference,

while interference cancellation (IC) also fails to provide significant gains whatsoever.

The study suggests that the usage of directional antennas transmission, such as beam forming or grid of beams at the UE, provide the best performance enhancement in the link, by limiting the interference power spatially. The gains perceived by these techniques are observed in both directions, DL and UL. Power control settings were also tested to mitigate the uplink interference.

4. **On-field verification of current latency values expected for C2 over LTE networks.**

   The study provides state-of-the-art reference about the achievable latency values in live operating LTE networks for an emulated C2 traffic channel. On-field verification is performed for this metric which is assessed in two different networks in urban locations, in order to show typical values observed and some of the challenges to maintain the target reliability.

   A dual-operator scheme is proposed in this thesis, to cope with the strict reliability requirements of the C2 using currently available technologies, prompting a more ready to market enabling feature. This thesis provides measurements-based assessment of the potential gains of such technique, while discusses its advantages.

5. **Introducing methods for identification of airborne users based on typical cellular radio measurements.**

   Some of the findings in this thesis show that the network can benefit of knowing a given user is UAV in stead of a regular terrestrial users. At the time of writing, it is still not possible to assure that this information will be made available to the network by explicit radio signaling from the UAV. Given the different interference scenario this thesis propose the usage of the radio measurements reported by the user as an UAV identification method.

   Different methods can be used to this end, such as deriving an analytical formula or the usage of several different machine learning techniques. Analyzing the best way to perform this task and investigate their limitations could be subject to an entire thesis in itself. The contribution of this research is to show the potential of using radio measurements as a predictive tool of the class of user.

6. **Cost and benefits assessment of reserving parts of cellular spectrum for dedicated C2 traffic.**

   A cost and benefit analysis is performed - using simulation methods - of protecting the C2 from undesired interference by reserving parts of

the cellular spectrum to dedicated C2 use. This assessment is made taken into consideration projections for the future demand of commercial UAVs and the amount of spectrum that should be reserved in different projected scenarios.

Scientific Publications

The main body of this thesis is encompassed by a collection of the papers. The state-of-the-art contributions aforementioned are presented in the following list of scientific publications:

Paper A: R. Amorim, P. Mogensen, T. Sorensen, I. Z. Kovacs and J. Wigard, "Pathloss Measurements and Modeling for UAVs Connected to Cellular Networks," *IEEE 85th Vehicular Technology Conference (VTC Spring)*, 2017, pp. 1-6.

Paper B: R. Amorim, H. Nguyen, P. Mogensen, I. Z. Kovács, J. Wigard and T. B. Sørensen, "Radio Channel Modeling for UAV Communication Over Cellular Networks," in *IEEE Wireless Communications Letters*, vol. 6, no. 4, pp. 514-517, Aug. 2017.

Paper C: R. Amorim, H. Nguyen, J. Wigard, I. Z. Kovács, T. B. Sorensen and P. Mogensen, "LTE radio measurements above urban rooftops for aerial communications," *IEEE Wireless Communications and Networking Conference (WCNC)*, 2018, pp. 1-6.

Paper D: R. Amorim et al., "Measured Uplink Interference Caused by Aerial Vehicles in LTE Cellular Networks," in *IEEE Wireless Communications Letters*, vol. 7, no. 6, pp. 958-961, Dec. 2018.

Paper E: I. Kovacs, R. Amorim, H. C. Nguyen, J. Wigard and P. Mogensen, "Interference Analysis for UAV Connectivity over LTE Using Aerial Radio Measurements," *IEEE 86th Vehicular Technology Conference (VTC-Fall)*, 2017, pp. 1-6.

Paper F: H. C. Nguyen, R. Amorim, J. Wigard, I. Z. Kovacs and P. Mogensen, "Using LTE Networks for UAV Command and Control Link: A Rural-Area Coverage Analysis," *IEEE 86th Vehicular Technology Conference (VTC-Fall)*, 2017, pp. 1-6.

Paper G: H. C. Nguyen, R. Amorim, J. Wigard, I. Z. Kovács, T. B. Sørensen and P. E. Mogensen, "How to Ensure Reliable Connectivity for Aerial Vehicles Over Cellular Networks," *IEEE Access*, vol. 6, pp. 12304-12317, 2018.

Paper H: R. Amorim, J. Wigard, I. Z. Kovács, T. B. Sørensen, P. Mogensen, "Enabling Reliable Cellular Communication for Aerial Vehicles", *Vehicular Technology Magazine*, 2019, **Submitted**.

Paper I: R. Amorim, J. Wigard, I. Z. Kovács, T. B. Sørensen, P. Mogensen, G. Pocovi, "Improving Command and Control Reliability for Drones with Multi-Operator Connectivity", *IEEE 89th Vehicular Technology Conference (VTC Spring)*, 2019.

Paper J: R. Amorim, J. Wigard, I. Z. Kovács, T. B. Sørensen, P. Mogensen, "Forecasting Spectrum Demand for UAVs Served by Dedicated Allocation in Cellular Networks", *IEEE Wireless Communications and Networking Conference (WCNC)*, 2019.

Paper K: R. Amorim, J. Wigard, H. Nguyen, I. Z. Kovács and P. Mogensen, "Machine-Learning Identification of Airborne UAV-UEs Based on LTE Radio Measurements," *IEEE Globecom Workshops (GC Wkshps)*, 2017, pp. 1-6.

Paper L: J. Wigard, R. Amorim, H. C. Nguyen, I. Z. Kovács and P. Mogensen, "Method for detection of airborne UEs based on LTE radio measurements," *IEEE 28th Annual International Symposium on Personal, Indoor, and Mobile Radio Communications (PIMRC)*, 2017, pp. 1-6.

Patents Disclosed

Novel solutions were developed during of the presented research and three of them were disclosed in the form of patent applications.

Contributions to Relevant Fora

Contributions to the relevant 3GPP study item [15] were made based on findings of this work. Of particular relevance, the height dependent channel model was presented to this forum and contributed to steer the channel model presented in the final version of the report, which provides extension for users in cellular networks at heights above 10 m.

Significant parts of this investigation were also presented in the form of reports for the SESAR 2020's DroC2om project. Some of the findings obtained through field measurements helped to set the foundation for the analysis of the potential of hybrid access schemes and the evaluation of the reliability of the wireless channel supporting the C2 [58]. Contributions were also made to the project based in the form of simulation results as part of the reporting about system concepts [59].

1.7.1 Simulator Features

The simulations performed throughout this study were developed using a Matlab-based proprietary Nokia-Bell Labs simulator. This system level simulator has been calibrated to evaluate the performance of mobile users in LTE networks. The design of new features in the simulator was a by-product of the implementation of UAV relevant scenarios. The main contributions to the simulator were:

- Height-dependent channel model for heights up to 120 m;
- User-specific power control settings, enabling the differentiation of terrestrial and aerial users;
- A directional antenna beam selection implemented on the UE side.

Other Contributions

Some of the findings presented in this work had provided support for two other publications related to this field of research:

- J. Stanczak, D. Kozioł, I. Z. Kovács, J. Wigard, M. Wimmer and R. Amorim, "Enhanced Unmanned Aerial Vehicle Communication Support in LTE-Advanced," 2018 IEEE Conference on Standards for Communications and Networking (CSCN), 2018, pp. 1-6.
- J. Stanczak, I. Z. Kovacs, D. Koziol, J. Wigard, R. Amorim and H. Nguyen, "Mobility Challenges for Unmanned Aerial Vehicles Connected to Cellular LTE Networks," Porto, 2018, pp. 1-5.

1.8 Thesis outline

This thesis is outlined in the form of a collection of papers, where the key research points and the outcomes of the analysis are presented by articles published or submitted to conferences or journals. Each of the following chapters in the main body of this thesis are formed by the relevant papers in that topic, that are preceded by an overview of the topic being discussed, some observations and a summary of the papers contributions. This summary provides the context for that paper within the main scope of the thesis and their relation with the other papers comprehended by this work. Some papers, whose findings may overlap concepts of more than one chapter, were assigned to the chapter that best fits a seamless progression of the storyline. The outline of the chapters are described below.

Chapter 1 Introduction: This current introductory chapter, which aims at presenting the motivation of the present work, a state-of-the-art review and the research questions and hypothesis. It also provides the contributions and the outline of the thesis.

Chapter 2 Path Loss Modeling: This chapter presents path loss modeling for airborne UAVs at different heights. The height-dependent models provided in this chapter, obtained by analysis of field measurements, set the background for the performance evaluation that compose the following chapters. It is composed by Papers A, B and C.

Chapter 3 Interference and Coverage Analysis: The unique propagation nature of the cellular-to-UAV communication presented in the previous chapter has implications on the radio coverage and interference. This chapter shows how the profile of interference experienced by UAVs differs from that observed by terrestrial users, in both DL and UL. It is also discussed in this chapter how this different profile of interference is potentially harmful for the C2. It is composed by Papers D, E and F.

Chapter 4 Performance Enhancement Techniques: Assuming a more stringent profile of interference can affect the known performance of cellular networks, a performance assessment is provided for the reliability levels measured and simulated under different scenarios. Moreover, for the most part in this chapter, technical enhancements are investigated and discussed as potential solutions to improve the C2 reliability. Papers G, H and I integrate this chapter.

Chapter 5 Dedicated Spectrum Assignment: This chapter is focused on debate the costs and benefits may be associated to dedicating cellular spectrum resources exclusively to C2, considering the projections about the size of fleet of commercial UAVs for the next twenty years. Simulations results are provided in this chapter to support the discussion which shows the estimations of the bandwidth required to provide coverage for different densities of UAV. This chapter is supported by paper J .

Chapter 6 Identification of Airborne UEs: This chapter covers the topic of dedicated solutions for UAVs. More specifically, the chapter provides discussion about how case-specific solutions can be implemented for UAV users sharing the spectrum with terrestrial users, in special, how the network can identify UAV users when no modifications on current standards are available, i.e. based only on

legacy radio measurements. Papers K, L are used as supporting references for the discussions presented.

Chapter 7 Conclusions and Future Work: The final chapter of this thesis wrap the main findings up and provide suggestions for future works.

References

[1] K. L. B. Cook, "The Silent Force Multiplier: The History and Role of UAVs in Warfare," in *2007 IEEE Aerospace Conference*, March 2007, pp. 1–7.

[2] FAA, "Integration of Civil Unmanned Aircraft Systems (UAS) in the National Airspace System (NAS) Roadmap," Tech. Rep., 2013.

[3] O. A. Martinez and M. Cardona, "State of the art and future trends on unmanned aerial vehicle," in *2018 International Conference on Research in Intelligent and Computing in Engineering (RICE)*, Aug 2018, pp. 1–6.

[4] M. M. et all, "Clarity from above. PwC global report on the commercial applications of drone technology," PwC, Tech. Rep., May 2016.

[5] SESAR Joint Undertaking, "U-Space Blueprint brochure," Publications Office of the European Union, Luxembourg, 2017.

[6] EUROCONTROL, "Roadmap for the integration of civil Remotely-Piloted Aircraft Systems into the European Aviation System," Tech. Rep., 2013.

[7] M. Neale and D. Colin, "ICAO RPAS MANUAL - C2 Link and Communications," Technology Workshop - Remotely Piloted Aircraft Systems Symposium, Mar. 2015.

[8] D. Colin, "RPAS - Required C2 Performance (RLP) Concept," JARUS, Tech. Rep., May 2016.

[9] R. J. Shively, A. Hobbs, B. Lyall, and C. Rorie, "Human performance considerations for Remotely Piloted Aircraft Systems (RPAS)," Remotely Piloted Aircraft Systems Panel (RPASP) - 2nd meeting, June 2015.

[10] International Civial Aviation Organization (ICAO), "Manual on Required Communication Performance (RCP)," ICAO, Tech. Rep. 9869 AN/462, 2006.

[11] "Characteristics of unmanned aircraft systems and spectrum requirements to support their safe operation in non-segregated airspace," ITU-R, Mobile, radiodetermination, amateur and related satellites services M.2171, 2009.

[12] F. L. Templin, R. Jain, G. Sheffield, P. Taboso-Ballesteros, and D. Ponchak, "Considerations for an integrated UAS CNS architecture," in *2017 Integrated Communications, Navigation and Surveillance Conference (ICNS)*, April 217, pp. 2E3–1–2E3–12.

[13] ——, "Requirements for an integrated UAS CNS architecture," in *2017 Integrated Communications, Navigation and Surveillance Conference (ICNS)*, April 2017, pp. 2E4–1–2E4–11.

[14] Qualcomm, "LTE Unmanned Aircraft Systems Trial Report," Qualcomm Technologies Inc., White Paper, May 2017.

[15] 3GPP, "Enhanced LTE support for aerial vehicles," 3rd Generation Partnership Project (3GPP), Technical Specification (TS) 36.777, Jan. 2018, version 15.0.0.

[16] NTT DOCOMO INC, Ericsson, "Study on Enhanced Support for Aerial Vehicles ," 3GPP TSG RAN Meeting 75, Tech. Rep. RP-170779, Mar 2017.

[17] International Civial Aviation Organization (ICAO), " Remotely Piloted Aircraft System (RPAS) Concept of Operations (CONOPS) for International IFR Operations," Available Online in https://www.icao.int/safety/UA/Documents/RPAS%20CONOPS.pdf, accessed in Dec. 2018.

[18] N. Hosseini, H. Jamal, D. W. Matolak, J. Haque, and T. Magesacher, "UAV Command and Control, Navigation and Surveillance: A Review of Potential 5G and Satellite Systems," in *IEEE Aerospace Conference*, Mar 2019.

[19] 3GPP, "Solutions for NR to support non-terrestrial networks," 3rd Generation Partnership Project (3GPP), Technical Specification (TS) 38.821, 2019, version 0.4.0.

[20] Y. Zeng, J. Lyu, and R. Zhang, "Cellular-Connected UAV: Potential, Challenges and Promising Technologies," *IEEE Wireless Communications*, pp. 1–8, 2018.

[21] GSMA, "GSMA Regulatory Position on Drones," Tech. Rep., August 2017.

[22] ——, "Using Mobile Networks to Coordinate Unmanned Aircraft Traffic," Tech. Rep., Nov. 2018.

[23] B. V. D. Bergh, A. Chiumento, and S. Pollin, "LTE in the sky: trading off propagation benefits with interference costs for aerial nodes," *IEEE Commun. Mag.*, vol. 54, no. 5, pp. 44–50, May 2016.

[24] 3GPP, "Study on channel model for frequencies from 0.5 to 100 GHz," 3rd Generation Partnership Project (3GPP), Technical Specification (TS) 38.901, Sep. 2017, version 14.2.0.

[25] S. Sun, T. A. Thomas, T. S. Rappaport, H. Nguyen, I. Z. Kovacs, and I. Rodriguez, "Path Loss, Shadow Fading, and Line-of-Sight Probability Models for 5G Urban Macro-Cellular Scenarios," in *2015 IEEE Globecom Workshops (GC Wkshps)*, Dec 2015, pp. 1–7.

[26] M. M. Azari et al., "Coexistence of Terrestrial and Aerial Users in Cellular Networks," in *Proc. IEEE Glob. Commun. Conf. Workshops*, Singapore, Dec 2017, pp. 1–6.

[27] S. D. Muruganathan, X. Lin, H.-L. Määttänen, Z. Zou, W. A. Hapsari, and S. Yasukawa, "An Overview of 3GPP Release-15 Study on Enhanced LTE Support for Connected Drones," Published in Arxiv. https://arxiv.org/ftp/arxiv/papers/1805/1805.00826.pdf, May 2018.

[28] U. Turke, B. Hiller, D. Gotz, I. Z. Kovacs, J. Wigard, A. Eisenblatter, M. Clergeaud, and N. van Wambeke, "DroC2om - 763601 - Models for Combined Cellular-Satellite UAS Communications," SESAR Joint Undetaking, Deliverable 3.1, April 2018.

[29] L. Gupta, R. Jain, and G. Vaszkun, "Survey of Important Issues in UAV Communication Networks," *IEEE Communications Surveys Tutorials*, vol. 18, no. 2, pp. 1123–1152, Secondquarter 2016.

[30] Y. Zeng, R. Zhang, and T. J. Lim, "Wireless communications with unmanned aerial vehicles: opportunities and challenges," *IEEE Communications Magazine*, vol. 54, no. 5, pp. 36–42, May 2016.

[31] A. Al-Hourani, S. Kandeepan, and S. Lardner, "Optimal LAP Altitude for Maximum Coverage," *IEEE Wireless Communications Letters*, vol. 3, no. 6, pp. 569–572, Dec 2014.

[32] Z. Becvar, M. Vondra, P. Mach, J. Plachy, and D. Gesbert, "Performance of Mobile Networks with UAVs: Can Flying Base Stations Substitute Ultra-Dense Small Cells?" in *European Wireless 2017; 23th European Wireless Conference*, May 2017, pp. 1–7.

[33] M. Erdelj, E. Natalizio, K. R. Chowdhury, and I. F. Akyildiz, "Help from the Sky: Leveraging UAVs for Disaster Management," *IEEE Pervasive Computing*, vol. 16, no. 1, pp. 24–32, Jan 2017.

[34] O. Esrafilian, R. Gangula, and D. Gesbert, "Learning to Communicate in UAV-aided Wireless Networks: Map-based Approaches," *IEEE Internet of Things Journal*, pp. 1–1, 2019.

[35] V. Sharma, M. Bennis, and R. Kumar, "UAV-Assisted Heterogeneous Networks for Capacity Enhancement," *IEEE Communications Letters*, vol. 20, no. 6, pp. 1207–1210, June 2016.

[36] J. Lyu, Y. Zeng, and R. Zhang, "UAV-Aided Offloading for Cellular Hotspot," *IEEE Transactions on Wireless Communications*, vol. 17, no. 6, pp. 3988–4001, June 2018.

[37] Qualcomm, "LTE Unmanned Aircraft Systems Trial Report," Qualcomm Technologies Inc., White Paper, May 2017.

[38] X. Lin, V. Yajnanarayana, S. D. Muruganathan, S. Gao, H. Asplund, H. Maattanen, M. Bergstrom, S. Euler, and Y. . E. Wang, "The Sky Is Not the Limit: LTE for Unmanned Aerial Vehicles," *IEEE Communications Magazine*, vol. 56, no. 4, pp. 204–210, April 2018.

[39] D. W. Matolak, "Air-ground channels & models: Comprehensive review and considerations for unmanned aircraft systems," in *2012 IEEE Aerospace Conference*, March 2012, pp. 1–17.

[40] ——, "Channel characterization for unmanned aircraft systems," in *2015 9th European Conference on Antennas and Propagation (EuCAP)*, April 2015, pp. 1–5.

[41] M. Simunek, F. P. Fontán, and P. Pechac, "The UAV Low Elevation Propagation Channel in Urban Areas: Statistical Analysis and Time-Series Generator," *IEEE Transactions on Antennas and Propagation*, vol. 61, no. 7, pp. 3850–3858, July 2013.

[42] M. Simunek, P. Pechac, , and F. P. Fontan, "Excess loss model for low elevation links in urban areas for UAVs," *Radio Engineering*, vol. 20, no. 3, pp. 561–568, 2011.

[43] D. W. Matolak and R. Sun, "Air–Ground Channel Characterization for Unmanned Aircraft Systems—Part III: The Suburban and Near-Urban Environments," *IEEE Transactions on Vehicular Technology*, vol. 66, no. 8, pp. 6607–6618, Aug 2017.

[44] R. Sun and D. W. Matolak, "Air–Ground Channel Characterization for Unmanned Aircraft Systems Part II: Hilly and Mountainous Settings," *IEEE Transactions on Vehicular Technology*, vol. 66, no. 3, pp. 1913–1925, March 2017.

[45] D. W. Matolak and R. Sun, "Air–Ground Channel Characterization for Unmanned Aircraft Systems—Part I: Methods, Measurements, and Models for Over-Water Settings," *IEEE Transactions on Vehicular Technology*, vol. 66, no. 1, pp. 26–44, Jan 2017.

[46] A. A. Khuwaja, Y. Chen, N. Zhao, M. Alouini, and P. Dobbins, "A Survey of Channel Modeling for UAV Communications," *IEEE Communications Surveys Tutorials*, vol. 20, no. 4, pp. 2804–2821, Fourthquarter 2018.

[47] N. Goddemeier, K. Daniel, and C. Wietfeld, "Coverage evaluation of wireless networks for unmanned aerial systems," in *2010 IEEE Globecom Workshops*, Dec 2010, pp. 1760–1765.

[48] T. Rappaport, *Wireless Communications: Principles and Practice*, ser. Prentice Hall communications engineering and emerging technologies series. Prentice Hall PTR, 2002.

[49] A. Al-Hourani and K. Gomez, "Modeling Cellular-to-UAV Path-Loss for Suburban Environments," *IEEE Wireless Communications Letters*, vol. 7, no. 1, pp. 82–85, Feb 2018.

[50] B. Galkin, J. Kibilda, and L. A. D. Silva, "Coverage Analysis for Low-Altitude UAV Networks in Urban Environments," in *Proc. IEEE Glob. Commun. Conf.*, Singapore, Dec. 2017, pp. 1–6.

[51] D. López-Pérez, M. Ding, H. Li, L. G. Giordano, G. Geraci, A. Garcia-Rodriguez, Z. Lin, and M. Hassan, "On the Downlink Performance of UAV Communications in Dense Cellular Networks," in *2018 IEEE Global Communications Conference (GLOBECOM)*, Dec 2018, pp. 1–7.

[52] G. Geraci, A. Garcia-Rodriguez, L. G. Giordano, D. Lopez-Perez, and E. Bjoernson, "Supporting UAV Cellular Communications through Massive MIMO," in *2018 IEEE International Conference on Communications Workshops (ICC Workshops)*, May 2018, pp. 1–6.

[53] L. Liu, S. Zhang, and R. Zhang, "Cooperative Interference Cancellation for Multi-Beam UAV Uplink Communication: A DoF Analysis," in *2018 IEEE Globecom Workshops (GC Wkshps)*, Dec 2018, pp. 1–6.

[54] W. Mei and R. Zhang, "Uplink Cooperative NOMA for Cellular-Connected UAV," *IEEE Journal of Selected Topics in Signal Processing*, pp. 1–1, 2019.

[55] V. Yajnanarayana, Y. . Eric Wang, S. Gao, S. Muruganathan, and X. Lin Ericsson, "Interference Mitigation Methods for Unmanned Aerial Vehicles Served by Cellular Networks," in *2018 IEEE 5G World Forum (5GWF)*, July 2018, pp. 118–122.

[56] W. Mei, Q. Wu, and R. Zhang, "Cellular-Connected UAV: Uplink Association, Power Control and Interference Coordination," in *2018 IEEE Global Communications Conference (GLOBECOM)*, Dec 2018, pp. 206–212.

[57] G. Geraci, A. Garcia-Rodriguez, L. Galati Giordano, D. López-Pérez, and E. Björnson, "Understanding UAV Cellular Communications: From Existing Networks to Massive MIMO," *IEEE Access*, vol. 6, pp. 67 853–67 865, 2018.

[58] T. B. Sørensen and R. Amorim, "DroC2om - 763601 - DroC2om - 763601 - Preliminary report on first drone flight campaign," SESAR Joint Undetaking, Deliverable 5.1, March 2018.

[59] I. Z. Kovács, , J. Wigard, N. van Wambeke, and R. Amorim, "DroC2om - 763601 - LTE/5G system concepts to provide support for both terrestrial communications and high reliability UAS data links," SESAR Joint Undetaking, Deliverable 4.1, May 2018.

Chapter 2 - Path Loss Measurements and Modeling

This chapter discusses the path loss modeling for the Unmanned Aerial Vehicle (UAV) scenarios and presents studies with models obtained from field measurements performed in live LTE networks.

2.1 Problem Description

2.1.1 Relevance of Path Loss Models

In the state-of-the-art review, presented in Section 1.6, the importance of path loss models for analyzing and planning the performance of communications networks was discussed. Such models are of great importance for the main goals of the present thesis, assessing the suitability of using cellular networks for providing Command and Control (C2) service for UAVs, in special their coverage and capacity [1].

A path loss model describes mathematically how the signal transmitted by a given source is attenuated as a function of the distance until it reaches the desired destination. In the lights of this function, it is possible to find out the maximum distance of coverage, i.e., the maximum distance where the received power is above the sensitivity threshold of the receiving devices for a given throughput [2].

Severe losses in the link budget indicate that the maximum allowed distance cannot exceed a few dozens of meters [3]. On the other hand, when the losses are very low, the theoretical coverage can extend for several kilometers [4].

As importantly, low propagation losses also indicate that the different transmit sources in the network are radiating significant interference power to the users that are connected to adjacent neighbor cells. Albeit it can sound counterintuitive at first, the low attenuation can lead to reduced average quality level of the received signal due to signal to interference plus noise ratio (SINR) [5]. This effect may reduce the overall network capacity, either in

terms of total throughput or in number of users that can be served [2].

2.1.2 Particularities of Aerial Models

The cellular network layouts are developed to optimize the network capacity for terrestrial users. It means that the radiated power, the antennas down tilt and the inter site distance are carefully designed to avoid the leakage of high interference power on the adjacent cells. This design takes into consideration the models that describe the propagation channel at ground level.

It is reasonable to infer that the transmission from a cellular base station to an airborne device is usually subject to much less obstacles in the radio path. By flying above buildings, vegetation and variations in the terrain, the flying UAV is much less surrounded by scattering elements. Fig. 2.1 shows an illustrative example of this effect. Observe from the situation depicted that it is expected that as the drone moves vertically away from the ground, the radio path is clearing from the obstacles.

By assuming that the propagation observed by a flying drone can be fundamentally different from what is observed at ground level, the terrestrial propagation models cannot be used for the aerial vehicles. One example of how these differences can impact the results is found in Fig. 2.2. The picture

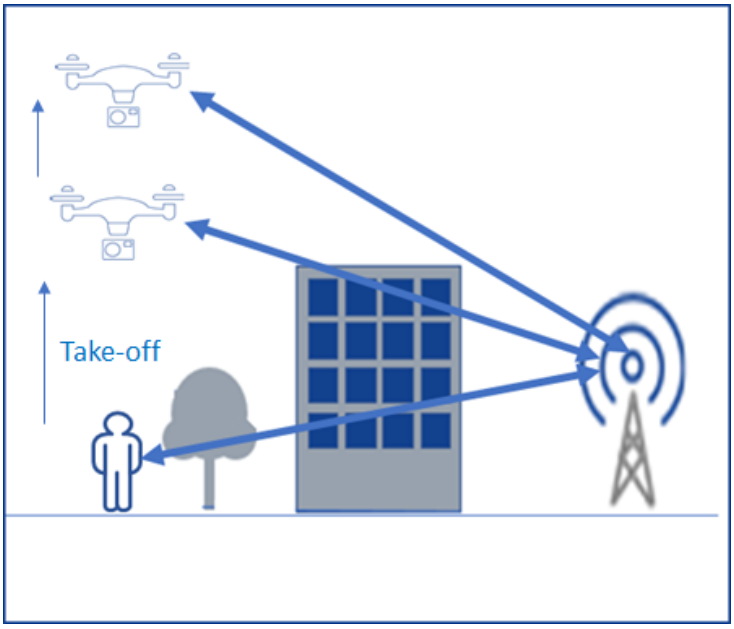

Fig. 2.1: Example of radio path for users at different heights.

shows raytracing estimations for the received power observed from a signal radiated by a single base station (BS) in a rural location in Denmark. Observe from the blue area at 1.5 m that, there is a strong attenuation of the signal outside a small area around the transmitter caused by the terrain variations. This effect is likely taken into consideration when designing the position of the neighboring sites in the network layout. As the UAV moves up, the terrain variations cannot confine the signal which spreads with high power for a large area, in spite of 4° of downtilt in the transmit antenna.

Hence, the performance predicted at terrestrial levels cannot be assumed similar for the airborne drones, as a consequence of the distinct path losses. In order to enable large scale verification of such assumptions, obtaining a statistical model for the propagation losses becomes important.

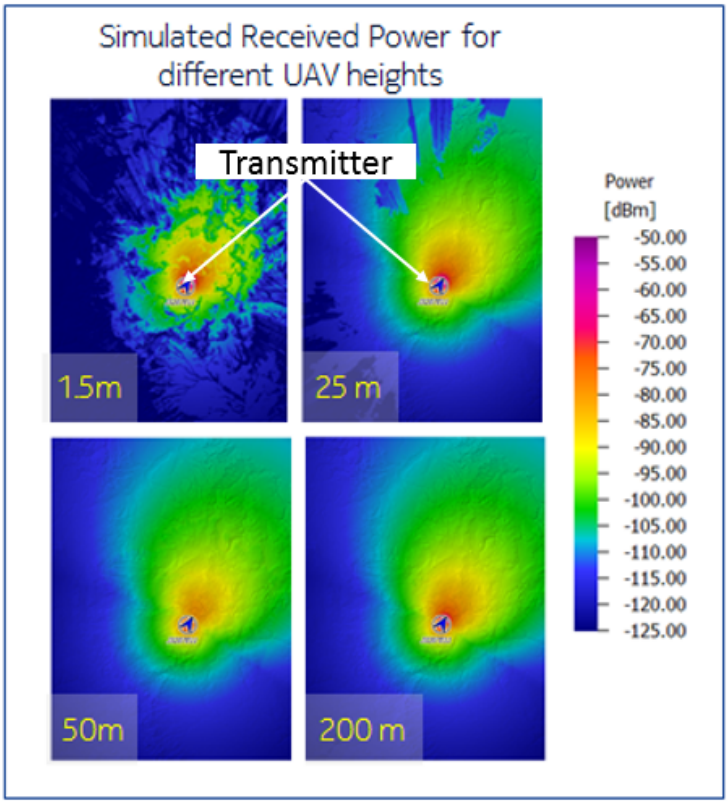

Fig. 2.2: Example of radio path for users at different heights.

2.1.3 Measurement Challenges

Deriving statistical path loss models relies on measurements collected in real scenarios. As more data becomes available in the literature, models will be presented and refined covering a larger number of scenarios and more refined they will be. Even models based on analytical techniques, such as raytracing tools, can be further calibrated based on field measurements, and are oftentimes much more complex to be widely used in comparison with the statistical models.

As Section 1.6 points out, in the early times of this research, there was a lack of such models for aerial devices connected to cellular base stations [6], which can be attributed to several factors.

First and foremost, the channel models commonly used for cellular networks were focused in providing service for terrestrial users, while commercial drones just recently became a tangible reality for the foreseeable future. On top of that, there are additional challenges because commercial UAVs are an incipient technology, namely the lack of expertise in performing such measurements and the challenging scenarios for collecting them.

In what concerns the expertise, the cellular networks community has worked with ground level measurements frameworks for decades (e.g. drive-test setups) and there are several equipments and commercial solutions that facilitate the data acquisition on the field. However, obtaining similar channel measurements from small devices flying at low altitudes imposes new requirements on the equipment setup. The framework for aerial measurements require a much more compact and lightweight setup, including all the equipment and its feeding batteries. Unlike drive-test setups, that are carried around by cars, small UAVs usually cannot take-off carrying heavy and bulky equipments. And even for light payloads, any additional weight represents a reduction in the flight autonomy. In this context, the expertise for doing aerial measurements is being developed as different research groups have been trying their innovative approaches to circumvent these limitations, for example using airships, weather balloons, captive balloons, or UAVs carrying small form equipments [7].

Moreover, there are additional challenges in the measurement scenarios. For the duration of this research, the rules for UAV flights restricted the range (limited by visual line of sight (VLOS)) and heights (up to 120 m) of the missions, driven by safety concerns [8]. The data acquisition of a single mission is therefore restrained to a small geographical area, driving up the costs and time spent for perform one set of measurements over extended areas. Additionally, the vertical movements of the UAV introduces one more dimension to be sampled, increasing the number of flights required for obtaining a model. It is one of the theoretical assumptions of this research that variations in heights at low altitudes impact the path loss model. Another problem is the

limited number of areas where UAVs can fly over. For example, flights over urban settings require express permission from authorities and are heavily affected by short VLOS distances.

All these reasons combined explain the lack of path loss models available when this research began, and they set the background for the measurement activities performed throughout this investigation. The work presented in this chapter has contributed to advance the state-of-the-art in channel models for UAVs connected to cellular networks.

2.2 Included Articles

Paper A. Pathloss Measurements and Modeling for UAVs Connected to Cellular Networks

In the timeline of this research, this paper reports the results of the first attempt, performed in June 2016, in creating a setup for measuring the path losses observed in the wireless channel for an aerial device. The measurement equipment, a cellular phone, is placed inside a winged UAV and attached to one carrier of a LTE operator (800 MHz) in rural Denmark. Measurements are collected at 20, 40, 60, 80 and 100 m of height.

As a first attempt, the setup used present some limitations. For example, there is radio signal attenuation caused by the fuselage of the UAV that encloses the measurement phone, introducing bias in the results. The cellular phone is not as precise as a radio scanner, specially with its internal antennas interacting with the UAV's fuselage. Also, as Fig. A.2 depicts, there is a limited flight range, and the most close-by cells are in constant line-of-sight (LOS) at all heights, biasing the final results.

In spite of these limitations, this paper brings valuable discussion of the degradation in the signal quality due to increased interference at higher heights and the causes that are associated with this phenomenon, such as the increased horizon distance, the clearance of the fresnel zones and the higher LOS likelihood. This first set of measurements also input valuable expertise used to develop the setups used in the other experiments.

Paper B. Radio Channel Modeling for UAV Communication Over Cellular Networks

This paper advances the contribution from A by using an improved setup to provide a path loss model obtained in rural locations of Denmark. Among the improvements developed for the setup presented in this article, it can be included: the flight lengths and the number of points collected were increased and the campaign was performed in two different locations, and also with more diversity on the position of the sites by measuring the network

of two different operators (LTE at 800 MHz) at the same time. Additionally, the setup for this experiment uses a radio scanner is used, attached underneath an hexacopter within a plastic box, which minimizes the losses due to the setup. Another point introduced by this paper is a drive-test reference performed at ground level, that enables the comparison of the models for airborne and terrestrial devices. The measurements were performed The set of heights analyzed in this paper are: 1.5, 15, 30, 60 and 120 m.

This paper produced incremental contribution to the state-of-the-art also brings a novel way of defining the path loss model by adding the height of the UAV into the equation. The article also provides analysis on the shadowing distribution at different flying heights.

Paper C. LTE Radio Measurements Above Urban Rooftops for Aerial Communications

This paper characterizes the urban scenario of propagation for UAVs. The measurements performed in this paper try to circumvent the limitations for flying at urban locations discussed in 2.1. For this goal, the setup used a construction crane and measured heights up to 40 m.

The main contribution of this paper is that it provides experimental measurements across different live LTE carriers (800, 1800 and 2600 MHz) and compare the results with the channel proposed in 3GPP for such scenarios [9]. The paper also investigates how the urban model obtained compares with the rural model previously presented in B.

Moreover, the article also brings the first detailed analysis of the interference profile, which is the main topic of the next chapter, by exploring the cell visibility and how close the neighbors are of the serving cell in the power domain.

2.3 Main Findings

2.3.1 Height-Dependent Path Loss Model

Papers B and C present channel models built upon the well known log-distance model [1] where the exponent is a function of the height: the more the UAV moves away from the ground level, more it approximates the free space exponent (2.0), while the exponents increases when approximating the ground ($\geq$3.0 at 1.5 m). The results presented in this paper, specially Paper B, were object of contribution the Third Generation Partnership Project (3GPP) [10] and the DroC2om project [11,12]. This result contributed in leading 3GPP to adapt their channel models for higher user equipment (UE) heights, such as those experienced by aerial vehicles [13]. Fig. 2.3 shows the main path losses for different UAVs heights following the model obtained

in Paper B. From this figure it is possible to observe that the signal radiated from neighbor cells located at 10 km of distance are expected to be received 30 dB higher at 120 m than at terrestrial levels.

These propagation models support other findings in the literature that show evidences of decrease in the radio path losses as the UAV moves up [5,14,15]. Another channel model proposed in the literature also built upon these references can be found in [16].

The height dependency of the path losses are not captured by the experiments performed in Paper A. The causes for this are outlined in Section 2.2. One of the main reasons may be related to the fact that the nearby sites (the most close-by depicted in Fig. A.2) are in constant LOS at all heights, biasing the results. The other papers have measured more than one location and more than one operator's network, to mitigate eventual biases produced by one specific layout. However, Paper A has showed field examples (Fig. A.4 and Fig. A.5) of how increases in heights can led to less obstruction in the radio path.

2.3.2 Height-Dependent Shadowing Standard Deviation

Alongside with the path loss exponent, the results presented in the Papers B and C have showed that the shadowing standard deviation also varies with the height. The radio signal becomes more predictable, i.e, shows less vari-

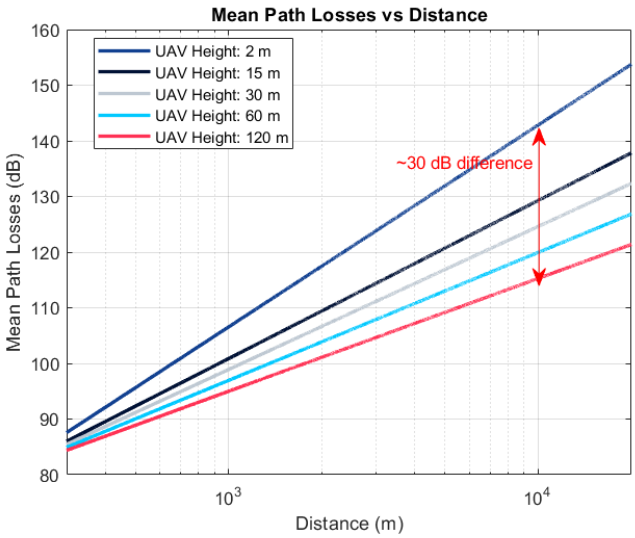

Fig. 2.3: Mean path losses versus distance, according to the channel model in Paper B.

ance, as the UAV heights increases, because some scattering elements in the radio path are removed. This also indicates that the received signal can be dominated by one or few delay paths, with high likelihood of LOS, which could be further confirmed by a characterization of the small scale elements of the radio path (see Section 2.4).

2.3.3 Cell Visibility

One important finding presented in these articles is the visibility of neighbor cells by the UAVs. This topic is an indication of the changes in the interference profile and will be object of further evaluation in Chapter 3.

In Paper A the results show that neighbor cells can be detected up to 12 km of distance. Paper B has showed that the sensitivity of the measurement equipment increases with height, caused by a rise on the noise-plus-interference floor. Albeit the sensitivity shows much more stringent values at 120 m than at terrestrial levels (see Fig. B.2), the measurement equipment has detected cells up to 22.2 km of distance. The number of cells detected at 120 m also increased significantly when compared to detection at terrestrial level (46 vs 26). The distribution of detected cells can be observed in Fig. 2.4, where it is possible to see that the detected cells are distributed over a wider range at 120 m.

This indicates that even sites farther away - but that fall below the sensitivity level - can potentially contribute with significant interference power. It is worth noting that 22.2 km is a fairly high distance: for a user at ground level, at sea level, the maximum theoretical reachable distance is approximately 29 km for one site with 40 m height. After this point, the signal is blocked by the Earth curvature [1].

These findings are supported by Paper C, that shows that the number of detected neighbors tend to increase as the user equipment moves away from the ground for three different network layouts(Fig. C.2). Paper C also suggests that the increased number of interfering neighbors approximates the serving cell in the power domain C.4.

2.4 Discussion

There are several parameters that can be used to characterize the radio channel. The articles presented in this chapter have focused on the large scale radio chanel parameters. The results indicate that an airborne device approximates LOS propagation with low shadowing variation as it moves away from the ground and suggests that the channel is dominated by one or a few multipaths.

Other parameters can also be used to characterize the wireless channel,

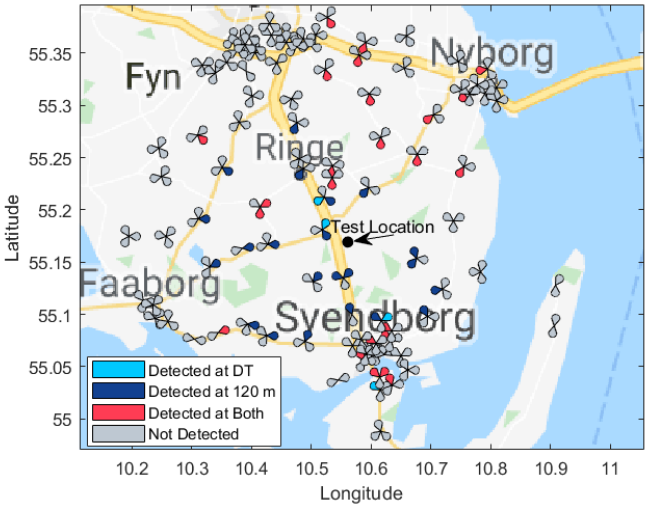

Fig. 2.4: Cells detected by the radio scanner in the experiments presented in Paper B. Results are shown for tests at terrestrial level Drive Test (DT) and at 120 m height

such as the Power Delay Profile (PDP). By assessing the PDP it is possible to determine if the received power indeed concentrates over the first few multipaths. When that is the case, there is a low variability on the radio channel, and there is not much diversity associated to the different antenna elements, limiting the implementation of Multiple Input Multiple Output (MIMO) solutions such as spatial diversity or multiplexing. On the other hand, because of the high likelihood of LOS and low losses in the wireless channel, there are references suggesting the UAV communication can benefit from the of beamforming on the realm of high frequency bands and also mmWave [17,18]. The investigation of massive-MIMO as a solution for C2 communication goes beyond of the scope of the present thesis.

It has pointed out in Paper A that due to the increased radio visibility distance, an airborne UAV could detect cells up to tens of km of distance. However, due to the sensitivity issues and the noise-plus-interference floor discussed in Paper B it was not possible to confirm this on the field for distances beyond 22.2 km. For this evaluation to take place, it would be required a transmitter fairly isolated from interference, and flights performed at significant distance. The author leaves this verification as a suggestion for future work.

Some of the results discussed in the papers presented by this chapter cover the issue of different interference profile observed by terrestrial and aerial users. This topic is the theme of Chapter 3 where it is discussed and

analyzed in further details.

References

[1] T. Rappaport, *Wireless Communications: Principles and Practice*, ser. Prentice Hall communications engineering and emerging technologies series. Prentice Hall PTR, 2002.

[2] A. R. Mishra, *Advanced Cellular Network Planning and Optimisation*. John Wiley & Sons, 2007.

[3] T. S. Rappaport, G. R. MacCartney, M. K. Samimi, and S. Sun, "Wideband Millimeter-Wave Propagation Measurements and Channel Models for Future Wireless Communication System Design," *IEEE Transactions on Communications*, vol. 63, no. 9, Sep. 2015.

[4] J. Laiho, A. Wacker, and T. Novosad, *Radio Network Planning and Optimization for UMTS*. John Wiley & Sons, 2001.

[5] B. V. D. Bergh, A. Chiumento, and S. Pollin, "LTE in the sky: trading off propagation benefits with interference costs for aerial nodes," *IEEE Commun. Mag.*, vol. 54, no. 5, pp. 44–50, May 2016.

[6] D. W. Matolak, "Air-ground channels & models: Comprehensive review and considerations for unmanned aircraft systems," in *2012 IEEE Aerospace Conference*, March 2012, pp. 1–17.

[7] A. A. Khuwaja, Y. Chen, N. Zhao, M. Alouini, and P. Dobbins, "A Survey of Channel Modeling for UAV Communications," *IEEE Communications Surveys Tutorials*, vol. 20, no. 4, pp. 2804–2821, Fourthquarter 2018.

[8] Drone Rules, "Regulations: Denmark (DK)," Available Online in http://dronerules.eu/en/professional/regulations/denmark, accessed in Mar. 2019.

[9] 3GPP, "Enhanced LTE support for aerial vehicles," 3rd Generation Partnership Project (3GPP), Technical Specification (TS) 36.777, Jan. 2018, version 15.0.0.

[10] Nokia, Alcatel-Lucent Shanghai Bell, "Evaluation Scenarios and Channel Models for Drones," 3rd Generation Partnership Project (3GPP), Technical Document (TDoc) R1-1704430, 2017, tSG RAN WG1 Meeting #88bis.

[11] T. B. Sørensen and R. Amorim, "DroC2om - 763601 - DroC2om - 763601 - Preliminary report on first drone flight campaign," SESAR Joint Undetaking, Deliverable 5.1, March 2018.

[12] T. B. Sørensen, R. Amorim, and M. López, "DroC2om - 763601 - Report of first drone flight campaign," SESAR Joint Undetaking, Deliverable 5.2, October 2018.

[13] 3GPP, "Study on channel model for frequencies from 0.5 to 100 GHz," 3rd Generation Partnership Project (3GPP), Technical Specification (TS) 38.901, Sep. 2017, version 14.2.0.

[14] N. Goddemeier, K. Daniel, and C. Wietfeld, "Coverage evaluation of wireless networks for unmanned aerial systems," in *2010 IEEE Globecom Workshops*, Dec 2010, pp. 1760–1765.

[15] Qualcomm, "LTE Unmanned Aircraft Systems Trial Report," Qualcomm Technologies Inc., White Paper, May 2017.

[16] A. Al-Hourani and K. Gomez, "Modeling Cellular-to-UAV Path-Loss for Suburban Environments," *IEEE Wireless Communications Letters*, vol. 7, no. 1, pp. 82–85, Feb 2018.

[17] G. Geraci, A. Garcia-Rodriguez, L. G. Giordano, D. Lopez-Perez, and E. Bjoernson, "Supporting UAV Cellular Communications through Massive MIMO," in *2018 IEEE International Conference on Communications Workshops (ICC Workshops)*, May 2018, pp. 1–6.

[18] Z. Xiao, P. Xia, and X. Xia, "Enabling UAV cellular with millimeter-wave communication: potentials and approaches," *IEEE Communications Magazine*, vol. 54, no. 5, pp. 66–73, May 2016.

Paper A

Pathloss Measurements and Modeling for UAVs Connected to Cellular Networks

Rafhael Amorim, Preben Mogensen, Troels Sorensen, Istvan Z. Kovacs and Jeroen Wigard

The paper has been published at the
IEEE 85th Vehicular Technology Conference (VTC Spring 2017)

© 2017 IEEE
The layout has been revised and reprinted with permission.

Abstract

This paper analyzes the radio channel between cellular network and Unmanned Aerial Vehichles (UAVs). The assessment is done by means of field measurements performed in a rural environment in Denmark. The tests were conducted in an operating LTE network (800 MHz), using a commercial cell phone placed inside the frame of a winged UAV. Trials were conducted with UAV flying at 5 different heights measured above ground level (20, 40, 60, 80 and 100m) and a pathloss regression line was obtained from the results. Thereafter, an analysis of downlink (DL) interference is performed for the reported measurements, which suggests that there is a height-related degradation on signal-to-interference levels. Three possible sources for this effect are also presented and discussed in this paper: expanded radio horizon at higher levels, line-of-sight (LOS) clearing and decreased obstruction of the first Fresnel zone. The importance of a better quantification of these factors are stressed as future work plans are described.

I Introduction

UAVs, also known as drones, have a promising potential to reduce risk, cost, and time deployment for many activities, such as buildings inspection or search and rescue missions. Most of this potential is yet to be explored, as the operational range for drones is still very limited. The current policy of many air space agencies is to limit UAVs operational ranges in order to ensure a safe usage of the airspace, resulting in strict regulations imposed to drones users, such as the requirement of visual line of sight between controler and UAV during all phases of the flight. [1].

One important enabler for future UAV activities is the deployment of a reliable communication and control link (C2), also known as control and non-payload communications (CNPC). The C2 link will be responsible for exchanging all flight-related communication for beyond line-of-sight applications, such as telemetry, air traffic information and remote commands. Although the C2 link is considered to be deployed in dedicated frequencies by many [2], cellular networks may already be able to offer operating ground infrastructure that could make C2 links more cost efficient and ubiquitous, and might be considered as an alternative. Not only limited to supporting the C2 link, the cellular networks are also strong candidates to be in charge of payload information, such as real-time footage or other messages to be carried to/from drones.

Hence, the 3D pathloss modelling is an important topic to be regarded as it will enable simulation models and a better performance assessment for UAVs using cellular network resources. The challenges of this topic are addressed in this paper based on airborne measurements. Although there are

several propagation models for typical cellular networks, their suitability for UAVs use case is yet to be proven since this propagation environment has its own specificities.

For ground users, radio waves propagating from base stations are subjected to phenomena as refraction, reflection and absortion caused by their interaction with buildings, trees, hills and other scattering objects present in the radio path between the transmitter and the receiver. In these scattering environments the signal is attenuated due to non line-of-sight propagation (NLOS). UAVs flying above rooftops and other obstructions are also subjected to these effects, but in a much smaller degree, while they also experience an increased likelihood of line-of-sight (LOS) transmissions.

On the other hand, by flying above the ground level, the UAV may observe an unobstructed path not only with the serving base station but also with many different interfering base stations in the same area. Because of this, assessments on interference levels for airborne UAVs are presented in this paper. It is worthy to mention that cellular networks are typically optimized for terrestrial usages which imposes some challeges to be discussed throughout this paper to their aerial usage.

A. Related Work

A significant contribution to this topic has been produced by the authors of [3] which have published a series of studies about air-to-ground (ATG) propagation channels based on measurements collected by large airbone UAVs.

Fig. A.1: Cumulus One. UAV used for measurements

The measurements were performed in C-Band (5060 MHz) and L-Band (968 MHz), being both the bands pointed out by ITU (International Telecommunications Union) as main candidates for dedicated C2 links. In [3] the measurements are performed for over-the-water flights and the results show that due to the smooth water surface, the model that best fits the measuremens are the curved earth 2-Ray model (CE2R). The “lobbing" effect caused by the second ray is more apparent for distances above 10km, and is more prominent on L-Band data. Measurements performed in a hilly suburban environment shown the presence of additional multipath components, deviating from the simple 2-Ray model. Linear fits using freespace pathloss model (FSPL) on log scale show standard deviations between 3.2 and 3.6 dB in L-Band, which is a good fit when compared to the range of 6-10 dB often observed on terrestrial cellular pathloss measurements [4]

In [5], measurements in mountainous environments are fit using a log-distance model with pathloss coefficients between 1.6 and 1.8, slightly less than the FSPL value, which the authors attribute to some waveguiding observed on the valley region. Near-urban environment is investigated in [6] and the pathloss shows a pattern approximated by FSPL for the measured distances.

B. Paper Contributions and Organization

All the measurements cited in subsection A. were taken on C-band and L-band empty bands, using a large UAV flying in heights around 500m-2km. This paper presents results collected in an operating LTE network at 800 MHz flying at current authorized heights for commercial UAVs (20-100m). It also presents assessmnet on the interference reported by the measurement device, regarding the cellular multicell environment. The final part of the paper is dedicated to a more detailed discussion about the challenges in obtaining a generic pathloss model, especially for interfering cells.

The paper is organized as follows: section II describe the measurements setup, while the results are discussed in section III. Then, a more detailed investigation in the height dependent factors that impact the propagation models for UAV-specific scenarios is presented in section IV. At last, future work planning and conclusions are presented, respectively, in sections V and VI.

II Measurements Setup

On July 2016, measurements took place at a small airport in the vicinity of Odense, Denmark. The airport is mostly served by infrequent chartered flights which enabled the authorization for UAV flying activities.

For this study, a winged UAV (Cumulus One) was used to perform the flights (see Fig. A.1). The cellular network data was collected by a regular cellular telephone (Samsung Galaxy S5), with the firmware adapted to allow the reading and reporting of radio measurements using Qualipoc software[1]. The cell phone was placed inside the UAV cavity, as depicted in Fig. A.1. Henceforth in this paper, this mounting will be referred as UAV-UE. It is worth to note that, as the UE was in the inner part of the UAV-UE mounting, the sensitivity of the measurements was reduced due to the attenuation of the UAV frame. Pre-flight measurements were conducted to quantify this effect, and they indicated penetration losses around 10 dB.

The cellular phone was programmed to measure a 20 MHz LTE carrier, with center frequency around 810 MHz, and the phone's serving cell was locked to be the same during all flights (see Fig. A.2). The selected cell is configured with 2-degrees electrical downtilt and is located at 22m height above the terrain. On average, at every 1s, the software recorded radio reports for the serving cell, including measurements like RSRP (reference symbol received power) and RSRQ (reference symbol received quality) [7].

The UE also reported some radio measurements for the neighbor cells. The number of neighbors and which neighbors are reported could not be defined in advance, as only cells discovered on each sampling interval were reported. For one cell to be detected, the UE must be capable of successfully separate its broadcast channel from the noise and interference power radiated by other adjacent cells. The power sensitivity for cell detection depends on the interference power at UE side: the heavier the interference, the higher the received power needs to be.

Once a cell is detected, the neighbor radio measurements are tagged with the physical layer cell identification (PCI) [8], which allows the mapping between them and their correspondent cells in operator's network. In LTE, there are 504 unique PCIs instances that can be attributed to the cells. Repetitions are managed by network planning to avoid neighbor cells to have the same PCI.

In the analysis presented in this paper, a circunference of 20km of radius around the landing zone was used as the search space for operator's cells. Reports collected by the UE were paired to cells in this region based on PCI numbers. The search area is limited to avoid ambiguity in cell mapping. Outliers samples whose PCI could not mapped within this area were discarded.

Antennas tilt and models were supplied by the network operator. Antennas radiation patterns and gains used in calculation were the same as provided by manufacturers datasheet. All transmitters have been assumed to have same wideband output power (49 dBm). Terrain altitude information

[1]More information about the Qualipoc software in https://www.rohdeschwarz.com/us/brochure-datasheet/qualipoc_android/

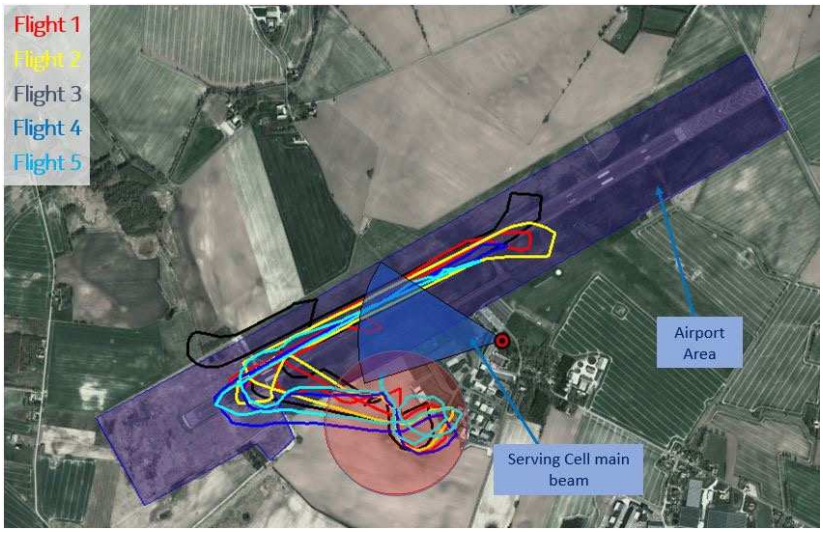

Fig. A.2: Flight zone demarcation.

was used to refine the calculation between base stations and the UAV-UE. The pathloss measurement was obtained from the difference between the transmitted power per received symbol (after applying antenna gains) and the RSRP. In order to mitigate the fast fading components in the measurements the collected samples were averaged by obtaining the local mean of samples in windows of length equal to 40λ [9], where λ represents the radio wavelength.

Due to UAVs legislation in Denmark, flights were limited to visual line-of-sight range and at a max of 100m height. Therefore, all 5 flight routes performed were within such bounds, as depicted in Fig. A.2. One of the goals of these measurements is to identify the effect of different heights on radio performance for the UAV-UE. Regarding this matter, in each measurement flight the controllers aimed at keeping the UAV-UE height as constant as possible. The flights heights, measured from ground level, followed an ascendant order with steps of 20m, i.e., the flight 1 was performed at 20m height, flight 2 was at 40m, and so on, up to flight 5, performed at 100m. To make the measurements comparable for these different heights the selected routes were similar for all 5 trials. The red circle on Fig. A.2 represent the area used as taking off and landing zone for the UAV, therefore UAV heights are not stable within this zone. The data collected in this area was not considered in the analysis.

III UAV-UE Measurements

A. Path Loss Modeling

Pathloss modeling was obtained by calculating the parameters α and β that best fit the measurements according to the log distance model widely used in previous literature [10]:

$$PL(d) = \beta + \alpha 10log_{10}(d) + X_0 \quad [dB] \tag{A.1}$$

where α accounts for the propagation coefficient (or pathloss exponent), β is a constant representing the close-in pathloss at a reference distance of 1m. X_0 is modelled as a random variable with Gaussian distribution, and zero mean and standard deviation σ, and represents the shadowing variation. In eq. A.1, PL, β and X_0 are described in dB and d is in meters.

For the sake of example, the results for the flight performed at 20m height are shown in Fig. A.3. The slope of the best fit line corresponds to α of 1.8, which is close to the exponent observed in freespace pathloss (FSPL), where $\alpha = 2$. The standard deviation of X_0 for this linear fit shows $\sigma = 5.4dB$. It is also possible to see in this figure, that due to the limitation on flight ranges for this campaign, there is a gap in the measurements for the range 1-4km, due to the absence of neighboring cells in this region that could be reported by the UE. Further tests are required to collect measurements that can fill this gap.

Even though the path loss exponent is below 2.0, there is an offset of approximately 20 dB between the collected samples and the reported measurements. This effect is probably related to an underestimation of the losses on the UAV fuselage. The pre-flight test was performed with the UAV-UE grounded, receiving the radio signal from its top part, while during the flights the arrival of the radio signals happened from the bottom or lateral parts of the UAV, which were reinforced to protect the phone inside the frame.

A summary with the results for all flight heights can be found in Table A.1. In all five flights the pathloss exponents are varying between 1.62 and 1.90, which are in line with the results presented for flight 1 and with values reported in [6]. and [11]. Although those values are below freespace propagation loss, it is important to remind that, by the own nature of the measurements, they are slightly biased downwards. It happens because the measurements are capped by the sensitivity threshold discussed in section II. This effect is also reinforced by penetration losses caused by UAV airframe, which causes an additional number of samples to be undetected, especially for the sites located further away from the flight region.

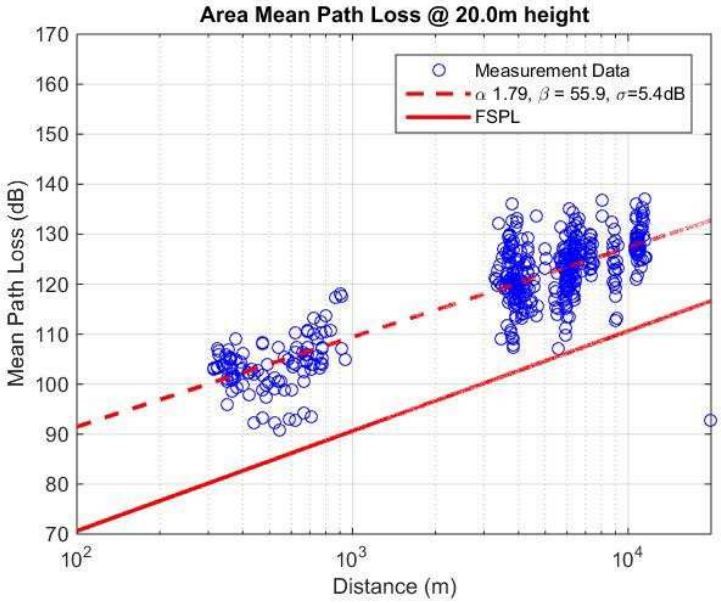

Fig. A.3: Path Loss Measurements with UAV-UE

Table A.1: Log-distance fit

UAV-UE Height	α	σ [dB]	β [dB]	$\overline{SINR}$ [dB]	Median RSRP [dBm]
20 m	1.79	5.4	55.9	17.3	-85.2
40 m	1.69	4.9	57.6	11.9	-86.5
60 m	1.74	5.4	54.8	9.0	-87.3
80 m	1.62	5.8	59.7	6.2	-89.6
100 m	1.90	5.2	48.8	5.8	-87.9

B. UE DL SINR vs UAV Height

Onwards in this paper, the expression SINR (signal-to-noise plus interference-ratio) will be used to refer to downlink (DL) SINR. The values of the median SINR and RSRP collected in each flight are also shown in Table A.1. In this table, it is possible to see that as the UAV goes up, the value of the median SINR for the serving cell, $\overline{SINR}$, decreases. The SINR degraded 11.5 dB when UAV-UE moved up from 20m to 100m. It is expected some variation on the received signal power for the different heights, first because of changes in the elevation angle between base station and UAV-UE, and second because increments in the 3D distances caused by increasing the distance in the height

dimension. However, no significant differences were identified in the median RSRP received from the serving cell, as reported in Table A.1. Therefore it is possible to infer there are stronger levels of interference for higher UAV-UE flights.

Another point worth to mention in Table A.1 is that the steepest degradation on SINR was recorded in height elevation from 20m to 40m. From flight 1 to flight 2, degradation recorded was 5.4dB, and then 2.9, 2.8 and 0.4 dB in subsequent ones. It indicates that the interference increase is more prominent for lower heights, while it is subjected to smaller variation due to height gains at higher levels.

IV SINR Degradation Causes

There are different factors that can cause the SINR degradation observed in previous section, and more measurements are needed in order to clarify how each of those factors impact final results, as related in section V. In this section, the main possible causes for this effect are presented in more details.

A. Expanded Horizon due to Earth curvature

Earth curvature imposes a limit on horizon range, which is the maximum straight path distance that do not intersect the planet's surface. Objects located beyond this range are not reachable in a straight path and are considered out of reach for optical communications.

For radio waves, the visual horizon may be expanded due to atmospheric effects. The dielectric constant of air varies with weather conditions and with height above ground. The height related variations cause eletromagnetic waves to bend as they were propagating in curved paths, keeping them closer to earth than they would be if travelling in a straight trajectory [4]. Approximating the Earth by a sphere of radius R, the radio horizon, D_{max}, between an UAV-UE and a base station with respective heights equal to $h_{ue} \ll R$, and $h_{bs} \ll R$, is by:

$$D_{max} \approx \sqrt{2kRh_{ue}} + \sqrt{2kRh_{bs}} \tag{A.2}$$

where k stands for the increase in radio range caused by atmospheric effects. Using the average value of $k = 4/3$ as suggested by ITU [12] for "standard" atmosphere conditions and assuming $R = 6370$ km, it is possible to simplify eq. A.2 to:

$$D_{max} \approx 4.12 \left(\sqrt{h_{ue}} + \sqrt{h_{bs}} \right) \tag{A.3}$$

where D_{max} is represented in kilometers and h_{ue} and h_{bs} are in meters. So, assuming constant base station altitudes in the network, the range of distances where it can still interfere with UAV-UE received signals depends on the device altitude. As a consequence, the UAV at higher altitudes has an expanded radio horizon, which can add several different sources of interference. Under such assumptions and considering ground-reference at sea level, with $h_{bs} = 25m$, the radio horizon for UAV-UE for the flights heights of section II can be roughly approximated by the values presented in Table A.2. It is possible to see that the radio horizon of the signal expands from 39km at 20m to 62km at 100m, increasing the "reachable" area in 2300 km^2, potentially adding hundreds of new sources of interference. At some point, however, it is expected that the increases in interference power asymptotically approaches to zero, with the altitude as radio horizon becomes very large enough that pathloss atennuation makes the new interference sources negligible.

Table A.2: Theoretical Radio Horizon

$UAV - UEHeight(m)$	20	40	60	80	100
Radio Horizon (km)	39.0	46.6	52.5	57.5	61.8

B. LOS probability

Figure A.4 shows how UAV height can impact the LOS clearing between network transmitters and the UAV-UE. In this figure, it is possible to see the altitude profile of the surface between a transmitter (Cell A), located close to the test area, and the UAV-UE. The surface profile includes buildings, trees and vegetations over terrain variation. The cell shown in this example corresponds to a sector where transmitter antenna is located at a height of 50 meters above ground level (19 meters of altitude). The UAV was placed in two different heights above ground - which is 16 meters of altitude at the landing zone - 20m and 40m. There is an obstruction to the line of sight between the network transmitter and the UAV at 20m height, probably caused by a building, which will cause attenuation to the transmitted signal. Once UAV moves up to 40 meters above ground in the same spot, there is no longer a LOS obstruction. Although this Cell's PCI was not identified by the UE in any measurements, the clearing of LOS would cause more interference power to be received by the UE.

In our measurement region, in South Denmark, the terrain is quasi-flat with no significant concentration of tall buildings in nearby cities. As so, the first meters above the ground correspond to the most significant gain in the LOS probability. The level of the first flight (20 m) probably see a very high gain compared to ground level, and future works must be done to test this hypothesis. Comparing the flight of the five trials described in section II, it

is expected that the clearing of obstructions is more relevant factor between the first two (20m and 40m), which are the trials that presented the largest degradation in SINR according to the Table A.1. Above 40m, major part of cells in the neighboring region tend to be in LOS, and gains in line of sight probability with height become smaller

Freespace propagation for most neighbor sites within radio horizon ranges is an unrealistic assumption for most current cellular network deployments. For example, considering a pedestrian user, such as $h_{ue} = 1.5$, freespace assumption would correspond to paths remaining unobstructed for more than 20 km. But, in real urban and suburban scenarios, horizon are limited by buildings, vegetation, terrain elevations and other obstacles which make ranges usually fall to some hundreds meters.

Consequently, the interference component of SINR is usually dominated by a group of few neighbor cells, as the signal radiated by the others become severely attenuation before reaching the UE. For a flying UAV-UE, however, the presence of blocking surfaces become less likely, as it tends to be isolated from obstacles and other scattering surfaces. So, as the UAV-UE gains altitude, it is more likely it obtains clearing in LOS with several base stations, and some of those whose effect could be neglected for a pedestrian user, can become a source of significant interference power.

Consider $P[LOS|d, h_{ue}]$ to be the LOS probability between an UAV-UE, flying at a height h_{ue}, and a base station separated by a distance d. The value of $P[LOS|d, h_{ue}]$ is hard to estimate and depends significantly on scenario characteristics. In a mountainous area, such as rural Norway, it may require a higher h_{ue} to obtain clearing with neighbor base stations. For a dense urban area, e.g. Manhattan, the presence of tall buildings may limit gains $P[LOS|d, h_{ue}]$, for values of h_{ue} lower than dozens of meters, but it will go close to 1 after UAV-UE clears the tallest rooftops in the area.

C. Fresnel Zones Obstructions

In some cases, the existence of LOS between two devices is not sufficient to assure free space-like propagation. If the path travelled by the radio signal is partly obstructed, i.e. obstacles block the radio waves in the first Fresnel zone between transmitter and receiver, additional losses will incur. These diffraction losses can add as much as 6 dB on top of the free space loss. As a rule of thumb, obstructions $> 40\%$ of the first Fresnel zone can cause significant excess in pathloss when compared to freespace propagation [4].

The first Fresnel zone defines the region around the LOS path where the excess path length is between 0 and $\lambda/2$, where λ represents radio wavelength. The zone is defined by an ellipsoid around the signal main path, whose radius r_1, is given by:

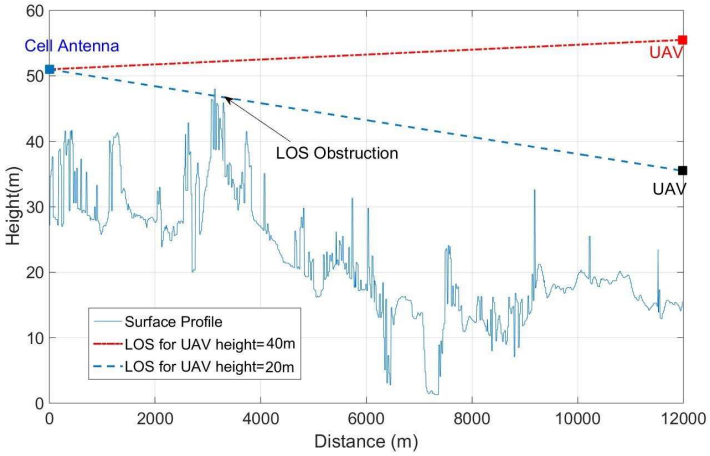

Fig. A.4: LOS and surface profile interaction for Cell A

$$r_1(d_0) = \sqrt{\frac{\lambda d_0 (D - d_0)}{D}}, \tag{A.4}$$

where D is the total distance between transmitter and receiver and d_0 is an intermediate distance, such as $d_0 \leq D$. The more obstructed is the Fresnel zone - in other words, the closer is the reflecting surface from the LOS path - the higher is the signal attenuation due to diffraction losses.

In Fig. A.5, it is possible to see how elevations in UAV heights may clear the first Fresnel zone. The first Fresnel zone is plotted for the link between the UAV-UE in two different heights and one of the neighbor cells in the test area (Cell 2). For UAV height equal to 20m, there is a clear obstruction (probably caused by a building) for $d_0 = 4.5km$ that block a significant part of the Fresnel one(50%), which can potentially cause severe diffraction losses. Moreover, there is another important obstruction for d_0 between 8 and 10 km, caused by the radio signal intersecting with the Earth's surface. Once UAV moves up to 40 meters of height, the first obstruction blocks a smaller fraction of the Fresnel zone and the second obstruction caused by Earth's surface is not observed. The latter is specially important, because buildings landscape can vary significantly between two different points in the flight route, but variations on the surface of the Earth tend to be much smaller in this region.

V Future Work

Airbore UAVs have degrees of freedom in the 3 dimensions, which introduce new variables to radio propagation modelling. Most common models used

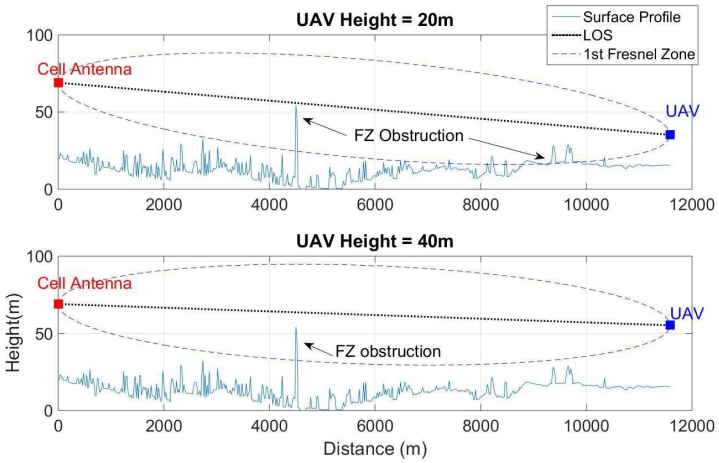

Fig. A.5: Fresnel zone plots for Cell 2

for cellular networks are usually adapted to pedestrian, vehicular and in-building users, and will probably not produce realistic results when used for UAVs case.

A lot of uncertainties need to be unveiled in order to obtain a better model for UAVs flying at a given altitude, as evidenced by section IV. At first, it is necessary to quantify what are the most important factors to be considered in different scenarios and for different UAV heights. Then, it is important to obtain parameters that can be used to better describe the 3D propagation environment for UAVs. After analytical models are refined for UAVs case, network simulations can be performed enabling a more detailed study of network performance for such atypical users.

Under this scope, new tests are being envisioned for the near future. The new set of tests should be conducted over larger sampling distances (multiple flights), and in a different area. It is also being discussed the possibility of flying with a portable radio scanner, although it requires more planning due to the high payload that limit the options of drones to be used. If possible, the scanner would allow the lock of measurements in many different PCIs, which would produce more precise results in what concerns the potential causes for height related SINR degradation explored in this paper. Another possibility that could be explored in the future is the use of air gliders for measurements, what could expand the possibilities for the test setups.

VI Conclusion

The set of cellular network measurements collected by the UAV-UE showed a pathloss slope that approximates freespace propagation for all five different heights measured. The measurement field was an open area with no obstructions between UAV and Base Station to cause significant signal attenuation, also no significant effect related to reflected paths were captured for the distances tested.

In all trials, measured values for pathloss slope are similar, with small variations caused by dynamic range limitation of measurement UE. However, it was observed a rembarkable SINR degradation between the lowest and highest flight levels. This result indicates the interference power increases with UAV-UE height. However, all neighbor cell measurements collected by UAV-UE show no power increase that could be accountable for the interference power increase.

Afterwards, a discussion on the challenges of obtaining a reliable path loss model for UAVs was presented, based on field measurements. Most part of uncertainties on pathloss modelling parameters for UAVs are height-related caused by changes on propagation environment. As it is pointed out, expanded radio horizon at higher altitudes, LOS likelihood and clearing of the first Fresnel zone are important radio factors that could observe significant variations within an area as a consequence of changes in UAV altitude. Future work is needed to quantify these effects in order to obtain a more realistic modelling for the propagation environment for UAVs.

Acknowledgment

The authors would like to thank UAS Danmark for the UAV used and for all support given during the measurements.

References

[1] EUROCONTROL, "Roadmap for the integration of civil Remotely-Piloted Aircraft Systems into the European Aviation System," 2013.

[2] FAA, "Integration of civil unmanned aircraft systems (uas) in the national airspace system (nas) roadmap," Tech. Rep., 2013.

[3] D. Matolak and R. Sun, "Air-ground channel characterization for unmanned aircraft systems - part i: Methods, measurements, and models for over-water settings," *IEEE Transactions on Vehicular Technology*, vol. PP, no. 99, pp. 1–1, 2016.

[4] J. Parsons, *The Mobile Radio Propagation Channel*. Wiley, 2000.

[5] R. Sun and D. W. Matolak, "Air-ground channel characterization for unmanned aircraft systems: The mountainous environment," in *2015 IEEE/AIAA 34th Digital Avionics Systems Conference (DASC)*, Sept 2015, pp. 5C2–1–5C2–9.

[6] D. W. Matolak and R. Sun, "Air-ground channel characterization for unmanned aircraft systems: The near-urban environment," in *Military Communications Conference, MILCOM 2015 - 2015 IEEE*, Oct 2015, pp. 1656–1660.

[7] " Evolved Universal Terrestrial Radio Access (E-UTRA); Physical Layer Measurements," 3GPP, Tech. Rep. TS 36.214 V8.7.0, September 2009.

[8] " Evolved Universal Terrestrial Radio Access (E-UTRA); Physical channels and modulation," 3GPP, Tech. Rep. TS 36.211 V8.9.0, December 2009.

[9] W. C. Y. Lee, "Estimate of local average power of a mobile radio signal," *IEEE Transactions on Vehicular Technology*, vol. 34, no. 1, pp. 22–27, Feb 1985.

[10] T. Rappaport, *Wireless Communications: Principles and Practice*, ser. Prentice Hall communications engineering and emerging technologies series. Prentice Hall PTR, 2002.

[11] D. W. Matolak and R. Sun, "Air-ground channel characterization for unmanned aircraft systems - part iii: The suburban and near-urban environments," *IEEE Transactions on Vehicular Technology*, vol. PP, no. 99, pp. 1–1, 2017.

[12] ITU-R, "Definitions of terms relating to propagation in non-ionized media," International Telecommunication Union, Recommendation P.310-9, Aug 1994.

Paper B

Radio Channel Modeling for UAV Communication Over Cellular Networks

Rafhael Amorim, Huan Nguyen, Preben Mogensen, István Z. Kovács, Jeroen Wigard and Troels B. Sørensen

The paper has been published in the
IEEE Wireless Communications Letters Vol. 6, Issue 4, pp.514-517, 2017.

© 2017 IEEE
The layout has been revised and reprinted with permission.

Abstract

The main goal of this paper is to obtain models for path loss exponents and shadowing for the radio channel between airborne Unmanned Aerial Vehicles (UAVs) and cellular networks. In this pursuit, field measurements were conducted in live LTE networks at the 800 MHz frequency band, using a commercial UAV. Our results show that path loss exponent decreases as the UAV moves up, approximating freespace propagation for horizontal ranges up to tens of kilometers at UAV heights around 100m. Our findings support the need of height-dependent parameters for describing the propagation channel for UAVs at different heights.

I Introduction

Unmanned aerial vehicles (UAVs), also known as drones, have been used for military applications for more than 20 years. More recently, technological developments regarding batteries, electronics and lightweight materials have made UAVs more accessible to the public, creating a boom in the market of small and medium scale UAVs. However, due to concerns with public safety most of their applications are still limited by countries regulations to visual-line-of-sight (VLOS) ranges and maximum heights between 100 and 150 m [1].

Emerging UAV applications present potential to reduce risk and cost for many commercial activities [2], but they would require larger operational ranges. The research community is putting efforts into creating solutions for a safe integration of drones in the airspace for beyond-VLOS flight ranges. An essential element in this is the development of a reliable communication link between the pilot/controller and the UAV.

The cellular networks are natural candidates to provide not only this link, known as CNPC (control and non-payload communication) [1,3,4] or C2 (communication and control link) [5], but also to serve data traffic for applications such as live streaming or sensor readings. Mobile operators already have ground infrastructures implemented and a ubiquitous coverage that can be adapted to serve such air-to-infrastructure links [6]. To study the feasibility of cellular-based communication for drones, a good understanding of the propagation channel between UAVs and ground stations is required. It is reasonable to assume the channel will present different behaviors for an aerial user when compared to a regular ground user. UAVs flying above rooftops, vegetation and terrain elevations, are more likely to observe radio path clearance to the base stations in the surrounding areas and therefore more likely to experience line-of-sight (LOS) propagations [6] for larger distances resulting in higher level of interference from a larger number of surrounding BSs [7].

Some efforts to characterize the aerial channel were presented by the authors of [8,9], where measurements were performed using single dedicated links at 900 MHz and 5 GHz bands, with large drones flying at heights between 500 m and 2 km, but the effect of height dependency is not directly assessed, neither heights below 150m, which are expected to be heavily used by commercial drones in the near future.

Some previous studies have suggested it is important to obtain a model that accounts for the dependency observed in the propagation channel to UE heights [3] [4]. In [10] the authors present a modification to the two-ray model which introduces variation in the path loss exponent according to the UE height, based on GSM and UMTS measurements collected by a stationary balloon located at 1900 m of the serving base station. Measurements in LTE using a flying UAV were reported in [7] and results suggest there is a clearance of the radio path, obtained with higher UE heights, reduces the shadowing variation while it increases the received signal power from the interfering cells and the number of visible neighboring cells, but no propagation model is presented.

The present work differs from the previous studies, as it directly assesses the effects of the LTE UAV-UE heights in the path loss exponent and shadowing variation, and proposes a height dependent modeling for both. A wider range of distances and diverse surrounding base stations are assessed using a flying LTE UAV-UE, connected to two real LTE networks at 800 MHz in Denmark.

This paper is organized as follows. The setup used in the trials and the data processing methodology are introduced in Section II. Section III present the measurements results, while the modeling of the height-dependent radio propagation channel is presented in Section IV. The paper follows with the conclusion in Section V.

II Measurement Setup and Data Processing

A measurement campaign was performed in October 2016, using the setup reported in Table B.1. The scanner was mounted underneath a commercial UAV connected to a dipole antenna, whose gain is small and assumed negligible for the purpose of this analysis, vertically placed as depicted in Fig.B.1. The scanner is capable of reporting radio measurements from up to 32 cells per recorded sample. The reports include the UAV GPS locations and reference signal received power (RSRP) and physical cell ID (PCI) from each detected cell. The measurements were repeated for two different Danish operators with independent networks and their results were combined to produce the outcome presented in Section III. The terrain profile and the location of sites in a radius of 35 km around the flight zone are showed in Fig.

Table B.1: Measurements Seutp Information

Setup Information	Value
Location	Fyn, Southern Denmark
Meas. Device	R&S® TSMA[1]
Technology	LTE
Band (MHz)	800
UAV Flight Speed	15 km/h
Avg. Sampling Rate	4 - 9 Hz
UAV-UE Antenna	Dipole
UAV Heights (m)	15, 30, 60, 120
Drive Test Height (m)	1.5

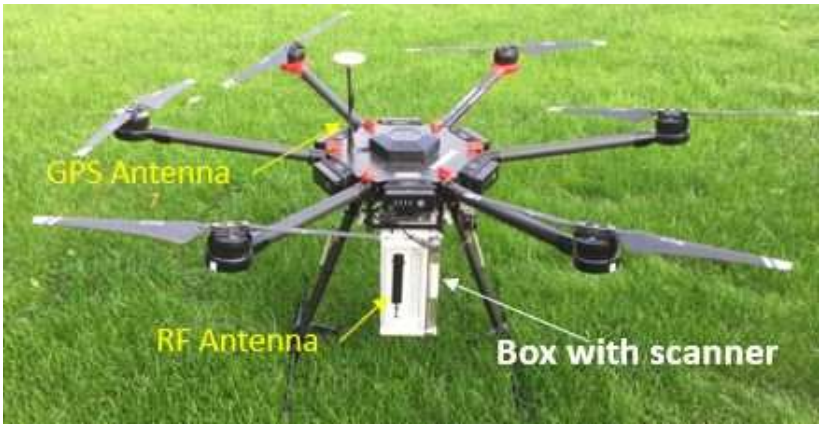

Fig. B.1: UAV-Scanner Mounting used for the measurements

B.2. The UAV was set to fly over two circular paths of 500m diameter, set 7 km apart from each other (see Fig. B.2). The UAV heights, measured from the take-off spot, according to the maximum limits allowed by local regulations. On ground, a reference drive-test (DT) was also performed on the nearby roads around the flying paths. During the drive test, the antenna is mounted on top of a car at 1.5 m height. With distances around 2 km from the closest BS, the propagation path is most of the time blocked by surrounding trees, buildings and hills, and therefore non line-of-sight is dominant condition in the drive test.

Each RSRP sample recorded by the scanner, R_i, recorded from a site at a distance d_i in meters, was translated into a path loss sample PL_i, according to the following equation

$$PL_i = P_{T_x} + G_a(\theta, \phi) - R_i \quad [dB], \tag{B.1}$$

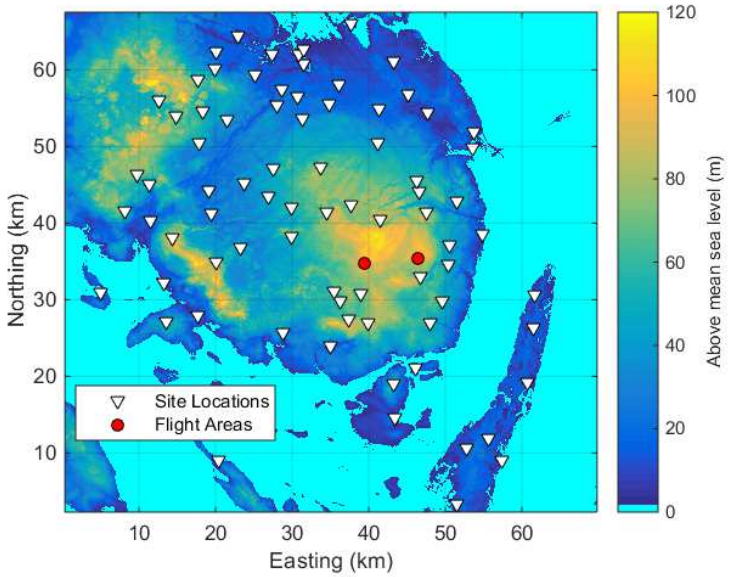

Fig. B.2: Site Locations and Terrain Profile for the measurement campaign in Fyn, Denmark

where P_{T_x} represents the average transmitted power per reference symbol in the network, and G_a is the antenna gain for the azimuthal θ and elevation ϕ angles measured between the base station and the UAV. The antenna gain is calculated through the horizontal interpolation algorithm (HPI) applied over the horizontal and vertical antenna diagrams, obtained from manufacturers. Example of antennas used in the networks include: Kathrein 80010699, Kathrein 80010647V01, among others. The calculation of elevation considers BS's and UAV's heights altogether with terrain topography. At the highest flight level, 120m, the UAV is flying above cellular base stations, which are usually downtilted for optimized ground coverage. However, distances ranges in this paper are limited to 1-22km and elevation angles were in the range of 0.25 to 2.9 degrees. When the geometrical elevation angle is added to antennas tilt, the maximum angle to the main beam of base station antennas is around 10 degrees, with more than 95% of samples below 7.5 degrees. In order to avoid the roll off region of the antenna patterns and miscompensation of the antenna gains in Eq. B.1, samples lying outside the -6dB vertical and horizontal lobes of the BS antenna pattern were filtered out from the analysis.

The effect of fast fading components in the measurements are mitigated by obtaining the local mean of samples for PL_i using windows of length equal to 40λ [11], where λ represents the radio wavelength at 800 MHz. The

pair of averaged path loss samples and distances, (PL'_j, d'_j) were then used to obtain a regression, in the least square sense, to fit a log-distance alpha-beta (AB) model, widely used in the literature [12]:

$$PL_{est}(d) = \alpha 10 \log_{10}(d) + \beta + X_\sigma \quad \text{[dB]}. \tag{B.2}$$

In Eq. B.2, PL_{est} represents the estimated path loss for a receiver located at a 3-D distance d (in meters) from the transmitter; α represents the path loss exponent and β is the intercept point with the line $d = 1$ m. Finally, X_σ is a random variable that accounts for shadowing variation modeled with normal distribution and standard deviation σ, assumed equal to the standard deviation of the regression residuals [12].

At very large distance, some path loss samples might be cropped, as the received power is not high enough to overcome the noise plus interference level so that the broadcast channel can be successfully decoded. The sensitivity level (PL_{sens}), i.e., path loss value when cropping occurs, is height-dependent as the interference increases with the flight height (it will become more evident in Section III). This cropping negatively affects the path loss analysis: it causes the path loss slope to be skewed downward, thus underestimating path loss exponent. Therefore, a threshold distance ($d_{max}(hu)$) is applied, where we removed samples greater than this distance to avoid the bias due to saturated samples. The choice of the threshold distance is important, as if it is set too high, the slope will experience the effect of cropping; if too low, a significant number of points will be removed from the analysis, and this might compromise the statistical significance of the regression values.

In our paper the threshold distance is selected as follows: First P_{sens} was defined as 99%-percentile of all measured PL'_j for a given height. The 99%-ile was chosen in order not to make the assumed sensitivity value too low due to outliers. Then, $d_{max}(h_u)$ was iteratively increased until the following stopping criteria is reached:

$$PL_{est}(d_{max}) \leq PL_{sens} - \sigma, \tag{B.3}$$

where $PL_{est}(d_{max})$ represents the estimated value for the path loss at d_{max}, using the regression presented in eq B.2, using all points that satisfy $d'_j \leq d_{max}(h_u)$.. Assuming a Gaussian shadowing distribution, $\approx 15\%$ of the samples at $d_{max}(h_u)$ are expected to be above $PL_{est}(d_{max}(h_u)) + \sigma$ (in the cropping region). The expected down-bias in the path loss slope using this criteria is within 0.1, and therefore, negligible for the later remarks presented in this paper.

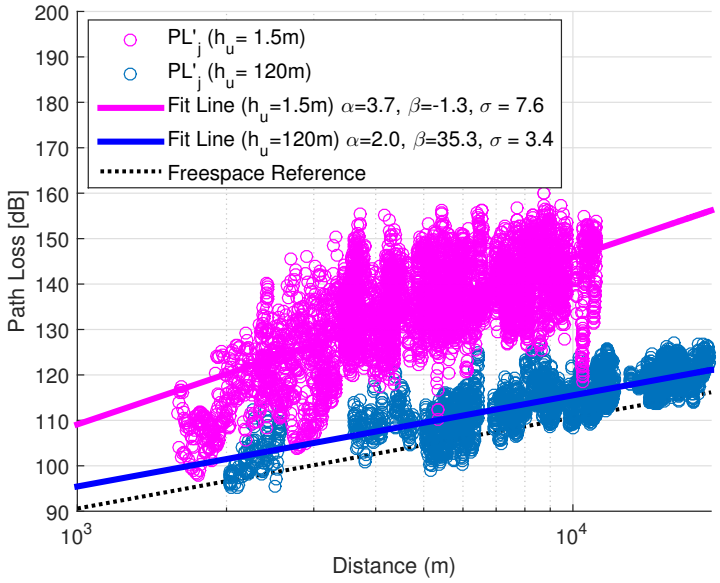

Fig. B.3: Path loss vs Distance - Measurement Results and regression model for UAV heights h_u = 1.5 and 120 m

Table B.2: Measurements Summary

h_u	Reg. Model Parameters			Avg. # Cells	PL_{sens} (dB)	d_{max} (km)
	α	β (dB)	$\sigma(dB)$			
1.5	3.7	-1.3	7.7	5.1	155.4	11.1
15	2.9	7.4	6.2	6.1	135.6	13.6
30	2.5	20.4	5.2	7.6	130.7	16.5
60	2.1	32.8	4.4	11.6	126.2	17.4
120	2.0	35.3	3.4	16.9	125.9	22.2

III Measurement Results

The results obtained through the methodology described in Section IV are presented in Fig. B.3, where it is possible to see that there is a clear reduction in path loss exponents as h_u increases, from 3.7 at ground level to 2.0 at 120 m. It results in significant differences in the path loss attenuation, specially for larger distances: for 3D distances close to 10 km the signal attenuation is 20 dB higher on ground level compared to the measurements at 120m.

The summary of the results for the other flight tests can be appreciated in Table B.2 that supports the expectations of better radio clearance at hig-

her heights, with the path loss exponent approaching free space propagation at higher flight levels [7]. In practical terms, such observation implies an expected increase in the interference level observed by UAVs, as well as a higher number of neighbor base stations being affected by UAV's transmissions. This claim is also supported by the average number of detected cells per sample that increased from 5.1 (DT) to 16.9 (120m). This height dependent behavior in the distance range and number of significant interference sources complies with previous results reported in [7]. It is also worth mentioning that the measurements suggest the signal power threshold increased at higher heights in all measured routes. This is exemplified by the value of PL_{sens} in Table B.2. This behavior might be attributed to the higher interference levels, and it indicates the number of significant interfering sites could be even higher, as some might not be identified due to falling short of the required signal-to-interference plus noise ratio (SINR) level.

Another finding that goes in line with the radio path clearance with height regards the observed values for the shadowing variation. For DT measurements it is approximately 7.6, which is aligned with reference values in the literature [13] for ground level measurements. As the UAV moves up this value decreases up to 3.4 dB, indicating a significant reduction in the shadowing variation. Part of the remaining variation might be attributed to the non-omni directional pattern of the receiver antenna and self-shadowing components.

IV Path loss Modelling and Discussion

The results in Sec. III made clear the propagation environment is significantly different for airborne UAVs and ground level users. Based on such observations, and in the work in [3], [4], [10] and [7], it is proposed here an extension of the model in Eq. B.2 using height-dependent parameters. Path loss exponents should decay with increases in UAV heights. In this paper, a logarithmic regression was used to obtain a group of height-dependent parameters to be used in eq. B.2. The logarithmic function was chosen assuming height-related radio path clearance, i.e. the path loss exponents reduction, is more prominent to small increments in elevation at low heights, where there are more concentration of buildings, vegetations and other obstacles. The height-dependent models are found in equations B.4-B.6.

$$\alpha(h_u) = \max(p_{\alpha_1} + p_{\alpha_2} \log_{10}(h_u),\ 2), \tag{B.4}$$

$$\beta(h_u) = p_{\beta_1} + p_{\beta_2} \log_{10}(\min(h_u,\ h_{FSPL})) \quad [dB] \tag{B.5}$$

$$\sigma(h_u) = p_{\sigma_1} + p_{\sigma_2} \log_{10}(\min(h_u,\ h_{FSPL})) \quad [dB], \tag{B.6}$$

where h_{FSPL} is the height where free space propagation is assumed ($\alpha = 2.0$). The values of p_1 and p_2 obtained based on the reported measurements are

exposed in Table B.3. Such parameters modelling serves as a reference for rural scenarios, and are valid for ranges limited to $h_u \leq 120$ and distance ranges similar to those in Table B.2, in a lightly hilly rural environment, with base stations height between 20 and 50 meters.

Using the slope and intercept estimation given by the height dependent model, and applying it to all measurements collected, the average offset between the measured samples and the estimated ones is equal to -0.3 dB, and the standard deviation for all heights was kept under the same values presented in Table B.2. It means the proposed height-dependent model is capable of providing a good model for the measured data, at expense of just two optimization variables per parameter.

Table B.3: Height-Dependent Model Parameters

Parameter	p_1	p_2
α	3.9	-0.9
β	-8.5	20.5
σ	8.2	-2.1

A visual example of the height dependent model using the parameters in Table B.3, is shown in Fig. B.4. The 95% confidence interval for the value of α estimated on the measured data is also shown, assuming X_σ to be Gaussian distributed (in which case the estimate is Student t-distributed [14]). These values suggest the difference among the exponents at higher levels ($h_u = 60$ or 120 m) compared to those at lower levels ($h_u = 1.5$ or 15) is statistically significant.

V Conclusion

This paper analyzed a set of live network measurements conducted with a radio network LTE scanner attached to an airborne UAV. Flights were conducted at heights compliant with current regulations, up to 120m. The results for the path loss exponents and the shadowing standard deviations imply better radio clearance as the UAV moves up. This finding is corroborated by the increase in the average number of detected cells at higher levels. A practical consequence of these observations is an expected SINR degradation at higher elevations, to be evaluated in future works.

In order to investigate the interference problem and evaluate mechanisms to deal with it, system level simulations are required. The main contribution of this paper is presented in Section IV. It proposes that path loss and shadowing parameters for airbone UAVs connected to cellular networks must follow height-dependent models, as a more efficient way of performing spatial prediction, as the radio path becomes more unobstructed with increases

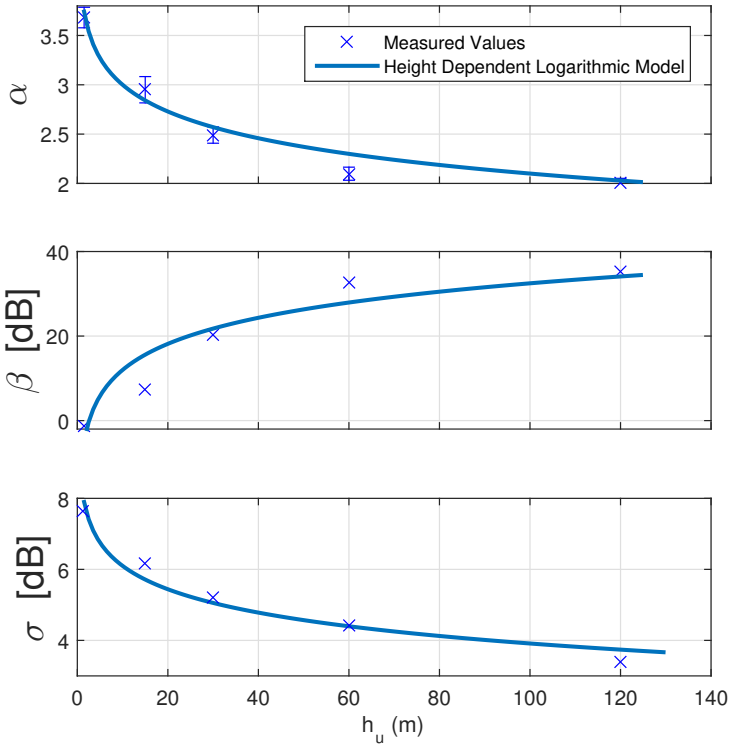

Fig. B.4: Height dependent models for the regression parameters of eq. B.2.

in height.

Acknowledgment

The authors would like to thank the team from DroneFyn Denmark which assisted in this research conducting the UAV Flights. And, also, we acknowledge the important contribution to the results by Rohde&Schwarz, which provided us the TSMA scanner used in the measurements.

References

[1] EUROCONTROL, "Roadmap for the integration of civil Remotely-Piloted Aircraft Systems into the European Aviation System," 2013.

[2] A. Foundry, Ericsson, and R. Space, "The Future of Drones According to the AT&T Foundry," AT&T Foundry and Rocket Space, Tech. Rep., October 2016.

[3] ZTE, ZTE Microelectronics and Tongji University, "Consideration on the channel model for LTE-based aerial vehicles," 3GPP TSG RAN WG1 Meeting, Tech. Rep. R1-1705163, April 2017.

[4] Nokia, Alcatel-Lucent Shanghai Bell Labs , "Evaluation Scenarios and Channel Models for Drones," 3GPP TSG RAN WG1 Meeting, Tech. Rep. R1-1704430, April 2017.

[5] FAA, "Integration of civil unmanned aircraft systems (uas) in the national airspace system (nas) roadmap," Tech. Rep., 2013.

[6] K. Welch, "Evolving cellular technologies for safer drone operation," Qualcomm 5G White Paper and Presentations, Tech. Rep., October 2016.

[7] B. V. D. Bergh, A. Chiumento, and S. Pollin, "Lte in the sky: trading off propagation benefits with interference costs for aerial nodes," *IEEE Communications Magazine*, vol. 54, no. 5, pp. 44–50, May 2016.

[8] D. W. Matolak and R. Sun, "Air-ground channel characterization for unmanned aircraft systems: The hilly suburban environment," pp. 1–5, Sept 2014.

[9] D. Matolak and R. Sun, "Air-ground channel characterization for unmanned aircraft systems: The near-urban environment," in *Military Communications Conference, MILCOM 2015 - 2015 IEEE*, Oct 2015, pp. 1656–1660.

[10] N. Goddemeier, K. Daniel, and C. Wietfeld, "Role-based connectivity management with realistic air-to-ground channels for cooperative uavs," *IEEE Journal on Selected Areas in Communications*, vol. 30, no. 5, pp. 951–963, June 2012.

[11] W. C. Y. Lee, "Estimate of local average power of a mobile radio signal," *IEEE Transactions on Vehicular Technology*, vol. 34, no. 1, pp. 22–27, Feb 1985.

[12] T. Rappaport, *Wireless Communications: Principles and Practice*, ser. Prentice Hall communications engineering and emerging technologies series. Prentice Hall PTR, 2002.

[13] V. Erceg, L. J. Greenstein, S. Y. Tjandra, S. R. Parkoff, A. Gupta, B. Kulic, A. A. Julius, and R. Bianchi, "An empirically based path loss model for wireless channels in suburban environments," *IEEE Journal on Selected Areas in Communications*, vol. 17, no. 7, pp. 1205–1211, Jul 1999.

[14] D. Altman, D. Machin, T. Bryant, and M. Gardner, *Statistics with Confidence: Confidence Intervals and Statistical Guidelines*. BMJ Books, February 2000.

Paper C

LTE Radio Measurements Above Urban Rooftops for Aerial Communications

Rafhael Amorim, Huan Nguyen, István Z. Kovács, Troels B. Sorensen and Preben Mogensen

The paper has been published in the
IEEE Wireless Communications and Networking Conference (WCNC), 2018

© 2018 IEEE
The layout has been revised and reprinted with permission.

Abstract

This paper focus on the investigation of aerial communications for drones connected to cellular networks in urban areas. Most of the previous measurement based channel models for urban environments do not extend to users located at heights above rooftops. On the other hand, UAVs are expected to fly at the very low level (VLL) airspace, in heights much lower than those covered by previous air-to-ground models. By means of field measurements, this paper presents height-dependent closed form expressions for the urban channel model (path loss slope and shadowing) extending to heights up to 40 m and compares the observed results with 3GPP reference models and previous studies. Measurements were conducted by a radio scanner attached to a construction-lift to measure the radio signal from three different live LTE networks (800, 1800, and 2600 MHz). Results suggest radio path clearance increases with height. As a consequence, it leads to an increase in number of cells in the detectable range and in the set of neighbors within 3 dB of the serving cell in the receiver, indicating neighbor cells are closer to each other in the power domain.

I Introduction

In recent years, an impressive growth on Unmanned Aerial Vehicles' (UAVs) market has been observed. This increase and the steady technological development of these devices are expected to enable a large number of new applications. It represents a market opportunity for cellular operators: UAVs will require data link connections, either for telemetry, command and control exchanges or potentially for real-time applications. In the first example, the data link must be highly-reliable due to safety concerns, in the latter it can demand high capacity, e.g. for real-time footage streaming.

Initial studies, such as [1], suggest UAVs are likely to create more severe interference conditions in the network, when compared to ground users, caused by a high-probability of radio line-of-sight (LOS) with several base stations. Cellular networks engineers have years of experience in planning and optimizing their infrastructure for ground coverage using prediction tools and simulators. While UAVs (also known as drones) are likely to fly above rooftops in urban areas, the legacy channel models used for this task do not extend for such heights. For instance, the reference ITU model for simulations consider user equipment (UE) heights up to 10 m [2] and 3GPP models extend to heights up to 22.5 m [3].

On the other hand, drones are expected to fly at the very low level airspace [4], with heights up to 300 m, much lower than those usually measured for modeling of air-to-ground path loss. Matolak and Sun have contributed with an extensive set of studies that evaluates measurements in different scenarios in [5] [6] [7] [8]. In these studies, measurements were performed for large

distances in dedicated links in C and L bands, and are focused on large UAV flying heights between 500 m and 2 km. In [7], the path loss slope observed in measurements collected on suburban/near urban scenarios is on the range of 1.5 to 2.0.

At the time of writing, the 3rd Generation Partnership Project (3GPP) holds a work item on enhanced support for aerial vehicles [9], which includes discussions on pathloss models and scenario definition to be used for simulation purposes. Current assumptions in [9] present a height dependent propagation model that extends the one previously presented in [3].

Other recent works, have addressed the clearance in the radio path with higher UE heights is observed in [10], where authors report reduced shadowing variation, increased intersite interference power and higher number of visible neighboring cells. In [11] a modified two-ray channel model was presented, introducing variation in path loss exponents according to the UE height, based on GSM and UMTS measurements collected by a stationary balloon. In a previous study, measurements were collected from two LTE operators at the 800 MHz band in a rural scenario with a scanner attached to a commercial UAV flying in heights up to 120 m [12]. The results showed radio path clearance as the UAV moves up: reduced shadowing variation, larger set of detected neighbor cells and path loss slope close to the theoretical free space path (FSPL) loss model. Analytical or theoretical models have also been previously proposed [13]. In [14], authors show the dependency of the losses with the elevation angle of the user by analyzing two opposed effects as the UAV moves up: the user moves outside the main beam of the antenna, but there is more clearance in the radio path.

This paper differs from the previous works by proposing a measurement-based propagation model for LTE users located above rooftops in urban scenarios that is independent of antenna patterns. Measurements are currently focused at low heights, where we assume some of future drones applications and services will be deployed, such as infrastructure maintenance, surveillance and last mile packet deliveries [15]. The measurements were performed in live LTE networks for 3 different frequencies (800, 1800 and 2600 MHz) on Northern Denmark. With the help of a construction lift it was possible to evaluate heights varying from ground level to up to 40 m. The learnings acquired with this setup will be used in the future in the designing of a setup for urban measurements with a real UAV. This work analyses the height dependency of the path loss slope for the model, and compare the observed values with those currently adopted by 3GPP RAN 1 work item.

This paper is organized as follows: Section II introduces the scenario, measurement setup and the data processing methodology used in this investigation. Results and conclusions are followed, respectively, in Sections III and IV.

II Measurement Setup and Data Processing

The measurement equipment used in the measurements is a R&S® TSMA[1] radio scanner. The device was set to scan three different frequencies from LTE live networks: 800, 1800 and 2600 MHz. Among the information saved on the measurement report are of particular interest for this paper: the device's GPS location and physical cell ID (PCI) and the average received power per LTE resource element (RE) [16] on the synchronization channel from serving and neighboring cells. The number of reported neighboring cells on each sample depends on the capability of the scanner of rightfully decode cell's synchronization channel. The signal-to-noise ratio (SINR) threshold values observed for this detection in the measurements is around -20 dB. The observed sampling rate in all trials was in the range of 3.4 and 7.5 Hz.

With the purpose of measuring the propagation channel at different heights, the scanner was mounted together with an omni-directional antenna on a 1.8m-height mast inside a construction lift's basket, and then, lifted from 5 to 40 m height, with incremental steps of 5 m. The basket was kept for 3 minutes on each of these levels, and lateral movements of 3-5 m were induced within this period, aiming at mitigate eventual bias caused by small scale fading. Due to limitations on the lift's mobility, this procedure was repeated on 10 different locations, to introduce sampling variability (see Fig.C.1). Additionally, reference measurements were collected on ground level, with the mounting carried by pedestrian users around each location.

The measurements took place in the city of Aalborg, in Northern Denmark. For reference of scenario's characterization, the urban population in the city is just above 110,000 people[2] with a populational density of ≈1000 inhabitants per km^2. More detailed information on the chosen locations is found on Table C.1, such as the average and 90%-ile of building heights in a 50 m radius around the measurement spot (showed in Fig. C.1). Table C.2 shows general information for the three networks, such as inter-site distance (ISD), mean transmitter heights and average downtilt in degrees, in the city center, within a radius of 4 km.

Table C.1: Locations Description

	Building Heights		
# of Locations	Avg. (m)	90%-ile (m)	Description
4	3.6 - 6.9	4.4 - 9.8	Low Residential Area
4	11.8 - 15.5	14.2 - 15.9	High Residential Area
2	4.4 - 5.1	5.8 - 7.1	Low Industrial Area

[1] https://www.rohde-schwarz.com/dk/brochure-datasheet/tsma/
[2] http://denmark.dk/en/quick-facts/facts

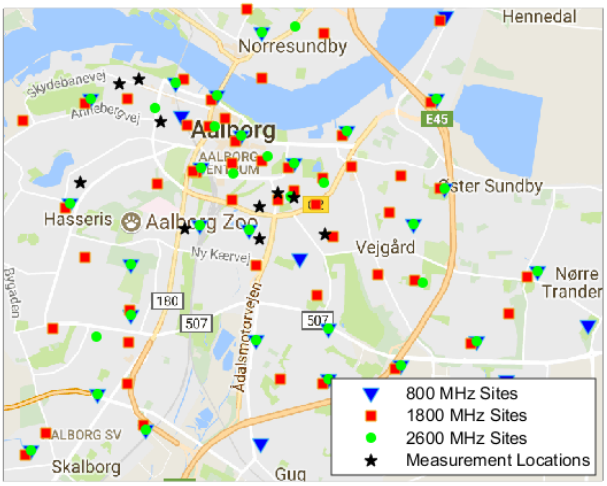

Fig. C.1: Map with measurement and site locations

Table C.2: Networks General Informaiton

Frequency (MHz)	ISD (m)	Avg. Tx. Height (m)	Avg. Downtilt (degrees)
800	850	26.2	5.5
1800	580	26.3	5.3
2600	690	25.3	5.8

The periodicity of saved measurement reports are internally controlled by the device based on multiple factors and cannot be directly controlled by the user. The recorded sampling rate observed for each height is showed in Table C.3.

Table C.3: Observed Sampling Rates

Height (m)	Sampling Rate (Hz)	Height (m)	Sampling Rate (Hz)
1.5	3.7	25	4.8
5	3.8	30	5.9
10	3.8	35	6.0
15	3.8	40	6.3
20	4	***	***

The data processing is similar to that previously used and detailed in [12]. Summarized here for the convenience of the reader: the PCI information was used to map the BS configuration, such as transmitted power, antenna used and site location. Pathloss samples were obtained by subtracting the measured power level from serving and neighboring cells from the EIRP (effective isotropic radiated power) of each base station. For the EIRP calculation the antenna gain used is calculated through the horizontal interpolation algorithm (HPI) applied over the horizontal and vertical antenna diagrams. Fast fading components are removed by applying local average on the path loss samples over windows of 40 wavelengths [17]. In order to avoid the roll-off region of the antenna patterns samples outside the -12 dB vertical and horizontal lobes were filtered out from the analysis. In [12], the threshold value was -6 dB, but it had to be relaxed for the purpose of this study, as it deals with much closer ranges to the base stations, to avoid all samples at the 2 highest lift levels would be excluded from the analysis due to the steep elevation angles.

The outcome of the processing phase was then used to obtain coefficients to fit a generalization of the close-in log-normal path loss model [18]:

$$PL(d, f, h) = \alpha(h) 10 \log_{10}(d) + PL_{ref}(f) + X_{\sigma}(h) \quad [dB] \tag{C.1}$$

where the variables d, f and h denote, respectively, the distance between BS and UAV (in m), the center frequency (MHz) and the UAV height above ground level (m). Besides, $\alpha(h)$ represents the height-dependent path loss slope and $X_{\sigma}(h)$ is a Gaussian variable with zero mean and standard deviation $\sigma(h)$ that accounts for the shadowing variation at the height h. Finally, PL_{ref} stands for the close-in path loss reference at 1m distance - assumed to be the theoretical free space path loss ($PL_{ref} = 20log_{10}(f) + 20log_{10}(4\pi)$).

A. 3GPP Reference Model

The working assumptions, at the time of writing, in the 3GPP study item on enhanced support for UAVs [9] [19] will be used for comparison purposes. Such a model is an extension of the well-known 3GPP model for the propagation channel for heights below 22.5 m that can be found in [20]. The measurement scenario differs from the assumptions of 3GPP in ISD (500 m) and antenna downtilt (10 degrees). For the convenience of the reader the model is repeated here in set of equations C.2 and C.3 for the line-of-sight (LOS) and non-line-of-sight (NLOS) cases, PL'_{LOS} and PL'_{NLOS}, respectively.

$$\begin{aligned} PL'_{LOS}(d) &= \begin{cases} PL_1(d) & \text{if } d_{2d} \leq d_{bp} \\ PL_2(d) & \text{if } d_{2d} > d_{bp} \end{cases} \quad \text{where} \\ PL_1(d) &= 28 + 22log_{10}(d) + 20log_{10}(f_c) \\ PL_2(d) &= 28 + 40log_{10}(d) + 20log_{10}(f_c) - 9log_{10}(d_{bp}^2 + \Delta_h^2) \end{aligned} \tag{C.2}$$

$$
\begin{aligned}
PL'_{NLOS} &= \begin{cases} \max(PL'_{LOS}(d), PL_3(d)) & \text{if } h_{ue} \leq 22.5 \\ PL_4(d) & \text{if } h_{ue} > 22.5, \quad \text{where} \end{cases} \\
PL_3(d) &= 13.54 - 39.08log_{10}(d) + 20log(f_c) - 0.6(h_{ue} - 1.5) \\
PL_4(d) &= 22.5 + (46 - 7log_{10}(h_{ue}))log_{10}(d) + 20log_{10}(f_c)
\end{aligned}
\tag{C.3}
$$

In these two set of equations, d stands for the total 3D distance between the BS and the UE, while d_{2d} represents the 2D projected distance regardless the difference in heights, Δ_h, between them. Also, d_{bp} is a breakpoint distance as calculated in [20] and depends on both, the center frequency f_c used for transmission and the UE heights h_{ue}. It is worthy noting that for UE heights, above 22.5 m there is no breakpoint distance for PL_{LOS} to be considered within the range supported by the model (5 km).

III Results

A. DL interference dependence on height

The work in [12] reported that the average number of cells detected increased with UE heights, due to the clearance in the radio path. The same behavior was observed during the urban measurements with the lift, as exposed in Fig. C.2. For all 3 frequencies, the number of cells tends to increase for the highest measurement compared to the ground level reference. The increase is specially high at 1800 MHz, which is the more dense network (see Table C.2), from 7.1 to 12.3. An interesting behavior is observed at 2.6 GHz, where the number of detected cells first decreases as the lift was elevated form ground level (6.2) to 20 m (4.3), where it starts increasing again up to 40 m (8.9). A cell is only recognized by the scanner if the synchronization channel is successfully decoded. If SINR is too low for that specific cell, it cannot be reported by the scanner. In some cases, if the signals from few cells are very strong, other neighbor cells may not be detected even if their signal levels are not so weak, due to the interference observed in synchronization channels. For 2.6 GHz, the clearance on the radio path of first few cells seems to have dominated at the first heights, increasing the interference levels on the sync channel and therefore reducing the overall number of detected cells. However, after 20 m of height, it seems that other cells further away also experience good radio clearance and their signals can overcome the SINR.

One can argue that power received from the strongest cell at higher heights could decrease, as the UE is moving away from the downtilted beams of the urban transmitter antennas. However, as showed in Fig. C.3, the radio clearance is the dominant phenomenon up to 40 m, as the strongest received power is around 20 dB higher at 40 m then at 1.5 m. On the other hand, radio clearance also brings more interference concerns. When interfering signals

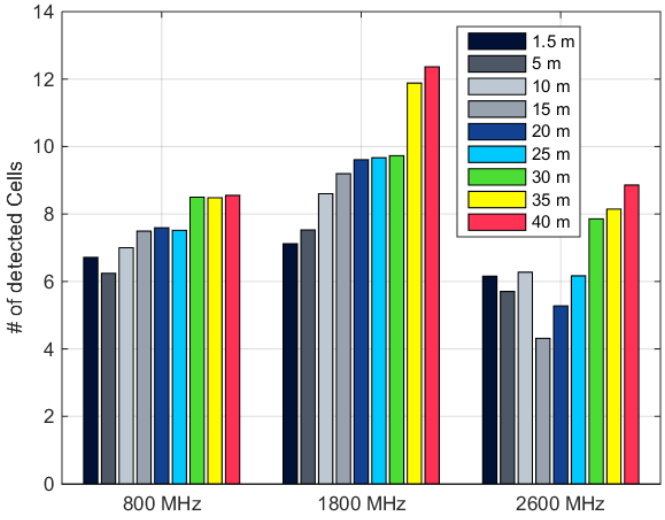

Fig. C.2: Avg. Number of Detected cells per sample

are closer in power domain the interference cancellation mechanisms at the received end tends to perform worse. Fig. C.4 shows the distribution of number of neighbor cells within 3 dB of the strongest (serving) cell signal. The number of neighbor cells lying in this power region tends to increase with UE heights. For instance, there are 2.6% (800 MHz), 4.2% (1800 MHz) and 7.4% (2600 MHz) samples with 4 or more sites within 3 dB of the serving cell at 40 m and less than 1% on ground level.

These two effects cited here can be even worse at higher heights. In [12] the average number of detected sites at 30 m is 7.6 and 16.9 at 120 m; and in [21] it is showed that at 120 m it is necessary to cancel the interfernece of the 4 strongest neighbors to obtain 3 dB of SIR gain.

B. Path Loss Measurements

Regarding the path loss model obtained from the measurements, two examples are presented in Fig. C.5 and C.6, which show respectively the results observed at ground level and at 40 m. The first consideration to be made regards the measured distances, which includes the range between 100 m and 5 km (similar across all trials). Hereafter, all path loss analysis are implicit referring to this range. For matters of comparison, the 3GPP model mentioned as reference is valid for distances between 10 m and 4 km. In these plots all values in y-axis was subtracted from PL_{ref} eliminates the frequency depen-

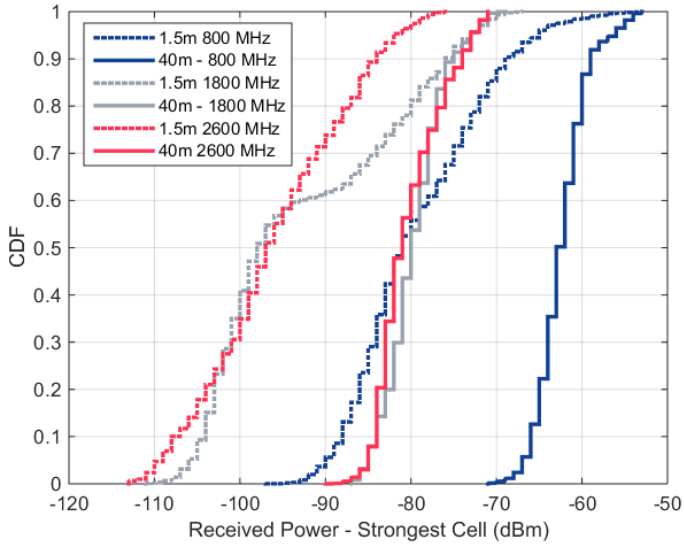

Fig. C.3: CDF: Avg. Received power (dBm) for first cell

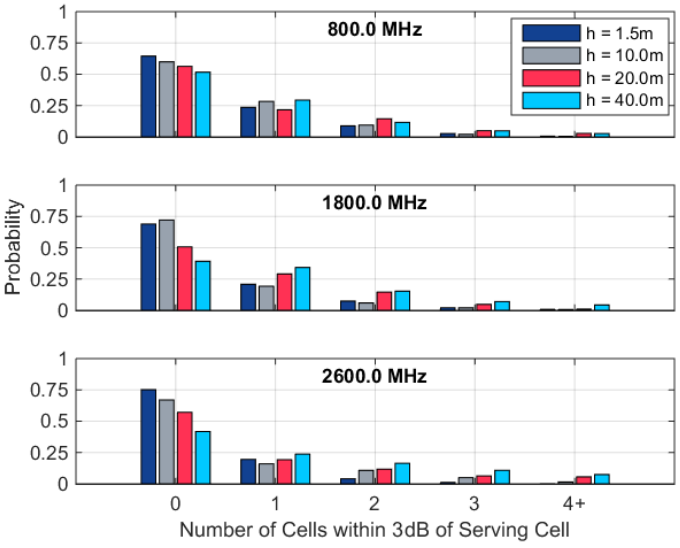

Fig. C.4: Distribution of number of cells within 3 dB of the serving cell

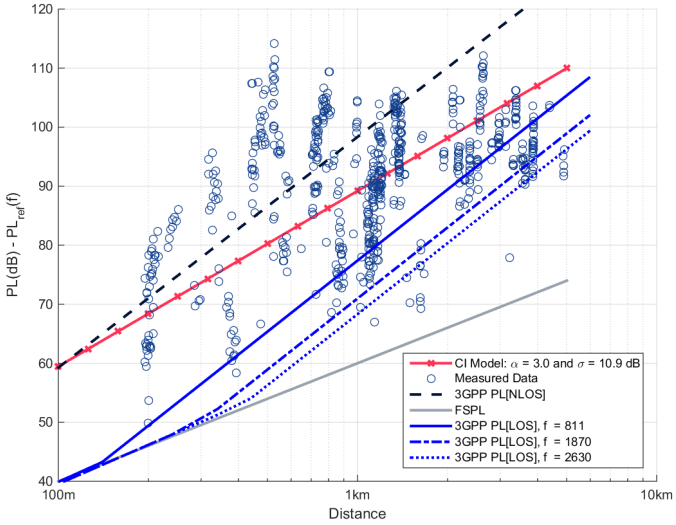

Fig. C.5: Path Loss Models at 1.5 m

dent component of $20log_{10}(f)$ in eq. C.1, so they can all be showed together regardless the frequency.

In Fig. C.5, at 1.5 m, it is possible to see the losses are much above FSPL reference line. At distances around 1 km, the excess losses (losses above FSPL reference) observed by the CI model line is about 30 dB. Also, most data samples are above 3GPP LOS model, and it seems 3GPP NLOS for is a better approximation of the measured values. On the other hand, in Fig. C.6, at 40 m, the measurement results are much closer to FSPL, with excess losses of 5 dB at 1 km; and much closer of 3GPP LOS model. It is worth noting that 3GPP NLOS model in this case is much more pessimistic than all recorded points, regardless the fact that current LOS probability model for such heights predicts values below 50% for this height [9].

A summary of the results is found in Table C.4, with the values that fit eq. C.1. It is also added to this table $\overline{E}_{LOS}$ and $\overline{E}_{NLOS}$, which are the average deviations from 3GPP model and the recorded data samples for the LOS and NLOS models, respectively: positive values represent underestimation, while negative values are an overestimation. In each row, one of these two values is marked in bold to represent the one that better approximates (in absolute values) our measurements. It is worth noting that $\overline{E}_{LOS}$ is always positive, while $\overline{E}_{NLOS}$ is always negative. The 3GPP NLOS seems to present better estimation for heights up to 5 m; while from 10 m onwards the LOS model

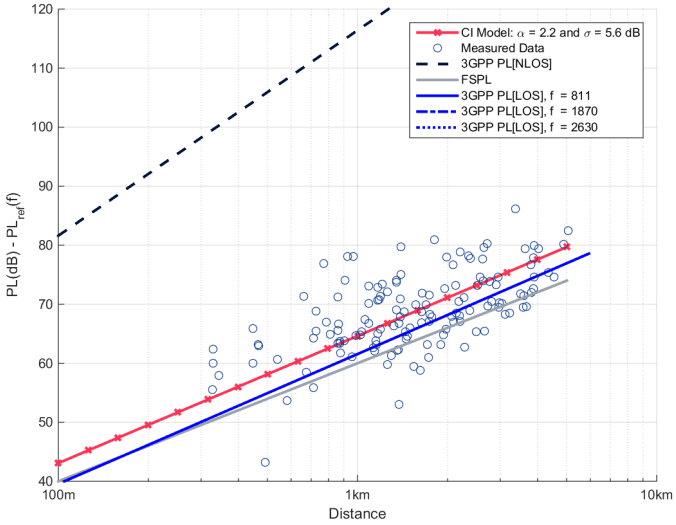

Fig. C.6: Path Loss Models at 40 m

is more representative, specially after $h_{ue} > 25m$ where it approximates FSPL behavior. This result is most likely related to the average building height in this area. In a more dense scenario, with taller buildings, the FSPL height is expected to increase.

The extended model used as of this writing, in [9] for $h_{ue} > 22.5m$ seems to be over-pessimistic. The model changes so abruptly that $\overline{E}_{NLOS}$ changes from -21.9 to -34.9, what cannot be attributed to changes in the measured data values, as showed by the values of α and $\overline{E}_{LOS}$.

Table C.4: Average difference from reference models

Height (m)	α	σ [dB]	$\overline{E}_{LOS}$	$\overline{E}_{NLOS}$
1.5	3.0	10.9	18.2	**-9.0**
5	2.8	11	20.9	**-13.1**
10	2.5	12.4	**13.5**	-18.4
15	2.3	9.3	**9.2**	-20.0
20	2.2	8.2	**5.2**	-21.9
25	2.2	6.7	**3.4**	-34.9
30	2.2	6.0	**3.6**	-33.4
35	2.2	5.9	**3.4**	-32.5
40	2.2	5.6	**3.1**	-32.7

C. Height Dependent Urban Path Loss Model

Compared to previous works, Table C.4 also shows the path loss slope and shadowing variation to reduces with UE gains in height, except for an outlier of σ when $h_{ue} = 10m$. Based on this, a logarithmic model was derived to create closed-form expressions for $\alpha(h)$ and $\sigma(h)$ in eq. C.1 to be used in evaluation of scenarios to the one described in this paper, i.e., in urban areas with average building heights below 20 m. The closed form expressions are presented in equations C.4 and C.4.

$$\alpha(h) = -0.64log_{10}(h) + 3.12 \tag{C.4}$$

$$\sigma(h) = -4.40log_{10}(h) + 13.51 \tag{C.5}$$

Fig. C.7 shows the closed-form expressions plotted against the measured values in Table C.4 and the height dependent model (HDM) for the rural measurements in [12]. The results in this paper show slope values smaller than those in [12], and higher shadowing deviation. It is important to note, though, besides the different types of environments, in this paper the distances are within the range of 100 m to 5 km, while the HDM Rural model was built using samples collected in a different range of distances, between 1.5 and 17 km.

IV Conclusion

A set of measurements were performed in urban scenarios in heights up to 40 m, to emulate radio performance of drones connected over cellular networks, in low-elevation flights and approximation and taking-off heights. Similar results were observed for three different frequencies (800, 1800 and 2600 MHz). Previous references have suggested increases in the number of detected cells at higher heights, but our findings suggest that at 40 m there already is an sensible increase in number of neighbors. Moreover, there is a substantial increase in the received power by neighbor sources, which will translate into heavier interference to be overcome by the BS-Drone link.

The main contribution of this paper is a urban height dependent path loss model based on real field measurements for UAVs connected to LTE networks. Our path loss investigations showed that above 25 m, 10 m above most buildings in the measured area, the propagation approximates the FSPL. When compared to reference values in 3GPP the measurements suggest that current work assumptions for PL_{NLOS} are too pessimistic and a bad predictions to what is observed on field. Also a height dependency is observed for the slope of the path loss line and also for the shadowing variation of the data samples. Closed-form expressions are provided for height-dependent models investigations in similar scenarios.

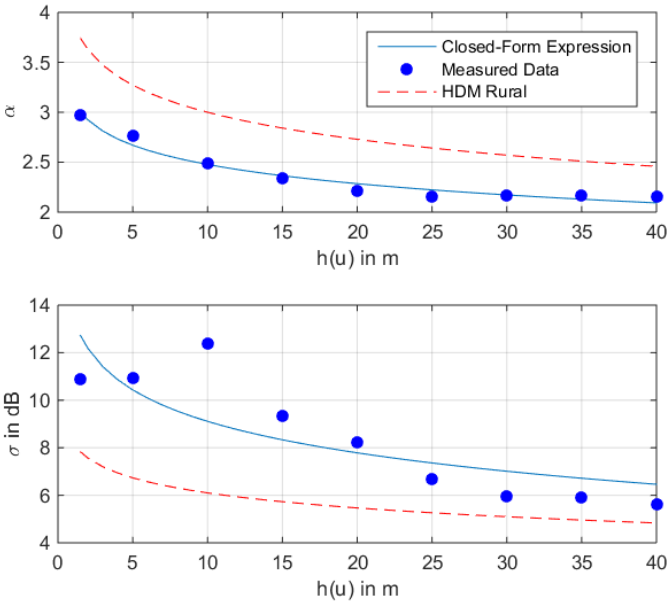

Fig. C.7: Height Dependent Models for α and σ

Next steps include using a real UAV to perform measurements at higher levels (up to 120 m), as a manner to investigate how these effects extend for such heights, and how the higher density of sites in urban areas impacts the interference analysis previously provided for rural scenarios.

Acknowledgment

This research has received funding from the SESAR Joint Undertaking under the European Union's Horizon 2020 research and innovation programme, grant agreement No 763601.

References

[1] M. M. Azari, F. Rosas, A. Chiumento, and S. Pollin, "Coexistence of terrestrial and aerial users in cellular networks," in *2017 IEEE Globecom Workshops (GC Wkshps)*, Dec 2017, pp. 1–6.

[2] "Guidelines for evaluation of radio interface technologies for imt-advanced," ITU-R, Mobile, radiodetermination, amateur and related satellites services M.2135-1, 2009.

[3] 3GPP, " Study on channel model for frequencies from 0.5 to 100 GHz," 3GPP, Tech. Rep. TS 38.901 V14.3.0, January 2018.

[4] EUROCONTROL, " RPAS air traffic management (ATM) concept of operations (CONOPS)," European Organisation for the Safety of Air Navigation (EUROCONTROL), Tech. Rep., February 2017.

[5] D. W. Matolak and R. Sun, "Air-Ground Channel Characterization for Unmanned Aircraft Systems - Part I: Methods, Measurements, and Models for Over-Water Settings," *IEEE Transactions on Vehicular Technology*, vol. 66, no. 1, pp. 26–44, Jan 2017.

[6] R. Sun and D. W. Matolak, "Air-Ground Channel Characterization for Unmanned Aircraft Systems Part II: Hilly and Mountainous Settings," *IEEE Transactions on Vehicular Technology*, vol. 66, no. 3, pp. 1913–1925, March 2017.

[7] D. W. Matolak and R. Sun, "Air-ground channel characterization for unmanned aircraft systems - part iii: The suburban and near-urban environments," *IEEE Transactions on Vehicular Technology*, vol. 66, no. 8, pp. 6607–6618, Aug 2017.

[8] R. Sun, D. W. Matolak, and W. Rayess, "Air-ground channel characterization for unmanned aircraft systems - part iv: Airframe shadowing," *IEEE Transactions on Vehicular Technology*, vol. PP, no. 99, pp. 1–1, 2017.

[9] 3GPP, "Enhanced LTE support for aerial vehicles," 3GPP, Tech. Rep. TS 36.777 V15.0.0, January 2018.

[10] B. V. D. Bergh, A. Chiumento, and S. Pollin, "Lte in the sky: trading off propagation benefits with interference costs for aerial nodes," *IEEE Communications Magazine*, vol. 54, no. 5, pp. 44–50, May 2016.

[11] N. Goddemeier, K. Daniel, and C. Wietfeld, "Role-based connectivity management with realistic air-to-ground channels for cooperative uavs," *IEEE Journal on Selected Areas in Communications*, vol. 30, no. 5, pp. 951–963, June 2012.

[12] R. Amorim, H. Nguyen, P. Mogensen, I. Z. Kovács, J. Wigard, and T. B. Sørensen, "Radio channel modeling for uav communication over cellular networks," *IEEE Wireless Communications Letters*, vol. 6, no. 4, pp. 514–517, Aug 2017.

[13] M. Mozaffari, W. Saad, M. Bennis, and M. Debbah, "Unmanned aerial vehicle with underlaid device-to-device communications: Performance and tradeoffs," *IEEE Transactions on Wireless Communications*, vol. 15, no. 6, pp. 3949–3963, June 2016.

[14] A. Al-Hourani and K. Gomez, "Modeling cellular-to-uav path-loss for suburban environments," *IEEE Wireless Communications Letters*, vol. PP, no. 99, pp. 1–1, 2017.

[15] K. Welch, "Evolving cellular technologies for safer drone operation," Qualcomm 5G White Paper and Presentations, Tech. Rep., October 2016.

[16] " Evolved Universal Terrestrial Radio Access (E-UTRA); Physical Layer Measurements," 3GPP, Tech. Rep. TS 36.214 V8.7.0, September 2009.

[17] W. C. Y. Lee, "Estimate of local average power of a mobile radio signal," *IEEE Transactions on Vehicular Technology*, vol. 34, no. 1, pp. 22–27, Feb 1985.

[18] T. Rappaport, *Wireless Communications: Principles and Practice*, ser. Prentice Hall communications engineering and emerging technologies series. Prentice Hall PTR, 2002.

[19] Ericsson , "Summary of Email discussion [89-10] on remaining details of channel modelling," 3GPP TSG-RAN WG1 #90, Tech. Rep. R1-1715084, August 2017.

[20] "Study on channel model for frequencies from 0.5 to 100 GHz," 3GPP, Tech. Rep. TS 38.901 V14.1.1, May 2017.

[21] I. Kovacs, R. Amorim, H. Nguyen, J. Wigard, and P. Mogensen, *Interference analysis for UAV connectivity over LTE using aerial radio measurements*. IEEE Vehicular Technology Society, 5 2017.

Chapter 3 - Interference and Coverage Analysis

The results presented in Chapter 2 and its related Papers suggests that airborne Unmanned Aerial Vehicles (UAVs) can be subjected to a different distribution of interfering sources in the power domain than that observed at terrestrial levels. In this Chapter, efforts are concentrated in further understand this profile of interference and how it can affect the performance of the Command and Control (C2) link.

3.1 Problem Description

The results previously presented in Chapter 2 show that the interference experienced by flying UAVs may come from several sources and those are close in the power domain. Moreover, such pattern would be identified not only in the edge, but in the whole cell area. To illustrate the growth in the number of interference sources, Fig. 2.4 shows the detected cells observed at terrestrial level and 120 m for the tests performed in Paper B.

The number of cells detected is higher at 120 m (46 vs 26), extending for a wider range, specially on the top right area of the map, albeit the radio scanner sensibility is more restrictive at this height (see B.2). It is worth pointing that because of the equipment sensibility some other significant sources of interference may not have been detected during the tests.

For the reminder of this thesis the concept of *interference profile* will be adopted. It refers to the distribution of the neighboring cells in the power domain: the received power difference between the first neighbors and the number of significant sources of interference.

The differences observed in the UAVs' interference profile can impact the link performance. On top of this, the efficiency of the interference mitigation techniques can also be reduced, by the absence of a clear dominant interfering, in which many of these techniques rely on. So it becomes important understanding how the interference profile differs for flying drones and what are the possible consequences of this effect.

3.1.1 Interference vs Coverage

The spatial reuse of frequency resources is one of the fundamentals of cellular communication that helps to amplify the system capacity. Because of the reuse of resources by different network elements, they can mutually interfere on each other. For example when one user equipment (UE) receives the power transmitted by other base stations than its serving one. The rising of the interference levels can cause a degradation in the signal to interference plus noise ratio (SINR), leading to a performance degradation.

Every communication link must operate above a certain SINR threshold, such that the received information can be successfully decoded by the receiver. When this condition is not met, the link is either experiencing poor coverage (high Block Error Rate (BLER)) or, in the worst cases, out of service coverage. For instance, in Long-Term Evolution (LTE) and LTE-Advanced (LTE-A), the Physical Downlink Control Channel (PDCCH) is the logical channel that sets up and manages the radio link, conveying the configuration information, scheduling grants. When there is a degradation in the PDCCH' SINR, below a threshold, Q_{in} the signal cannot be received by the user and the connection is assumed to be in outage. If the problem persists for a certain period of time, a radio link failure ensues. For avoiding the radio link failure, within this period of time, the SINR must improve above a recovery threshold Q_{out} [1].

The LTE-A system use robust coding to protect the PDCCH against severe interference levels [2], but in extreme situations, more advanced interference management solutions may be required to preserve the performance of the aerial UE's link, as it will be presented in Chapter 4.

Different solutions have been used to manage the inter-cell interference in cellular networks and prevent the lack of coverage at cell edge. The 2G systems adopt the frequency spatial reuse, whereas the 3G systems use code multiplexing [3]. In 4G LTE and LTE-A network, more advanced and adaptive solutions were developed to handle the inter-cell interference problem, such as inter-cell interference coordination (ICIC) and Coordinated Multipoint (CoMP).

3.1.2 Downlink Interference

The interference is intrinsically related with the traffic load. In current systems, the downlink (DL) is more heavily loaded than the uplink (UL), hence more likely to experience severe interference conditions. To cope with the rampant growth in the traffic load, CoMP and ICIC solutions were developed for the management of inter-cell interference [4].

The ICIC and enhanced inter-cell interference coordination (eICIC) solutions aim at coordinate the resource usage across the network transmitters

to improve the link performance by mitigating the inter-cell interference [5]. The solutions may be time, frequency or power based [6]. In the time and frequency solutions, there is a trade-off between interference mitigation and the cells capacity. In these techniques, multiple base stations try to avoid "collision" in their transmissions by negotiating the time/frequency resources each of them will transmit. In the power-based solutions, the power of transmission of one or more nodes is adjusted to avoid interference to the other base stations.

The hypothesis unveiled by the results presented in Chapter 2 and Fig. 2.4 is that the differences in the interference profile may compromise the deployment of techniques such as eICIC and CoMP. By coordinating just a few neighbor cells may provide very low performance gains, whereas the complexity of managing many neighboring cells in a large area is unattractive and difficult with multiple areas to be coordinated overlap.

The CoMP solutions are usually deployed to enhance the connectivity of users in the cell edge, where the SINR and two or more cells are received with similar power levels, and they can be of two kinds: the Joint-Transmission Joint Transmission Coordinated Multipoint (JT-CoMP) and the Coordinated Scheduling/Beamforming Coordinated Scheduling/Coordinated Beamforming Coordinated Multipoint (CS/CB-CoMP) [4]. In the first case, JT-CoMP, multiple cooperating transmitters are used simultaneously to convey data for a user equipment. It aims at improving the system performance by transforming strong interfering neighbor cells into co-serving cells. In the CS/CB-CoMP, the information is transmitted to the user only by the serving cell, while the scheduling of transmissions and the choice of beamforming allocations are coordinated between neighbor cells to reduce the overall interference.

3.1.3 Uplink Interference

In UL the LTE network's base stations are in the receiving end of the radio link. In this case, the total interference experienced by the receiver is caused by the power received from all other devices that are not associated to that base station. In other words, the other-cell's users are source of interference in UL.

Hence, the lower path losses experienced by one UAV do not change the interference profile it experiences. But it can change how it affects the other users - either terrestrial or other UAVs -,increasing the interference radiated toward other cells.

On the other hand, based on the fact multiple base stations will receive the UAV transmission with high power, Joint Reception Coordinated Multipoint (JR-CoMP) can be used to improve the UL performance. In the JR-CoMP the information received across several base stations is combined to enhance the

robustness of the conveyed signal.

The papers presented by this chapter assess the profile of interference observed and caused by UAVs and evaluate how it impacts the performance of CoMP and eICIC techniques presented in Section 3.1. Albeit, the CS/CB-CoMP and the power domain eICIC are not directly assessed in these papers, Section 3.4 provides a discussion about their expected performance, based on the other results presented and on account of contemporary works published in the literature on the duration of this study.

3.2 Included Articles

Paper D. Measured Uplink Interference Caused by Aerial Vehicles in LTE Cellular Networks

The UL interference caused by UAVs is investigated in this paper by means of field measurements. A mobile phone connected through an operational LTE-A network is set to transmit repeatedly a large file to a remote server, emulating a full-buffer transmission. Tests are performed in a rural location at two heights: ground level and at 100 m. The main metric used in this analysis is the rise of interference over thermal noise in all base stations within 15 km radius of the transmission site.

Because the measurements are taken in an operational network, the interference generated by the network's subscribers is a lurking variable that could bias the results. In order to minimize this effect, the tests are performed between 2-5 AM, when the network load reaches its minimum, and the results compared with the benchmarking of each cell collected in the seven days prior to the test.

The advantage of this uplink setup is that it measures the interference rise and each base station is affected individually, which means that there is no sensibility variation between the tests performed at ground and at 100m.

The paper analyzes the number of cells affected and compare the total interference rise observed on each of them for both cases. It also discusses strategies to mitigate the high-interference power caused by the airborne transmission at 100 m, once it seems to affect the whole area.

Paper E. Interference Analysis for UAV Connectivity over LTE Using Aerial Radio Measurements

This paper assesses an empirically measured data set to characterize the radio interference observed by UAVs connectivity over LTE. For this analysis, the data-set is split into 4 sub-scenarios, based on the network density and the signal to interference Ratio (SIR) distribution. In each sub-scenario, measurements are performed in five heights: 1.5m, 15, 30, 60, 120 m.

Thereafter, the paper evaluates the probability of obtaining performance enhancement in the radio link using network interference management techniques available in LTE, as described in Section 3.1. The DL solutions analyzed in the paper are JT-CoMP and Interference Rejection Combining (IRC). By considering an ideal IRC scheme, the calculations presented in the paper assumes all the contribution of the neighbor cells are removed from the SINR, and therefore has similar performance gains as provided by an ICIC scheme. The analysis in UL is focused on the performance gains provided by JR-CoMP.

The simplified mathematical models provide an upper bound for the performance gain enabled for each technique. Evaluations are focused in interference coordination among up to the four first neighbors, ranked by the measured received power.

Paper F. Using LTE Networks for UAV Command and Control Link: A Rural-Area Coverage Analysis

The impact of the DL interference in the network coverage is assessed in this paper by system level simulations. This study's motivation is assessing the hypothesis that the main limiting factor for the DL C2 coverage is the interference.

Using a height-dependent path loss model, the coverage area is examined by the predicted SINR for different network loads. For the purposes of this paper, the outage is defined as the situation where the predicted SINR does not exceed the threshold level for PDCCH reception. The performance is evaluated at 5 different heights: 1.5, 15, 30, 60 and 120. The impact of the profile of interference in the results presented is discussed throughout the paper, as having more cells significantly contributing for the interference shows seems to influence the system performance.

The paper also compares the perfomance enhancement provided at ground level and at 120 m, by removing one source of the interference via ideal interference cancellation (IC), which has a similar effect then using time/frequency ICIC in the first neighbor. Additionally, the work also glances at other performance enhancement techniques, which is the focus of the next chapter, by proposing the usage of macro-diversity access across two different networks to improve the overall coverage of the C2 link.

3.3 Main Findings

3.3.1 SINR degrades with increases in UAV height

The investigations presented throughout these papers have demonstrated a degradation in the SINR is expected with increases in UAV's height up to 120

m, albeit the signal's received power tends to increase, in spite of the antennas down tilt. The increase in the serving cell received power is supported by the findings in Papers D and F. On the other hand, the rise in the total interference power outweighs the gains in the received signal, and the SINR degrades.

The degradation in SINR is reported in Paper E, where the mean SIR measured at lower heights is significantly better than the values reported at 60 and 120 m for all four sub-scenarios evaluated (Fig. E.2). These results are summarized in Figure 3.1, where it is possible to see that in all sub-scenarios a degradation in SIR between 5 and 13 dB is observed comparing the values at terrestrial level and at 120 m. It is also worth noting in this picture that even the high-SIR scenarios (at terrestrial level) experience a steep degradation with increases height, as the distance range of the interfering base stations increases.

Paper F also reports similar degradation. In the simulations, -6 dB is used as the SINR threshold for the PDCCH reception. In other words, the C2 link is assumed to be in outage for SINR values below this threshold. The average SINR simulated under full-load assumptions shows an outage increase from 4.2% at 1.5 m to 51.7% at 120 m.

The density of sites (conversely the inter-site distance (ISD)) and the network load both seem very important parameters in the degradation of the

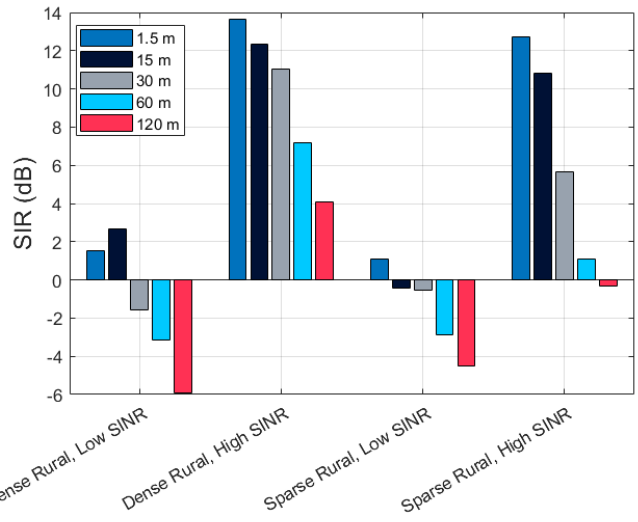

Fig. 3.1: DL SIR degradation for the four sub-scenarios evaluated in Paper F for different UAV heights.

SINR, as expected. The outage drops from 51.7% to 27% at 120 m, by increasing the ISD from 2.2 to 5 km Fig. F.6.

The full-load assumption provides a worst-case scenario upper bound for the outage, but real operational networks do not operate close to the full capacity. In most cases, the network load is around 10-30%. The simulations show that the outage at 120 m decreases to 1.9% assuming a fractional load of 25% (Fig. F.7).

It is worth noting that these degradations cannot be attributed to the losses in the received signal. This can be observed from Fig. 3.2, where the spectrum efficiency, measured by the throughput per Physical Resource Block (PRB) used, is assessed in different scenarios, using the setup described in Paper D, i.e. using UL full buffer transmissions. The DL traffic is generated by the feedback from the FTP transmissions. The rural scenario refers to that described in the reference paper. Information about the urban an suburban scenarios, can be found in [7].

3.3.2 No clear dominant source of interference in DL

The results corroborate the hypothesis that, the higher is the UAV the less likely it will observe a clear dominant interfering cell. Evidences for this are provided, for example, by the analysis of the Dominant Interferer Ratio (DIR) presented in Paper E. The results show that the DIR tends to degrade as the

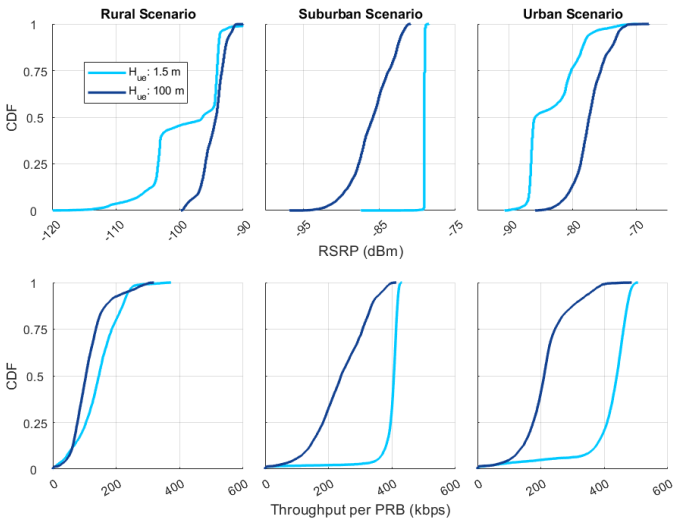

Fig. 3.2: Spectrum efficiency degradation with height for the three scenarios reported in [7].

UAV height increases (see Fig. E.2) In all four sub-scenarios evaluated, the DIR is much lower at 120 m than at 15 m as reported in Fig. 3.3, with a variation between 5 and 6 dB, indicating that the neighbor cell with strongest received power do not stand out compared to the others in the power domain as it does at lower heights.

This is further illustrated in this paper by time-traces of SIR and DIR, that are provided as example for one of the sub-scenarios at 15 m and at 120 m. In the first case, the DIR varies between -9 and 9 dB, while in the second it oscillates between -10 and 4 dB (Fig. E.3 and Fig. E.4). Moreover, the Physical Channel Indicator (PCI) reported for the first strongest interfering cell shows more changes at 120 m than at 15 m (Fig. E.5. This implies the neighbor cells are close to each other in the power domain and more susceptible to vary with small changes in the radio channel (Fig. E.5).

A similar evidence is found in Paper D. Albeit the paper is more focused on the UL, it provides the DL Reference Signal Received Power (RSRP) for the cells in the monitored area that could be detected by the transmitting phone. The RSRP analysis show that more cells are detected at 120 m, than at 1.5 m. Besides, the average power received for the first neighbors are more narrowly distributed, as presented in Fig. D.4.

Further, in paper F, the average DIR simulated assuming a fractional load of 50% drops from -1.7 dB at 1.5 m to -7.1 dB at 120 m (see Fig. F.8).

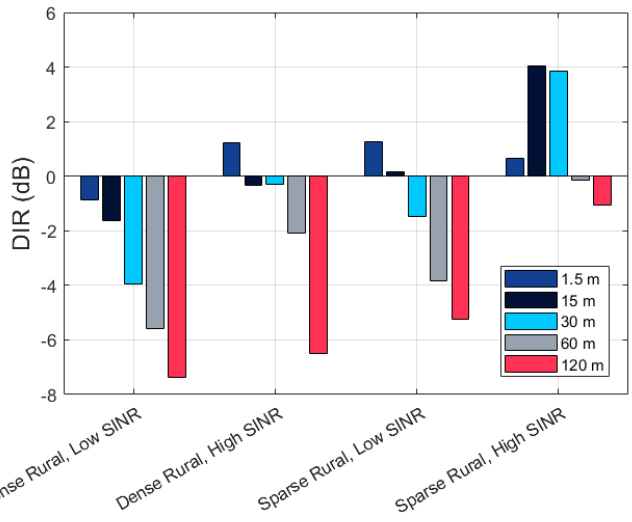

Fig. 3.3: DIR degradation for the four sub-scenarios evaluated in Paper F for different UAV heights.

3.3.3 Less effective ICIC and CoMP in Downlink

As a consequence of the lack of a dominant clear source of interference and low expected DIR, the ICIC and CoMP strategies are less effective to improve the C2 performance.

The paper E addresses the probability of observing a 3 dB gain in the SIR by applying JT-CoMP and IRC. The paper assumes all detected cells are loaded, i.e, are sources of interference in the SIR formula. On the other hand, it may have been the case that some significant interfering cells were not detected because of the increased interference-plus-noise floor on the measurement equipment.

Results show that for low SIR scenarios, at least three cooperating cells are required to provide SIR gain for UAVs flying above 30 m. But it is also discussed that there are practical challenges in implementing such solution. The constant changes in the neighbor cells require frequent adaptation of the set of cells cooperating. The required signaling and delays involved in this process may offset the theoretical gains of CoMP.

The IRC technique evaluated in the same paper is expected to offer similar gains than those provided by the time/frequency ICIC. The data shows that removing just the first interfering cell can provide limited gain in sparse networks, but it is insufficient in the other cases. In order to provide any gain, at least 3 or 4 interfering signals are required to be canceled. The number could be even higher if significant interfering cells were left out by the rise in the interference-plus-noise floor of the equipment. This finding is similarly demonstrated by Paper F, where canceling the first interfering cell produces less gain in SINR at 120 m, than at ground level.

3.3.4 Increased noise rise in Uplink

In Section 3.1, it was discussed how the UL interference caused by airborne UAVs could differ from those coming from terrestrial users. These assumptions are supported by the analysis of field measurements performed in D.

A full-buffer transmission was repeated at ground level and at 100 m. The rise of interference over thermal noise metric attributed to these transmissions was much higher for the latter case. The number of cells impacted in a 15 km radius increased from 8 to 20. Also, the average magnitude of the interference over thermal noise rise increase in 3.7 dB in the cells impacted by the 100 m transmission. The paper provides ideas to mitigate this impact, in special, the use of directional transmission, that could limit the power radiated toward network base stations outside the main direction of the transmission. This concept is explored in more details in the next chapter.

Moreover, the results also indicate the extent of the area impacted by the aerial transmission can be significantly larger. One cell 30 km away from the

test location, outside the zone of analysis, was measured with significantly high DL power, suggesting the UL transmissions would contribute to a noise of approximately 8 dB in this cell. It is worth noting that at such distances, a 30 m-high base station would likely be hidden behind the Earth curvature from a terrestrial user [8].

Although, the SINR degradation is not expected in UL, the JR-CoMP proves to be an alternative to improve the C2 UL performance, as shown in Paper E. The results show the gains are limited to a certain scenarios and require at least 2 or more cells coordinating.

In addition to the rural scenario reported in Paper F, the test was later repeated in two other scenarios - urban and suburban - as reported in [7]. In all the cases the number of interference victim cells increased significantly, as well as the average noise rise caused by the UL transmission, as it is shown in Fig. 3.4.

3.3.5 Network diversity shows good potential for perfomance enhancement

The macro diversity access proposed in Paper F shows good potential to enhance the performance of C2. Assuming an user can have simultaneous access to more than one operator, it may profit from the different network

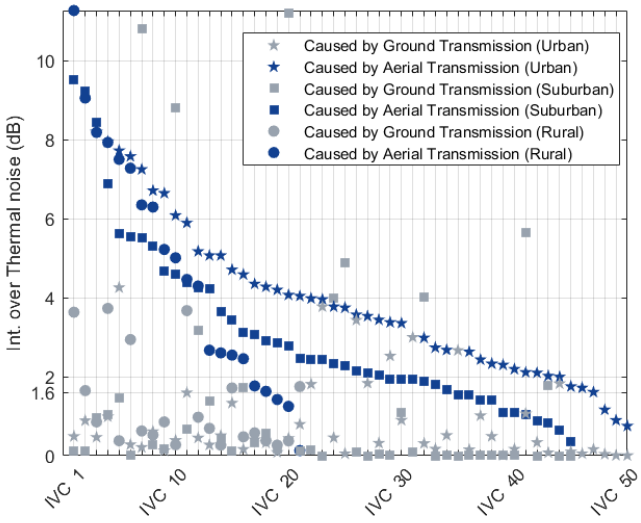

Fig. 3.4: Interference over thermal noise (IoT) measured in the interference victim cells during the UL full buffer transmissions for the three scenarios reported in [7].

layouts: sites locations, ISD, antennas orientations, etc. Unless both operators are in outage at the same time, the user can rely on the other operator if one of them goes in outage.

In the simulations results presented in the paper, the link outage for two different network layouts is 19.7% and 7.25% in a scenario with 50% of fractional load in the network. By using selective diversity, the outage drops to 1.8 %, as depicted in Fig. 3.5.

These results are the first glance in this paper of how different techniques can enhance the performance of C2 link. Chapter 4 will discuss other alternatives for enhancing the performance of C2 link to values close to the Third Generation Partnership Project (3GPP) requirements.

3.4 Discussion

The findings presented in this chapter show that, as previously hypothesized, the heights of the UAV impact the profile of interference experienced and caused by these users in the cellular network. Of most importance in this chapter is the DL SINR degradation associated with lack of a clear dominant interfering cell.

The C2 is a critical link that expects high reliability levels. Thus, the degradation in performance must be handled by interference mitigation techni-

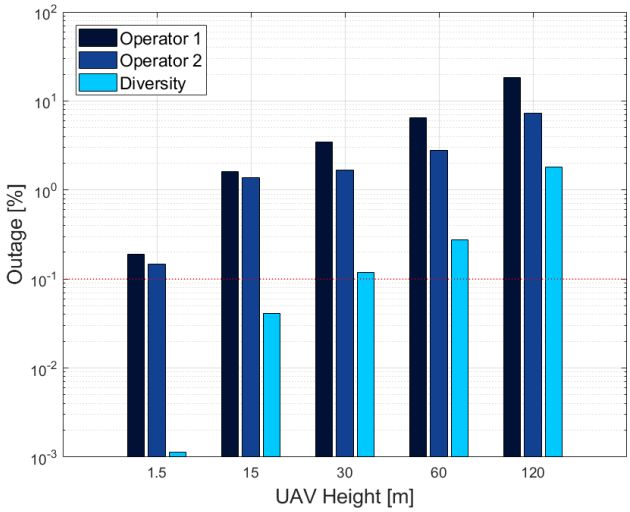

Fig. 3.5: Reliability increase against outage by means of network diversity for the full-load simulations presented in Paper F.

ques, in order to guarantee the performance requirements. The inter-cell interference management techniques provided by LTE-A, ICIC and CoMP, are not expected to provide significant performance enhancement at low complexity deployments.

First of all, the number of cells to be coordinated increase in the UAVs case, and the same is valid for the area where these cells are distributed. Moreover, as many cells are reported in similar levels in the power domain, there are more changes in the most significant neighbor cells. This could lead to frequent redefinitions in the set of coordinating cells. These factors combined can lead to a significant increase in the complexity of managing such solutions.

For the JT-CoMP, the signaling and delays involved in updating frequently the set of coordinating cells can outweigh the gain in performance. Moreover, if several transmitters are used to jointly transmit to a single user, the network capacity is affected.

When time/frequency ICIC is used, the cells must negotiate in which time/frequency resources each of them is allowed to transmit. Coordinating the resource allocation policy among several cells may be very complex and, in special, difficult to scale when multiple UAVs require access in different networks' cells. Further, it would also lead to diminished network capacity. Similar gains and drawbacks are expected by the CS/CB-CoMP.

Because of this, other interference mitigation solutions must be deployed to guarantee performance enhancement of the C2 link. The next chapter is focused on discuss in more details these techniques and their potential in improving the C2 reliability.

For the UL case, the interference caused by the UAV is significantly higher when compared to a terrestrial user, and it also impacts a large area and number of cells. On the other hand, the C2 UL required throughput - 60-100 kbps - is very low when compared to cellular broadband applications. This means the amount of resources occupied for a given UAV' C2 is low, minimizing the impact caused. Moreover, the expected number of UAVs [9] is very small compared to the number of terrestrial mobile UEs [10].

However, UAVs are likely to transmit in UL with very high data rate, for example, for live video streaming. In this case, even for small number of UAVs per cell, the increased interference may be a problem to be addressed by the mobile network.

References

[1] F. Capozzi, D. Laselva, F. Frederiksen, J. Wigard, I. Z. Kovacs, and P. E. Mogensen, "UTRAN LTE Downlink System Performance under Realistic Control

Channel Constraints," in *2009 IEEE 70th Vehicular Technology Conference Fall*, Sep. 2009, pp. 1–5.

[2] 3GPP, "Evolved Universal Terrestrial Radio Access (E-UTRA); Physical channels and modulation," 3rd Generation Partnership Project (3GPP), Technical Specification (TS) 36.211, Dec. 2009, version 8.9.0.

[3] A. R. Mishra, *Advanced Cellular Network Planning and Optimisation*. John Wiley & Sons, 2007.

[4] D. Lee, H. Seo, B. Clerckx, E. Hardouin, D. Mazzarese, S. Nagata, and K. Sayana, "Coordinated multipoint transmission and reception in LTE-advanced: deployment scenarios and operational challenges," *IEEE Communications Magazine*, vol. 50, no. 2, pp. 148–155, February 2012.

[5] A. S. Hamza, S. S. Khalifa, H. S. Hamza, and K. Elsayed, "A Survey on Inter-Cell Interference Coordination Techniques in OFDMA-Based Cellular Networks," *IEEE Communications Surveys Tutorials*, vol. 15, no. 4, pp. 1642–1670, Fourth 2013.

[6] D. Lopez-Perez, I. Guvenc, G. de la Roche, M. Kountouris, T. Q. S. Quek, and J. Zhang, "Enhanced intercell interference coordination challenges in heterogeneous networks," *IEEE Wireless Communications*, vol. 18, no. 3, pp. 22–30, June 2011.

[7] T. B. Sørensen and R. Amorim, "DroC2om - 763601 - DroC2om - 763601 - Preliminary report on first drone flight campaign," SESAR Joint Undetaking, Deliverable 5.1, March 2018.

[8] ITU-R, "Definitions of terms relating to propagation in non-ionized media," International Telecommunication Union, Recommendation P.310-9, Aug. 1994.

[9] Federal Aviation Authority, "FAA Aerospace Forecast, Fiscal Years 2018-2038," Tech. Rep., March 2018.

[10] Cisco, "Cisco Visual Networking Index: Forecast and Trends, 2017–2022," white paper, Nov. 2018.

Paper D

Measured Uplink Interference Caused by Aerial Vehicles in LTE Cellular Networks

Rafhael Amorim, Huan Nguyen, Jeroen Wigard, István Z. Kovács, Troels B. Sørensen, David Z. Biro, Mads Sørensen and Preben Mogensen

The paper has been published in the
IEEE Wireless Communications Letters Vol. 7, Issue 6, pp.958-961, 2018.

© 2018 IEEE
The layout has been revised and reprinted with permission.

Abstract

Aerial users, such as unmanned aerial vehicles (UAVs), experience different radio propagation conditions than users on the ground. This is a concern regarding the integration of such users in the cellular networks in the near future. This paper investigates the impact of uplink transmissions from an aerial user equipment. Full buffer transmissions were performed by a device at ground level and also flying attached to a UAV at 100 m height. The field measurements show a higher number of cells affected by the aerial transmission, with an increase of up to 7.7 dB in the interference over thermal noise in cells within 15 km of the test location. This letter also assesses two strategies to reduce the uplink interference caused by aerial users: UAV's cruise height control and directional transmissions. Results show the directional transmission is a more promising technique and have the advantage of not reducing the uplink received power.

I Introduction

Unmanned Aerial Vehicles (UAVs), also known as drones, are experiencing a market surge boosted by technological developments in recent years. Data connectivity is one of the key enablers for beyond visual line-of-sight (BVLOS) flight ranges, which can help to unleash an emerging potential. Besides the control link between UAVs and their users, many applications may require high data rate connectivity, such as surveillance, infrastructure monitoring, and media streaming [1]. Cellular networks are ubiquitous, have a ready-to-market implemented infrastructure and are capable of supporting broadband applications. Therefore, they arise as natural candidates to provide UAVs's connectivity.

The Third Generation Partnership Project (3GPP) has opened a work item on enhanced support for aerial vehicles [2] to set common ground for performance evaluation of such devices. At the time of writing, current channel models are assumed to be height dependent and approximate freespace propagation as UAV moves up. In [3] authors use stochastic geometry to show that the aerial devices present higher line-of-sight (LOS) probability than users on the ground. Preliminary results in [4] and [5] indicate this may change the interference patterns commonly observed in cellular networks.

Understanding how less severe path losses impact the performance of both new aerial and legacy users is a topic of interest for network operators [6]. This paper is focused on the performance assessment of uplink (UL) transmissions, i.e., from the user equipment (UE), either ground or aerial, to the base station (BS). Previous studies in [7] and [8] use downlink (DL) field measurements to estimate the UL interference power observed by the neighbor cells detected in the experiment. Results indicate a significant increase

in the UL interference power as a function of the UE height.

In the present work, UL field measurements were performed in a rural area in Denmark, using a live Long-Term Evolution (LTE) carrier at 800 MHz. A test phone performed transmissions at two different heights: on ground level and attached to an airborne UAV at 100 m, a height compatible with many UAV's commercial applications. A collaboration with the network operator enabled the assessment of the impact of such transmissions in all the co-channel cells within a 15 km radius area. Based on the observations, the paper discusses the challenges of implementing interference coordination techniques and presents two other possible countermeasures to the high interference. The first, UAV cruise height control, is based on observations made in [9,10] that UAVs' height may be optimized, offering a trade off between throughput and interference in adjacent cells. The second strategy, directional array of antennas at the UAV, tries to minimize the interference without sacrificing the user throughput based on evidences presented in [11].

The remainder of this letter is organized as follows: Section II addresses the setup and details of the field measurements; Section III shows the measured results and discuss their implications. Final remarks are found in Section IV.

II Field Measurements Setup

A. Network Scenario

The monitored area includes 50 live operating cells distributed over 17 sites. Reference information for the base stations, such as average, maximum and minimum values for antennas downtilt and transmitter heights, is found in Table D.1. In order to minimize the impact to and from other users in the network, the measurements were performed at night, between 2-5 AM. In this time window, the average UL cell measured in the two weeks previous to the test was only 2 percent.

Table D.1: Monitored Cells Information

	Average	Minimum	Maximum
Height (meters)	37.2	27.5	54
Downtilt (degrees)	5.2	3	8

B. Test Device and Operation

The tests were carried out with an R&S QualiPoc[1] Android smartphone. In order to obtain a full-buffer behavior, a large test file (approximately 400 MB) was repeatedly transmitted by the device, that was locked to a 10 MHz LTE carrier in the 800 MHz band. The tests, which had 15 minutes of duration, were repeated three times for each of the two cases: the terrestrial UE (TUE), from a static ground position at 1.5 m, and the airborne UE (AUE) at 100 m, with the smartphone attached to a UAV flying in circles of 7 m radius.

C. Measurements

For this analysis the interference over thermal noise power (IoT) in the network cells was provided by the telecom operator. This performance indicator reports the median of the noise rise in LTE Physical Uplink Shared Channel (PUSCH) [12] sub-bands over periods of 15 minutes. For each test, starting and ending time were synchronized with the report generated at the base stations.

Reports were also collected by the phone software. UL measurements include phone's average transmit power, number of Physical Resource Blocks (PRBs) used and throughput in PUSCH channel. DL measurements include physical cell indicator (PCI) and reference signal received power (RSRP) [12] for the serving cell and for some detected neighbors. During the trials, sampling rates observed were around 0.8-2 Hz.

III Results and Discussion

Before comparing the impact on UL in the two cases, it is important to understand how these transmissions compare to each other, especially regarding the transmit power. Figure D.1 shows the CDF of three metrics recorded by the phone across all tests: UL transmit (Tx) Power, PRBs used in PUSCH Channel and PUSCH throughput. Despite UL power control in LTE base stations, UE is transmitting close to its maximum power, 23 dBm, in both cases, indicating a power-limited throughput due to the path loss. A slightly lower average output power, 22.8 dBm, is observed by the AUE, compared to the TUE (23.0 dBm). In addition, TUE and AUE also show similar average resource usage, occupying 42.8 and 40.8 PRBs respectively, which indicates similar power spectral density in both cases. Also, the bandwidth used was close to the maximum number of PRBs available for PUSCH in a 10 MHz bandwidth (46), corroborating the assumption of low network load generated by other users.

[1]More information about the Qualipoc software in https://www.rohdeschwarz.com/us/brochure-datasheet/qualipoc_android/

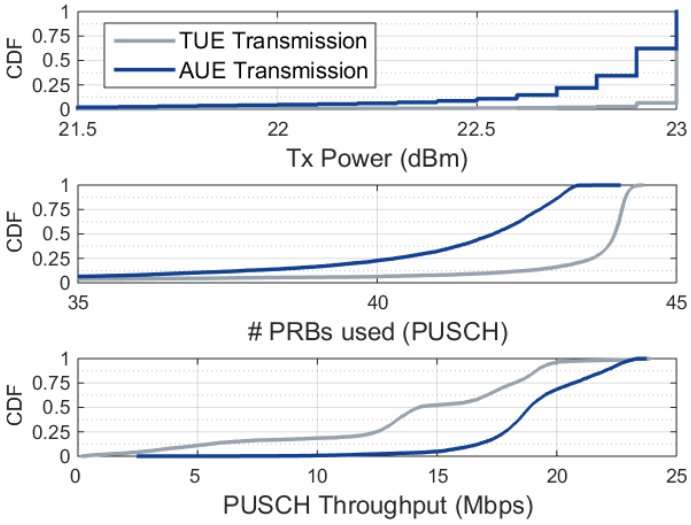

Fig. D.1: Cumulative Density Fucntion (CDF): Recorded Tx Power, PRB usage and UL throughput for the transmissions using the terrestrial user equipment (TUE) and the airborne user equipment (AUE).

Despite these similarities, the median throughput obtained during aerial transmissions is 32.5 percent higher than that observed at ground level (18.9 versus 14.2 Mbps). This can be attributed to lower coupling losses, as indicated by the phone reports. The AUE case reported higher average Modulation and Coding Scheme (MCS) than the TUE case, 23.7 versus 18.7, and higher median serving cell DL Reference Signal Received Power (RSRP), -94 dBm versus -101 dBm. It is worth noting that the TUE and the UAV are not connected to the same serving cell. The TUE's serving cell is 3.8 km away, but the AUE made a handover to a farther serving cell (13.7 km away) after taking off, probably because its new elevated position was in a low gain region of the closest cell's antenna.

The IoT was evaluated to quantify the impact of such transmissions to the cells in the vicinity. The average IoT for each base station across the three tests was used as a metric for comparison. The previous two weeks of measurements, within the same time frame (2-5 AM), was used as a baseline value for each cell. If the IoT for either AUE or TUE exceeds the 99th percentile of the baseline plus 0.5 dB, the cell is considered an Interference Victim Cell (IVC). This is motivated on the ground that it is more likely that the transmissions of the test device caused the outlier, rather than statistical variation.

A total of 20 cells were classified as IVCs. Fig. D.2 shows all IVCs ranked

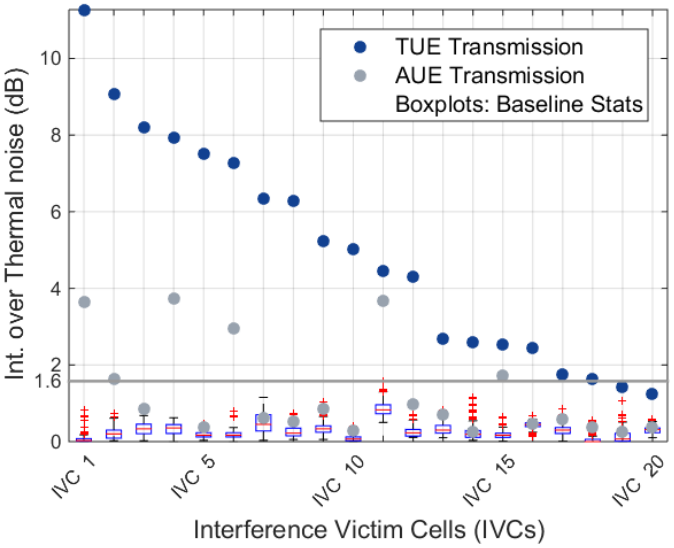

Fig. D.2: Interference over Thermal Noise (IoT) per Interference Victim Cells (IVCs). IVCs indexes are ranked by higher IoT values.

by the higher IoT in the AUE test. The same figure shows the boxplots for the IoT distribution in the baseline data for each IVC. The IoT reference line at 1.6 dB marks the highest IoT baseline value observed. It is possible to see that the IoT caused by the AUE is much higher than that caused by a similar transmission at ground level. For instance, only in 6 cells the IoT caused by the TUE is above the 1.6 dB reference line, while 18 cells exceed this threshold for the AUE transmission. The average IoT increase is 3.7 dB, with peaks between 7.1 and 7.7 dB (IVCs 1, 2, 3 and 5), in spite of the downtilted antennas, which should partially reject the transmission received from the UAV.

Fig. D.3 shows the spatial distribution of the IVCs on the map. IVCs 7, 18 and 19 are located behind a hill from the test location perspective, and interference prediction tools would not account for harmful signal levels originated by the test location. This effect will be especially important for interference prediction in urban areas, where buildings are accounted for significant interference containment.

Predefining the set of neighbor cells for interference coordination will be difficult as results indicate the set of impacted cells varies with height. Moreover, optimizing a coordinated scheduling for AUE over such a large set of impacted cells would lead to significant reduction in overall resource availability in the network. Besides, it may be too complex to be performed

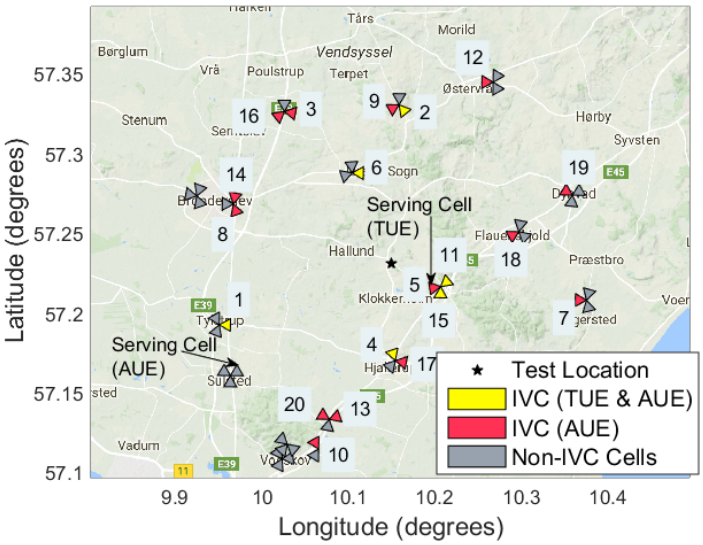

Fig. D.3: IVC cells map distribution. Numbers identify the IVC index.

in real time, especially when several UAVs are using broadband services at the same time. This paper analyses two strategies to mitigate the interference caused by an AUE without dealing with resource coordination: 1) cruise height control and 2) directional antennas transmission.

The radio reports collected by the UE may provide valuable information to estimate the IoT reduction that can be achieved by both techniques. The DL RSRP seems to provide good estimation for the coupling losses between UE and surrounding cells, despite the frequency duplexing [8]. Fig. D.4 shows how DL RSRP measurements correlate to IoT values, for the cells the phone was able to detect. It is possible to see that the regression line performs a good estimation for the potential UL interference power. It is important to note that cells outside the monitored area were also detected by AUE with high RSRP. The most significant case was observed at a cell located approximately 30 km from the test location, whose median RSRP of -97 dBm estimates an IoT of about 8 dB.

Results in [4] and [6] indicate increasing UAV height tend to decrease DL interference. Assuming the network and the AUE can negotiate the cruise height, constrained to UAV's application requirements, it is possible to reduce the interference power in both UL and DL. In this letter it is estimated the UL IoT reduction obtained by decreasing AUE's height to 50 and 25 m. For this calculation, it is first estimated the path loss difference between 100

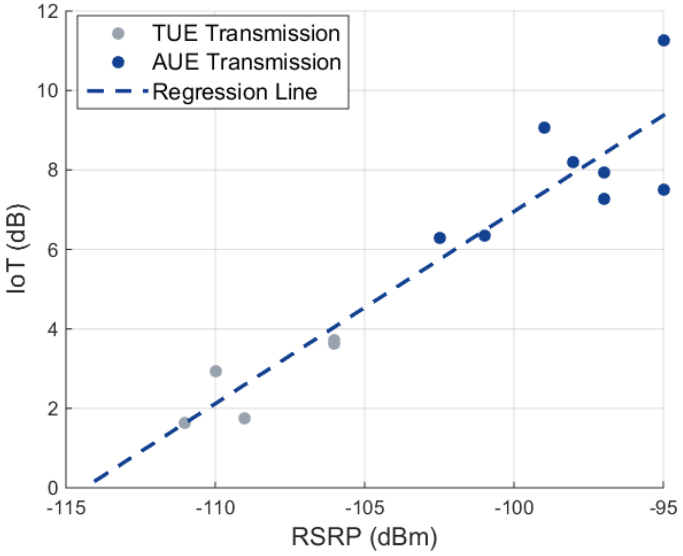

Fig. D.4: IoT versus downlink reference symbol received power (RSRP) from neighbor cells.

m (test height) and the two target heights (50 m and 25 m) using the channel model proposed in [5]. Then, the IoT reduction correspondent to such decrease in received power is estimated by applying the linear relation given by the slope of the line in Fig. D.4. No changes in BSs's antenna gains are considered, as changes in the elevation angle are assumed negligible due to the distances between most IVCs and the test location (>10 km) [13]. If this calculation results in a very low estimated IoT for a given cell, the baseline median for that cell is used as a lower boundary to account for residual IoT in the network.

Results are shown in Fig. D.5, where it is possible to see that lower AUE heights lead to smaller IoT at the IVCs. At 50 m, the estimated IoT is on average 2.1 dB higher than the values measured for the TUE. This value decreases to 0.9 dB at 25 m. Nevertheless, this solution reduces the serving cell RSRP that would drop from -94 dBm, at 100 m, to -99 dBm (50 m) and -104 dBm (25 m), which indicates a trade-off between interference and AUE throughput.

The other solution relies on the fact most commercial UAVs are not restricted to small form factor and therefore they may deploy an array of antennas with directional pattern to mitigate the UL and DL interference with the advantage of causing minor impact on the serving cell signal. To evaluate this potential, it was estimated the IoT reduction obtained by applying the

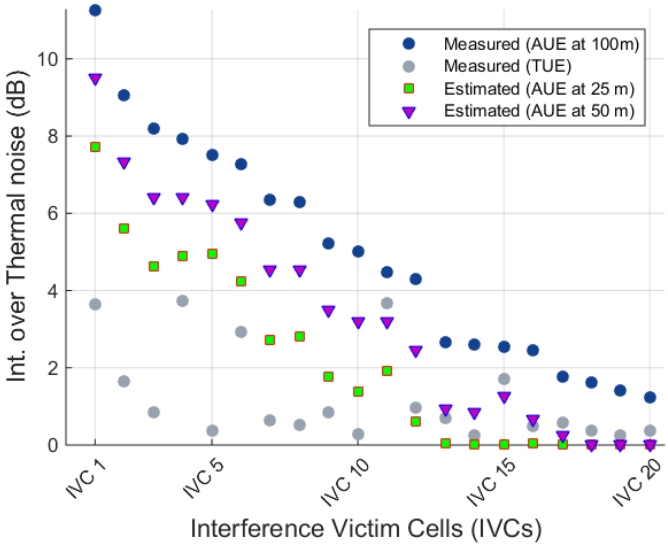

Fig. D.5: IoT measured in the tests compared to estimated values obtained for AUE at 25 and 50 m. The estimations consider the differences in path loss for different heights in the channel model proposed in [5].

directional antenna pattern suggested in [2] and shown in eq. D.1 (in dB). In this equation, the main direction, $\theta = 0°$, is the direction of maximum antenna gain, G_{max}, set to 0 dB, and θ_{3dB} is the half-power beam width.

$$G(\theta) = G_{max} - \min\left[12\left(\frac{\theta}{\theta_{3dB}}\right)^2, 20\right] \tag{D.1}$$

Results were estimated considering a wide-beam case where $\theta_{3dB} = 70°$ and a perfect alignment, that means the UAV antenna main direction point towards the serving cell. Results in Fig. D.6 show significant IoT reduction obtained with the use of directional antennas in the AUE. The IoT values are similar to that observed by the TUE transmission, with an average difference of 0.3 dB. Additionally, as the effective transmit power in the main direction is the same of the reference case, the throughput towards the serving cell will remain unchanged. However, the directional beam can not prevent high interference levels at cells located close to the serving cell, for example IVC 1 (see Fig. D.3). Furthermore, estimations show the applied wide beam is robust to misalignment up to $\pm 15°$ from the perfect alignment direction.

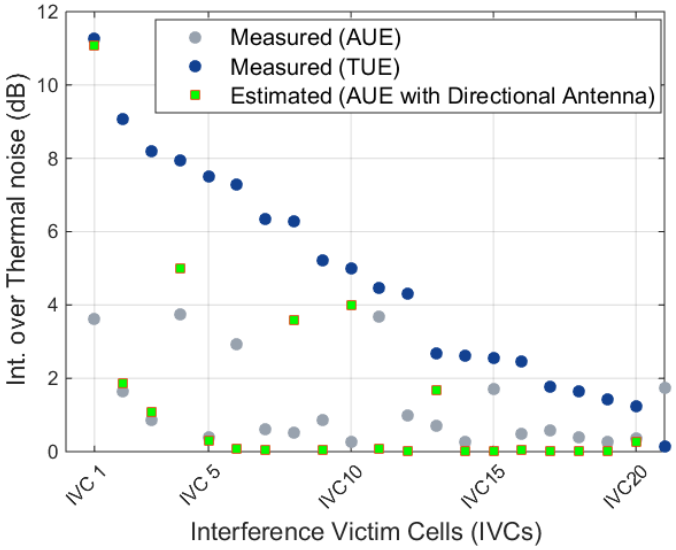

Fig. D.6: Measured IoT versus the estimated IoT from introducing a directinoal antenna model on the AUE.

IV Conclusion

This paper presents one of the challenges of having UAVs connected to the LTE cellular networks. Measurements were conducted by having a test phone transmitting full-buffer data at two heights, 1.5 m and 100 m. Results show similar UL transmit power and allocated resources, but the UAV at 100 m tends to cause significantly more interference than the UE at 1.5 m. The UAV causes an interference over thermal noise (IoT) 3.7 dB higher on average than that caused by the terrestrial UE. The differences in IoT peak at between 7 and 8 dB, with high interference measured in cells up to 14 km away, but results indicate this distance may be as high as 30 km. Both the UAV cruise height control and the use of directional antennas at the UAV side showed potential to reduce the interference caused by UAVs to values comparable to those observed due to a terrestrial UE. The latter seems to be more promising at it can be achieved without reducing the user throughput.

Acknowledgment

This research has received funding from the SESAR Joint Undertaking under the European Union's Horizon 2020 research and innovation programme,

grant agreement No 763601. The research is conducted as part of the DroC2om project. Authors would also like to acknowledge the contribution of Steffen Hansen and Daniel Kappers to the UAV flights.

References

[1] Qualcomm, "Evolving cellular technologies for safer drone operation," Qualcomm Technologies Inc., White Paper, Oct. 2016.

[2] 3GPP, "Enhanced LTE support for aerial vehicles," 3rd Generation Partnership Project (3GPP), Technical Specification (TS) 36.777, Jan. 2018, version 15.0.0.

[3] B. Galkin, J. Kibilda, and L. A. D. Silva, "Coverage Analysis for Low-Altitude UAV Networks in Urban Environments," in *Proc. IEEE Glob. Commun. Conf.*, Singapore, Dec. 2017, pp. 1–6.

[4] B. V. D. Bergh, A. Chiumento, and S. Pollin, "LTE in the sky: trading off propagation benefits with interference costs for aerial nodes," *IEEE Commun. Mag.*, vol. 54, no. 5, pp. 44–50, May 2016.

[5] R. Amorim et al., "Radio Channel Modeling for UAV Communication Over Cellular Networks," *IEEE Wireless Commun. Lett.*, vol. 6, no. 4, pp. 514–517, Aug. 2017.

[6] M. M. Azari et al., "Coexistence of Terrestrial and Aerial Users in Cellular Networks," in *Proc. IEEE Glob. Commun. Conf. Workshops*, Singapore, Dec 2017, pp. 1–6.

[7] I. Kovacs et al., "Interference Analysis for UAV Connectivity over LTE Using Aerial Radio Measurements," in *Proc. IEEE 86th Veh. Tech. Conf. (VTC Fall)*, Toronto, Canada, Sept. 2017, pp. 1–6.

[8] Qualcomm, "LTE Unmanned Aircraft Systems Trial Report," Qualcomm Technologies Inc., White Paper, May 2017.

[9] M. Mozaffari et al., "Unmanned Aerial Vehicle With Underlaid Device-to-Device Communications: Performance and Tradeoffs," *IEEE Trans. on Wireless Commun.*, vol. 15, no. 6, pp. 3949–3963, June 2016.

[10] A. Al-Hourani, S. Kandeepan, and A. Jamalipour, "Modeling air-to-ground path loss for low altitude platforms in urban environments," in *Proc. IEEE Glob. Commun. Conf.*, Austin, USA, Dec. 2014, pp. 2898–2904.

[11] H. C. Nguyen et al., "How to Ensure Reliable Connectivity for Aerial Vehicles Over Cellular Networks," *IEEE Access*, vol. 6, pp. 12 304–12 317, 2018.

[12] 3GPP, "Evolved Universal Terrestrial Radio Access (E-UTRA); Physical channels and modulation," 3rd Generation Partnership Project (3GPP), Technical Specification (TS) 36.211, Dec. 2009, version 8.9.0.

[13] A. Al-Hourani and K. Gomez, "Modeling Cellular-to-UAV Path-Loss for Suburban Environments," *IEEE Wireless Commun. Lett.*, vol. 7, no. 1, pp. 82–85, Feb. 2018.

Paper E

Interference Analysis for UAV Connectivity over LTE Using Aerial Radio Measurements

I. Kovacs, R. Amorim, H. C. Nguyen, J. Wigard and P. Mogensen

The paper has been published in the
IEEE 86th Vehicular Technology Conference (VTC-Fall) 2017.

© 2017 IEEE
The layout has been revised and reprinted with permission.

Abstract

The use of Unmanned Aerial Vehicles (UAV) for civilian and commercial services has experienced a significant increase in the past couple of years. Emerging UAV enabled services, however, require extended beyond-visual-line-of-sight geographical range. One key regulatory requirement for these services is that the radio communication link must reliably cover a wide(er) area, when compared to the visual-line-of-sight range radio links currently used. Standardized cellular systems such as Long Term Evolution UMTS (LTE), are an obvious candidate to provide the radio communication link to UAVs. In this paper, we use empirical measurements in live rural LTE networks to assess the impact of uplink and downlink radio interference on the UAV radio connectivity performance. Further, we provide a baseline analysis on the potential of interference mitigation schemes, needed to provide a reliable radio connectivity to the UAVs.

I Introduction

Small and medium Unmanned Aerial Vehicles (UAV) have rapidly became a commercial success in the past couple of years due to relatively low price tags, easy operation and many vendors offering various solutions [1]. Therefore, regulatory actions have been triggered in almost all markets to ensure the safe operation of UAVs. For typical UAV use, without special regulatory permissions, there are three key regulatory requirements [2–4]: i) visual-line-of-sight (VLOS) to the operator controlling the UAV, ii) maximum flight altitude allowed and, iii) 'no-flight' exclusion zones where UAV operations are not allowed.

The wireless remote control of the UAVs is generally using short (up to 200m) or medium (up to 1km) range radio communication technologies, such as WLAN or its proprietary variants, typically operating in unlicensed frequency bands. Many of the emerging commercial applications target large(r) scale operations, up to 100's of km, such as for oil/gas pipeline or power line surveillance purposes [1]. Although, the WLAN-based technologies can also provide longer radio range operation, going beyond-visual-line-of-sight (BVLOS), wide geographical areas are still difficult and expensive to service with these technologies and, most of the time, require special regulatory permission [2–4].

Recently, there have been several studies reported analyzing radio connectivity to small/medium UAVs using (existing) cellular networks and standardized technologies, such as LTE or LTE-Advanced [5–14]. The cellular approach has significant advantages over today' s solutions: i) provides truly wide area radio coverage, ii) the quality of the radio communication link can be fully controlled and, iii) large scale control and tracking of the UAVs can be

integrated and provisioned via a specialized regional or country traffic management service. Using cellular networks to communicate with airborne devices comes, however, with certain challenges. Outdoor cellular networks are planned and typically optimized to provide the best possible service to user devices located at ground level, or at low elevations relative to the deployed network antenna. Hence, signal coverage and interference at higher altitudes, where typical UAVs operate, need to be carefully investigated [6–13].

In this paper, we address one of the key radio communication challenges for UAV connectivity over LTE: interference. We approach the problem from an empirical point of view and use radio measurements from a live LTE cellular networks, performed with an airborne UAV [7,9]. The main contributions of our work, compared to results reported earlier in [5,7], are the investigation of four different rural radio scenarios and the estimation of interference mitigation versus the UAV flying height. In Section II we provide a summary of these radio channel measurements. Section III presents the interference scenario characterization and analysis based on the radio measurement data. In Section IV we provide the estimated upper bound performance gain when applying selected interference mitigation techniques, available today in LTE/ LTE-Advanced networks. In Section V we discuss the results in relation to the previous studies and highlight standardization aspects. Conclusions and future work are outlined in Section VI.

II UAV Radio Measurements

A. Investigated radio scenarios

The UAV radio channel measurements have been performed in Southern Denmark, on October 2016, in two different locations, 7 km apart from each other, as depicted in Fig. E.1. The measurements were conducted in two different live operating LTE networks in the 800 MHz band, with base station heights ranging from 19 to 50 m, and electrical antenna down-tilt angles between 0o and 9o. The radio environment is characterized by typical Danish rural buildings with average heights below 10 m and a terrain profile with varying heights between 30 and 80 m [7].

B. Equipment

The measurements analyzed in this paper were collected with a Rohde & Schwarz mobile network scanner [14] mounted underneath a commercial hexacopter drone, remote controlled by a licensed pilot via a traditional WLAN radio link. A vertical oriented dipole receiver antenna with approx. 60o beam-width was used. The network scanner's sampling rate was between 5 to 9 Hz, depending on the number of cells detected. The equipment

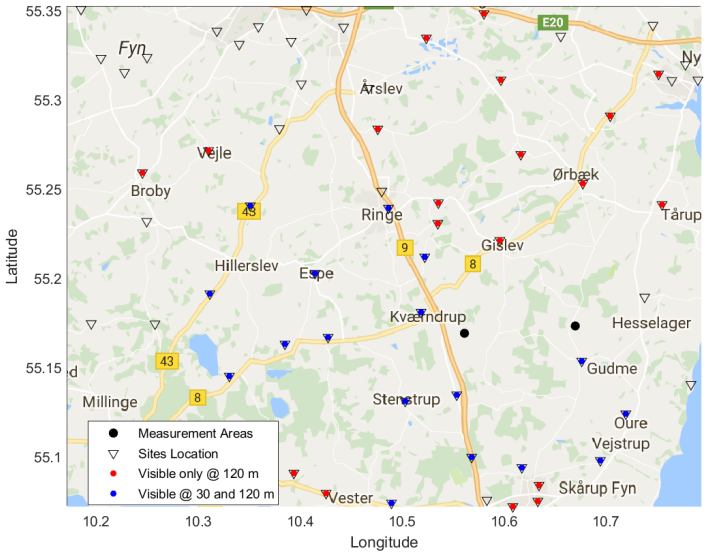

Fig. E.1: Live rural LTE cellular network layout utilized for the UAV radio measurements.

is capable to record the LTE standard compliant Physical Channel Indicator (PCI) and Reference Signal Received Power (RSRP), per resource element, values, from up to 32 different cells (frequencies), in each sampling time step. The RSRP and PCI from both network operators have been recorded simultaneously. The RSRP data has been used to investigate both downlink (DL, network-to-UAV) and uplink (UL, UAV-to-network) spatial and temporal interference patterns in each of the networks. For the purpose of this study, the recorded PCI values have been anonymized and translated to unique cell indices.

C. Measurement Campaign

In each measurement location, the UAV was flying at approximately 25 km/h in circular paths of 500 m of diameter, once at each constant height at 15, 30, 60 and 120 m above the takeoff position altitude. Additional drive tests have been performed in the same areas at the same speed, with the same radio network scanner, with the mobile antenna mounted at 1.5 m height, on top of a driving car. To estimate the average path loss between the LTE cells and the UAV locations, the measured downlink RSRP values have been used combined with the transmit power information of the radio cells from the two operator networks. The serving cell is selected based on the strongest mea-

sured RSRP. All other received co-channel RSRP values are then considered as interfering signals when no interference mitigation is applied.

III Interference Analysis

We characterize the measured rural scenarios by extracting the mean LTE site deployment density (inter-site distance) and the estimated probability, during the performed UAV flights, to have an average downlink signal-to-interference ratio (SIR) at the UAV-UE below 0 dB. The former parameter can be derived from the publicly available network geo-data in the region of interest [15]. The SIR is calculated for each time step, under the assumption of full interference in the frequency band of each of the networks, according to the formula E.1.

$$SIR_0 = 10\log_{10}\left(\frac{RSRP_{sci}}{\sum_{k=1,k\neq sci}^{N} RSRP_k}\right)[dB] \tag{E.1}$$

where the serving cell index is sci and the total number for detected (recorded) cells is N, at a given UAV height. As an example, Figure E.1 indicates the set of cells which have been detected and measured at different UAV heights. The SIR_0 metric is calculated for each time step during the UAV flights.

While the full interference SIR_0 metric might not be totally representative for real-life operation of UAV-UE, because of different carrier loads and cell selection mechanisms, it does help us in our first step to characterize the scenario. We used the 0 dB SIR 'threshold' assuming that this is the maximum downlink SIR where any downlink interference mitigation scheme could be needed. We exclude the receiver noise from the (downlink and uplink) analysis due to being predominantly in interference-limited scenarios. The four distinct rural radio sub-scenarios identified are summarized in Table E.1.

Table E.1: Monitored Cells Information

Sub-scenarios investigated (all UAV heights)	**Probability for DL SIR_0 below 0dB**	
	High (> 20%)[1]	**Low (< 20%)**
"Dense" rural: average ISD = 2.2 km	Sub-scenario #1	Sub-scenario #2
"Sparse" rural: average ISD = 3.8 km	Sub-scenario #3	Sub-scenario #4

[1]The 20% probability limit was observed in the measurement data analysis

A. Downlink (Network-to-UAV)

A typical metric used to characterize the DL interference in cellular networks is the dominant interference ratio (DIR), defined as the ratio between the power of the dominant (strongest) interfering signal (cell index *dici*) and the sum power of all other interfering signals, when no interference mitigation is applied [16].

$$DIR = 10\log_{10}\left(\frac{RSRP_{dici}}{\sum_{k=1,k\neq sci,k\neq dici}^{N} RSRP_k}\right)[dB] \tag{E.2}$$

where DIR values correspond also to *full interference* assumption.

Fig. E.2 presents a summary of the four sub-scenarios in terms of time-averaged (over all time steps) SIR_0 E.1 and DIR E.1. It is immediately evident that UAV UE locations at 15 to 120 m heights are experiencing significantly different SIR_0 and DIR compared to the ground UEs at 1.5 m height. It can also be observed that the channel conditions change vs. UAV height, which indicates that the performance of interference mitigation schemes would also be different at different UAV heights. These results also provide a strong motivation for a new channel modeling approach which is UAV height dependent [9].

To get more insight into the UAV radio channel behavior, Fig. E.3 and Fig. E.4 show, for two of the UAV heights, the time traces of the serving and dominant interfering cell indices, along with time traces for the estimated SIR_0 and corresponding DIR.

The first observation we make is on the range of the DIR values, between -9 dB and +9 dB at 15 m UAV height, and between -10 dB and -4 dB at 120 m UAV height. This indicates that in these UAV scenarios there might not always be one clear 'dominant' interfering cell and instead several cells contribute equally to the received interference. Second, for both UAV flight heights, it is clearly visible that the dominant interfering cell can change between consecutive time steps, as expected. In Figure E.5 we summarize the cell change rates of the serving cell and the dominant interfering cell. The absolute values for this metric clearly depend on the selected flight path and speed of the UAV. In our experiments the UAV flight path and speed were kept constant at each height. While only the low SIR_0 sub-scenarios (#1 and #3) show high rates for serving cell changes, in all sub-scenarios the interfering cell change rates are relatively high and decreases versus the increasing UAV height. These results have a direct impact on the practical performance gain of network based interference mitigation schemes as detailed in Section A..

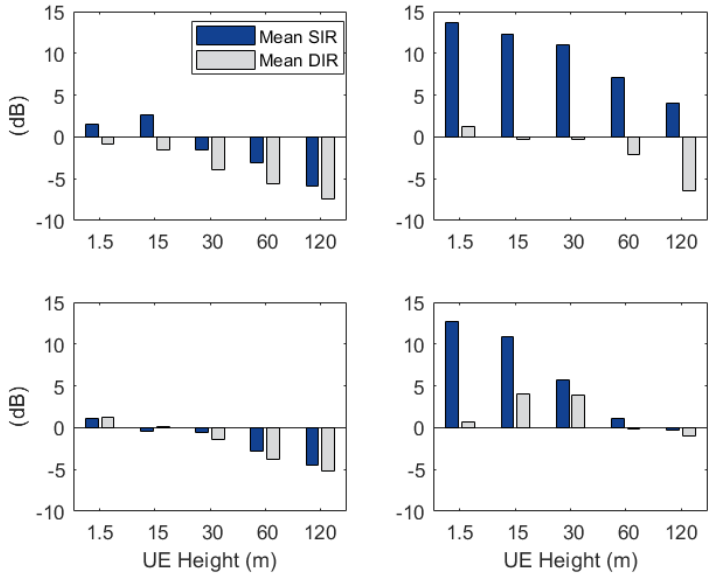

Fig. E.2: Summary of the the estimated full load downlink SIR_0 and DIR in the investigated sub-scenarios (see Table E.1 for row-column layout).

B. Uplink (UAV-to-Network)

The key metric we extract in this uplink analysis is the received interference power levels from any UAV location as received in the $k-th$ non-serving cells in each time step, $P_{RX0,k}$. The UL received signal power is estimated using the total coupling-loss (CL) values, estimated as described in Section C., and the standard 3GPP LTE UL open loop power control (OLPC) mechanism in the serving cell [17]. For simplicity, we assume a maximum UE transmit power per LTE subcarrier of P_{TXMAX}=12.2 dBm (23 dBm per physical resource block) and OLPC parameters set to P_0 = -90.8 dBm and α = 0.8.

$$P_{Rx0,k}(RX0,k) = min(P_{TXMAX}, P_0 + \alpha.Cl_{sci}).CL_k[dBm] \tag{E.3}$$

The UL SI(N)R cannot be analyzed directly, as we have not measured actual UL LTE transmissions from other UEs. The serving cell is determined using the same procedure as described in Section A.. Figure E.6 shows the box-and-whiskers statistics for the received power statistics for ground UE locations and three UAV UE heights. The serving cell (S) and the top 10 most interfered cell (DI1 to DI10) are included. The uplink interference power levels are in the range between -120 dBm and -110 dBm at ground UE and 15m UAV height, and between -110 dBm and -105 dBm at 120 m UAV

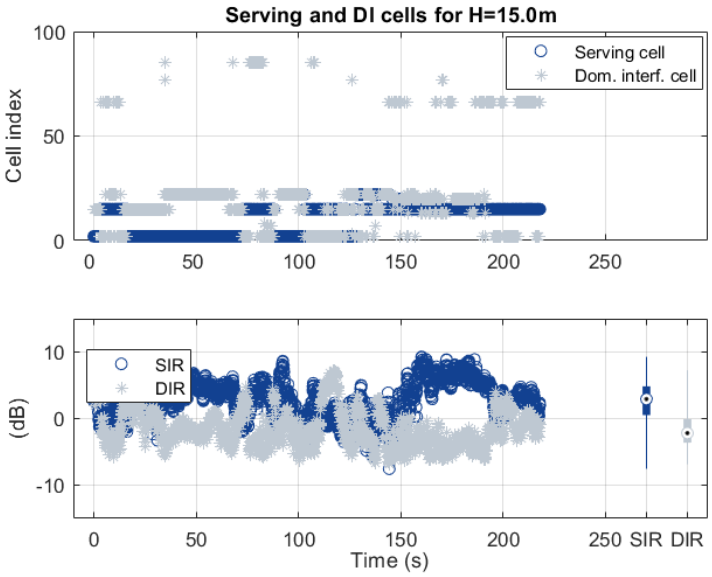

Fig. E.3: Example downlink time traces for UAV flying at H=15m height, in sub-scenario #1 (see Table E.1).

height. Up to UE heights of 15 m there are 4 interfered cells within 10 dB below the average serving cell power level. However, at 120m UAV height all 10 interfered cells are within this 10 dB range. This indicates that an UL UAV transmission will likely have a strong impact on a larger number of neighboring cells. The implications of these observations are discussed further in Section B..

Figure E.7 presents a summary of the UL average received power at serving cell and at the 3 most interfered cells. We can note that although the sub-scenarios have been 'defined' based on downlink SIR_0 (see Table E.1), there is a very good correlation between the downlink (Figure E.2) and uplink (Figure E.7) radio channel metrics in each of the sub-scenarios. In the low SIR_0 sub-scenarios (#1 and #3) the uplink interference is stronger and the first 3 most interfered cell experience similar interference power levels. However, in the high SIR_0 sub-scenarios (#2 and #4) the uplink power level at the most interfered cell is generally 5-10 dB higher compared to the next interfered cells.

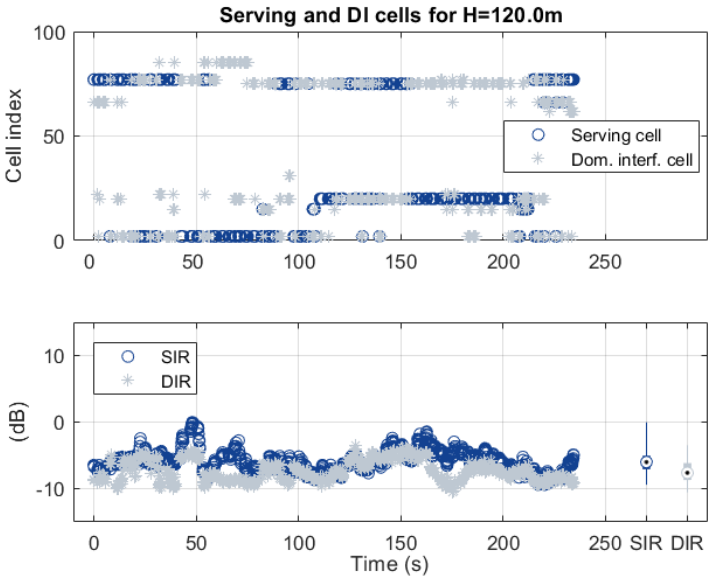

Fig. E.4: Example downlink time traces for UAV flying at H=120m height, in sub-scenario #1 (see Table E.1).

IV Interference Mitigation

In this section, we evaluate the upper bound gains for the most common DL and UL interference mitigation techniques available in today's LTE-Advanced networks. Inter-cell interference coordination (ICIC), beamforming and macroscopic diversity techniques are discussed in Section V.

In general, any DL SIR gain (SIR_{gain}) or UL received power gain (P_{RXgain}) from an interference mitigation scheme would provide sufficient system level gain only when is applied to a sufficiently high number of UE or eNB transmissions. Further, the performance gains are mostly achievable when the initial interference levels are sufficiently high and/ or received power levels are low. We translate these two conditions into two simple conditional probability metrics:

- DL: *Probability to achieve SIR gain of at least 3 dB conditioned by an initial-SIR of maximum 0 dB (set based on Figure E.2):*

$$\begin{aligned} Prob_{DLIM-gain} &= Prob(SIR_{gain} > 3dB | SIR_0 \leq 0dB) \\ \text{with} \quad SIR_{gain} &= SIR_{IM} - SIR_0 \quad [dB] \end{aligned} \tag{E.4}$$

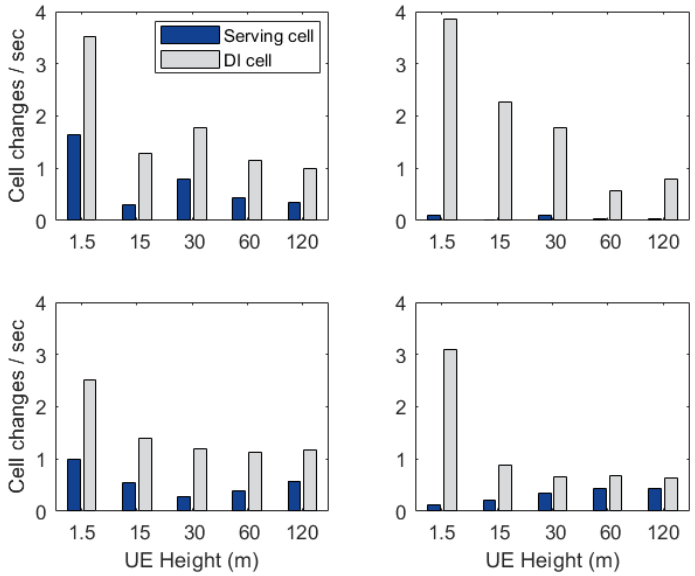

Fig. E.5: Summary of the the estimated cell change rates in the investigated sub-scenarios (see Table E.1 for meaning of row-column layout)

- UL: *Probability to achieve signal power gain of at least 3 dB conditioned by an initial received subcarrier power of maximum -105 dBm (set based on Figure E.7).*

$$\begin{aligned} Prob_{ULIM-gain} &= Prob(P_{RXgain} > 3dB | P_{RX0} \leq -105dBm) \\ \text{with} \quad SIR_{gain} &= P_{IM} - P_{RX0} \quad [dB] \end{aligned} \tag{E.5}$$

These gain probability metrics are analyzed in the next sections for different interference mitigation schemes, IM.

A. Downlink Interference Mitigation

For DL interference mitigation, we look at interference rejection combining (IRC) with ideal rejection at the UE [16], and joint cooperative multi-point transmission (JT-CoMP) with coherent combining [18]. These are simplified models and yield, of course, only an upper bound for the achievable SIR gain. There are four cases analyzed in each of the four sub-scenarios (see Table I), corresponding to when the first 1, 2, 3, or 4 strongest interfering signals (cell indices $i1$, $i2$, $i3$ and $i4$) are cancelled out (rejected), in case of the IRC scheme,

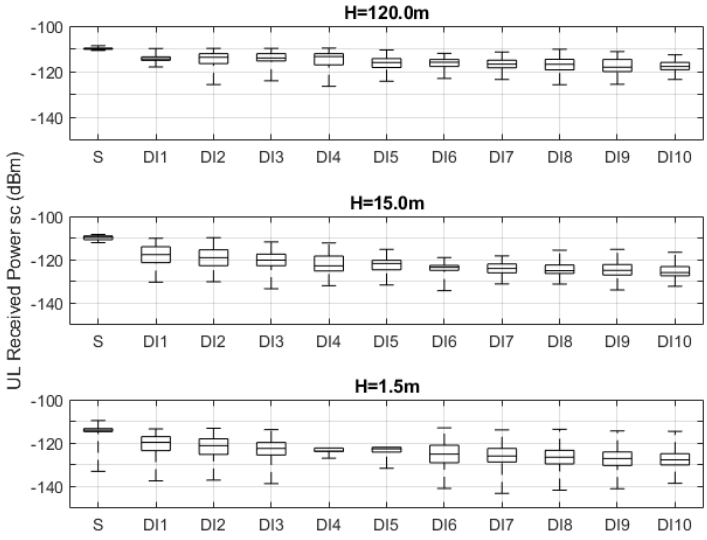

Fig. E.6: Example uplink received power statistics for ground UE locations (1.5m) and two UAV UE heights (15m and 120m), in sub-scenario #1 (see Table E.1). S: serving cell; DI1 to DI10: the top 10 most interfered cells.

according to E.6 or, are coherently combined, in case of the JT-CoMP scheme, according to E.7.

$$SIR_{DLIRC,i1...i4} = 10\log_{10}\left(\frac{RSRP_{sci}}{\sum_{k=1,k\neq sci,k\neq i1...i4}^{N} RSRP_k}\right) \tag{E.6}$$

$$SIR_{JTCoMP,i1...i4} = 10\log_{10}\left(\frac{RSRP_{sci} + \sum_{k=i1...i4} RSRP_k}{\sum_{k=1,k\neq sci,k\neq i1...i4}^{N} RSRP_k}\right) \tag{E.7}$$

UE Interference Rejection

Figure E.8 presents the DL IRC SIR gain probability metric (ProbDLIRC-gain) in the four sub-scenarios, calculated using E.1, E.4 and E.6. We can immediately see the impact of the average SIR_0 and DIR values depicted in Figure E.2. First, cancelling out only the dominant interfering signal is insufficient, but it can help to a certain degree in sparse networks with low SIR_0 (mostly at higher UAV heights, sub-scenario #4). Second, to experience any significant likelihood for IRC gains, 3 or 4 interfering signals need to be cancelled

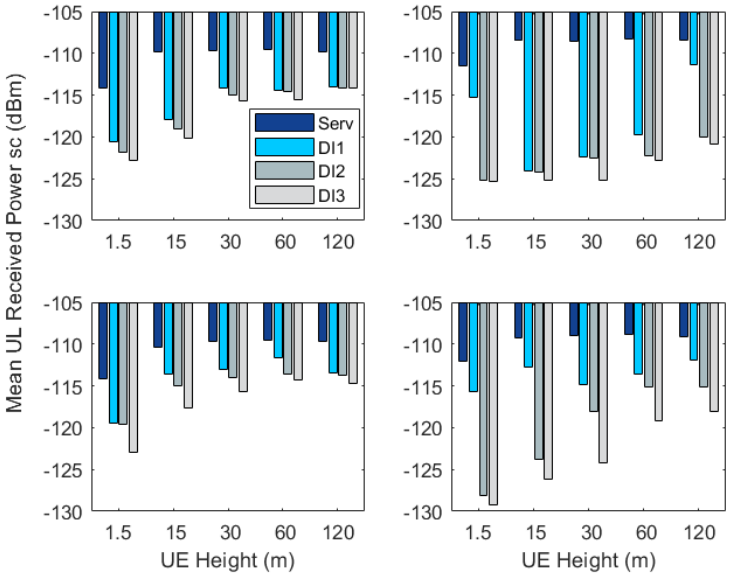

Fig. E.7: Summary of the uplink average received (subcarrier) power levels in the investigated sub-scenarios (see Table E.1 for meaning of row-column layout)

out at the UE side. The 'outlier' result in sub-scenario #1 at 15 m is explained with the results in Figure E.2: combination of higher SIR_0 and lower DIR at 15m compared to 1.5 m height. The practical performance of the DL IRC schemes is not expected to be impacted by the dominant interfering cell changes (Figure E.5) if the UE receiver algorithm can estimate the interference signal.

Network JT-CoMP

Figure E.9 summarizes the JT-CoMP SIR gain probability metric (ProbJTCoMP-gain) in the four sub-scenarios, calculated using E.1, E.4 and E.7. Note the correlation between the cases with low average DIR combined with low SIR in Figure E.2, and the JT-CoMP gain vs. number of cooperating cells in Figure E.9. In the low SIR_0 sub-scenarios (#1 and #3), whenever the DIR is close to 0 dB, a 2-cell JT-CoMP (1 serving + 1 cooperating) is sufficient to achieve the maximum gain. Cooperation of one additional cell is sufficient to achieve maximum gain also for UAV heights above 30m. Only in one of the high SIR_0 sub-scenarios (#2) gain from JT-CoMP is achievable, and only for UAV heights above 60m, with the cooperation of 2-3 cells.

The practical performance of the DL JT-CoMP scheme is impacted by

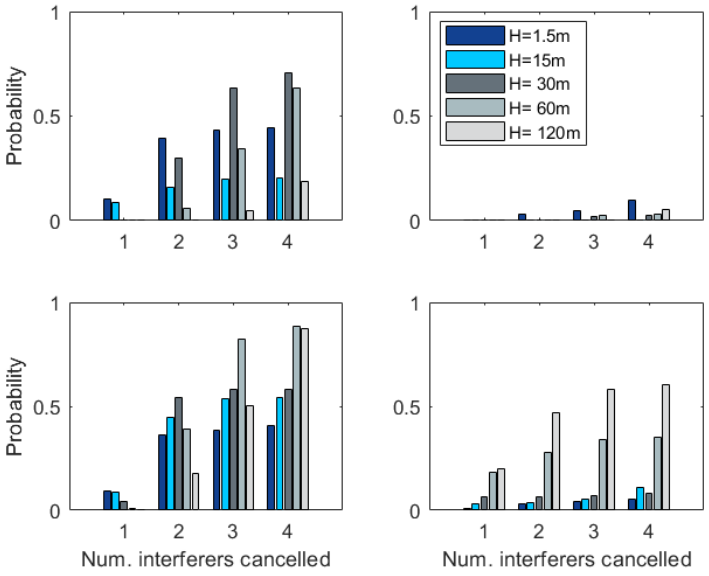

Fig. E.8: Summary of the the DL IRC 3dB SIR gain probability results in the investigated sub-scenarios (see Table E.1 for meaning of row-column layout)

the changes in the dominant interfering cells (Figure E.5), any change in the cooperating cell set requires signaling between the involved cells, and the resulting transmission delays can easily negate the JT-CoMP gains. While, this aspect certainly requires a more detailed study, it is important to know the expected upper bound performance from DL JT-CoMP like schemes. rr

B. Uplink Interference Mitigation - Network JR-CoMP

For UL interference mitigation, we look at joint cooperative multi-point reception (JR-CoMP) with coherent combining [17]. Like in the downlink, the (idealistic) assumption we use for JR-CoMP is that the signals received at the 1, 2, 3 or 4 most interfered cells can be coherently combined.

$$P_{JRCoMP,i1...i4} = 10\log_{10}\left(RSRP_{sci} + \sum_{k=i1...i4} RSRP_k\right) \quad [dBm] \tag{E.8}$$

Figure E.10 summarizes the JR-CoMP signal gain probability metric (ProbJRCoMP-gain) in the four sub-scenarios, calculated using E.2, E.5 and E.8. The first notable result is that cooperation of 2 cells is insufficient to achieve the target 3 dB gain. The reasons are the relatively large difference between received

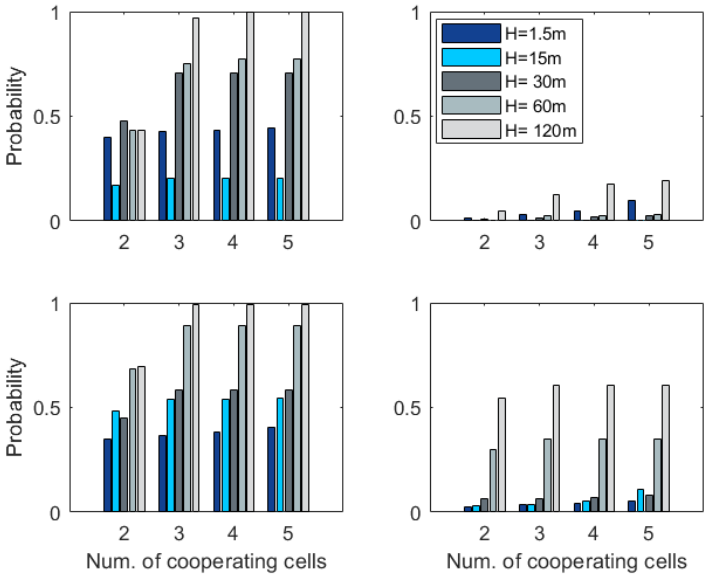

Fig. E.9: Summary of the DL JT-CoMP 3dB SIR gain probability results in the investigated sub-scenarios (see Table E.1 for meaning of row-column layout)

power levels between the serving cell and the most interfered cells, see Figure E.7. The gain probabilities start to be significant when 3 or 4 cells are used and, mostly for UAV heights above 30m. Further, in the scenarios with low interference (sub- scenario #2 and #4, Figure E.7) the JR-CoMP scheme generally does not provide significant gain for UAV heights below 60m, while at least in certain rural locations, it can still be useful for UAV heights above 60m. Note that, in case of JR-CoMP, the cells required to cooperate can be selected based on the "most interfered cell" approach like what we have used in Section B. and Figure E.6. This means that there is likely no need for frequent re-configuration of the cell sets involved in the joint reception scheme, thus signaling overhead (delays) can be minimized.

V Discussions

Like the previous studies [5,6], our investigation also show that in downlink (network-to-UAV), several dominant interfering signals can be detected by a UAV. These interference scenarios potentially require, either a more complex interference cancelling receiver at the UAV and/ or, a downlink multi-cell cooperation scheme involving a minimum of 2-3 cells. The IRC and JT-CoMP

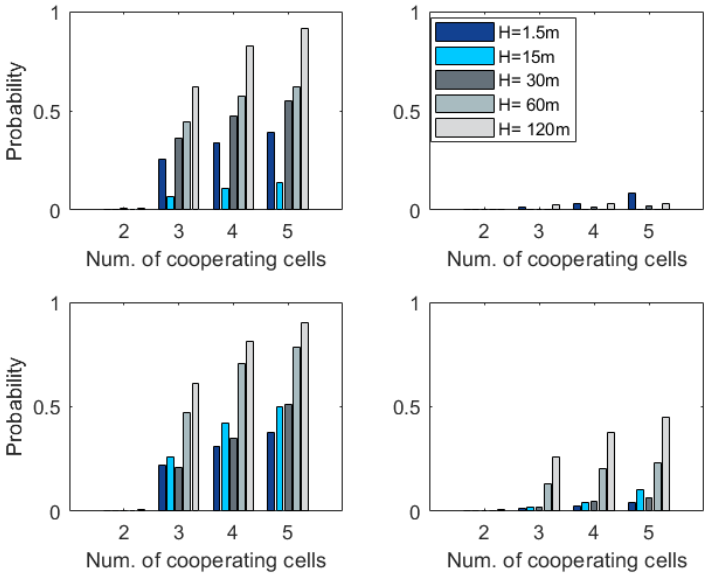

Fig. E.10: Summary of the UL JR-CoMP 3dB gain probability results in the investigated sub-scenarios (see Table E.1 for meaning of row-column layout)

schemes evaluated in this paper show high potential gains, depending on the network deployment density and UAV location, even in the same rural scenario. Receive beamforming at the UE side can be utilized in combination or as alternative to the IC, depending on the UE complexity. The practical DL JT-CoMP gains depend on the selection of the cooperating cells. In case of UAVs, our results show that the rate of change in the interfering cells decreases vs. UAV height so it becomes easier to achieve reasonable JT-CoMP gains compared to scenarios with ground level UEs. Based on the same observations, downlink coordinated scheduling or coordinated beamforming [17] have certainly practical potential in the UAV scenarios. Downlink inter-cell interference coordination and macroscopic diversity, have been extensively studied for ground UE scenarios in [18,19]. For UAV scenarios, the same techniques could still be applied, but require further investigations due to the different propagation conditions (fast fading, path loss, slow fading).

In uplink (UAV-to-network), our results show that the number of interfered cells almost doubles in case of UAVs compared to the ground locations. To mitigate this interference, either JR-CoMP or beamforming (UE and/or network) techniques will be required. Our results disclosed that a minimum of 3-cells JR-CoMP is needed for the gains to be sufficiently high.

Another technique to be considered in further investigations to improve

the UAV radio link reliability is the radio network diversity, where the macroscopic diversity is applied between the at least two separate networks or frequency layers.

Clearly, further work is required to provide detailed analysis and appropriate solutions for UAV radio communications when using existing LTE networks. At the time of writing this paper, the 3rd Generation Partnership Project (3GPP) has just started standardization activities in this area e.g., [8–13]. Our results in terms of the analyzed downlink and uplink interference mitigation gains provide a strong motivation for introducing a new, UAV height dependent channel modeling approach [9].

VI Conclusions

In this paper, we have presented an extensive analysis of the radio interference for UAV connectivity over LTE. We have used empirical radio channel measurements performed at ground level and four typical UAV heights (15, 30, 60 and 120m) where we have recorded the radio signal levels from two live LTE networks deployed in a typical rural area (Denmark). Based on the measurement data we have characterized the UAV scenarios in terms of typical downlink and uplink radio channel metrics, and we have estimated the potential gains from downlink and uplink interference mitigation techniques. Our results show that interference conditions at UAV heights change drastically compared to the typical ground level locations, for which the radio network has been optimized.

Future work must focus on detailed evaluation of interference mitigation schemes combined with radio resource management tailored to the expected UAV radio traffic. It is also part of future work to evaluate how the UAV radio traffic impacts the 'normal' ground level broadband traffic and overall radio capacity.

References

[1] M. Mazur and et all, "Clarity from above. pwc global report on the commercial applications of drone technology," PwC, Tech. Rep., May 2016.

[2] EUROCONTROL, "Roadmap for the integration of civil Remotely-Piloted Aircraft Systems into the European Aviation System," 2013.

[3] FAA, "Integration of civil unmanned aircraft systems (uas) in the national airspace system (nas) roadmap," Tech. Rep., 2013.

[4] , "Global Drone Regulations Database," https://droneregulations.info/, available March 30, 2017.

[5] Qualcomm, "Evolving cellular technologies for safer drone operation," Qualcomm Technologies Inc., White Paper, Oct. 2016.

[6] B. V. D. Bergh, A. Chiumento, and S. Pollin, "LTE in the sky: trading off propagation benefits with interference costs for aerial nodes," *IEEE Commun. Mag.*, vol. 54, no. 5, pp. 44–50, May 2016.

[7] R. Amorim et al., "Radio Channel Modeling for UAV Communication Over Cellular Networks," *IEEE Wireless Commun. Lett.*, vol. 6, no. 4, pp. 514–517, Aug. 2017.

[8] 3GPP TSG RAN WG1, "R1-1704429 – Requirements of Connectivity Services for Drones," Meeting #88bis, april 2017.

[9] ——, "R1-1704430 – Evaluation Scenarios and Channel Models for Drones," Meeting #88bis, april 2017.

[10] ——, "R1-1704431 – Interference Mitigation Aspects for Drone Connectivity," Meeting #88bis, april 2017.

[11] ——, "R1-1704701 - Preliminary results for interference distribution for aerial vehicles," Meeting #88bis, april 2017.

[12] ——, "R1-1705026 - System level performance and interference mitigation techniques for aerial vehicles," Meeting #88bis, april 2017.

[13] ——, "R1-1705163 - Consideration on the channel model for LTE-based aerial vehicles," Meeting #88bis, april 2017.

[14] Rohde & Schwarz, Mobile Network Testing, "R&S TSMA Autonomous Mobile network Scanner," june 2016.

[15] "Danish Mast Database," http://www.mastedatabasen.dk, available March 30, 2017.

[16] G. Pocovi, B. Soret, M. Lauridsen, K. I. Pedersen, and P. Mogensen, "Signal quality outage analysis for ultra-reliable communications in cellular networks," in *2015 IEEE Globecom Workshops (GC Wkshps)*, Dec 2015, pp. 1–6.

[17] 3GPP, " Evolved Universal Terrestrial Radio Access (E-UTRA); Physical Layer Procedures," 3GPP, Tech. Rep. TS 36.213 V14.2.0, Mar. 2017.

[18] D. Lee, H. Seo, B. Clerckx, E. Hardouin, D. Mazzarese, S. Nagata, and K. Sayana, "Coordinated multipoint transmission and reception in lte-advanced: deployment scenarios and operational challenges," *IEEE Communications Magazine*, vol. 50, no. 2, pp. 148–155, February 2012.

[19] V. F. López, K. I. Pedersen, and B. Soret, "Interference characterization and mitigation for different lte-a deployments," *EURASIP Journal on Wirelss Communications and Networking*, December 2015.

Paper F

Using LTE Networks for UAV Command and Control Link: A Rural-Area Coverage Analysis

Huan Cong Nguyen, Rafhael Amorim, Jeroen Wigard, István Z. Kovács, Preben Mogensen

The paper has been published in
IEEE 86th Vehicular Technology Conference (VTC-Fall) 2017.

© 2017 IEEE
The layout has been revised and reprinted with permission.

Abstract

In this paper we investigate the ability of Long-Term Evolution (LTE) network to provide coverage for Unmanned Aerial Vehicles (UAVs) in a rural area, in particular for the Command and Control (C2) downlink. The study takes into consideration the dependency of the large-scale path loss on the height of the UAV, which is derived from actual measurements, and a real-world cellular network layout and configuration. The results indicate that interference is the dominant factor limiting the cellular coverage for UAVs in the downlink: outage level increases from 4.2% at 1.5 m height to 51.7% at 120 m under full load condition. Lower network loads or larger inter-site distances reduces the interference and thus improves the coverage significantly: outage at 120 m is reduced to only 1.9% under network load of 25% for example. Similar effects are expected to be achievable by static or dynamic interference coordination schemes. In addition, ideal interference cancellation (IC) scheme with ability to remove completely the dominant interferer shows less effective for UAVs than for users on the ground. On the other hand, macro network diversity has very good potential for drones, as not only it improves the coverage, but also the reliability of the C2 link.

I Introduction

According to [1] the sales of consumer Unmanned Aerial Vehicles (UAVs) will increase tenfold by 2021. In [2] the commercial applications of UAV technology are allowing companies from agriculture to film-making industry to create new business and operating models, which in turn creates global market value estimated over $127.3 billion. This increasing interest in drones, as they also are called, is one of the best signs of how lower pricing can drive the Internet of Things (IoT). Currently regulations in most countries only allow for operating drones when there is visual line of sight (VLOS), but it is expected that beyond visual line-of-sight (BVLOS) operations will be allowed provided there is a reliable Command and Control (C2) link to the drone. This is very important to ensure safe drone operations: in the uplink, i.e. from a drone to base station (BS), the control link is used to update the Unmanned Aircraft System Traffic Management (UTM) or flight control unit with the drone location, plus potentially further information which the control function can utilize to make its decisions. And in the downlink (towards the drone), it allows the control function to change the the drone direction to avoid potential collisions, or to command a range of sensor/actuator functions on board of the drone.

One attractive means to provide this C2 link is to utilize the existing cellular networks, in particular the LTE systems. However, such a network is not designed for aerial coverage, since its base station (BS) typically uses

down-tilted antenna optimized for the ground users. Also the radio characteristics for drones are different than for users on the ground, as the higher the drone's altitude, the less blockage from buildings, vegetations, hills, etc it experiences. This positively affects the desired serving cell's signal as this will increase, but at the same time it will also boost the interference. This is reported in [3], where one of the biggest issues for cellular connectivity for drones is the interference the drones suffer at increasing height.

In this paper we quantify the ability of cellular networks to support the drone's C2 downlink by investigating a real-world LTE network in Fyn, Denmark. The area is chosen because it represents a typical rural area, where BVLOS operation is expected to be first granted due to less stringent safety and security requirements than in an urban scenario. Here a measurement campaign was performed to characterize the large-scale path loss and shadow fading properties for flying drones at different height. There are several similar works in literature, such as in [3,4]. But all of them are limited in measured distance and number of observations, and thus not usable to derive a statistically-sufficient empirical height-dependent path loss model for drones. Our measurement is followed by an analysis through simulations, taking into consideration this dependency of the path loss and shadowing on the height of drone. Our study focuses on the impact of drone's height, network's inter-site distance (ISD) and load level on the C2 downlink's coverage, which is measured as the percentage of drone locations in outage, i.e. the experienced signal to interference plus noise ratio (SINR) is below a certain threshold. In addition, we also investigate several potential mechanisms to increase coverage, namely interference coordination, interference cancellation (IC) and network diversity. To the best of our knowledge, no such coverage analysis for drones is available in literature.

The outline of this paper is as follows: in Section II we derive the single-slope large-scale path model for drones from measurement, and present the network layout and assumptions used in our simulations. Section III shows results from our drone coverage analysis, while Section IV investigates the application of IC technique and network diversity to improve the coverage. Finally, conclusions are drawn in Section V.

II Methodology and Assumptions

A. Propagation Model

To capture the large-scale path loss model for drones, a measurement campaign was performed at two locations in Fyn, Denmark. This is a typical rural area with terrain profile's variation between 40 and 120 m above mean sea level. A R&S TSMA mobile network scanner, mounted on a DJI Matrice

Fig. F.1: The measurement equipment mounted on the drone is monitoring live LTE networks.

600 drone (see Fig. F.1), was set to measure Reference Signal Received Power (RSRP) simultaneously from two Danish LTE networks at 800 MHz. The drone was set to fly two circular paths of 500 m diameter, which were 7 km apart from each other. Measurements were done at four different heights (h_{UAV}): 15, 30, 60 and 120 m, which were selected according to the maximum limit allowed by regulations. The desired height is measured relatively to the ground at taking-off point, and then the drone kept a constant altitude[1] during flight. A drive-test is also performed on the ground as reference, where the received antenna is placed on top of a car at 1.5 m height. Propagation loss, considering isotropic antennas at transmit (Tx) and receiver (Rx), is extracted from the measured signal strength, taking into account transmit power, BS and drone positions, altitudes and antenna patterns. For more detailed information on the measurement setup and path loss extraction procedure, please refer to [5].

Fig. F.2 shows the measured path loss for user equipment (UE) height of 1.5 and 120 m. For simplicity, we choose to model the large-scale path loss vs distance with the single-slope Alpha-Beta model [6]:

$$PL_{AB}(d) = 10\alpha \log_{10}(d) + \beta + \mathrm{X}_{\sigma_{h_u}} \quad \text{[dB]} \tag{F.1}$$

where $PL_{AB}(d)$ is the path loss over the 3D Tx-Rx distance d (in meters), α is the path loss slope, β is the floating intercept (in dB) and $\mathrm{X}_{\sigma_{h_u}}$ is the normal-distributed shadow fading term with zero mean and standard deviation σ_{AB}.

[1]Throughout this paper, we define height as elevation measured with respect to the underlying ground surface, while altitude is elevation above mean sea level.

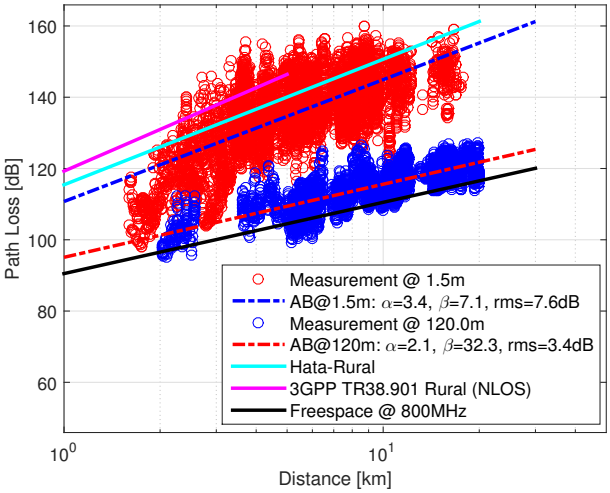

Fig. F.2: Measurement vs well-known rural path loss models.

As can be seen from Fig. F.1, the measured path loss slope is 3.4 at 1.5 m, which is similar to that of existing rural path loss models such as Okumura-Hata [7] or Third Generation Partnership Project (3GPP) NLOS RMa [8]. At 120 m, the measured path loss slope is close to free-space path loss (i.e. $\alpha = 2$). Table F.1 summarizes the height-dependent parameters for the path loss model, which are used in the next sections to evaluate the coverage of existing LTE network for drones in a rural area.

Due to the height-dependent path loss slopes, the serving cell's signal strength becomes stronger when an UE is elevated from 1.5 to 120 m. The negative effect is that the interference also gets stronger and becomes the limiting factor for drone coverage. A hint of the interference problem from the measurement campaign is that the scanner at 120 m detects 16.9 neighboring cells in average, compared to only 5.1 at 1.5 m. In the next sections, the adverse effect of interference on the cellular network's coverage performance for drones will be examined more closely via simulations.

B. Simulation Assumptions

We choose to investigate the drone coverage under the same environment as the measurement campaign: the study takes into account the whole island of Fyn, which is around 70x70 km in dimension, excluding Odense city and the surrounding sea (see Fig. F.4), as we focus on rural area only. The area is divided into a grid of 100x100 m pixels, and at the center of each pixel one drone is dropped during simulation. A real-world network layout is implemented

Table F.1: Measurement Summary

h_{UAV}	AB Model			Detected Cells (average)
	α	β	σ_{AB}	
1.5 m (DT)	3.4	7.1	7.6	5.1
15 m	2.8	12.9	6.2	6.1
30 m	2.5	20.6	5.2	7.6
60 m	2.1	32.0	4.4	11.6
120 m	2.1	32.3	3.4	16.9

in our simulation, which includes actual BS's location, height, antenna pattern, bearing and down-tilting. The BS heights range from 19 to 50 m above the ground, and down-tilting angles are from 0 to 9^o. BSs are transmiting at 49 dBm over a bandwidth of 20 MHz at 800 MHz band, while their cable loss is assumed to be 1 dB. Terrain profile is considered via the inclusion of a Digital Elevation Map (DEM), and drones are assumed to always fly above the terrain at a constant height. A shadow fading map is generated for each cell with correlation distance of 100 m, and the shadowing correlation between sites and co-located cells are 0.5 and 1, respectively. The standard deviation for shadow fading is height-dependent and given in Table F.1. We assume that the drone's antenna gain is small and neglectable, and it suffers 2 dB loss due to blockage from the fuselage. The LTE system considered in our simulation has 2x2 Multiple Input Multiple Output (MIMO).

In this paper our focus is on the C2 downlink, i.e. control traffic is being sent from a BS toward a drone. As envisioned in [9], the link requires an application data rate of 30 kbps, which if we assume 100% overhead from Radio Link Control (RLC), Medium Access Control (MAC) and higher layer protocols will result in a physical data rate of 60 kbps. With the most robust modulation and coding scheme [10], this requires at most 4 out of 100 usable Physical Resource Blocks (PRBs), if we assume continuous transmission and an LTE system bandwidth of 20 MHz. This means that it is not difficult from a capacity point of view to support the C2 downlink data rate. However, the cellular network must be able to provide this critical link with 99.9% reliability [9], but in reality, a LTE device cannot operate at arbitrary low SINR: at some point the LTE system will break down and thus no throughput is possible even if resources are available. Specifically, an Radio Link Failure (RLF) is said to occur when the SINR first drops below -8 dB and then remains below -6 dB during 1 s [11]. Therefore, in our analysis, we choose -6 dB as minimum required SINR for LTE to deliver the C2 link, and define *outage* as the percentage of drone locations experiencing SINR below this threshold. The 99.9% reliability in [9] in our analysis is understood as the cellular network must be able to provide C2 link coverage for at least 99.9% of the geographical rural

Table F.2: Key Simulation Parameters

Parameter	Value
Simulation area	70 x 70 km
Grid resolution	100 x 100 m
Network layout	229 sites (676 cells)
Average inter-site distance	2.2 km
Transmit power	49 dBm
System bandwidth	20 MHz
Carrier frequency	800 MHz
BS's cable loss	1 dB
Drone fuselage blockage loss	2 dB
MIMO configuration	2x2
2D shadowing correlation distance	100 m
Shadowing correlation	0.5 (sites), 1 (cells)
Min. downlink throughput requirement	60 kbps
Min. SINR requirement	-6 dB

area, which is hereafter referred to as *99.9% availability*. In another words, the outage level must be maintained at below 0.1% for flying drones. Table F.2 gives an overview of key simulation parameters used for generating results presented in the following sections.

III Coverage Analysis

A. Coverage under full-load assumption

In this section we investigate the cellular network's ability to provide coverage for drones under the assumption that the network is fully loaded, i.e. all neighboring cells have data to transmit in downlink and thus cause interference to the receiver. This is the worst-case scenario and serves as the lower bound result. The SINR cumulative distribution function (CDF) under the full-load assumption is given in Fig. F.3 for different drone height. The SINR at ground level (1.5 m) is also included. With average ISD of 2.2 km, the CDF is close to the that of the 3GPP Macro Case #3 regular network [12], which has an average ISD of 1.7 km. At 120 m height, the overall SINR drops significantly compared to that of 1.5 m, and thus the outage is soaring from 4.2% to 51.7%. Fig. F.4 illustrates drone locations in outage (yellow dots) at 120 m height, where the experienced SINR is below -6 dB. In general coverage is only available in small regions around those BSs (brown dots). The SINR degradation is due to the increased interference, not because of the re-

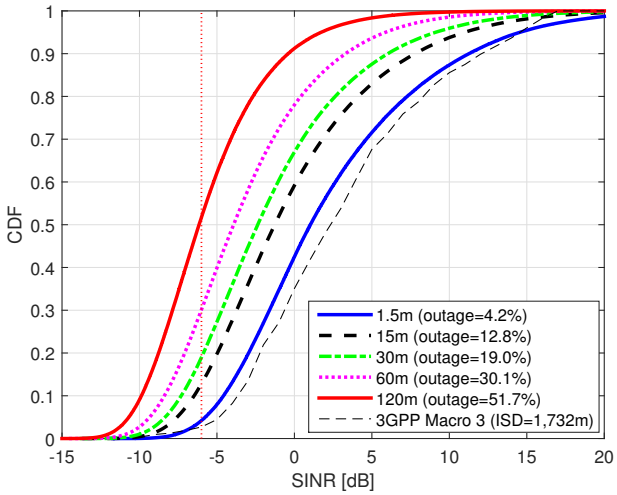

Fig. F.3: SINR CDF under full-load assumption. Red dotted vertical line indicates minimum required SINR of -6 dB.

duction of the best server's received power. Fig. F.5 shows that the received power actually improves significantly with the increased height, even though BS antennas are down-tilted and optimized for terrestrial users. At the 50 percentile the received power increases from -58.7 dBm at ground level to -43.1 dBm for drones at 120 m.

B. Impact of inter-site distance

Since different network operators might have different ISD in the rural area, in this section we discuss the impact of changing network density on the performance of drone's C2 link. To create networks with higher ISD for investigation, we apply a minimum ISD filter on the current network, according to the following process: We start with the first entry in the list of available sites, and remove any sites in the list that has distance less than a filtering distance (d_{filter}) of 1.5, 3.2 or 4.8 km from the chosen one. Then we move to the next entry of the updated list and apply again the same procedure of distance-based filter. The process is repeated until the last entry in the list is reached. This results in three new network layouts with average ISD approximately 3.0, 4.0 and 5.0 km, respectively. Fig. F.6 illustrates the SINR for different ISDs under the full-load assumption. The outage level for 5.0 km ISD is 27%, approximately half of the network outage for the original 2.2 km ISD. Even though this number is still high compared to the afore-mentioned desired availability of 99.9%, this finding indicates that by reducing the net-

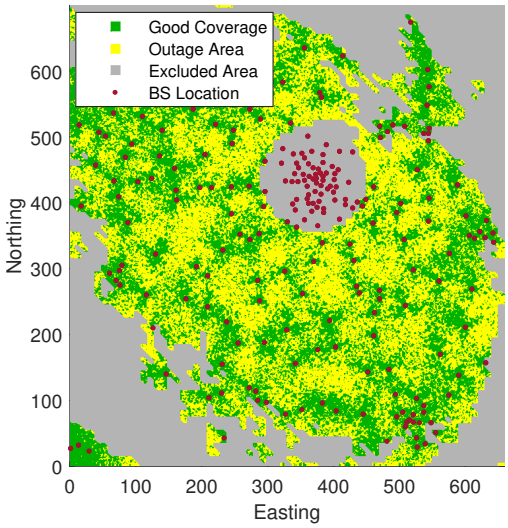

Fig. F.4: Outage map at 120 m under full-load assumption. Easting and Northing scale is 100x100 m pixel.

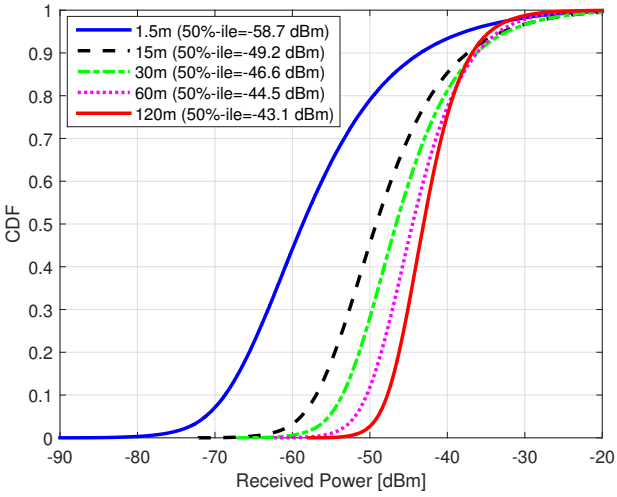

Fig. F.5: The CDF of best server's received power.

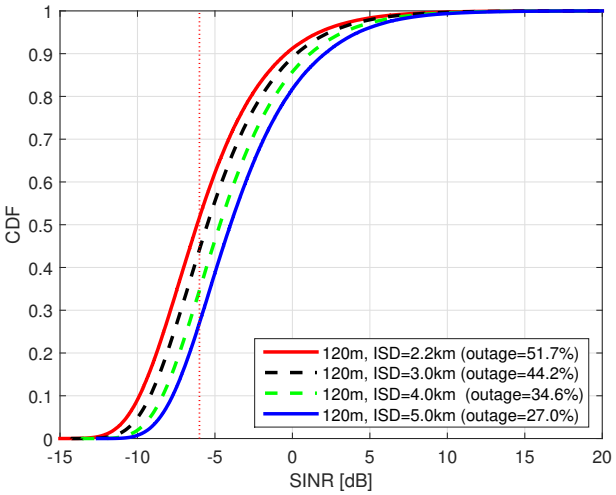

Fig. F.6: SINR CDF for different ISDs under full-load assumption. Red dotted vertical line indicates minimum required SINR of -6 dB.

work density, interference is also diminished at the expense of having less resources per area.

C. Coverage under fractional load assumption

Cellular networks today operate at load levels lower than 100%. In this section we look at the coverage for drones, assuming that the network has average loads of 25%, 50% and 75% of its total capacity. To generate the SINR CDF for a desired network load of 25% for example, a Monte Carlo simulation is run for 1000 realizations to collect sufficient statistics. At each realization we randomly choose 75% of the neighboring cells and mute all the interference caused by them towards the current serving cell. The results are shown in Fig. F.7. The SINR CDF for network load of 25% indicates that the outage is only 1.9%, which is much lower than the value of 51.7% under the full load assumption. In other words, the cellular network can provide drone coverage up to 98.1% of the locations if its load is kept at 25%.

This result, together with the understanding from Section B., hints in the direction that interference coordination / avoidance schemes can be used to lower the outage and thus improve the availability for the C2 link. By muting or lowering the transmit power on those sub-frames reserved for drone's C2 link on neighbor cells within a certain radius, such a scheme can potentially help network operators to get closer to the strict requirement of 99.9% availability. However, the interference coordination scheme needs to be ca-

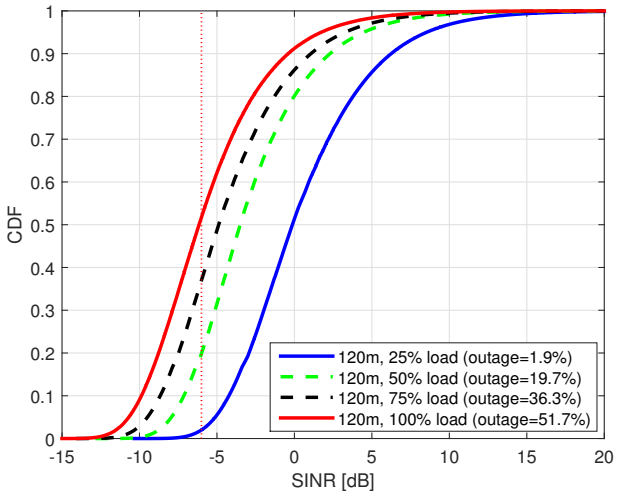

Fig. F.7: SINR CDF under various load levels. Red dotted vertical line indicates minimum required SINR of -6 dB.

refully designed to limit the corresponding capacity penalty for terrestrial users sharing the same network. It is important to note that the increased interference affects both data and control channels for UAVs, and therefore it is essential that the scheme is designed to mitigate interference for both types of channel.

IV Outage Mitigation Techniques

In this section we discuss the application of IC and network diversity as methods for reducing outage.

A. Interference Cancellation

We assume an ideal receiver-side donw-link IC algorithm, which is able to mute completely the dominant interferer. Fig. F.8 shows the performance of the IC scheme at the ground level and 120 m height under the 50% network load assumption. We choose to investigate the interference mitigation technique under this network load to reflect the fact that in reality cellular networks are not always fully loaded [13]. For drones at 120 m, the IC scheme helps to reduce outage from 19.7% to 11.8%. Nevertheless, it is evident from the figure that the scheme becomes less effective at 120 m than at ground level, as for all SINR values the distance between the curves with and without IC decreases, around 1 dB compared to a value of 3 dB for the ground level. The

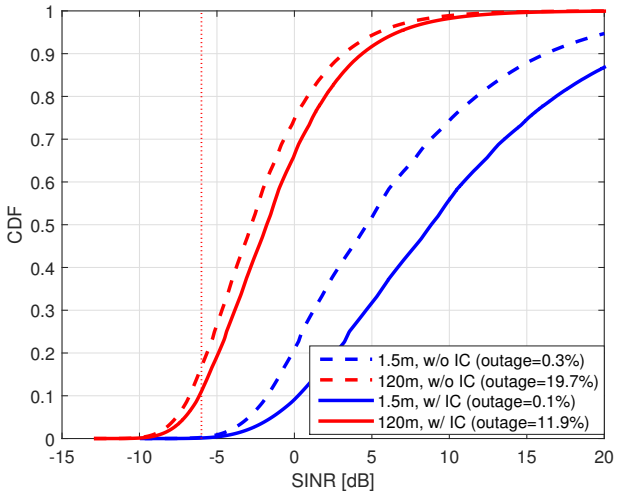

Fig. F.8: SINR with and without IC under the 50%-load assumption. Red dotted vertical line indicates minimum required SINR of -6 dB.

reason is that more neighboring cells are visible at 120 m and contributing to the interference level. Fig. F.9 shows for various height the dominant-to-rest interference ratio (DIR), which is ratio of the dominant interferer to the aggregated power of the rest of the interferers. It is clear that the dominant interferer's contribution becomes less significant with increasing height. Thus removing only the dominant interferer has less impact on reducing the overall interference.

B. Macro Network Diversity

Another way of improving the availability is to connect drones to more than one network at the same time. The drone is in this section assumed to connect to two independent LTE networks simultaneously. The first network (Operator 1) has been described in Section B., while the second (Operator 2) has larger ISD of 3.8 km. We also apply the real-world network layout and BS configuration for Operator 2 in our simulations. Both networks operate on 800 MHz band, but they are not sharing the spectrum nor site locations. Operator 2 is assumed to have the same transmit power and system bandwidth as Operator 1. As the drone can utilize both networks to obtain the C2 data, the outage in case of macro network diversity is defined as number of drone locations that experience both networks having SINR lower than -6 dB. Table F.3 shows the outage in percentage for Operator 1 and 2 separately. As expected due to larger ISD the network of Operator 2 has lower

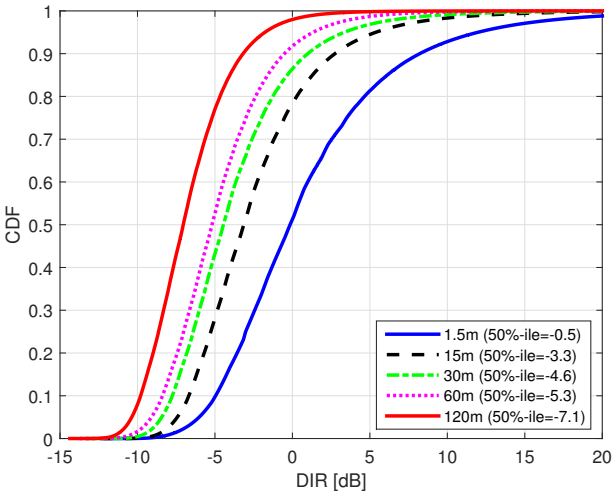

Fig. F.9: DIR for different height under the 50%-load assumption.

Table F.3: Outage Level (%) at 50% Network Load

h_{UAV}	Operator 1	Operator 2	Diversity
1.5 m	0.30	0.15	0.00
15 m	1.61	1.38	0.04
30 m	3.43	1.69	0.12
60 m	6.54	2.77	0.27
120 m	19.7	7.25	1.80

outage in general. For example, the outage from Operator 1 and 2 at 120 m is 19.7 and 7.25%, respectively. By combining the best SINR from the two networks using selection diversity, we can achieve a much lower outage level (1.8%). Macro network diversity, therefore, is an important technique to be considered for drones, as it is useful not only for increasing availability, but also for improving reliability, for example to avoid service disruption due to handover failure.

V Conclusions

In this paper we discuss the cellular coverage for the drone's C2 in downlink. It is envisioned that drones will be allowed to operate BVLOS first in rural area, and such a link is important to ensure safe remote operations. The existing LTE networks are a natural candidate to provide C2 link for drones. The study takes into consideration the dependency of the large-scale path loss on

the drone's height, which is derived from actual measurement in rural area of Fyn, Denmark. Simulations are performed using a real-world LTE network's layout and configuration. First, the results indicate that, while it is not difficult to fulfill the minimum physical layer data rate requirement of 60 kbps in the downlink in terms of resources, ensuring a minimum -6 dB SINR for drones can be challenging. At high altitude the coverage is significantly limited due to interference, since path loss becomes close to free-space with increasing height, thus boosting the interference levels received by the drone. Under the full-load assumption, outage level for the drones at 120 m soars to a staggering number of 51.7%, compared to 4.2% for the ground users. Secondly, results with lower network load and larger distance to the interfering base stations indicate that lower interference leads to significantly better coverage. This points to the potential of interference coordination schemes to improve the availability. Third, interference cancellation (IC) scheme, which removes completely the dominant interferer, seems to be much less effective for drones than for UEs on the ground, as interference experienced by drones consists of more sources than the interference of ground users. Finally, applying network diversity, or having drone connected to two independent networks at the same time, is proven to be useful, as it not only improves the coverage but also the reliability.

References

[1] "Consumer Drone Sales to increase Tenfold to 67.7 Million Units Annually by 2021," Tech. Rep., July 2016.

[2] "Clarity from above: PwC global report on the commercial applications of drone technology," Tech. Rep., 2016.

[3] B. V. D. Bergh, A. Chiumento, and S. Pollin, "LTE in the sky: trading off propagation benefits with interference costs for aerial nodes," *IEEE Communications Magazine*, vol. 54, no. 5, pp. 44–50, May 2016.

[4] N. Goddemeier, K. Daniel, and C. Wietfeld, "Role-Based Connectivity Management with Realistic Air-to-Ground Channels for Cooperative UAVs," *IEEE Journal on Selected Areas in Communications*, vol. 30, no. 5, pp. 951–963, June 2012.

[5] R. Amorim, H. Nguyen, P. Mogensen, I. Kovacs, J. Wigard, and T. Sørensen, "Radio channel modelling for uav communication over cellular networks," *I E E E Wireless Communications Letters*, 5 2017.

[6] H. C. Nguyen, I. Rodriguez, T. B. Sorensen, L. L. Sanchez, I. Kovacs, and P. Mogensen, "An Empirical Study of Urban Macro Propagation at 10, 18 and 28 GHz," in *2016 IEEE 83rd Vehicular Technology Conference (VTC Spring)*, May 2016, pp. 1–5.

[7] M. Hata, "Empirical formula for propagation loss in land mobile radio services," *IEEE Transactions on Vehicular Technology*, vol. 29, no. 3, pp. 317–325, Aug 1980.

[8] 3GPP, "Technical Specification Group Radio Access Network; Study on channel model for frequencies from 0.5 to 100 GHz," 3rd Generation Partnership Project (3GPP), TR 38.901, Mar. 2017. [Online]. Available: http://www.3gpp.org/dynareport/38901.htm

[9] Nokia and A.-L. S. Bell, "Requirements of Connectivity Services for Drones," 3rd Generation Partnership Project (3GPP), Contribution R1-1704429, 2017. [Online]. Available: http://www.3gpp.org/ftp/TSG_RAN/WG1_RL1/TSGR1_88b/Docs/R1-1704429.zip

[10] 3GPP, "Evolved Universal Terrestrial Radio Access (E-UTRA); Physical layer procedures, v14.2.0," 3rd Generation Partnership Project (3GPP), TR 36.213, Mar. 2017. [Online]. Available: http://www.3gpp.org/dynareport/36213.htm

[11] ——, "Evolved Universal Terrestrial Radio Access (E-UTRA); Mobility enhancements in heterogeneous networks, v11.1.0," 3rd Generation Partnership Project (3GPP), TR 36.213, Jan. 2013. [Online]. Available: http://www.3gpp.org/dynareport/36839.htm

[12] H. Holma and A. Toskala, *LTE for UMTS: Evolution to LTE-Advanced*, 2nd ed. Wiley.

[13] "Sustainable traffic growth in LTE network," Tech. Rep., 2017.

Chapter 4 - Performance Enhancement Techniques

The previous chapter has analyzed the increase in the interference as a function of the height that Unmanned Aerial Vehicles (UAVs) are expect to fly in cellular networks. The present chapter will investigate different techniques for performance enhancement and evaluate how they can bring the Command and Control (C2) reliability to values similar of the Third Generation Partnership Project (3GPP) requirements.

4.1 Problem Description

The problem of interference has been discussed in the previous chapters, where the signal to interference plus noise ratio (SINR) degradation was pointed out for UAV's communication. This chapter and its related papers present a performance assessment of the C2 link regarding 3GPP requirements. They also focus on evaluating performance enhancement techniques in their potential of improving the C2 reliability.

Modern cellular technologies use robust channel coding techniques for protecting the data from the wireless channel conditions by introducing redundancy in the data [1]. These techniques are able to correct most of the errors in the received message introduced by the wireless channel. This allows the wireless link to successfully transmit messages even in poor SINR conditions. On the other hand, the data's redundancy utilizes physical resource that could be used for "new" data. Thus there is a trade-off: too much redundancy represents an inefficient use of the spectrum, whereas too few redundancy leads to too many errors in the reception.

In Long-Term Evolution (LTE), this trade-off is balanced by the usage of adaptive Modulation and Coding Scheme (MCS) [2]. The robustness in the transmission is dynamically decided by the scheduler, usually aiming at achieving a target Block Error Rate (BLER) in the first HARQ transmission. The target BLER is designed by the network engineers as a compromise between optimizing the capacity of the wireless channel and robustness against non corrected errors.

The usage of very low MCS, i.e. more robust transmissions, is inferred from the previous chapters for the UAV use case. It means high consumption of network resources. In very loaded scenarios, the requirement of several physical resources by the UAV users may delay the delivery of packets, impacting the latency Key Performance Indicator (KPI). This is one of the hypothesis investigated in this chapter.

Furthermore, the effect ot the target BLER, usually set to approximately 10 % in cellular networks, is also discussed in this chapter. Every time one packet is received with error, it has to be retransmitted, which incurs additional delay on delivering the messages. This work analyzes the impact of retransmissions on the reliability of the C2 link, regarding the transmissions should be completed within 50 ms [3].

Beyond the latency challenges, it is of paramount importance to guarantee that the radio control information is correctly decoded by the user. If a LTE device cannot decode and interpret the Physical Downlink Control Channel (PDCCH) correctly, the link will behave poorly and a radio link failure may occur [4]. In this thesis, this factor is also taken into consideration when analyzing the performance of the C2 link.

Because of the challenges aforementioned, the increased interference harms the reliability of the C2 link. Besides the analysis of the C2 performance, this thesis proposes and evaluates techniques for mitigating the inter-cell interference and enhance the reliability of the C2. The key techniques evaluated in this chapter are the following:

- inter-cell interference coordination (ICIC);
- interference cancellation (IC);
- user equipment (UE)'s directional antenna beams;
- uplink (UL) power control; and
- network diversity

.

4.1.1 Potential Enhancements of the LTE Physical Layer

Fig. 4.1 presents a schematic of the LTE sub-frame and shows one example of the resource allocation used for the the reference symbols [5]. The columns represent the OFDM symbols, while the rows in the grid are the subcarriers. Reference symbols are always continuously transmitted in the 1st, 5th, 8th and 12th OFDM symbol of the sub-frame, using a known sequence, such that the users can estimate the effects of the radio channel when decoding the received signal.

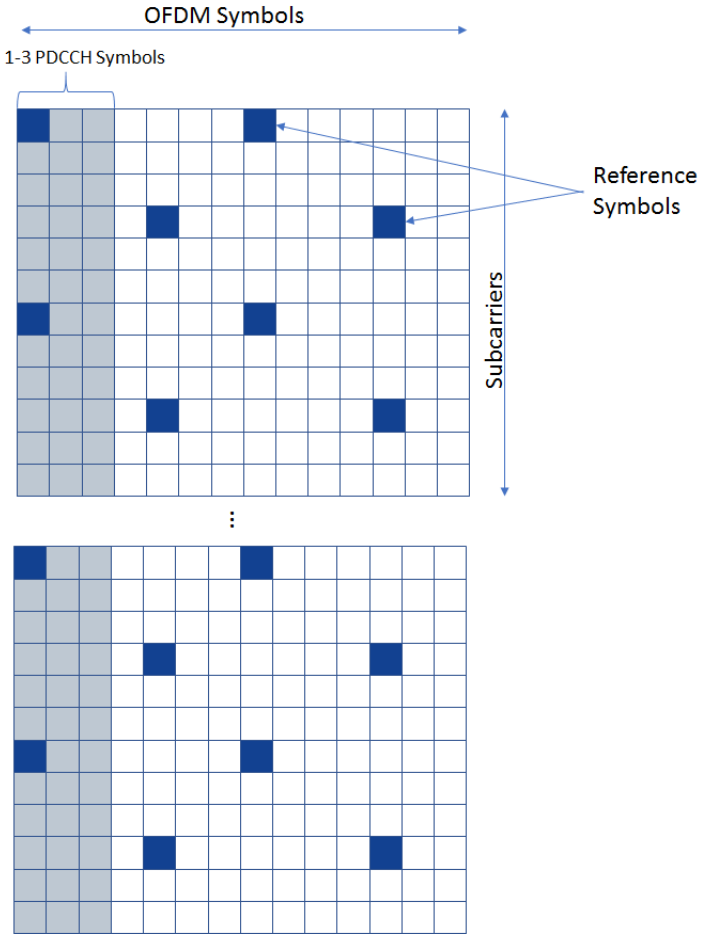

Fig. 4.1: Exemplification of PDCCH and cell specific reference symbols allocation in a LTE subframe according to [5].

To minimize the interference between reference signals of neighbor cells, the position of the reference symbols illustrated in Fig. 4.1 is cyclically shifted according to the cell Physical Channel Indicator (PCI). An airborne UAV receives interference from multiple sources, the power received from the continuously transmitted reference symbols accumulates to raise the interference power through the entire bandwidth , in those OFDM symbols containing reference symbols. This can cause some performance degradation in the C2 transmission even under low network load assumptions.

Besides the problem with the cell-specific reference symbols transmissions, the allocation policies for the PDCCH also create challenges for some

performance enhancement techniques. The PDCCH carries all relevant information transmitted by the network for the management of the radio connection. It includes, for example, the UL transmission grants and the reconfiguration of radio parameters. This important control channel is always wideband transmitted in the first one to three Orthogonal Frequency Division Multiplexing (OFDM) symbols in Fig. 4.1.

In order to find the radio management information directed to them, users must scan the PDCCH. For that reason, it has to be available for all users in in the cell area. Consequently, there is limited support for directional transmissions (e.g. beamforming or grid of beams) of the control channel in LTE.

4.1.2 Inter-Cell Interference Coordination

The ICIC technique has been previously discussed in Chapter 3. Previous results have indicated that ICIC gains are expected to be very limited for a small number of cells coordinated, while involving a high number of cells in the coordination set tends to increase significantly the computational complexity and the capacity loss. These issues are illustrated in more details in this subsection.

The ICIC is a resource allocation management strategy that aims at reducing the transmission "collision" probability between one given cell and its set of strong interfering neighbors. For this, neighbors cell are prevented to transmit in the same resources by negotiating the allocation policies through signaling messages.

In 3GPP release 8, defined ICIC to be used in frequency domain. It means some frequency resource blocks in the LTE sub-frame are reserved for one particular cell within a coordination group [6]. This can reduce the interference in the data channels, however, the PDCCH as illustrated in 4.1, is not allocated in different frequency resources. Therefore, the PDCCH cannot be protected from harmful interference.

Although the PDCCH interference problem was not a relevant issue for terrestrial users served by macro-network deployments, it became a problem in heterogeneous networks. To address this problem, the enhanced ICIC (e-ICIC) was introduced in 3GPP release 10 [7]. In this case, the cell victim of interference was protected through an entire sub-frame, whereas the neighbor cells transmit a blank or almost blank (very low power) subframe [8].

So, the ICIC and e-ICIC techniques available cannot completely remove the interference from neighbor cells in control channels, because of LTE frame structure, but they can provide significant mitigation. However, the size of the coordination sets, discussed in Chapter 3, are also a challenge for the applicability of ICIC for the UAV use case, because of both complexity and capacity loss.

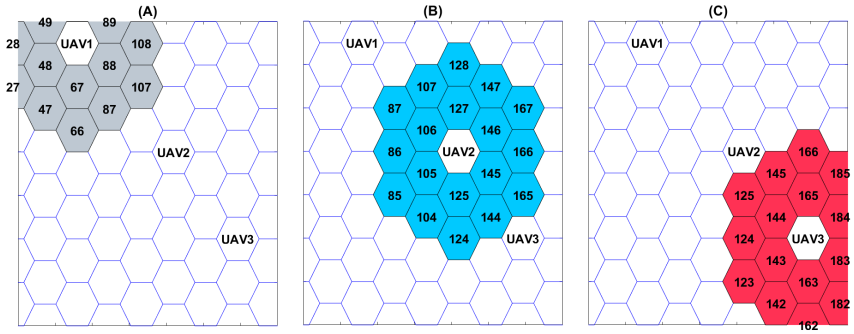

Fig. 4.2: Illustration of ICIC coordination groups for three UAVs in the network. Coordinated cells are highlighted and the numbers represent unique identifiers for the cells on the grid. (A) shows the coordination group required by $UAV1$, while (B) and (C) shows the groups for $UAV2$ and $UAV3$ respectively.

These challenges are illustrated in Fig. 4.2 that shows a snapshot of an hexagonal grid of cells, representing the area covered on the ground by different eNodeBs. In this figure, there are three airborne UAVs, each associated with a different cell, as depicted. For the sake of the discussion, it is assumed that the ICIC should remove the interference of the first two rings of interfering cells to protect the C2 performance. These results in three different coordination sets, that are shown in Fig. 4.2 (A), (B) and (C), respectively. The numbers presented for the cells in the coordination set, represent the unique identifier number attributed to each cell on the grid. Observe that, albeit the three UAVs are distant to each other on the grid, some cells belong to two coordination group: cells 87 and 107 belong to coordination groups 1 and 2, while 6 cells (124, 125, 144, 145, 165, 166) belong to groups 2 and 3.

Cells that belong to more than one group will be muted by the policies of two groups, which tends to increase the muting patterns and this can cause severe capacity degradation. To avoid this situation, a coordination among the three groups would be required, but that would increase even more the managing complexity. It is reasonable to argue from the scenario in Fig. 4.2, which presents only 3 UAV, that by scaling the density of UAVs, this problems will increase rapidly.

In this chapter, the focus is on analyzing the required size for coordination groups and the loss of capacity expected, in order to evaluate the feasibility of ICIC deployments for C2.

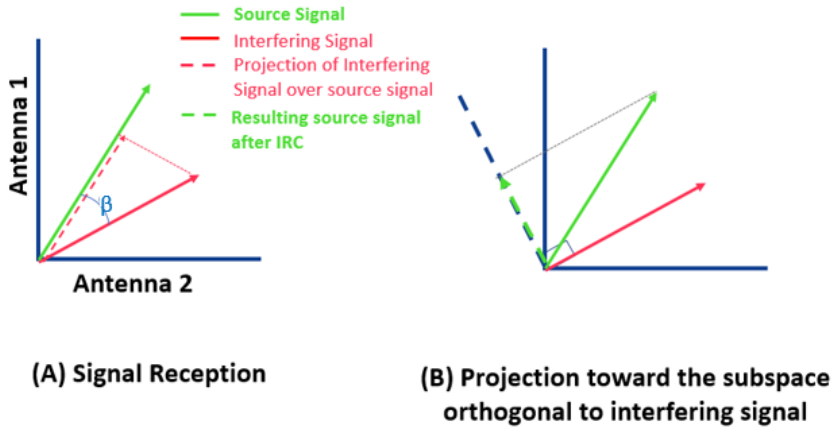

Fig. 4.3: Algebraic analogy of linear interference cancellation. The received signals (A) are projected toward the subspace orthogonal to the interfering signal (B), suppressing the contribution of the interference in this subspace.

4.1.3 Interference Cancellation

Interference management techniques are typically implemented in the network side. LTE Release 11 was the first to adopt interference suppression/mitigation at the UE terminal, by introducing the Interference Rejection Combining (IRC) [9].

The IRC utilizes linear combination of the signal received by the different antennas of the mobile terminal to suppress the interference. Fig. 4.3 illustrates the algebraic principle. The signal and interference received are estimated by the mobile terminal with their respective contributions in the subspace formed by the receiving antennas. Then, the signals are projected over a subspace orthogonal to the interfering signal to be canceled [10]. The orthogonal projection suppresses the interfering signal, but it also contributes to attenuate the received symbol by a factor of $\sin\beta$, where β is the angle between the received signal and the subspace orthogonal to the interference.

The process can be performed successively to $N-1$ signals, where N is the total number of receiver antennas, a process known as Successive Interference Cancellation (SIC). The disadvantage, though, is the reduction on the desired signal power (see Fig. 4.3. In practice, the number of antennas currently implemented in mobile terminals is relatively small, usually limited to 2 or 4 at low frequency bands. This limitation is an implication of the minimum distance required to guarantee decorrelation between the antennas [11], that prevents multiple antennas to be placed in miniaturized handheld devi-

ces. These spatial challenges may be overcome in future UAVs applications by using higher frequencies or by smart placing of the antennas onto the UAVs body.

However, the interference suppression achieved by IRC is not ideal, and its performance depends on different factors. Besides the quality of the channel estimation, a low Dominant Interferer Ratio (DIR) tends to degrade the IRC performance [10,12]. This is shown by the analytical example of a N_R-antennas deployment with M interfering neighbor cells in the following set of equations. Before the rejection of the received power from the dominant cell, I_0, the signal to interference plus noise ratio, $SINR$, is given by:

$$SINR = \frac{S}{N + I_0 + \sum_{i=1}^{M-1} I_i} \tag{4.1}$$

where S is the received power from the desired signal, while N represents the thermal noise power and I_i is the received power from the i-th neighbor. Likewise, the DIR can be defined as:

$$DIR = \frac{I_0}{N + \sum_{i=1}^{M-1} I_i}. \tag{4.2}$$

After the rejection operation is performed, the signals are projected into a subspace orthogonal to the dominant interfering cell, as depicted in Fig. 4.3. So, the resulting SINR, $\overline{SINR}_0$ in the output of this process is:

$$\overline{SINR}_0 = \frac{S}{N + \sum_{i=1}^{M-1} \sin \alpha_i' I_i} \sin^2 \alpha. \tag{4.3}$$

where α represents the angle between the received signal and the first interfering, and α_i is the angle between the first interfering and the i-th neighbor. For a high number of receiving antennas, $N_R \to$ inf the expected angle between two random vectors increases and approaches 90 deg in the limit [10]. Therefore, in the best case, where the channels are completely uncorrelated and the number of antennas is very high, then $sin(\alpha) \to 1$ and $sin(\alpha_i') \to 1, \forall i$. Hence, from (4.1) and 4.3, the expected IRC_{gain} is given by:

$$IRC_{gain} = \frac{\overline{SINR}_0}{SINR} = \frac{N + I_0 + \sum_{i=1}^{M-1} I_i}{N + \sum_{i=1}^{M-1} I_i} = 1 + \frac{I_0}{N + \sum_{i=1}^{M-1} I_i} = 1 + DIR \tag{4.4}$$

The concept of non-linear processing for interference rejection is introduced in 3GPP Release 12. The Network Assisted Interference Cancellation and Suppression (NAICS) relies on assistance from the network side to perform a more efficient cancellation of the interfering streams in the received signal and, because of this, requires tight coordination. Examples of assistance information that can be shared with the UE are [13] about the transmission in the neighbor cells:

- Presence or absence of Interference;
- Control Format Indicator (CFI);
- Physical Downlink Shared Channel (PDSCH) allocation;
- modulation and coding configuration;
- virtual cell ID;
- etc.

Albeit more efficient, the performance of the NAICS also relies on a high DIR (> 3dB). However, these solutions are more complex, and are usually limited to one neighboring cell being rejected.

In the light of the findings presented in Chapter 3, where multiple interfering sources are expected, the analysis in this chapter focuses on the IRC, which is analyzed in terms of the maximum performance gain for ideal cancellation of the first 1-4 neighbors. The results are discussed in regards of the IRC inefficiencies for low DIR and high number of interfering neighbors.

4.1.4 Uplink Power Control

In mobile networks, the UL transmit power varies with the radio path loss between the mobile terminal and the eNodeB. When the user is very close to the eNodeB, transmitting with maximum power would make the SINR much above the required target for the maximum throughput supported by the system. In other words, the terminal's power will be wasted, whereas it will be causing more interference to neighbor cells. To account for this, cellular networks utilize UL Power Control (PC) mechanisms. Their main goal is providing enough power to achieve the service required SINR, while minimizing the interference caused to neighboring cells [14].

The PC can be implemented either by closed-loop (CLPC), open-loop (OLPC) or a combination of both. This investigation will focus in the Open Loop Power Control (OLPC), but most of the discussions presented here can be extended for the Closed Loop Power Control (CLPC), without loss of generality. The simplified version of OLPC's formula for the UE's transmit power, P_T, is given by the following equation [15].

$$P_T = min(P_{max}, P0 + \alpha PL + 10log_{10}M) \tag{4.5}$$

where P_{max} is the UE maximum allowed power for transmission, usually equal to 23 dBm in LTE; PL is the estimated path loss; M represents the number of LTE's Physical Resource Block (PRB) allocated for that user; while $P0$ and α are network-specific design parameters. $P0$, is the target uplink received power per scehduled PRB and, in a certain extent, defines an offset

level for the transmit power of UL users in a given cell, while α, between 0 and 1, defines the path-loss compensation factor.

By setting $\alpha = 1$, the network designer wants full-compensation of the radio path loss. It is possible to see, in a close inspection of (4.5), that the average received power of all users tend to be the same, in spite of their location in the cell. This represents lower variability of UL throughput among users, at the cost of decreased throughput for the users with lower path losses [16] and for the overall cell throughput [17].

On the other hand, fractional compensation of the path loss tends to be more aggressive for users in the cell edge, that will have to face a larger non-compensated path loss [16]. As a consequence for this fact, if $\alpha < 1$ then UAVs will have better spectral efficiency and cause harmful levels of interference in the other users, as they expect much lower average path loss than terrestrial users in the same cell.

Some studies have demonstrated that the value of α that maximizes the cell capacity depends on scenario aspects, such as the propagation coefficient [17]. In practical cases, the choice of α depends on the network configuration and project decision, and is typically the same for all users in the network.

The value of $P0$, in LTE systems, is actually a combination of two component factors: a user related and a cell related [18]. Currently, although, the user related component is seldom used in real deployments, because it is not common prioritize one user or application in current networks.

But, as aforementioned, when $\alpha < 1$, UAVs can be unfairly favored. In order to circumvent this effect, the value of $P0$ can be adjusted for the different classes of users (UAVs and terrestrial) to minimize the interference caused by UAVs. The reference papers presented by this chapter evaluate the UL interference caused by UAVs and the effects of having a smaller $P0$ set for this class of user. In recent 3GPP specifications, which were partially impacted by the discussions presented in this thesis, the values of α may also be user specific, as for attending different requirements for terrestrial UEs and UAV-UEs [19].

Although the C2 requires low throughput, hence likely low resource usage per UAV, there are some factors that can contribute to the increase of the UL interference. UAVs can also transmit high throughput data, besides the C2 link, for example when performing a live video streaming. Some of the results presented in this chapter also discuss the impact of the high throughput transmission on UL by the UAVs.

4.2 Included Articles

Paper G. How to Ensure Reliable Connectivity for Aerial Vehicles over Cellular Networks

This paper presents a extensive campaign of system level simulations, aiming at evaluating the C2 performance when UAVs share 20 MHz of LTE spectrum (800 MHz) with the terrestrial users. The simulaion scenario is a typical rural network, generated based on the network settings provided by a real LTE-Advanced (LTE-A) provider in rural Denmark. This layout is comprised by 179 cells distributed over a 40x40 km area, with an average of 10 users uniformly distributed over the area. Eiter 1 % or 10 % of these users are UAV in the scenarios analyzed.

In the downlink (DL), the allocation of resources assumes a 100 kbps guaranteed bit-rate C2 application for the UAVs, whereas terrestrial users's traffic is modeled as an FTP application and is served using a "best-effort" allocation. The parameters for the terrestrial traffic model is chosen to enable simulations at two load points: *medium*, with approximately 30 % of resource (PRB) utilization, and *high* (67 %).

The UL resources are equally distributed between active UAVs, modeled as full-buffer traffic, and the terrestrial users, intermittent full buffer, active when there is data to be transmitted in DL . As discussed in 3.4, the resource usage expected for UL C2 transmissions is very low, and so, not expected to heavily increase the average interference level in the network. The full-buffer assumption enable the analysis of more heavily UL traffic implemented by the UAVs, for example full-HD live streaming [20].

The paper assesses DL and UL performance of both types of users through several KPIs, such as SINR, throughput and C2 outage. Most importantly, the paper assesses the outage probability and the average time in outage. One user is said to be in outage if its DL SINR goes below -8 dB, where the radio connectivity is assumed to be lost because the PDCCH cannot be decoded. The UE is kept in outage until the SINR goes above -6 dB, recovering the PDCCH. The choice of these thresholds is suggested in [3].

First, it is established a baseline for the performance of ground users and UAVs when sharing the resources with each other. Thereafter, interference mitigation techniques are deployed specifically to the UAV users, in order to improve the reliability of the C2 link. The techniques are split into two groups: network-based and user-based. The network-based techniques are ICIC and the UAV-specific power control settings, meanwhile user-based solutions are IC and directional antenna beam selection.

Paper H. Enabling Reliable Cellular Communication for Aerial Vehicles

The main goal of this paper is to provide a high-level discussion on the techniques that could be used to support C2 requirements over cellular communications. Besides it extends some of the work previously presented in this thesis for different scenarios.

The advantages and disadvantages of using cellular networks for C2 are discussed throughout the paper, in special, the challenges regarding the connectivity performance. The paper elaborates on the problem of interference by showing an extension of the work presented in D. The UL full-buffer measurements are shown for two different scenarios in this work, urban and rural.

Then, as in Paper G, simulations are performed to evaluate the performance of the C2, this time evaluated over an urban scenario. The paper also explores techniques for performance enhancement are investigated according, similarly to Paper G.

Looking forward to the future of C2 over cellular networks, the paper provides an insightful discussion about the enhancements on the physical layer of 5G New Radio that circumvent some of the flaws of LTE-A in what regards C2 applications.

Paper I. Improving Command and Control Reliability for Drones with Multi-Operator Connectivity

In this work, a measurement setup is created to emulate the C2 traffic exchanged by a client-server application. The client is installed onboard a real UAV and the server is remotely located in Aalborg University. The connectivity to the client is provided via two mobile phones connected through two different cellular networks.The UAV flies at three different heights (15, 40 and 100 m) in five designated routes in an urban scenario. A drive-test is also performed to provide ground level reference.

The end-to-end latency between the transmission of a packet and its reception (in UL or DL) is measured with the assistance of Global Positioning System (GPS)-based synchronization, while radio connectivity KPIs are recorded by the mobile phones. [21]. The latency measurements are used to evaluate the reliability of cellular networks in delivering the C2 packets within 50 ms.

Based on the reliability measurements collected over both operators,an assessment of the main causes of failures observed on the field is provided in the paper, including evaluation of the radio link KPIs. Besides, how network settings can be adapted to enhance the reliability.

The paper also provides in-field assessment of a theoretical dual-network

hybrid access strategy. In this scheme, the UAV is connected through two operators at all times. Client and server send the C2 messages through both operators simultaneously. The messages are considered received when they are received for the first time through any of the two operators.

4.3 Main Findings

4.3.1 Outage increases significantly with terrestrial traffic and UAV height

According to the results presented in Fig. G.3, the percentage of time in outage – where the PDCCH cannot be decoded – increases with the UAVs height. As depicted in Fig. 4.4, when the simulated network operating at 10 % of load, the average time in outage for a terrestrial user is 0.18 %, whereas a UAV flying at 120 m experiences an average time in outage of 5.53 %. This value is higher than 1.13%, which is the outage observed for a terrestrial UE under high load (67 % of resource usage). The airborne UAV at 120 m experiences outage of 23 % under the high traffic load conditions.

This degradation is caused by the increase in interference. When the simulated network operating at 10 % of load, the average DL SINR is close to 15 and 7 dB for UAVs flying at 15 and 120 m heights, respectively, whereas terrestrial users experience approximately 4 dB of average SINR. However, when the network is more heavily loaded, the interference accumulates much faster in the UAV connection. With a 67 % operational load in the network, the decrease in average SINR are approximately 3, 15 and 12 dB, respectively, at 1.5, 15 and 120 m.

4.3.2 Limited potential in downlink interference cancellation

The results obtained by interference cancellation in DL do not show promising potential to solve the outage issue. In the simulations presented in Paper G and Paper H, an ideal interference cancellation is assumed for up to 3 neighbor cells. In other words, the contribution of the three neighbor cells with highest power level is discarded from the interference for a given UAVs.

In Paper G, which uses the rural scenario simulations, the outage for an UAV flying at 120 m under high load conditions improves from 23 % to 10 %. The outage is more than halved, but it is still far beyond the 0.1 % outage requirements of 3GPP. Similar results are also observed for the urban scenario simulated in Paper H.

Considering real deployments, the cancellation obtained is not likely to be ideal, especially when there is no clear dominant interfering cell, which is likely to be the case for UAVs, as discussed in Chapter 3. Because of this, the

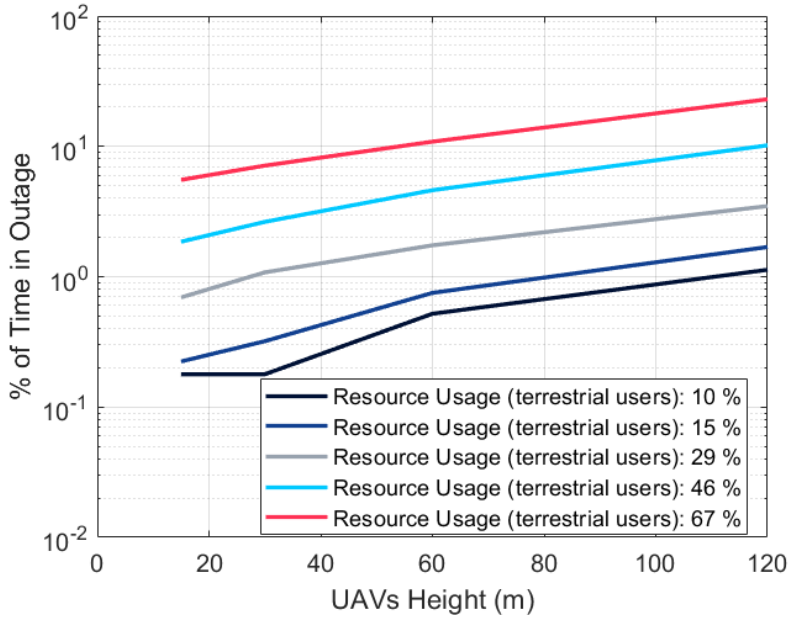

Fig. 4.4: Percentage of time in Outage versus UAV height for the simulations performed in Paper G.

gains may be even more limited in such high load scenarios.

Moreover, increasing the number of canceled cells to obtain the desired gain may also not be attainable, due to practical challenges. Besides the fact the neighboring cells are close to each other in the power domain, it would require increased number of receiving antennas deployed and, a significant increase in the complexity of the receiver [9].

4.3.3 Inter-Cell Interference Coordination limits the network capacity

Chapter 3 discussed how the usage of e-ICIC is limited when just few cells are coordinating. It also states that, on the other hand, increasing too much the number of coordinating cells can be rather complex to manage.

In spite of the established practicalities, from the research perspective,it is important to understand how much cells would be required to coordinate, the area covered by these cells, as well as the overall capacity loss inflicted to the network. Because of this, the ICIC is reexamined in the papers provided in this chapter. The method chosen is the time/frequency coordinated scheduling.

Implementing a true ICIC policy with several cells in each coordinating set is a very complicated problem that would require a dedicated analysis on its own. When multiple cells are considered to be part of one set, this set is likely to cover a very large area. Consequently, if many cell sets are formed in the simulation area, some cells can belong to multiple groups simultaneously. For this reason, the method implemented in the simulations is just an upper bound for the ICIC gain that would be experienced by an UAV: the cells are removed from the set of interfering cells for that user when the SINR is calculated.

When the network is operating with high load, the outage cannot be reduced to the levels required by coordinating 10 cells (2% of outage). In the urban scenario, not even 20 coordinating cells can achieve the 99.9 % reliability (Fig. G.18), as 0.2 % of outage is observed (Fig. H.3), although this value is quite close, especially when considering the inaccuracies of other modeling elements.

In what concerns the complexity of managing such large sets of coordinating cells, it is worth noting that the 10th neighbor has more than 60% of probability of being located more than 10 km away from the serving cell (See Fig. G.20).

Further, Paper G provides a simplified analysis of how much potential would be capped from the network, by using exclusively ICIC to protect the C2 links. In this case, the UAVs served by a given cell are packed into the same Transmission Time Intervals (TTIs), to minimize the amount of coordination required. Then, it is calculated the SINR required to convey all the 1250 B of information for each UAV and how much PRBs should be used. For the sake of simplicity, the UAVs of the other cells are ignored in this analysis. Calculations are performed for one, two and four UAVs users in the serving cell, while they are assumed to transmit every TTI, every 10th TTI or every 50th TTI.

In the writing process of this thesis, it was realized that Tables G.3 and G.3 presented mistakes due to typo and usage of inaccurate formula used to fill the cells. The corresponding results are corrected in this thesis, as presented in Tables 4.1 and 4.2. Table 4.1 shows the allocation requirements, in PRB and SINR, for the most conservative MCS to achieve the required throughput (100 kbps). As explained in Paper G, the SINR is the minimum between the -6 dB required to keep the PDCCH error below 2% [22] and the SINR for 10% BLER for the chosen MCS.

In order to achieve the required SINR, neighbor cells have to be muted by ICIC to mitigate the interference. The results in Table 4.2 show the amount of cells that must be muted to guarantee the required SINR 90 % of the time. Although this value is below the 99.9% reliability, it is used for demonstrate the challenges in using ICIC for the UAVs. In Table 4.2, the capacity loss observed for high load conditions, caused by muting cells transmission, va-

Table 4.1: ICIC Allocation Requirements

# of UAV in the cell	TTI allocation	MCS Requirements	
		PRB per UAV	SINR
1	Every TTI	9	-6.0
1	Every 10 th TTI	80	-4.7
1	Every 50 th TTI	100	1.6
2	Every TTI	9	-6.0
2	Every 10 th TTI	50	-4.0
2	Every 50 th TTI	50	5.0
4	Every TTI	9	-6.0
4	Every 10 th TTI	25	-2.3
4	Every 50 th	25	14.6

Table 4.2: ICIC Capacity Loss for the Coordination Set

# of UAV in the cell	TTI allocation	Coordination Set Size		Capacity Loss	
		Low Load	High Load	Low Load	High Load
1	Every TTI	0	3	0 %	3x100 %
1	Every 10 th TTI	0	8	0 %	80 %
1	Every 50 th TTI	10	>20	20 %	>40 %
2	Every TTI	0	3	0 %	3x100 %
2	Every 10 th TTI	0	9	0 %	90 %
2	Every 50 th TTI	> 20	>> 20	> 40 %	$\gg$ 40 %
4	Every TTI	0	3	0 %	3x100 %
4	Every 10 th TTI	2	14	20 %	140 %
4	Every 50th	>20	>> 20	> 40 %	$\gg$ 40 %

ries between 40 % and 300 % – or 3x100 %, i.e., the capacity loss equivalent of 3 cells muted – compared to the capacity of a single cell with 20 MHz of bandwidth.

Minimizing the number of TTIs in which the UAVs are allowed to transmit, tends to minimize the capacity loss to a certain extent, at the expenses of larger coordination sets. For instance, when there is one UAVs in the cell, the number of cells in the coordination set varies between 3 and more than 20, according to the period between UAV's TTIs. This implies a large area to be coordinated. Fig. G.20 shows that, in the simulated scenario, the 5-th strongest neighbor is located farther than 10 km in 40 % of the cases, and the

10-th neighbor is more than 20 km away in 10 % of the cases.

Based on this results, it is reasonable to assume that e-ICIC faces a scalability problem when the needs of the UAVs in the other cells are also considered. However, for medium load conditions, when the interference is significantly lower, the number of cells in the coordination set is much smaller. This suggests that, in combination with other techniques that mitigate the overall interference even in high loaded cases, ICIC could show some potential.

4.3.4 User-specific Power Control shows potential for minimizing UL interference

In LTE networks, radio management policies and rules are frequently applied to all users in the network. But, as extensively discussed throughout this thesis, the performance of UAVs and terrestrial users are fundamentally different, due to their radio propagation channel conditions.

Because the radio losses are much smaller from the perspective of an aerial user, while the UL interference experienced by both, terrestrial and aerial, are alike, the power control settings can be more conservative for UAVs.

In Papers G and H, the simulations are performed assuming users transmit a full-buffer traffic application. Even though the number of UAVs make just 1 % of the users in the simulation, reducing the P0 in 6 dB - compared to the value set for terrestrial users (P0 = -98 dBm per PRB) - has demonstrated an effective way of minimizing the UAV induced interference (see Fig. G.16 and Fig. H.4). As a consequence, there is a perceived increase in the average throughput experienced by terrestrial users - which corresponds to the majority of simulated users. Surely, the UAVs' throughput is slightly reduced, but the main point of this experiment is that provides a tool for the network designer to prioritize either UAVs or terrestrial applications in UL.

Such findings have been submitted for the 3GPP study item on cellular support for UAV and has contributed to the decision presented in the report [3], that envisions the usage of different power control settings for UAVs, who should be treated as a different class of users.

4.3.5 Antenna Beam Selection has great potential to enhance the SINR and decrease the outage

The main advantage of using a directive antenna pattern on the UAV-UE is that it provides a user-centric approach, that do not require or depend on any implementation on the network side.

The directional antenna beam rejects the unwanted signal that comes from sources outside the main direction, which in most cases can reduce significantly the interference, while it amplifies the reception in the direction of the main signal.

Table 4.3: Median end-to-end latency measured (ms) in Paper I

	Operator 1		Operator 2	
	DL	UL	DL	UL
Drive Test (DT)	14.6	27.1	17.2	31.6
15 m	14	24.4	17.1	31.1
40 m	14.3	25.1	17.8	32.1
100 m	14.9	24.6	16.6	34.2

In the simulations, a directional grid of beams is implemented in the user end, and every simulation step, the beam said to be active is that maximizing the Reference Signal Received Quality (RSRQ). In Paper G, the average DL SINR at the high load point increases from -5 to 0 dB when the grid of two beams is used (Fig. G.9). Likewise, the outage probability drops from 23 % to 0.3 %. Yet, by implementing a grid with 6 directional beams, the reliability of 99.9 % is achieved.

Paper H does not show the results for implementations with 6 beams, but, in the urban scenario simulated, the reliability goes up from approximately 80 % to 99.8 % in the high load condition by implementing just 4 beams.

It is worth noting that by achieving the reliability requirement even under the stringent network load simulated, the grid of beams shows promising potential to enhance the performance of real C2 deployments.

The main goal of deploying a grid of beams at the UAV-UE is to increase the robustness of the C2 DL against the interference. But as a by-product, it also improves the UL performance. It mitigates the interference induced by the UAV in the network, providing throughput gain for the terrestrial users similar to those reported by a reduction of 6 dB in P0, but without sacrificing the throughput of the UAVs. Instead, by directing most of the UAV's transmission power to the direction of the serving base station, the grid of beams causes the UAVs' throughput to double in the simulations.

4.3.6 Current network deployments cannot cope with C2 latency requirements

The C2 traffic model was emulated in a field trial performed in a urban scenario in Denmark and the results reported in Paper I. The end-to-end latency is measured for the packets exchanged in both UL and DL. The results shows that the 3GPP requirements are challenging for current LTE-A deployments. Albeit the median end-to-end latency measured is significantly below the 50 ms threshold (see Table 4.3), less than 99.9 % of C2 packets fulfills this requirement.

In fact, radio connectivity failures in LTE transmissions cause a long-tail

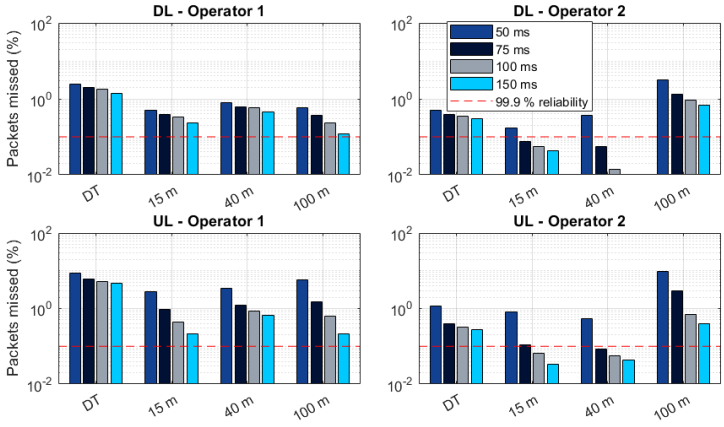

Fig. 4.5: Percentage of packets received above different latency thresholds for the measurements presented in I

in the distribution of the measured latency. As discussed in Paper I, when these happen, several consecutive packets are affected, until the problem is solved (usually from a re-establishment of the connection or a handover). Fig. 4.5 shows that because of this long-lasting peaks of delays, relaxing the latency requirement does not alleviate much the problems in achieving 99.9 % of reliability, especially at 100 m height.

4.3.7 Dual-Network hybrid performance approximates C2 requirements

The position of the eNodeBs, the orientation and tilting of network's antennas, and the site density are all related to the network planning and are customized differently in different networks. Also, the load balancing and total load varies between the operators. Thus, the correlation among instantaneous delays observed across the operators should be low. On the other hand, there are some degree of correlation expected, as it is common that multiple networks share site installations, for economical and practical reasons, and also the wired backhauling.

It is worth to remember that the 3GPP requirements is set for the delay between UAV and eNodeB, which is smaller than the end-to-end delay measured in our study. This means that the values measured provide good insight about the performance not only of the air interface but for the whole C2 system.

So, a dual-operator hybrid access is proposed such that the UAV is simultaneously connected to the controller through two operators. In the proposed

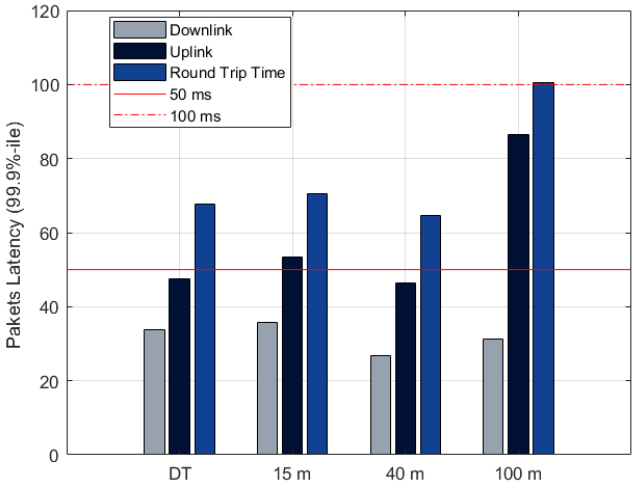

Fig. 4.6: 99.9%-ile of received packets for DL, UL and round-trip time (RTT) for the hybrid access strategy [5].

scheme, the messages are always sent through the two links and considered received when they are first rightly decoded through any of the two links. This rather simple implementation is transparent for the network operators, and do not require any technical modification on their part.

The results show that the hybrid access scheme has potential to improve the latency of both UL and DL. Fig. 4.6 shows the 99.9% -ile for the packets' latency for UL, DL, where it is possible to see that the end-to-end delay reaches the 99.9 % reliability for most cases. There is one case, UL at 100 m, where the requirement was not reached. Yet, the other solutions discussed in this paper, such as the directional transmission, or the addition of more networks into the hybrid access strategy could easily enhance the results to desired level. Fig. 4.6 also shows the RTT, which measures the DL and UL delay combined. The results indicate that messages can be exchanged back-and-forth between UAV and controller with a total latency below 100 ms.

Assuming total independence between the latency experienced over different networks, the hybrid access reliability, R_{ha}, for a given latency will be given by:

$$R_{ha} = 1 - \prod_{i=1}^{M} (1 - R_i) \tag{4.6}$$

where R_i is the the reliability of the i-th operator within the latency threshold

and M is the total number of networks in the hybrid access scheme. However, as observed across our measurements the results are slightly worse than described by this equation, probably caused by some residual correlation across the networks as previously explained.

4.3.8 Some aspects of LTE-A physical layer can be further improved in future technologies

Besides the grid of beams technique, the performance of C2 links can also benefit from improvements in the physical layer of cellular technologies. Paper H presents an insightful discussion of some of these aspects.

The field measurements presented in Section H.III where performed at night time, where almost no traffic load is present in the network, however, the interference increase was noticeable when comparing the measurements at 100 m with the ground level reference. This can be attributed to the quiescent interference caused by the reference symbols, as discussed in Section 4.1.1. The next generation of cellular technologies envisioned by 3GPP, the 5G New Radio (NR), mitigates this problem by introducing user-specific reference symbols [23]. The main advantage is that those are not continuously transmitted and do not create "background" interference even in the absence of cell load.

Latest releases of LTE-A also have enhanced the PDCCH allocation, by introducing the concept of enhanced PDCCH (e-PDCCH), where user-specific PDCCH allocations are performed, aiming at enabling the channel's directional transmission [24]. However, the e-PDCCH is more an "add-on" than a native feature of LTE, and tends to be inefficient. For example, the space of search of user-specific e-PDCCH must be previously defined in PDCCH that is still required to initiate the transactions between end user and network [24]. The NR technology allows, by design, the allocation of PDCCH in user specific positions, increasing the flexibility for deploying directional transmissions of the control channel [23].

4.4 Discussion

The service provided to UAVs by terrestrial LTE networks designed for terrestrial coverage is likely to provide less reliability, specially under heavy load circumstances. In the absence of interference, the network physical layer is easily capable of delivering 100 kbps within 50 ms, however, because of the interference, it cannot achieve such performance at 99.9% of the time. Throughout this chapter, several techniques to minimize the impact of the interference were presented and discussed.

4.4.1 Downlink Performance Enhancement

In DL, the network coordination provides an inefficient way to handle these challenges, as the interference is caused by multiple sources. First, the absence of a clear dominant interferer limits the potential gain of removing one or a few sources of interference. On the other hand, muting several interfering cells creates very large coordination sets that extends over a large area, which is complex to manage and very difficult to scale.

Likewise, there is also some challenges to effectively deploy IRC solutions at the UAV side. The expected gain depend of the DIR, which tends to be low, as multiple sources of interference are expected. In theory, it is possible to remove several interfering cells using SIC, but it will require the implementation of several receiving antennas on the UAV side. Moreover, this cannot be done indefinitely, as the power of the receiving signal is also subject to some attenuation at every iteration.

It is possible, though, that in combination with other more efficient strategies, both of these techniques can be proved more efficient.

Besides these two methods, other two methods, both based on implementations at the UAV side have showed more efficiency to enhance the C2 performance. These methods are advantageous because they do not require changes in the network specifications, development of new technical solutions nor expensive investments in the network deployment.

The use of directional antennas at the UAV-UE side has proven very efficient to mitigate the DL interference. By maximizing the RSRQ, the method proposed tends to choose the antenna receiving less interference from the medium. It is noteworthy that the proposed scheme is not an optimized beamforming strategy, rather, it simply proposes using multiple antennas oriented in different predetermined directions and choosing the one that maximizes the RSRQ. Although it can be implemented in the UE, regardless any assistance from the network operator, it can be beneficial if technical solutions on the network side are developed to handle such use cases. The reason behind it is that handovers and mobility measurements can be degraded by considering a very directional transmission on the UE side.

Another solution that has demonstrated significant potential for enhancing the reliability KPI was the usage of hybrid access solutions at the UAV-UE, where the device transmits/receives the C2 messages simultaneously through multiple operators. The hybrid access solution can be implemented transparently from the network point of view, as emulated in our measurements.

The networks may also assist the hybrid access performance, by using multiple carrier solutions in the transmission. The principles would be the same: sending/receiving duplicates of the C2 messages through multiple frequency carriers. Usually, the instantaneous load in different network carriers

are different of each other, so it is the interference. If it becomes a network-assisted solution, it can be adjusted dynamically, deciding on the usage of multiple carriers depending on whether the current interference is high or not.

Other technological enhancements of the physical layer are also envisioned for 5G technology and they can help to improve the overall system performance. For instance, user-specific reference signals will reduce the pilot pollution, whereas user specific PDCCH will offer more flexibility for directional transmissions and enable beamforming solutions for the control channels as well. The DL transmit beamforming can also be an attractive solution to be used either standalone or in combination with the directional beams of the UE [25,26]. The next generation of cellular technology includes the usage of higher frequencies, increasing the number of beams available in the network [27]. However, it is important to remember that, with multiple interfering sources, the adaptation of the direction of "nulls" and "peaks" of antenna gain may be a complex task to manage [25].

4.4.2 Uplink Performance Enhancement

The uplink interference is rather limited for the C2, as the amount of resources occupied tends to be small for the periodicity and size of the C2 messages. However, outside the scope of the C2, the UAV can also use broadband applications in UL, with live streaming being the classical example of such cases.

In this case two strategies have proved beneficial. From the network point of view, it is possible to minimize the interference by adopting different PC parameters specifically for the UAV. Albeit it slightly decreases the UAV throughput, it cause a lower overall degradation of the performance of other users in the network. From the UE point of view, the minimization of the UL interference is a by-product of the deployment of the directional transmissions used for enhancing the DL performance, as they minimize the number of cells affected in the network.

The measured delayion UL is also a point of concern according to the measurement results. Few aspects in the network design can also be tweaked, to minimize the link latency. In LTE the UL Hybrid Automatic Repeat Request (HARQ) retransmissions take place at least 8 ms after the first message is conveyed. Considering additional delays observed in the network, withing a few retransmissions the user approximates the 50 ms threshold of latency. This is a similar problem than that faced by Voice over LTE (VoLTE) users and can benefit from similar solutions.

First, it is possible to adopt a more conservative BLER target for the first transmission, by adopting more robust MCS for C2 links. This would lead up to more resource consumption in the first transmission, but would reduce the number of retransmissions required. Another option is to enable the UL TTI

bundling used for VoLTE users, when the data is preemptively retransmitted in consecutive TTIs when the channel conditions are bad, minimizing the time spent for redundant versions to be transmitted.

References

[1] D. J. Costello and G. D. Forney, "Channel coding: The road to channel capacity," *Proceedings of the IEEE*, vol. 95, no. 6, pp. 1150–1177, June 2007.

[2] 3GPP, "Evolved Universal Terrestrial Radio Access (E-UTRA); Multiplexing and channel coding," 3rd Generation Partnership Project (3GPP), Technical Specification (TS) 36.212, Sep. 2016, version 14.0.0.

[3] ——, "Enhanced LTE support for aerial vehicles," 3rd Generation Partnership Project (3GPP), Technical Specification (TS) 36.777, Jan. 2018, version 15.0.0.

[4] F. Capozzi, D. Laselva, F. Frederiksen, J. Wigard, I. Z. Kovacs, and P. E. Mogensen, "UTRAN LTE Downlink System Performance under Realistic Control Channel Constraints," in *2009 IEEE 70th Vehicular Technology Conference Fall*, Sep. 2009, pp. 1–5.

[5] 3GPP, "Evolved Universal Terrestrial Radio Access (E-UTRA); Physical channels and modulation," 3rd Generation Partnership Project (3GPP), Technical Specification (TS) 36.211, Dec. 2009, version 8.9.0.

[6] ——, " Evolved Universal Terrestrial Radio Access (E-UTRA) and Evolved Universal Terrestrial Radio Access Network (E-UTRAN); Overall description; Stage ," 3GPP, Tech. Rep. TS 36.300 V8.12.0, Mar. 2010.

[7] ——, " Evolved Universal Terrestrial Radio Access (E-UTRA) and Evolved Universal Terrestrial Radio Access Network (E-UTRAN); Overall description; Stage ," 3GPP, Tech. Rep. TS 36.300 V10.12.0, May 2015.

[8] ——, " Evolved Universal Terrestrial Radio Access (E-UTRA); Requirements for support of radio resource management ," 3GPP, Tech. Rep. TS 36.300 V16.0.0, Jan. 2019.

[9] H. Holma, A. Toskala, and J. Reunanen, *LTE Small Cell Optimization: 3GPP Evolution to Release 13*. John Wiley and Sons, 2016.

[10] Y. Léost, M. Abdi, R. Richter, and M. Jeschke, "Interference rejection combining in LTE networks," *Bell Labs Technical Journal*, vol. 17, no. 1, pp. 25–49, June 2012.

[11] W. C. Y. Lee, "Antenna spacing requirement for a mobile Radio base-station diversity," *The Bell System Technical Journal*, vol. 50, no. 6, pp. 1859–1876, July 1971.

[12] V. Fernández-López, K. I. Pedersen, and B. Soret, ""Interference characterization and mitigation benefit analysis for LTE-A macro and small cell deployments"," *EURASIP Journal on Wireless Communications and Networking*, vol. 2015, no. 1, p. 110, Apr 2015. [Online]. Available: https://doi.org/10.1186/s13638-015-0344-z

[13] 3GPP, " Study on Network-Assisted Interference Cancellation and Suppression (NAIC) for LTE," 3GPP, Tech. Rep. TR 36.866 V12.0.1, Mar. 2014.

[14] C. U. Castellanos, D. L. Villa, C. Rosa, K. I. Pedersen, F. D. Calabrese, P. Michaelsen, and J. Michel, "Performance of Uplink Fractional Power Control in UTRAN LTE," in *VTC Spring 2008 - IEEE Vehicular Technology Conference*, May 2008, pp. 2517–2521.

[15] R. Mullner, C. F. Ball, K. Ivanov, J. Lienhart, and P. Hric, "Contrasting Open-Loop and Closed-Loop Power Control Performance in UTRAN LTE Uplink by UE Trace Analysis," in *2009 IEEE International Conference on Communications*, June 2009, pp. 1–6.

[16] N. J. Quintero, "Advanced Power Control for UTRAN LTE Uplink," Master's thesis, Aalborg University, 2008.

[17] M. Coupechoux and J. Kelif, "How to set the fractional power control compensation factor in LTE?" in *34th IEEE Sarnoff Symposium*, May 2011, pp. 1–5.

[18] 3GPP, " Evolved Universal Terrestrial Radio Access (E-UTRA); Physical layer procedures ," 3GPP, Tech. Rep. TS 36.300 V15.14.0, Jan. 2019.

[19] ——, " Evolved Universal Terrestrial Radio Access (E-UTRA); Radio Resource Control (RRC); Protocol specification," 3GPP, Tech. Rep. TS 36.331 V15.4.0, Feb. 2019.

[20] M. M. et all, "Clarity from above. PwC global report on the commercial applications of drone technology," PwC, Tech. Rep., May 2016.

[21] G. Pocovi, T. Kolding, M. Lauridsen, R. Mogensen, C. Markmller, and R. Jess-Williams, "Measurement Framework for Assessing Reliable Real-Time Capabilities of Wireless Networks," *IEEE Communications Magazine*, vol. 56, no. 12, pp. 156–163, December 2018.

[22] D. Laselva, F. Capozzi, F. Frederiksen, K. I. Pedersen, J. Wigard, and I. Z. Kovacs, "On the Impact of Realistic Control Channel Constraints on QoS Provisioning in UTRAN LTE," in *2009 IEEE 70th Vehicular Technology Conference Fall*, Sep. 2009, pp. 1–5.

[23] 3GPP, "NR; Physical channels and modulation," 3GPP, Tech. Rep. TS 38.211 V15.0.0, Jan. 2018.

[24] S. Ye, S. H. Wong, and C. Worrall, "Enhanced physical downlink control channel in LTE advanced Release 11," *IEEE Communications Magazine*, vol. 51, no. 2, pp. 82–89, February 2013.

[25] G. Geraci, A. Garcia-Rodriguez, L. G. Giordano, D. Lopez-Perez, and E. Bjoernson, "Supporting UAV Cellular Communications through Massive MIMO," in *2018 IEEE International Conference on Communications Workshops (ICC Workshops)*, May 2018, pp. 1–6.

[26] Z. Xiao, P. Xia, and X. Xia, "Enabling UAV cellular with millimeter-wave communication: potentials and approaches," *IEEE Communications Magazine*, vol. 54, no. 5, pp. 66–73, May 2016.

[27] T. S. Rappaport, G. R. MacCartney, M. K. Samimi, and S. Sun, "Wideband Millimeter-Wave Propagation Measurements and Channel Models for Future Wireless Communication System Design," *IEEE Transactions on Communications*, vol. 63, no. 9, Sep. 2015.

Paper G

How to ensure reliable connectivity for aerial vehicles over cellular networks

Huan C. Nguyen, Rafhael Amorim, Jeroen Wigard, István Z. Kovács, Troels B. Sørensen and Preben Mogensen

The paper has been published in
IEEE Access Vol. 6, pp. 12304-12317, 2018.

© 2018 IEEE
The layout has been revised and reprinted with permission.

Abstract

[1] *Widely deployed cellular networks are an attractive solution to provide large scale radio connectivity to unmanned aerial vehicles. One main prerequisite is that co-existence and optimal performance for both aerial and terrestrial users can be provided. Today's cellular networks are, however, not designed for aerial coverage, and deployments are primarily optimized to provide good service for terrestrial users. These considerations, in combination with the strict regulatory requirements, lead to extensive research and standardization efforts to ensure that the current cellular networks can enable reliable operation of aerial vehicles in various deployment scenarios. In this paper, we investigate the performance of aerial radio connectivity in a typical rural area network deployment using extensive channel measurements and system simulations. First, we highlight that downlink and uplink radio interference play a key role, and yield relatively poor performance for the aerial traffic, when load is high in the network. Secondly, we analyze two potential terminal side interference mitigation solutions: interference cancellation and antenna beam selection. We show that each of these can improve the overall, aerial and terrestrial, system performance to a certain degree, with up to 30% throughput gain, and an increase in the reliability of the aerial radio connectivity to over 99%. Further, we introduce and evaluate a novel downlink inter-cell interference coordination mechanism applied to the aerial command and control traffic. Our proposed coordination mechanism is shown to provide the required aerial downlink performance at the cost of 10% capacity degradation in the serving and interfering cells.*

I Introduction

The market for Unmanned Aerial Vehicles (UAVs), flying in the very low level (VLL) airspace [1], is rapidly growing and emerging commercial use cases are being developed day by day. Besides aerial photography and film-making, UAVs become very useful for agricultural or pipe-line inspection, package delivery and disaster-relief applications. In general, it can be said that UAVs, also commonly referred to as *drones*, are used to streamline operations, to reduce risks and to improve efficiency [2].

Current regulations in most countries limit drone operations to the cases in which there is visual line of sight (VLOS) between an UAV and its pilot. However, it is expected that beyond visual line-of-sight (BVLOS) operations will be allowed for extended flight range, provided there is a reliable Command and Control (C2) link to the drone. The C2 link is critical to safe operations of the drones. In the uplink (UL), i.e. from a drone to a base sta-

[1]This research has received funding from the SESAR Joint Undertaking under the European Union's Horizon 2020 research and innovation programme, grant agreement No 763601. The research is conducted as part of the DroC2om project.

tion (BS), the control link is used to update the Unmanned Aircraft System Traffic Management (UTM) or flight control unit with the drone location, plus potentially crucial information, such as telemetry and sensor readings, which the control function can utilize to make its decisions. In the downlink (DL), from BS towards the drone, the C2 link allows the control function to change the drone's flight path to avoid potential collisions, or to command a range of sensor/actuator functions on board of the drone. As one example, the DL C2 can be used to maneuver the UAV, when its originally-designed route crosses the path of a manned vehicle (e.g. helicopter) that suddenly needs to land for an emergency.

Cellular networks are an attractive solution to provide the C2 connectivity. In particular, current Long-Term Evolution (LTE) based systems present many advantages such as: an already in place infrastructure that provides almost full coverage, therefore minimizing the investments; shared resources with terrestrial UEs (TUEs) to reduce the operational costs; flexible scheduler and multiple access to maximize resource usage efficiency. For very remote rural areas, and UAVs at the limit of VLL airspace, cellular coverage can be complemented with satellite. In this paper, we will concentrate on the parts of the network with full, or close to full, coverage. The biggest challenge is that cellular networks are not designed for aerial coverage, since their base stations typically use down-tilted antennas optimized for TUEs.

Not surprisingly various regulatory committees are striving for specifying the rules, which UAV operations must conform to, in order to ensure a robust and well-organized transition towards the "Aerial Vehicles era". It is critical that this transition shall occur without impacting the legacy functionalities and deployments. Among those organizations addressing UAV use cases, one can find also the Third Generation Partnership Project (3GPP), responsible for standardizing worldwide cellular technologies, such as Universal Mobile Telecommunications System (UMTS) (so-called: 3G) or LTE (4G). In March 2017, a 3GPP study item: "Enhanced support for Aerial Vehicles" was approved [3], aimed at preparing LTE networks to support a new type of user equipment (UE), likely to emerge in cellular networks in the imminent future: airborne users flying at heights up to 300 m above the ground level. These works include the development of propagation channels and line-of-sight (LOS) probability models, and the assessment of coverage and capacity provided by cellular networks to UAV's connectivity [3].

It is important to note that several previous works have proposed the usage of UAVs as relay nodes and aerial BSs, for example [4,5], in order to improve the overall system capacity, but this is a fundamentally different problem as the one we are trying to solve in this paper. Throughout this work, UAVs are treated as airborne UEs connected to terrestrial cellular networks.

The radio propagation channel for UAVs flying above buildings, terrain roughness and other forms of obstruction is considerably different from those

observed by a TUE on the ground. For instance, the work in [6] shows that the LOS probability between a TUE and UAV increases monotonically with the elevation angle between the two devices, and therefore to UAV heights. Although this study is based on TUEs being served by a UAV-BS, the same rationale should apply to the case, where UAVs are users connected to the BS. Measurements conducted in [3,7] for the case of LTE showed the implications of higher UAV heights due to radio path clearance: higher number of neighbor cells observed, increased interference power, and reduced shadowing variation.

Besides radio clearance, the effect of antenna down-tilt should also be taken into account. As previously mentioned, the BS's antennas in cellular networks are down-tilted in order to optimize the terrestrial coverage, and this will impact the quality of the link between BS and UAV. The combination of the two effects are well described in [8], where the authors propose a channel model that adjusts a ground level model, by introducing a compensation function depending on the angle between UAV and BS. The reference for the model parameters are field measurements collected at 850 MHz for a BS with a monopole antenna. In [9], a modified two-ray model is presented to account for variations in the path loss exponent and antenna gains according to UE height.

In [10], a generic height-dependent channel model is proposed for UAV in a rural environment based on field measurements (see Figure G.1), for heights up to 120m. Besides its simplicity, the model also provides a tool to evaluate the channel for different types of antennas, and captures the effects caused by side lobes of highly-directive antennas as commonly deployed in cellular systems. The simulations and analysis in this paper are performed using this channel model.

In cellular networks, the BS's inter-site distance (ISD) is designed according to ground level channel models and the density of TUEs. The ISD is therefore not optimized for the different propagation environment perceived by UAVs. As a result of this, and the radio path clearance, their radio performance tends to be negatively impacted due to a significant increase in interference levels [11]. Using the model in [10], the studies in [3,12] showed that highly loaded scenarios present a challenge for UAV coverage due to the interference levels observed, while the work presented in [13] disclosed that the interference mitigation gain depends significantly on the scenario's radio characteristics.

This paper presents an evaluation of specific UAV interference mitigation techniques by means of simulations, and its main goal is to evaluate how well existing techniques, traditionally optimized for TUEs, perform when applied to UEs mounted on drones. Different techniques are investigated for UL and DL cases, which are split in two groups: terminal-based and network-based solutions.

Fig. G.1: Preparation for UAV channel measurement: Our pilot is mounting the R&S scanner on the DJI Matrice 600 drone.

Terminal-based solutions assume UE operations are compatible with 3GPP's specifications, regarding power level and number of transmit antennas. The 3GPP Release 8 dictates that a UE can use 2, and up to 4 antenna elements [14]. Implementations with more elements is not practically precluded, provided the number of 'visible' elements to the radio network in any given transmission fulfill the 3GPP requirements. The size, geometry and degrees of freedom in the UAV movement, opens up several possibilities for multiple antenna deployments and interference mitigation techniques. As one example, the 3GPP study item [3] has concluded that the usage of beamforming solutions implemented on the UAV side presents the potential to increase the signal to interference plus noise ratio (SINR) in both DL and UL. Usually, UE-side beamforming imposes some additional challenges for deployments, such as high-complexity processing and proper handling of handover events. In this paper, a more simplistic approach is investigated, where UAV characteristics are explored to produce an array of directional antenna beams in combination with antenna selection on the UAV side.

Interference cancellation is another terminal-based solution investigated in this paper. 3GPP Release 8 UEs can implement either interference cancellation (IC) or Interference Rejection Combining (IRC), and the performance

of these techniques in LTE networks have been previously evaluated for TUEs [15]. However, the interference observed by UAVs differ from previous models, as several interfering sources are expected instead of a few dominant ones [13]. In this paper we extend the evaluation of IC performance under such a new scenario.

The network-based solutions presented in this paper are restricted to practical interference mitigation schemes that do not require significant changes on the network side, i.e. without modifying the type or number of BS antenna elements, their tilts, or carrier frequencies (e.g. use of dedicated carriers). This ensures that that the LTE network remains optimized for TUEs. The first network-based solution considered in the paper is the optimization of UL Open Loop Power Control (OLPC) parameters. As UAVs tend to have lower propagation losses and higher number of interfering BSs compared to TUE, applying the same UL power constraints will result in UAVs radiating high interference power to many neighboring BSs. In this paper, we evaluate a solution where different power control settings are applied to UAVs and TUEs. The solution assumes that the network is capable of identifying the airborne state of UEs, which can be achieved for legacy networks [3,16].

Different inter-cell interference coordination (ICIC) solutions have been previously studied for LTE, e.g. [17]. The general concept is that neighbor cells coordinate the data transmission to reduce the overall interference levels. In general, the improvements in SINR are obtained at the expense of capacity loss, as some BSs are prevented to transmit in some radio resources. Our paper proposes and evaluates the potential benefits and capacity costs of implementing a novel inter-cell coordination mechanism for the DL C2 traffic of the UAVs served in the network.

The remainder of this paper is organized as follows. Section II features an overview of the height-dependent channel model used. Section III describes our system level simulator and its key parameters, while reference simulation results are presented in Section IV. Assessments on the interference mitigation techniques are made in Section V and VI, and finally the conclusions are presented in Section VII.

II Height-Dependent Rural Propagation Model

In a previous study, we have performed a measurement campaign at two locations in Fyn, Denmark, to characterize the propagation channel between terrestrial BSs and UAVs in a rural scenario. The readers are encouraged to refer to [10] for detailed information on the measurement campaign, and the derivation of a large-scale path loss model for UAVs. Here the proposed height-dependent path loss model, which is applied in our simulations, is briefly presented for the sake of completeness. It takes the following form:

$$PL_{\text{AB}}(h_u, d) = 10\alpha_{h_u} \log_{10}(d) + \beta_{h_u} + X_{\sigma_{h_u}} \quad \text{[dB]} \tag{G.1}$$

where $PL_{\text{AB}}(h_u, d)$ is the mean path loss taking into account: (a) the 3-dimensional (3D) distance d between BS and UAV, and (b) the UAV's height h_u. Both distance and height are in meters. The term α_{h_u} is the path loss slope, β_{h_u} is the floating intercept (in dB), and $X_{\sigma_{h_u}}$ is a normal-distributed random variable with zero mean and standard deviation σ_{h_u}, which represents the large-scale shadow fading.

Table G.1: Rural Height-Dependent UAV Propagation Model

h_u	Model's Parameters			Detected Cells (average)
	α_{h_u}	β_{h_u}	σ_{h_u}	
Ground (1.5 m)	3.7	-1.3	7.6	5.1
15 m	2.9	7.4	6.2	6.1
30 m	2.5	20.4	5.2	7.6
60 m	2.1	32.8	4.4	11.6
120 m	2.0	35.3	3.4	16.9

The channel model parameters extracted from our measurements, according to the best-fit of G.1, are presented in Table G.1. It is important to note that they are changing with height: First, a slope of 3.7 at ground level is observed, which is close to that of existing rural propagation models, such as Okumura-Hata [18] or 3GPP non line-of-sight (NLOS) Rural Macro (RMa) [19] model. When the height of the UAV increases, the measured slope decreases and approaches the value of 2, i.e. free-space path loss. Second, the shadow fading variation, σ_{h_u}, is also reduced with height: Approximately 7.6 dB is observed at 1.5m, whereas at 120 m it is only 3.4 dB. Both indicate that the propagation path from a ground BS to an elevated drone is often clear from obstacles, which increases the received signal strengths seen at/from the drone. As a result, the number of neighboring cells detected by the drone is also increased with height, which implies stronger interference in both UL and DL [3,12]. The interference seen from the drone, or caused by it, will be analyzed in greater detail in Section IV. We assume that the propagation channel becomes height-independent after 120 m, since increasing height at this point does not improve the radio path clearance further. Therefore, the channel model's parameters at 120 m can be applied for higher heights.

III System Level Simulator

Our analysis is based on a simulation framework for quantitative investigation of user mobility, with focus on the 3GPP LTE technology, which is described in [20–22]. In this section we introduce the modeling assumptions, parameters and Key Performance Indicators (KPIs) used in our simulations.

A. Modeling Assumptions

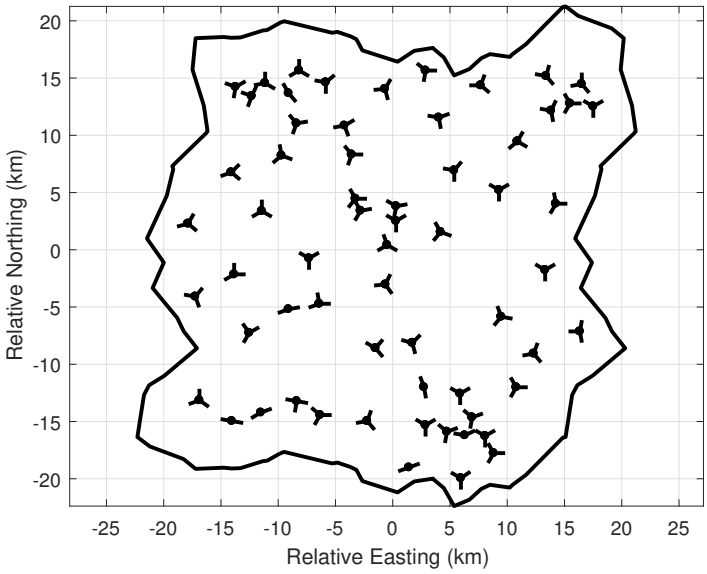

Fig. G.2: Rural network layout, including 179 cells, for simulation evaluation. Dark solid line demarcates network border.

A network of C cells is considered, where each cell c is described by a set of properties, including its 3D position, antenna pattern, bearing, tilting and transmitting power. To make the study more realistic, an actual 800 MHz LTE network, depicted in Figure G.2, is imported into our simulation: The network consists of 179 cells covering a 40 km x 40 km area in Fyn (Denmark), where the measurements presented in Section II have been performed. This is to ensure that the path loss model is applied in the same environment in which it was measured. The average ISD is 3 km, and the network is wrapped around to introduce interference at the network edge.

There are U users dropped uniformly in 2-dimension within the network. All TUEs are assumed to be at 1.5 m, while all UAVs are dropped at a given

height, specified by the simulation scenario. The users move along linear trajectories in random directions through the network at a constant velocity. User mobility is constrained to be within the network border to remain in coverage. When a UE reaches the border, it will bounce back following a random direction. At time instant t the position of user u is described by the location function $p_u(t)$. We utilize the height-dependent propagation channel model, introduced in Section II, in the calculation of received power $R_c(p)$ from the antenna of cell c towards any location p on the map:

$$R_c(p) = P_{\mathrm{DL}} - PL_{\mathrm{AB}}(h_u, d_{c,p}) + G_c(\phi_{c,p}, \theta_{c,p}) \quad [\mathrm{dBm}] \tag{G.2}$$

where P_{DL}, measured in dBm, is the transmitting power from cell c, and G_c is the antenna gain (in dB) in the direction of location p. The $d_{c,p}$, $\phi_{c,p}$ and $\theta_{c,p}$ are the 3D distance, azimuth and elevation angle between cell c and location p, respectively. When UE is moving, all these parameters are time-dependent.

The cell c serving user u at time instant t is defined by the connection function $c = x_u(t) \in \{1, 2, 3...C\}$. As the user moves through the network, its serving cell can change via Handover (HO) procedure according to 3GPP specifications. The user continuously measures Reference Signal Received Quality (RSRQ) level from all cells, and once a neighboring cell becomes better than the serving cell by an offset Δ_{A3} for a period of time TTT, i.e. A3 event, the HO procedure is triggered. Using the approach in [20], the instantaneous wideband DL SINR $\gamma_{u,c}(t)$ of user u at time instant t (from the serving cell c) can be approximated by:

$$\gamma_{u,c}(t) R_c(p_u(t)) - 10 \log_{10} \left[\sum_{i \neq c} \rho_i(t) 10^{\frac{R_i(p_u(t))}{10}} + 10^{\frac{N}{10}} \right] \quad [\mathrm{dB}] \tag{G.3}$$

in which N is the thermal noise power in dBm, and $\rho_i \in [0, 1]$ is the load in the i^{th} cell at time t, indicating that a cell with lower load, ρ_i is close to zero, produces lower interference.

The SINR determines how much DL throughput a user can get with a given number of assigned Physical Resource Blocks (PRBs). The UE is said to be in 'outage', if its DL SINR gets below a threshold Q_{out} such that communication is no longer possible. This might happen due to either too low signal from serving cell or too high total interference from all neighboring cells. Another threshold, Q_{in}, is defined as having much higher probability of reception than Q_{out}, and once the DL SINR is better than Q_{in} the communication channel is assumed to be back to normal. In our simulation, Q_{out} and Q_{in} are chosen according to [3] as -8 dB and -6 dB, respectively. The duration in which the user's SINR goes below threshold Q_{out} and until it becomes better than Q_{in} is defined as the *time in* Q_{out}. If the user is in Q_{out}

for longer than a period of T_{310}, it is considered to experience a Radio Link Failure (RLF), and therefore a recovery procedure will be triggered, i.e. the user disconnects from the current cell and starts searching for a better serving cell.

In LTE, the UL power control is implemented as a combination of Open Loop Power Control (OLPC) and Closed Loop Power Control (CLPC) [23]. In this study, we focus only on the usage of OLPC, because it is simple and does not require feedback information from serving BS. The algorithm can be described as follows:

$$P_{\mathrm{UL}} = \min\left\{P_{\mathrm{UL}}^{\max}, \mathrm{P0} - \Delta_{\mathrm{P0}}^{u} + \alpha PL_{\mathrm{est}} + 10log_{10}M\right\} \quad [\mathrm{dBm}] \tag{G.4}$$

in which P_{UL} and $P_{\mathrm{UL}}^{\max}$ are respectively the UE's actual and maximum allowed transmit power. P0 is a parameter designed according to the target signal to noise ratio (SNR) [23]. Also, $\alpha \in [0, 1]$ is the fraction of estimated path loss (PL_{est}) to be compensated, and M represents the number of PRBs allocated to the UE in the UL. The term Δ_{P0}^{u}, called P0 offset, is specific to our approach for mitigating interference from UAVs, which is described in more details later in Section A..

B. Simulation Parameters and KPIs

The most important parameters for our simulations are summarized in Table G.2. The radio mobility parameters follow the assumptions used in the 3GPP Aerial Vehicle performance studies [3]. Each cell has 10 users on average, i.e. counting both TUEs and UAVs. In DL, the TUE traffic pattern is modeled as File Transfer Protocol (FTP) sessions, where both packet size and arrival time are Poisson-distributed random variables. By keeping the mean packet size constant at 20 Mbit and varying the mean arrival time from 20 to 80 s, we control the *downlink offered load* in the network. The load is measured as the percentage of PRBs being scheduled, averaged over all cells and simulation steps. The UAV is assumed to have only C2 data in DL, which is modeled as a Constant Bit Rate (CBR) traffic of 100 kbps, or equivalently 1250 Bytes every 100 ms. Our DL scheduler prioritizes the C2 traffic over the FTP traffic, meaning that the C2 will be scheduled first, and then the remaining resources will be divided equally among the connected TUEs which have FTP data to receive. Users are assumed to be in *idle-mode*, if there is no DL data to be transmitted. A user switches from idle to *connected-mode*, when DL packet arrives at the buffer, if it is not currently in RLF. Once the data buffer is clear, the user returns to idle-mode. For the UL data traffic of both TUEs and UAVs, we assume a full buffer traffic model, in which UL transmission is off when the DL is in either idle-mode or in RLF. In other words, the UL traffic load in our simulations will also be lower, when the DL

offered load is reduced and/or when the outage probability is high due to RLF.

The main KPI's used in this paper for assessing the impact of deploying UAVs on the network performance are listed below. Each of these KPIs is evaluated separately for TUEs and UAVs.

- **DL SINR**: Average UE DL connected-mode SINR, which is the $\gamma_{u,c}(t)$ gathered under the condition that the UE has data to receive and not in RLF, and averaged over all UEs and time instants.
- **DL throughput**: Average UE DL throughput, collected under the same condition as the DL SINR.
- **Outage probability**: Estimated as percentage of time instants that a UE is in Q_{out} relative to the total simulation time, averaged over all UEs.
- **Average time in Q_{out}** : Duration for time in Q_{out} averaged over all Q_{out} occasions and UEs.
- **UL SINR**: Average UE UL SINR, which is defined the same way as the DL SINR above, but for UL resources. Details on UL SINR calculation used in the simulations are found in [21].
- **UL throughput**: Average UE UL throughput corresponding to the UL SINR.

IV Reference Simulation Results

This section looks at the impact of UAV deployment on cellular network performance in both DL and UL. The performance numbers presented in this section are the reference points for discussing the gain of interference mitigation techniques in Sections V and VI.

A. Downlink Performance

Figure G.3 shows the average SINR, which is collected for UAVs and TUEs separately, as a function of the offered load. The *Ref* refers to the case when all users in the network are TUEs, and the *Hxm* is where UAVs account for 1% users and fly at a constant height of x meters. As the traffic load increases, TUEs in the *Ref* case are subjected to only a slight DL SINR degradation: The average SINR drops from 3 dB to 1 dB as the offered load jumps from 10% to 67%. On the other hand, it is evident that the UAV SINR is a function of both network load and the height at which the UAVs are deployed. At the lowest load point, the UAVs experience better SINR than TUEs in general,

Table G.2: Key Simulation Parameters

Parameter	Value
Simulation area	40 x 40 km
Number of cells (C)	179 cells
Average network ISD	3.0 km
Cell's transmit power (P_{DL})	49 dBm
System bandwidth	20 MHz
Carrier frequency	800 MHz
MIMO configuration	2x2
2D shadowing correlation distance	100 m
Shadowing correlation	0.5 (sites), 1 (cells)
Total number of users (TUE + UAV)	1790 (average 10 per cell)
User velocity	30 km/h
TUE DL traffic	FTP model
TUE DL packet size	20 Mbit on average
UAV DL C2 traffic	CBR model
UAV DL C2 data rate	100 kbps
UL traffic for TUE and UAV	Full buffer model
Threshold Q_{out}	-8 dB
Threshold Q_{in}	-6 dB
RLF timer (T_{310})	1 s
RSRP and RSRQ measurement error	1.22 dB
HO event	A3 with Δ_{A3} = 2 dB
HO Time to trigger (TTT)	160 ms
Maximum UL transmit power ($P_{\mathrm{UL}}^{\mathrm{max}}$)	23 dBm
Power control P0	-98 dBm per PRB
Power control α	0.8

partially due to the gain from better serving cell signal strength. However, when the load increases, their SINR drops quickly: At 120 m the UAV SINR falls from 7 dB to -5 dB, if network load increases from 10% to 67%. That is a significant 12 dB reduction, compared to merely 2 dB for TUEs in the same situation. It indicates that the UAV DL connection is much more sensitive to network load than the TUE. The UAV SINR is also degraded with increasing height: At 67% load the SINR goes from 0 dB at 15 m to -7 dB at 250 m, corresponding to 7 dB degradation. This degradation is more or less constant vs. the offered traffic load points.

The DL SINR degradation can be explained by observing the average interference vs offered load introduced in Figure G.4. Increasing the offered load leads to higher interference as expected, but the degradation is much

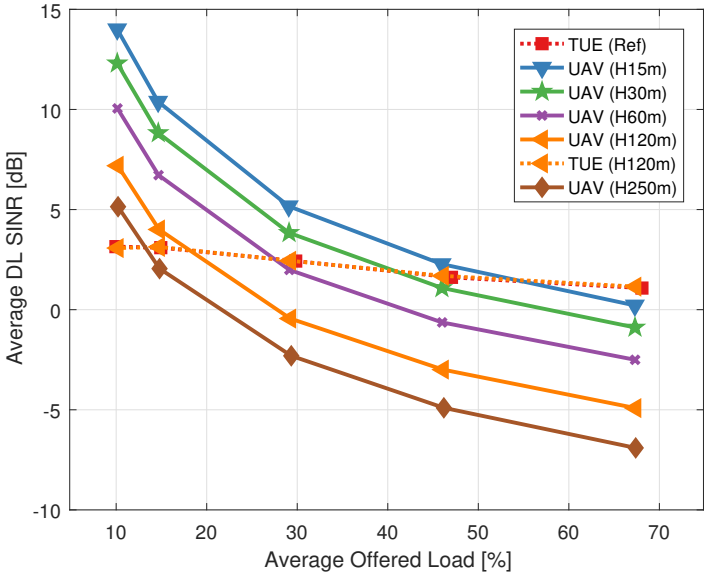

Fig. G.3: SINR experienced during data transmission vs. offered load. *Ref* indicates the case without any UAV, while *Hxm* refers to cases where UAVs accounts for 1% users in the network and fly at constant height of x m.

faster for the UAVs than the TUEs: Up to 12 dB difference is experienced, when load changes from 10% to 67% for the UAVs at 120 m, while the corresponding value for the TUEs is only 3 dB. This is due to the fact that clearance of the radio propagation path for UAVs leads to improved signal strength from the serving cell, but also increased level of interference seen from the neighboring cells. The DL interference experienced by the UAVs is also a function of UAV height: It gradually increases until the UAVs reaches 120 m, and then decreases again. This is due to two reasons: Firstly, the path loss slope goes down steadily to 2, i.e. free-space path loss, for UAV heights from 15 m to 120 m, and remains constant with further increase of UAV height. Therefore, if the UAV is moving upwards up to 250 m, the path loss starts to increase because the 3D distance increases, while the slope is constant. Secondly, as the elevation angle increases with the UAV height, the BS antenna gain is also reduced, which might introduce further loss in the total link loss. The increase of total link loss reduces both serving cell's signal strength and neighboring cells interference, but nevertheless the combined effect is that the SINR is still reduced at 250 m compared to 120 m. From both Figure G.3 and G.4, we can see that the DL performance of the TUEs is not impacted by the presence of UAVs, since the TUE SINR and interference curves in *Ref* (no

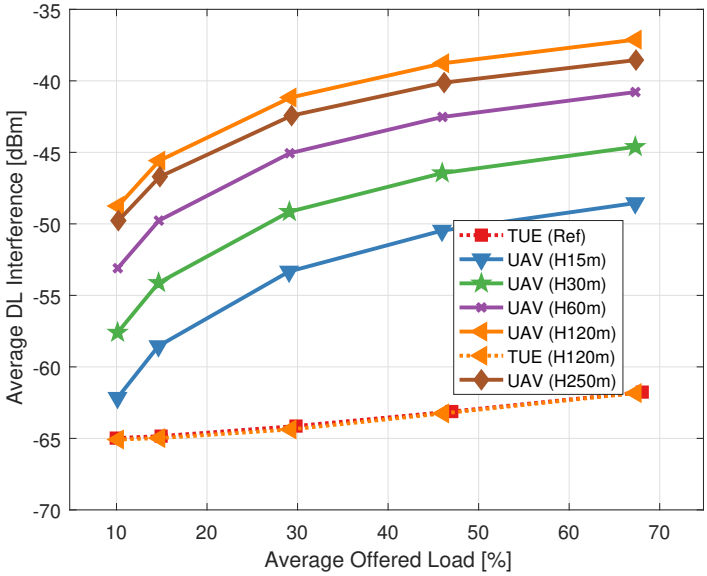

Fig. G.4: Interference experienced during data transmission vs. offered load. *Ref* indicates the case without any UAV, while *Hxm* refers to cases where UAVs accounts for 1% users in the network and fly at constant height of x m.

UAVs) and *H120m* case, i.e. 1% UAV flying at 120 m, are essentially identical.

Additionally, Figure G.5 shows the outage probability as a function of offered load. Due to higher interference and thus worse DL SINR, the UAVs tend to suffer from larger outage than TUEs in general. At 67% load point, the outage probability for TUEs and UAVs at 120 m is 1.5% and 23%, respectively. Increasing the UAV height further to 250 m makes the situation even worse, i.e. the outage is increased to 42% for the same traffic load point. As the DL performance is essential for providing C2 link for drones, keeping outage probability low is critical. In the 3GPP discussions the target reliability was set to 99.9%, which could be understood that less than 0.1% outage is required. Similar to [3], our simulation results also indicate that downlink interference is a key obstacle to achieve the required DL performance, and therefore interference mitigation techniques are needed to improve the reliability of the C2 link in this type of deployment scenario.

To avoid swamping readers with results from all load points and heights, in the next sections we focus only on two traffic load points, *medium* and *high*, which correspond to the 30% and 67% downlink load in Figures G.3- G.5, respectively. The UAV height is also often fixed at 120 m, unless otherwise stated.

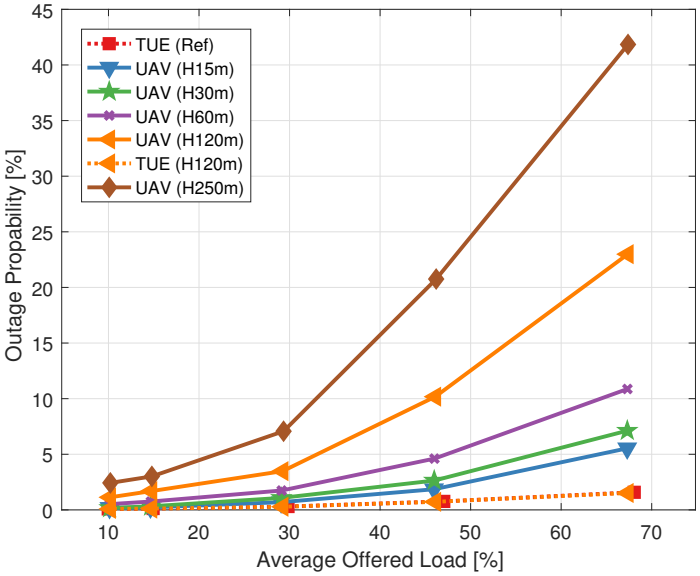

Fig. G.5: Outage probability vs. UAV height. *Ref* indicates the case without any UAV, while *Hxm* refers to cases where UAVs accounts for 1% users in the network and fly at constant height of x m.

B. Uplink Performance

This section discusses the impact of UAVs on the UL performance of the network.

Figure G.6 illustrates the DL outage probability, average UL SINR and throughput for UAVs at different heights. Similarly, the UL performance of TUEs is shown in Figure G.7. A few observations can be made: First, when an UAV flies at increased heights, it experiences better propagation conditions, and therefore its UL transmissions can potentially cause higher noise rise in the neighboring cells in a larger area compared to TUEs at the same location. Due to such an increase in UL interference, generally both UL SINR and throughput of UAVs and TUEs drop with increasing UAV height. This impact is less visible in the high load scenario, compared to the medium load one. At the high load, the UAV DL outage probability is much higher, i.e. many UAVs are in RLF and not able to transmit in UL, resulting in their lower impact in the network. Comparing the cases with UAVs at 15 m with 250 m in the medium load scenario, the UL SINR for TUEs reduces about 2 dB, while average UL throughput drops from 2.4 Mbps to 1.8 Mbps, or a 25% degradation. On the other hand, in the high load case, the UL SINR

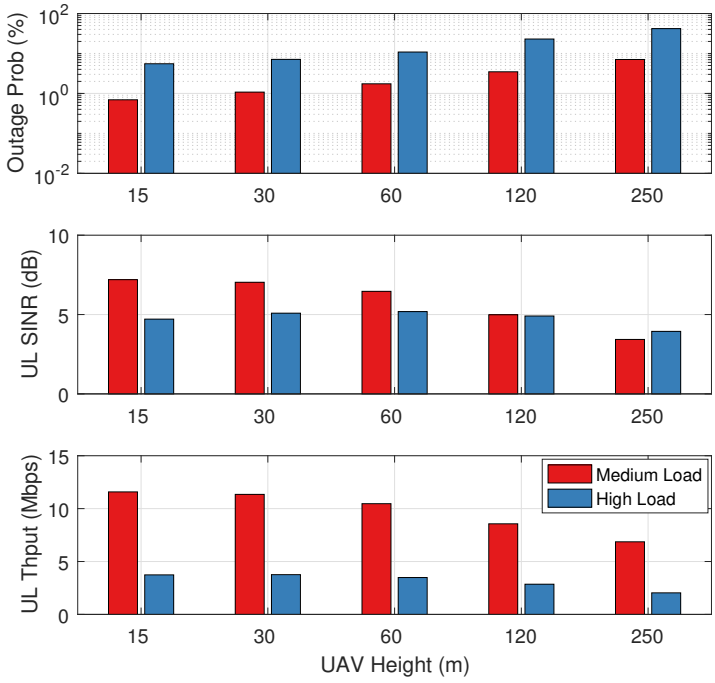

Fig. G.6: UAV outage probability, average UL SINR and throughput vs. UAV height. UAVs account for 1% users in the network and fly at a constant height.

for TUEs is degraded by only 0.5 dB, and virtually no change in average UL throughput is visible. The higher UAV outage probability for UAV heights above 120 m also causes the TUE UL SINR in the high load scenario to be better than that of the medium load. Secondly, both UAV and TUE tend to achieve much higher UL throughput at medium load, because in this case, the available bandwidth is shared between a smaller number of active UEs. For example, an UAV at 120 m in the medium load scenario has in average three times more PRBs allocated than in the high load. Lastly, due to the improved propagation channel, UAVs always enjoy higher average connected-mode UL SINR and throughput than the TUEs.

In conclusion, the presence of UAVs has a negative impact on the UL performance of the TUEs. Again, interference mitigation techniques are likely to be required to reduce such impact, and in the next sections we will look at several candidate solutions for mitigating UAV interference and compare their performance.

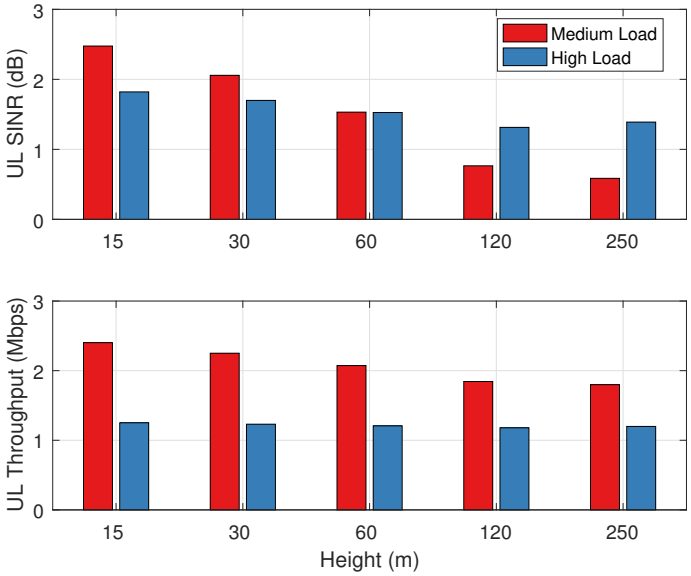

Fig. G.7: Average TUE UL SINR and throughput vs. UAV height. UAVs account for 1% users in the network and fly at a constant height.

V Terminal-based interference mitigation techniques

Assuming that no network upgrades are introduced, we consider first interference mitigation techniques applicable to the UE side. Techniques based on simple antenna combining and/or selection are achievable at a relatively low complexity, even when 3GPP Release 8 UEs are used on the UAVs. Here we select two potential schemes: antenna beam selection and interference cancellation.

A. Antenna beam selection

Antenna selection with 2 or more directional antenna elements can be equivalent to a very simple beam selection, when assuming the antenna elements are mounted on the UAV body at the right spacing and angles/orientations. As an example, in case the UAV can rotate its fuselage in the azimuth plane while keeping the flight direction, then 1 or 2 antenna elements are sufficient to generate a 'beam' towards the serving cell. Or, in case the UAV degrees of freedom are more restricted, at least 4 antenna elements need to

be mounted to provide four beams in the azimuth plane. In the elevation plane, the simple antenna selection described above might not be applicable, unless a larger number of antenna elements can be accommodated on the UAV fuselage. Certainly, higher gains can be expected when both azimuth and elevation antenna beamforming or selection is available. Henceforth, our assumption is that antenna beam selection at the UAVs is applied only in the azimuth plane, and an omni-directional elevation radiation pattern is used.

We select an antenna beam radiation pattern modeled as a $sinc()^2$ function, with -3 dB beam-widths of approximately 90 deg, or 50 deg in the azimuth plane. The modeled beam patterns provide +6.6 dBi gain in the main direction and -13 dB front-to-sidelobe attenuation, which can be considered to account for the non-ideal orientation and/or shape of the beams. A simple setup with a grid of 2, 4 or 6 fixed beams is used (fixed relative to the UAV fuselage) to emulate a practical antenna selection mechanism. These options are depicted in Figure G.8, along with the corresponding possible beam orientations on the UAV. Our choice for antenna beam model is different from the assumptions used in the 3GPP UAV studies reported in [3] and, in our opinion, provides a setup better aligned with all the other network and UAV deployment assumptions we make in this paper.

The evaluated beam selection algorithm is based on the standard RSRQ measurements performed at the UAV terminal side, and without any requirement for feedback from the serving cell. First, for each detected cell, serving and interfering, the maximum RSRQ is determined across all the possible antenna beam orientations, i.e. 2, 4 or 6 beams, depending on the configuration used. This RSRQ, and the corresponding Reference Signal Received Power (RSRP) values, are used as input to the usual 3GPP mobility mechanisms, cell (re)selection and hand-over. In the second step, the antenna that maximizes the RSRQ for the serving cell is selected. We further assume that the same antenna beam orientation is used for both downlink and uplink transmissions, from and to the serving cell.

Downlink Results

Figure G.9 shows the average downlink SINR and throughput improvements for the UAVs, when the antenna beam selection is applied (2, 4 or 6 fixed beams). The reference case, presented in Section IV, is assuming omni-directional UE antenna for UAVs, and is labeled as "0" number of beams.

In the medium load scenario, we can immediately notice a significant SINR improvement over the omni-directional case, already when using a grid of 2 fixed beams. In the high load case, the UAVs would need to use a grid of at least 6 fixed beams in order to experience similar SINR improvements. Analyzing the average throughputs, however, we can conclude that the target of 100 kbps is achievable in both low and high load conditions, when a grid

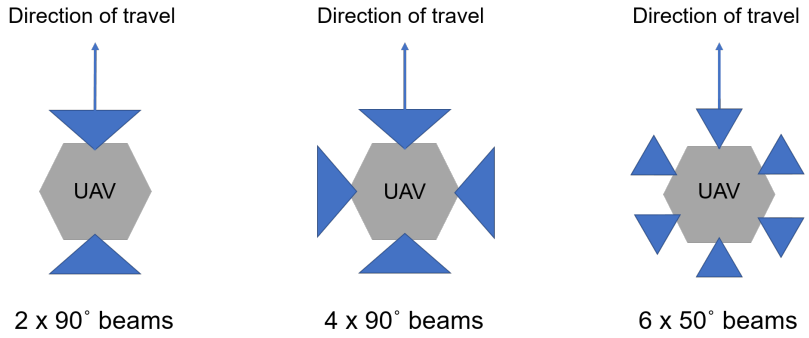

Fig. G.8: Modeled antenna beam configurations for the UAV.

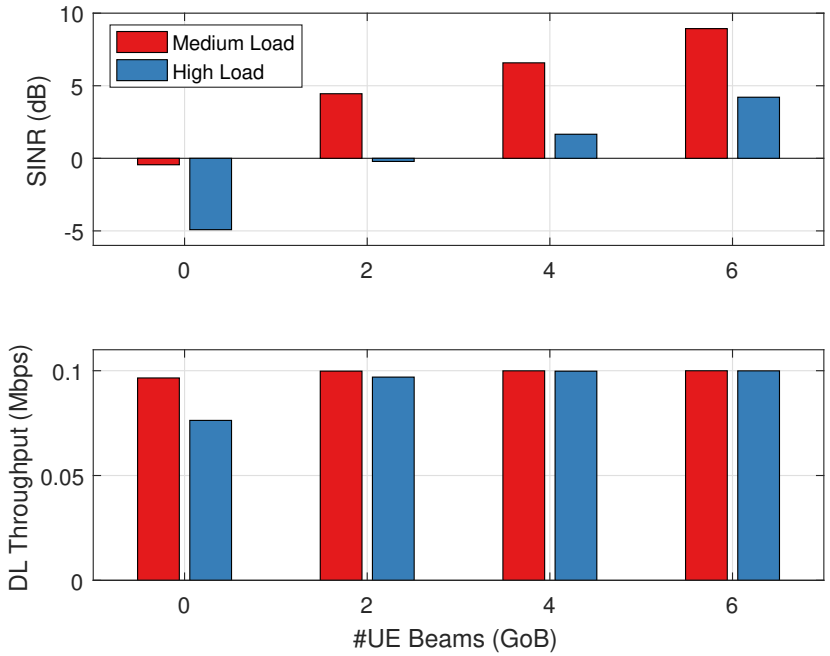

Fig. G.9: Average UAV DL SINR and throughput vs. number of antenna beams. UAVs account for 1% users in the network and fly at constant height of 120 m.

of at least 4 fixed beams is used.

Further, Figure G.10 shows the outage probability and average time in Q_{out}, when antenna/beam selection is applied.

In the reference case, the outage probability is high, 5% and 22% for medium and high load cases, respectively. In order to achieve outage probabi-

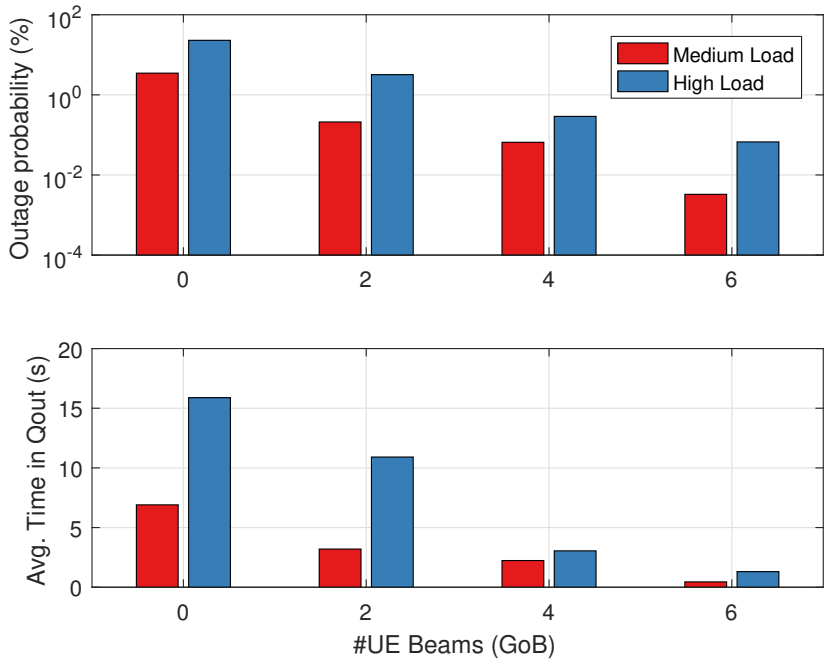

Fig. G.10: UAV outage probability and average time in Q_{out} vs. number of antenna beams. UAVs account for 1% users in the network and fly at constant height of 120 m.

lities below 1%, similar to the conclusions from the downlink SINR analysis, the UAVs need to use a grid of at least 4 or 6 fixed beams, depending on the traffic load. It is remarkable that, when a grid of 6 beams is used, the outage can be as low as 0.1% even in the high traffic load case.

The average time in Q_{out} results show similar trends as the outage probability versus the number of beams used. Here the important conclusion is that only a minimum of 0.5 s and 1.2 s time in Q_{out} is achievable, even when a grid of 6 beams is used, improving significantly the interruption times that should be taken into consideration in the design of the UAV communication link.

In order to disclose the impact of changing the number of UAVs, we have also analysed the cases when UAVs account for 10% users in the network. For brevity, these results are not shown here. The first conclusion is that the downlink performance of the UAVs depends on the number, and traffic demand, of the TUEs. This leads to results indicating performance improvement, especially in terms of outage and time in Q_{out}, when there are more UAVs and less TUEs in the network. The second conclusion is that the advantage from using antenna beams on the UAVs remains significant, and at 10%

UAV penetration an outage probability below 0.01% can be achieved with a grid of 6 fixed beams.

Finally, it is confirmed that the downlink performance of the TUEs is not affected by the use of antenna beams at the UAVs, regardless of the UAV penetration. This is natural, due to the low UAV CBR traffic demand (100 kbps per UAV) relative to the high available cell capacity, and because the downlink transmissions to the UAVs generate the same amount of average inter-cell interference, with or without antenna beams at the UAVs. The TUEs can achieve average downlink throughputs of 6 Mbps and 2.5 Mbps in medium and high traffic load conditions, respectively. The average downlink performance of the TUEs is practically determined by the number of TUEs and their traffic demand.

Uplink Results

Next we analyse the UL performance. Figure G.11 shows the average UL SINR and throughput improvements for the UAVs, when the antenna beam selection is applied (2, 4 or 6 fixed beams). As a consequence of the favorable propagation conditions at 120 m height, the UAVs experience very good average UL SINR already without the use of antenna/beams. Nevertheless, the results show a non-negligible improvement in both average UL SINR and throughput, when a grid of 4 or 6 fixed beams is used, although more so in the medium load case.

The impact of UAV antenna beam selection is visible on both the UL SINR and throughput for the TUEs in Figure G.12. The use of a grid of 6 beams on the UAVs, results in up to 30% average throughput gain for the TUEs. This gain can be explained by the lower average inter-cell interference generated by the UAV UL transmissions due to their directional antenna beams.

The impact of the UAV penetration on the uplink performance KPIs for UAVs and for TUEs has been also investigated. For brevity, these results are not shown here. As expected, the increased number of UAVs leads to significantly lower UL performance for all UEs in the network: up to 36% and 45% degradation for UAVs and TUEs, respectively. The use of a grid of 6 beams on the UAVs remains beneficial, and can partially mitigate the increased interference, due to higher number of UAVs.

B. Interference cancellation

More recent LTE releases presented features to improve interference cancellation when compared to the baseline of a Release 8 UE. Release 11 was the first to introduce IRC, by adopting a Minimum Mean Square Error (MMSE) receiver, which suppresses interference by linearly combining the received signals at UE antennas [24]. In Release 12, non-linear processing is intro-

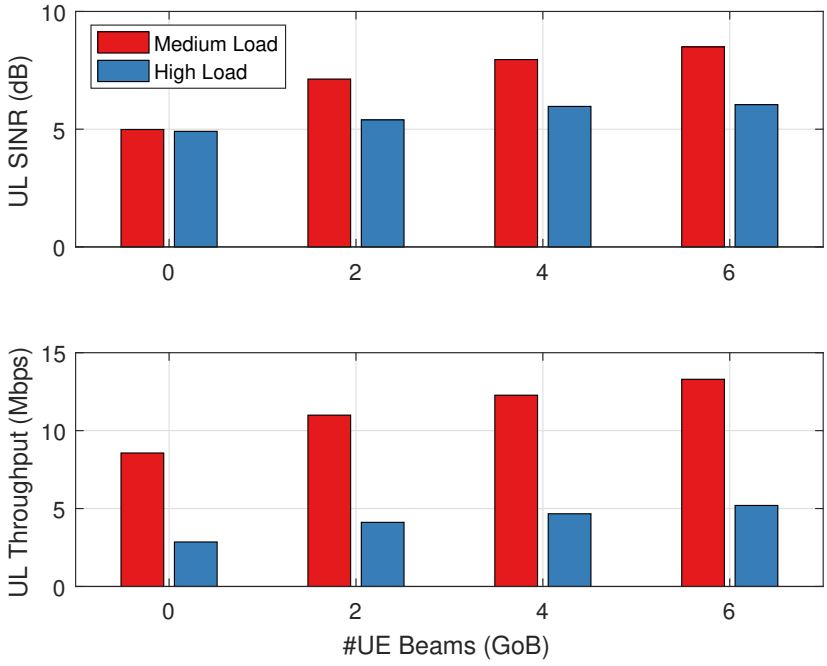

Fig. G.11: Average UAV UL SINR and throughput vs. number of antenna beams. UAVs account for 1% users in the network and fly at constant height of 120 m.

duced with the Network-Assisted Interference Cancellation and Suppression (NAICS), which involves reconstructing the interfering signal and subtracting it before decoding the desired signal [24]. Even more advanced receivers are implemented in 3GPP Release 13 UE and beyond.

In this subsection, we quantify the potential of IC technique by assuming the perfect removal of 1 to 3 interferers. We note here that a 3GPP Release 13 UE with a minimum of 4 antenna elements would at best be able to cancel out 3 interfering signals; or alternatively, reject two strong interferers and receive data through the two remaining beams.

The ideal IC is modeled by canceling cells in order of the RSRP levels of the interfering cells, i.e. starting with the cell with the strongest RSRP. A cell is included in the interference cancellation irrespective of its actual load. For the DL SINR this means that (G.3) is modified such that $\rho_i(t)$ equals zero for the i^{th} cell, whose signal is canceled out or ideally rejected by the UE receiver.

In Figure G.13, we show the gain in terms of outage probability and average time in Q_{out} versus the number of cells canceled out for both the medium and high load cases. The outage decreases most for the high load case, as in the high load case removing the first x interfering cells reduces

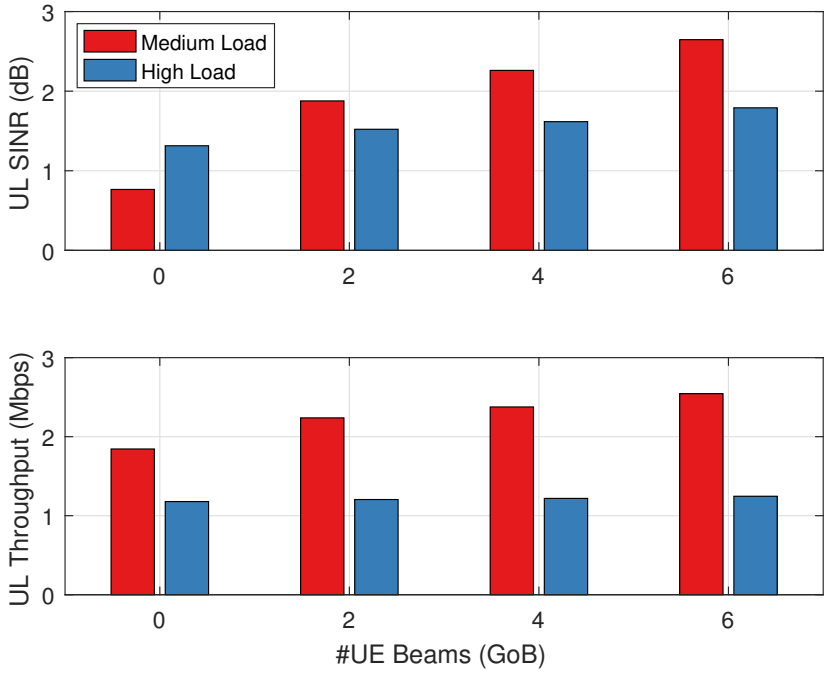

Fig. G.12: Average TUE UL SINR and throughput vs. number of antenna beams. UAVs account for 1% users in the network and fly at constant height of 120 m.

interference power more than in the case of low load. Also the time in Q_{out} decreases, but both the improvement in outage probability and average time in Q_{out} are in general lower than the improvements we have seen for the grid of fixed beams in the Section A.. A reason for this is that part of the outage is caused by pure coverage issues, which cannot be improved by removing sources of interference. But it can be improved by a grid of fixed beams, which besides limiting the interference also provides a gain in the serving cell direction. This effect may also be observed in Fig. G.14, where the high load case shows low SINR, and therefore, a high outage in throughput sense, even for 3 canceled interfering cells.

VI Network based interference mitigation solutions

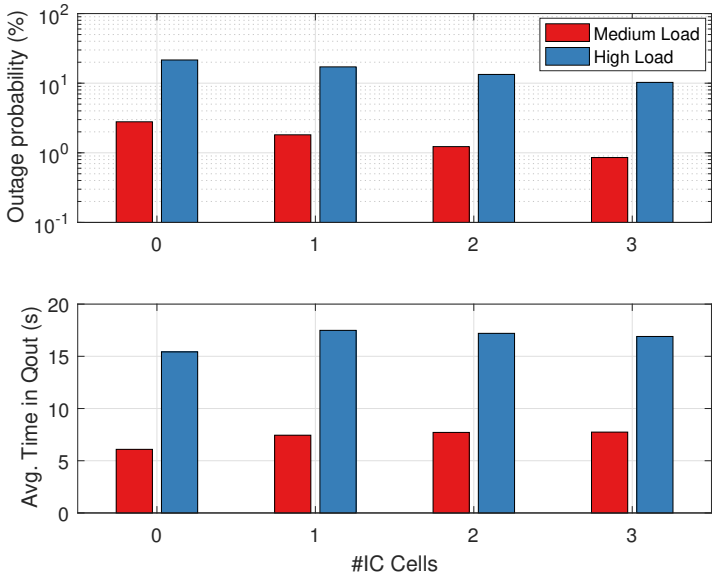

Fig. G.13: UAV outage probability and average time in Q_{out} vs. number of interfering cells whose signal was canceled. UAVs account for 1% users in the network and fly at constant height of 120 m.

A. Power control

In LTE networks, the power control parameters P0 and α, as in (G.4), are optimized in order to minimize the user's battery consumption and system's overall intra-cell interference, while maintaining good UL performance. In interference-limited networks, decreases in α, for example, will minimize the transmitted power of users close to cell edge. However, under-compensation of these parameters may cost significantly in terms of system throughput and UL outage. Usually, P0 and α are defined based on statistical information at BSs by network engineers.

Considering the significant differences in the propagation observed by TUEs and UAVs, we analyze the solution where the BSs use different settings for the different UE classes [3]. The term Δ^{u}_{P0} in (G.4) was introduced to introduce an offset in P0 for the different UE classes. In our study, it is zero for all TUEs, and a value between 0 and 12 dB for UAVs.

Figure G.15 illustrates the average UAV UL SINR and throughput, when Δ^{u}_{P0} increases from 0 to 12 dB for UAVs. As expected, when UAVs reduce their transmitted power, their SINR and throughput are also degraded. In the medium load scenario, the UAV throughput drops from 8.6 Mbps to

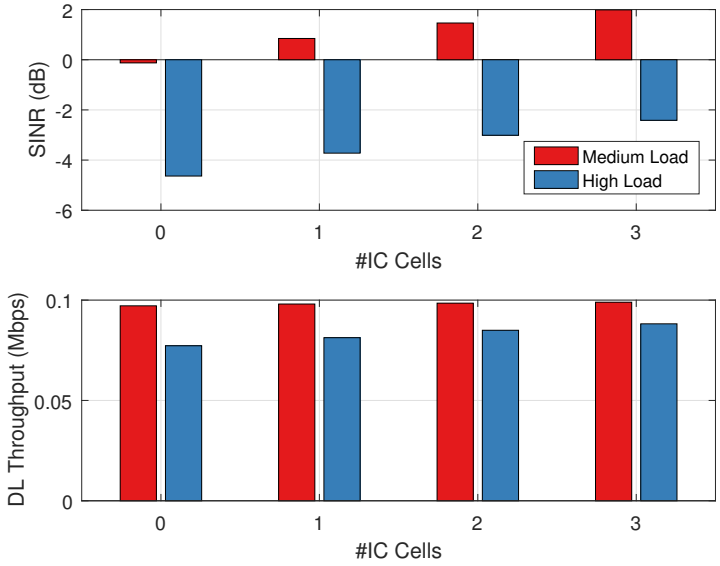

Fig. G.14: Average UAV DL SINR and throughput vs. number of interfering cells whose signal was canceled. UAVs account for 1% users in the network and fly at constant height of 120 m.

3.1 Mbps, or 64% reduction. This is the price to pay for using power control to reduce UAV's interference in the UL.

In Figure G.16 the average TUE UL SINR and throughput are shown as function of UAV's P0 offset. When UAVs lower their transmitted power, interference is reduced, and therefore TUE's SINR and throughput are improved: Throughput increases from 1.8 Mbps to 2.8 Mbps, or 56%, when P0 goes from 0 to 12 dB in the medium load scenario, even though UAVs represent just 1% of the users. In the high load case, due to a large number of UAVs are in outage, the effect of power control becomes much less significant. This approach has the advantage of not causing impact for TUEs output power distribution.

B. Inter-cell interference coordination

Several standardized inter-cell interference coordination solutions exist. The simplest downlink ICIC scheme was introduced in 3GPP Release 8, and is purely based on inter-cell signaling and does not require any UE-side functionality. The general idea is to coordinate the usage of radio resources between cells to optimize the cell edge SINRs. The enhanced and further enhanced ICIC (eICIC and feICIC) solutions have been developed in 3GPP Releases 10

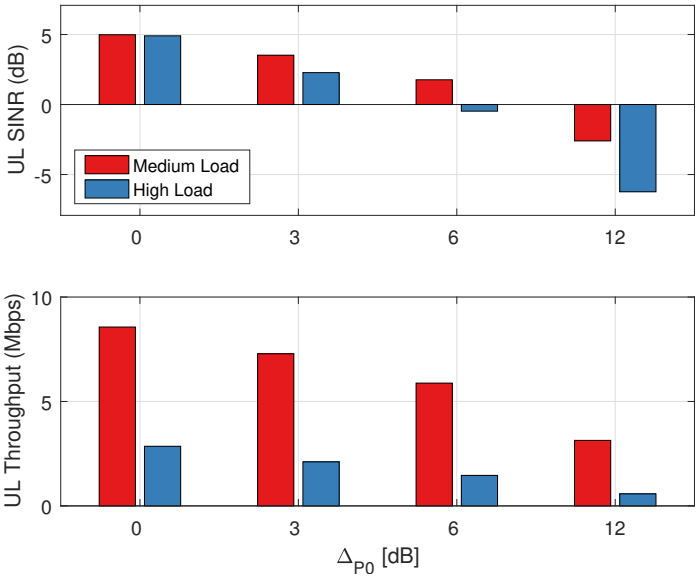

Fig. G.15: Average UAV UL SINR and throughput vs. UAV P0 offset. UAVs account for 1% users in the network and fly at constant height of 120 m.

and 11 for heterogeneous network deployments, targeting interference mitigation between macro base stations and small cells [17]. The main component is to suppress or blank sub-frames of the interfering BS. This allows the serving BS to schedule transmissions during these quiet sub-frames. When the Almost Blank Subframes (ABS) scheme is utilized, control channels can still be transmitted to ensure backwards compatibility. In LTE Release 11, the terminals are able to apply interference suppression as well, for better reception on the control signaling, allowing for "full blanking" of the downlink sub-frames.

The (f)eICIC solutions are applicable also between macro BSs, thus, in principle, can be considered as candidate solutions in our UAV investigations as well. The C2 link can be sent to an UAV according to the different generalized allocation schemes shown in Figure G.17:

a) Dynamic scheduling (reference): scheduling the available data every Transmission Time Interval (TTI) according to proportional fair scheduling. This maximizes the scheduling gains, but is the most challenging scheme for the control signaling between cells, as very frequent coordination may be required, thus increasing the control plane load on X2.

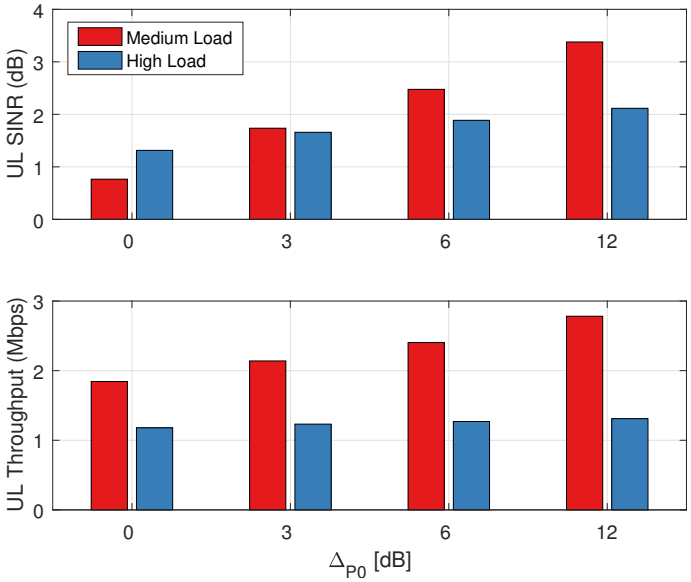

Fig. G.16: Average TUE UL SINR and throughput vs. UAV P0 offset. UAVs account for 1% users in the network and fly at constant height of 120 m.

b) Fixed PRB scheduling: scheduling every TTI, but on preallocated PRBs. This enables slow coordination between the cells, as the resources to be muted or transmitted at lower power in the interfering cells do not change frequently, but it comes at the cost of a lower frequency diversity gain.

c) Packing the data in few TTIs: in this scheme UAVs are only allowed to transmit every x^{th} TTI. The data for all served UAVs is packed in these TTIs, so that all neighboring cells easily can mute their resources in these TTIs. Coordination is rather simple, as the resources are well-known and semi-static. Benefit over the second scheme is that this scheme also provides interference coordination for the Physical Downlink Control Channel (PDCCH).

We model the effect of blank sub-frames by assuming that the downlink transmission from the corresponding cells is muted in the corresponding TTIs and PRBs. For completeness we include here the cases where 1 up to 20 interfering cells are muted. We evaluate the impact of transmission muting in a similar way, as we did for the interference cancellation in Section B.: (G.3) is modified so that $\rho_i(t)$ equals zero for the i^{th} cell, whose signal is muted. In Figure G.18, we show the gain in terms of outage probability and

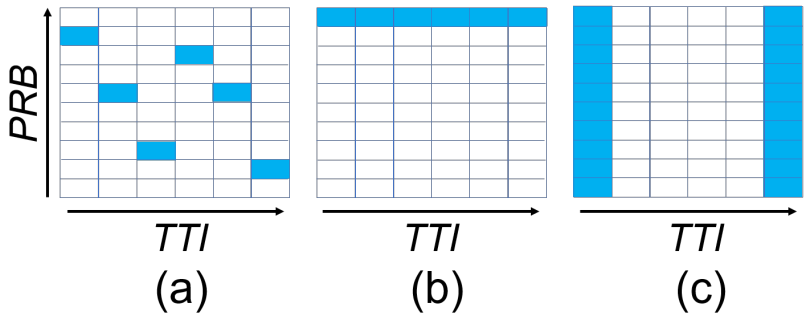

Fig. G.17: Different allocation schemes for the UAV C2 data: (a) dynamic scheduling, (b) fixed PRB scheduling, and (c) packing the data in a few TTIs.

average time in Q_{out} versus the number of cells muted for both the medium and high traffic load cases. The results for up to 3 cells muted are the same as presented in Section B.. The notable result is the extreme case when the strongest 20 interfering cells are muted and the resulting outage drops below 0.01%. This indicates that the scenario becomes practically noise limited from the UE perspective, even in the high load scenario.

In the following, we compare the scheduling configurations shown in Table G.3. In the first column, the number of UAVs in the serving cell are listed, the second column shows how often in time domain the UAVs are scheduled, the third and fourth column list the required number of PRBs and required SINR for the most conservative Modulation and Coding Scheme (MCS) possible to deliver C2 link data to an UAV. Note that we only consider UAVs in the serving cell, and assume for now that there are no UAVs in the cells around the serving cell. All UAVs are always scheduled in the same TTI, to minimize potential coordination signaling between cells. The required DL SINR is the maximum between the minimum required SINR for the PDCCH (-6 dB at 2% error rate [25]) and the required SINR for reaching 10% Block Error Rate (BLER) at the first transmission. We consider that every UAV sends 1250 B every 100 ms and one full retransmission is considered to reach high reliability.

It can be seen from the Table G.3 that when we pack the UAV's transmission in fewer TTIs, or when we pack more UAVs in a TTI, the required SINR increases as the MCS increases, due to the data to be sent in less PRBs. Now the question is, how we can achieve the required SINR for the different cases, and how many cells we need to mute. This can be deducted from the curves shown in Figure G.19, where the cumulative distribution function (CDF) of the DL SINR in high load is shown for a different number of interfering cells muted. We can see that if the required SINR is -6 dB, then we need to

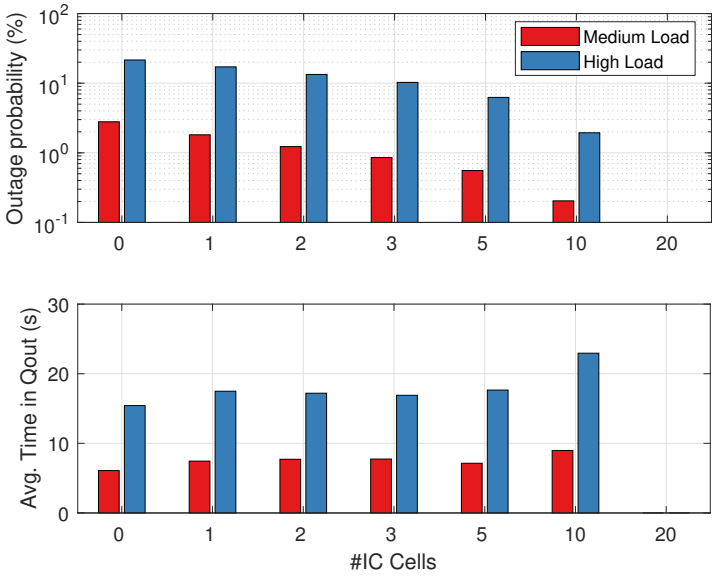

Fig. G.18: UAV outage probability, and average time in Q_{out} vs. number of IC cells muted. UAVs account for 1% users in the network and fly at constant height of 120 m.

Table G.3: Considered scheduling configurations for downlink UAV C2 traffic

#UAV	TTI	#PRB	Required SINR
1	Every	9	-6.0 dB
1	10^{th}	80	-4.7 dB
1	50^{th}	100	1.6 dB
2	Every	9	-6.0 dB
2	10^{th}	80	-4.0 dB
2	50^{th}	100	-6.0 dB
4	Every	9	-6.0 dB
4	10^{th}	80	-2.3 dB
4	50^{th}	100	14.6 dB

remove 3 cells in the case of high traffic load, to obtain an outage below 10%.

By comparing the CDFs from Figure G.19 and the required SINR from Table G.3 we can find the number of cells to be muted for the different cases. The result of this comparison is summarized in Table G.4, where also the medium load case is represented.

It can be seen that at medium load, as long as we do not pack the UAVs

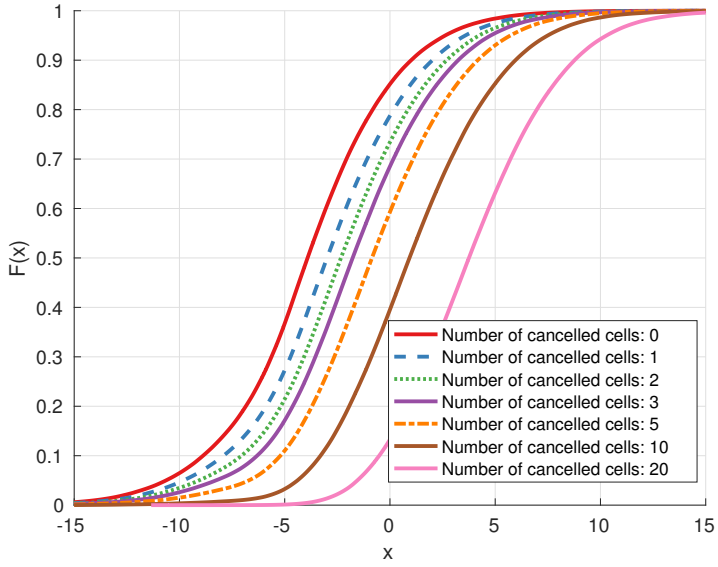

Fig. G.19: UAV DL SINR distribution in high load scenario. UAVs account for 1% users in the network and fly at constant height of 120 m.

Table G.4: Number of cells to be muted in case of low load and high load for the considered scenarios

#UAV	TTI	Muted Cell(s)		Capacity Loss	
		Medium	High	Medium	High
1	Every	0	3	9%	309%
1	10^{th}	0	8	8%	90%
1	50^{th}	10	20	20%	40%
2	Every	0	3	18%	318%
2	10^{th}	0	9	10%	110%
2	50^{th}	>20	$\gg$20	>40%	N/A
4	Every	0	3	36%	336%
4	10^{th}	0	14	10%	110%
4	50^{th}	>20	$\gg$20	>40%	N/A

data in very few TTIs, no coordination is needed, while at high load, medium to extensive coordination is needed. Note that scheduling every TTI becomes PDCCH limited at high load, which means we need to mute full TTIs. Therefore, scheduling every 10^{th} TTI becomes the most attractive option, as it does not require coordination between more than 10 cells. The last two columns

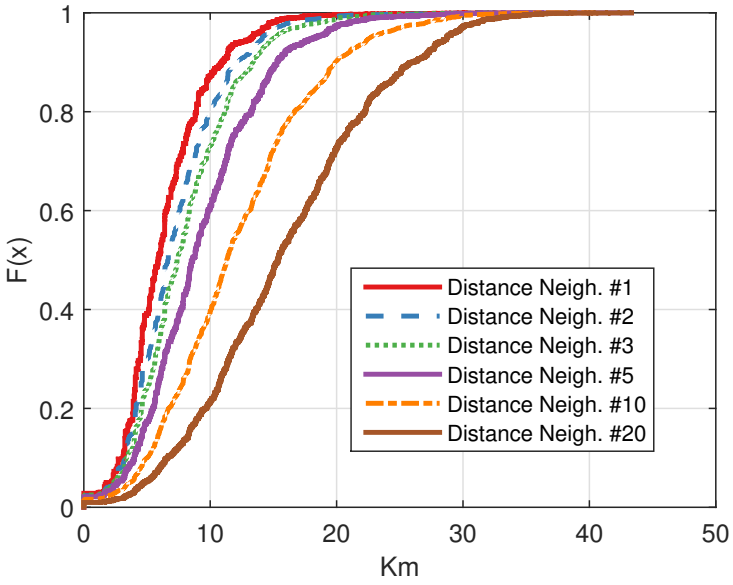

Fig. G.20: CDF of the distance to the strongest interferers for the rural area in Denmark.

of Table G.4 show the loss in available capacity for TUEs as percentage of full cell capacity. It can be seen that the coordination is costly, especially in the high load case. With one UAV in the cell and scheduling it every 10^{th} TTI, it corresponds to losing 90% of a full cell capacity (shared over 9 cells). With one UAV, it is more attractive to schedule it every 50^{th} TTI, leading to a loss of 40% but spread over 20 cells. When having more UAVs, the scheduling needs to be more often and the capacity loss increases. Note that having 2 UAVs, which requires muting over 9 cells, corresponds to 2 drones per 10 cells, twice as much as the low drone density in the simulations shown in the previous sections.

Even though coordination may only be required between 10 cells, it may require coordination over a large area, as is shown in Figure G.20, where the CDF of the distance to the x^{th} interfering cell can be seen. It can be seen that the strongest interferer may be as far away as 15 km, while capturing the first 10 cells with 90% likelihood requires covering an area of 20 km around the serving cell. However, the coordination for the C2 link can be rather slow, as the traffic can be assumed to be rather constant and therefore the TTI's to be coordinated do not change often. If there are also UAVs in the neighboring cells, they can be coordinated by fixing the PRB per UAV, i.e. allocating frequency slices to each of them in a rather static fashion.

VII Conclusion

Widely deployed cellular networks are an attractive solution to provide large scale radio connectivity to aerial vehicles. One main prerequisite is that co-existence and optimal performance for both aerial and terrestrial users should be provided even though deployments are primarily optimized to provide good service for terrestrial users. In this paper, we investigate the performance of aerial radio connectivity in a typical rural area network deployments, using extensive channel measurements and system simulations. We highlight that downlink and uplink radio interference play a key role and yield relatively poor performance for the aerial traffic when load is high in the network. As a consequence, we analyze two groups of interference mitigation schemes under the constraint of minimal network upgrades required: terminal based and network based solutions.

In terms of terminal based interference mitigation solutions, we show that interference canceling and antenna beam selection can both improve the overall, aerial and terrestrial, system performance to a certain degree, with up to 30% throughput gain and an increase in the reliability of the aerial radio connectivity to above 99%. As network based solutions, we have analyzed the open loop uplink power control and a novel downlink inter-cell interference coordination. By setting a 3 dB to 6 dB lower P0 value for aerial users compared to the terrestrial users, the uplink power control mechanism can improve the average uplink throughput performance of terrestrial users. This improvement comes, however, at the cost of a degraded uplink throughput for aerial aerial users, and indicates that the power control alone might not be sufficient to adequately mitigate uplink interference.

Our proposed downlink inter-cell interference coordination mechanism is applied to the aerial users' command and control traffic. We show that inter-cell coordination is required in high load scenario, and up to 8 cells need to be muted to support 1% aerial user penetration. The cost of this solution is 10% terrestrial capacity degradation in each of the muted cells.

The results summarized above indicate that some practical, and relatively low complexity, interference mitigation schemes have good potential, when utilized in currently deployed rural LTE networks. Our findings also highlight that there are clear limitations of these interference mitigation techniques, especially when the overall network performance needs to be maintained for higher penetration of connected aerial vehicles. It is therefore also clear that further research and standardization activities are needed.

Acknowledgment

We would like to thank Steffen Hansen, our drone pilot, and other colleagues at Aalborg University for supporting this work.

References

[1] *"RPAS air traffic management (ATM) concept of operations (CONOPS)"*, European Organisation for the Safety of Air Navigation (EUROCONTROL), Feb 2017. [Online]. Available: http://www.eurocontrol.int/publications/

[2] *"Drones are about to fill the skies within the next 5 years"*, Business Insider Intelligent Report, Jun 2016. [Online]. Available: http://www.businessinsider.com/

[3] 3rd Generation Partnership Project; Technical Specification Group Radio Access Network;, *"Study on Enhanced LTE Support for Aerial Vehicles (Release 15),"* 3GPP TR 36.777 V0.4.0 (2017-11).

[4] M. Mozaffari, W. Saad, M. Bennis and M. Debbah, *"Unmanned Aerial Vehicle With Underlaid Device-to-Device Communications: Performance and Tradeoffs,"* in IEEE Transactions on Wireless Communications, vol. 15, no. 6, pp. 3949-3963, June 2016.

[5] Z. Xiao, P. Xia and X. g. Xia, *"Enabling UAV cellular with millimeter-wave communication: potentials and approaches,"* in IEEE Communications Magazine, vol. 54, no. 5, pp. 66-73, May 2016.

[6] A. Al-Hourani, S. Kandeepan and S. Lardner, *"Optimal LAP Altitude for Maximum Coverage,"* in IEEE Wireless Communications Letters, vol. 3, no. 6, pp. 569-572, Dec. 2014.

[7] B. V. Der Bergh, A. Chiumento and S. Pollin, *"LTE in the sky: trading off propagation benefits with interference costs for aerial nodes,"* in IEEE Communications Magazine, vol. 54, no. 5, pp. 44-50, May 2016.

[8] A. Al-Hourani and K. Gomez, *"Modeling Cellular-to-UAV Path-Loss for Suburban Environments,"* in IEEE Wireless Communications Letters, vol. PP, no. 99, pp. 1-1.

[9] N. Goddemeier, K. Daniel and C. Wietfeld, *"Role-Based Connectivity Management with Realistic Air-to-Ground Channels for Cooperative UAVs,"* in IEEE Journal on Selected Areas in Communications, vol. 30, no. 5, pp. 951-963, June 2012.

[10] R. Amorim, H. Nguyen, P. Mogensen, I. Z. Kovács, J. Wigard and T. B. Sørensen, *"Radio Channel Modeling for UAV Communication Over Cellular Networks,"* in IEEE Wireless Communications Letters, vol. 6, no. 4, pp. 514-517, Aug. 2017.

[11] M. M. Azari, F. Rosas, A. Chiumento, S. Pollin, *"Coexistence of Terrestrial and Aerial Users in Cellular Networks,"* in 2017 IEEE Globecom, Singapore, 2017, pp. 1-6

[12] H. Nguyen, R. Amorim, J. Wigard, I. Kovács, and P. Mogensen, *"Using LTE Networks for UAV Command and Control Link: A Rural-Area Coverage Analysis"*,. IEEE Vehicular Technology Society, 5 2017.

[13] I. Z. Kovács, R. Amorim, H. C. Nguyen, J. Wigard, P. Mogensen *"Interference analysis for UAV connectivity over LTE using aerial radio measurements,"* 2017 IEEE 86th Vehicular Technology Conference (VTC Fall), Toronto, Canada, 2017, pp. 1-5.

[14] M. Kottkamp, A. Roessler, J. Schlienz, *"LTE-Advanced Technology Introduction"*, Rohde & Schwarz, August 2012

[15] Y. Ohwatari, N. Miki, T. Asai, T. Abe and H. Taoka, *"Performance of Advanced Receiver Employing Interference Rejection Combining to Suppress Inter-Cell Interference in LTE-Advanced Downlink,"* 2011 IEEE Vehicular Technology Conference (VTC Fall), San Francisco, CA, 2011, pp. 1-7.

[16] J. Wigard, R. Amorim, H. Nguyen, I. Kovács, and P. Mogensen, *"Method for Detection of Airborne UEs Based on LTE Radio Measurements,"* IEEE Communications Society, 5 2017

[17] K. I. Pedersen, B. Sorret, S. B. Sanchez, G. Pocovi and Hua Wang, *"Dynamic Enhanced Intercell Interference Coordination for Realistic Networks"*, IEEE Trans. on Veh. Tech., VOL.65, No.7., July 2016

[18] M. Hata. *"Empirical formula for propagation loss in land mobile radio services,"* IEEE Transactions on Vehicular Technology, 29(3):317–325, Aug 1980.

[19] 3GPP. Technical Specification Group Radio Access Network; *"Study on channel model for frequencies from 0.5 to 100 GHz"*, TR 38.901, 3rd Generation Partnership Project (3GPP), March 2017.

[20] I. Viering, M. Dottling and A. Lobinger, *"A Mathematical Perspective of Self-Optimizing Wireless Networks,"* 2009 IEEE International Conference on Communications, Dresden, 2009, pp. 1-6.

[21] I. Viering, A. Lobinger, and S. Stefanski, *"Efficient Uplink Modeling for Dynamic System-Level Simulations of Cellular and Mobile Networks,"* EURASIP Journal on Wireless Communications and Networking, August, 2010.

[22] I. Viering, B. Wegmann, A. Lobinger, A. Awada and H. Martikainen, *"Mobility robustness optimization beyond Doppler effect and WSS assumption,"* 2011 8th International Symposium on Wireless Communication Systems, Aachen, 2011, pp. 186-191.

[23] R. Mullner, C. F. Ball, K. Ivanov, J. Lienhart and P. Hric, *"Contrasting Open-Loop and Closed-Loop Power Control Performance in UTRAN LTE Uplink by UE Trace Analysis,"* 2009 IEEE International Conference on Communications, Dresden, 2009, pp. 1-6.

[24] H. Holma,A. Toskala,J. Reunanen, *"LTE Small Cell Optimization: 3GPP Evolution to Release 13"*, John Wiley and Sons, 2016

[25] D. Laselva, F. Capozzi, F. Frederiksen, K. I. Pedersen, J. Wigard and I. Z. Kovács, *"On the Impact of Realistic Control Channel Constraints on QoS Provisioning in UTRAN LTE"*, IEEE VTC Fall 2009.

Paper H

Enabling Reliable Cellular Communication for Aerial Vehicles

R. Amorim, J. Wigard, I. Z. Kovács, T. B. Sørensen and P. Mogensen

The paper has been submitted to
IEEE Vehicular Technology Magazine for possible future publication.

© 2019 IEEE
This paper has been submitted for peer-review consideration and possible publication.

Abstract

Due to safety concerns, a reliable radio communication link is a key component in the future application of Unmanned Aerial Vehicles, as it will enable Beyond Visual Line-of-Sight operations. In terms of cost and deployment time, radio communication for aerial vehicles will greatly benefit from the ready to market infrastructure and ubiquitous coverage of cellular networks. Cellular networks are optimized for terrestrial users, and the different propagation environment experienced by aerial vehicles poses some interference challenges. In this article, system level simulations are used to assess interference mitigation solutions that can improve aerial link reliability. Thereafter, we discuss how the 5G New Radio flexible air interface, and beamforming-suited frequencies, favor the integration of UAVs into cellular networks by offering better ground for interference management solutions.

At the time of the writing, this paper is still under peer-review and pending decision by the respective publication editor. Regarding the rules for parallel publication, the paper has not been included in the public version of the thesis. The reader is encouraged to contact the author or the referred publication channel for a copy of the paper.

Paper I

Improving Command and Control Reliability for Drones with Multi-Operator Connectivity

R. Amorim, J. Wigard, I. Z. Kovács, T. B. Sørensen, P. Mogensen and G. Pocovi

The paper has been accepted for publication in
IEEE Vehicular Technology Conference 2019.

© 2019 IEEE
The layout has been revised and reprinted with permission.

Abstract

In this work, we analyze the end-to-end latency measured in a client-server application that emulates the traffic requirements for the Unmanned Aerial Vehicle (UAV)'s Command and Control (C2) link. The connectivity is provided by two real LTE-A networks to a client attached to a flying UAV. Measurements are performed at 4 different heights: ground level, 15 m, 40 m and 100 m. In single operator scenarios, the reliability measured at the target latency, 50 ms, was between 99.6 % and 97.6 % in downlink, and 91.3% and 99.4% in uplink. These results are below the 99.9 % target reliability defined for UAVs and they show that several consecutive packets can be missed when the radio link connectivity degrades, leading to high (> 1 s) values for the 99.9%-ile of latency. To circumvent this, a dual-operator hybrid access scheme is proposed in this paper. The results show that the hybrid access strategy managed to reach the performance requirements in most cases. The solution shows potential to enable C2 over cellular networks, without requiring optimization or modifications in the network.

I Introduction

Air traffic regulators and safety authorities have addressed the importance of the C2 link for enabling beyond visual line-of-sight (BVLOS) flight for UAVs [1,2]. This link is responsible to send the commands from the flight controller to the UAV as well as updates on the flight mission and other important information regarding the airspace. It also conveys the telemetry from the UAV and readings from its sensors to the flight controller. The C2 link is, therefore, a critical piece of the UAV flight and must be reliable in all phases of the flight.

The growth in the UAV market and its expansion to BVLOS missions represent great commercial potential for communication providers, such as cellular networks [3]. In a recent study item, presented in [4], the Third Generation Partnership Project (3GPP) has provided connectivity requirements for the C2 link. There are three main indicators that should be observed: latency, reliability and data rate. The requirements set by 3GPP are symmetric, i.e. they are the same for the traffic transmitted and received by the UAV. The throughput requirement is set at 60-100 kbps, and each packet should be received within 50 ms of latency with a reliability of 99.9 %.

Previous studies have reported the challenges of providing highly reliable radio connectivity for UAVs using current cellular networks [5–9].

Some experimental works found in the state-of-the-art indicate that the average latency figures in cellular networks may be above the C2 requirements [10]. But, there is a lack of studies emulating the expected C2 traffic type. It is important to evaluate the performance of cellular networks for the

C2 traffic, because throughput, reliability and latency are dependent of each other [11,12].

The work presented in [12] has also indicated that the usage of a dual-operator hybrid access can improve the system results by adding diversity, while offering robustness against radio link failures in one of the network links.

In this paper, eventual shortcomings of live LTE-A networks in providing C2 connectivity for UAVs are evaluated. A custom setup is used where the UAV carries an onboard client application that exchanges data packets via cellular networks with a remote server [13].

Thereafter, the measurements are used to demonstrate how a simple, client-side, hybrid access solution can significantly improve, and almost overcome, the outages incurred due to latency in the operator access network.

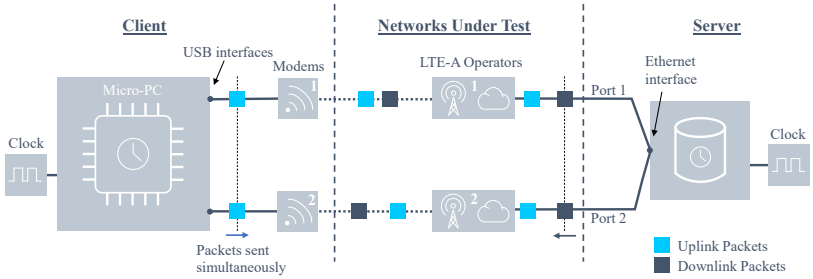

Fig. I.1: Diagram of the Client-Server setup used in the field measurements.

Henceforth in this paper, the legacy nomenclature of cellular networks will be adopted: downlink (DL) will refer to the traffic generated by the cellular network towards the UAV, while uplink (UL) will refer to the traffic generated in the opposite direction.

The remainder of this paper will be organized in the following manner. Section II will detail the setup used in the tests and Section III will describe the scenario for the field measurements alongside information about the flight missions performed. Then, results will be presented for the single-operator and dual operator setup, respectively, in Sections IV and V. At last, further discussions and final remarks are covered by Sections VI and VII, respectively.

II Setup Description

In order to evaluate the performance of the C2 link over cellular networks, the end-to-end traffic between a UAV and its controler is emulated by two elements: a client, attached to a flying UAV, and a server, remotely located

at Aalborg University. Figure I.1 shows a diagram of the whole setup and its key parts. A short description of the functionalities is added in the following paragraphs. For the readers interested in a more detailed description of the measurement framework and its components, those are found in [13].

In the server, a User Datagram Protocol (UDP) traffic generator creates packets following the 3GPP traffic model proposed in [4] for the evaluation of C2 link. In other words, it generates a fixed data rate traffic, with 10 *kbits*-sized packets being sent every 100 ms. The traffic generator sends time-stamped numbered packets with 10 *kbits* (1250 bytes) of size at the instants $t_s = t_0 + k * 100$, where t_s is given in ms, t_0 is the moment where the exchange of information is started and $k = 1, 2, 3...$ represents the numbered packets. The server is attached to a clock synchronized by Global Positioning System (GPS), which marks every packet with its transmission time given in microseconds.

The client consists of a small form factor computing board. The connectivity to the client is provided via Universal Serial Bus (USB) by two smartphones connected to two different cellular networks. A UDP traffic generator and a GPS-based clock perform similar functions as described for the server, except that the transmission instants are offset by approximately 50 ms. The packets are transmitted by the two phones via cellular network connections, each of them associated to a different live LTE Danish network. These two smartphones have a modified firmware which allows an application software to record radio link information such as the Reference Signal Received Power (RSRP), Reference Signal Received Quality (RSRQ), transmitted power, etc[1]. It is worth noting that these data connections are treated as any other eMBB data connection, without any C2/drone specific optimization in the two mobile networks.

A similar receiving process is performed by both client and server. The numbered time-stamped UDP packets are received and the One-way Delay (OWD) calculated by subtracting the generation time from the current receiving time. GPS-based clocks provide a synchronization accuracy in the order of approximately $10\mu s$.

III Evaluation Scenario

The tests took place in an urban environment of Aarhus, the second largest city in Denmark. The flight paths were designed to follow the safety regulations for UAVs issued by Danish authorities by the time of the tests. Given that a continuous visual line of sight (VLOS) is required for the entirety of the UAV mission, the paths followed the city streets and were limited to lengths

[1]More information about the Qualipoc software in `https://www.rohdeschwarz.com/us/brochure-datasheet/qualipoc_android/`

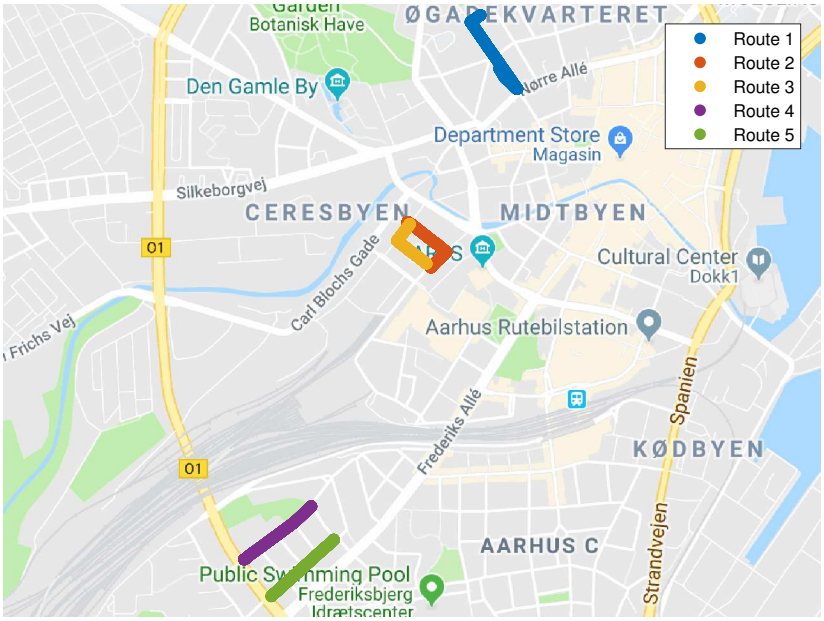

Fig. I.2: Map of the area in Aarhus where flights were performed.

of up to 350 m, in order to prevent surrounding buildings and other obstacles to block a clear VLOS between UAV and the pilot.

Five different routes were chosen for these tests as depicted in Fig. I.2. Routes 1 ($\approx$ 350 m of length), 2 and 3 ($\approx$ 210 m each) perform turns around street corners, while routes 4 and 5 ($\approx$ 270 m each) are long straight lines. The UAV speed was set to 2 m/s and flights were repeated at 3 different heights: 15 m, 40 m and 100 m. For comparison, Drive Tests (DTs) were also performed on each route with the mounting box attached on top of the car. For safety reasons, the car speed was set to approximately 4-6 m/s, because of the local traffic conditions. The drive tests were performed three times in each route, to provide a similar number of samples obtained for each flying height.

The two Mobile Network Operator (MNO) networks used in the test have LTE sites deployed in three different frequencies: 800 MHz, 1800 MHz, 2600 MHz. The phones were not locked to any specific frequency, and the carrier which the phones were attached to depended on the mobility and load balancing settings defined by each operator.

IV Single Operator Results

The 3GPP defines that a maximum latency of 50 ms should be osberved in the one-way path between eNodeB and UAV. The setup presented in this paper is capable of measuring the end-to-end (E2E) delay, which includes the time spent between eNodeB, Core Network and the Public Internet access [13]. Compared to the delay on the air-interface, which 3GPP's requirements refer to, the impact of these additional paths in the results is estimated to be on average between 5-10 ms. This assumption is based on literature reference, where a previous study have demonstrated an average round-trip time (RTT) of 7.5 ms in a ping from a computer located at Aalborg University towards the server [14].

In other words, the latency results provided in this paper should be interpreted as an upper bound for the air interface OWD between eNodeB and UAV. It is important to note that some of the numbered packets transmitted by the client-server setup were not received by the counterpart, probably because of failures in the radio connection. These packets are accounted in the final results as presenting infinite E2E delay for purposes of evaluation.

Figure I.3 shows the complementary CDF of the OWD measured in the packtes received in DL, obtained after aggregating the measurements over the 5 routes for each height. For convenience, 99.9 % reliability and 50 ms delay lines are highlighted in the chart. At the 0.1%-ile, none of the evaluated scenarios achieves the 50 ms target.

The measurements on Operator's 1 network shows the worst performance for the DT, where the amount of packets received with reported latency equal or larger than 50 ms is 2.4 %, much higher than the 0.1 % requirements of 3GPP. For the other heights, the number of packets above the target latency is ranging between 0.5 and 0.8 %. But even though these results are closer to the target, adding some flexibility in latency requirements would not easily lead the number of lost packets to below 0.1 %, as the charts show.

A summary of the 99.9%-ile is presented in Table I.1. The results for Operator 1 shows that such high level of reliability was not reachable for the DT and flying test at 40 m, because several packets have not been received, probably caused by radio connectivity issues. For the other two cases a latency between 150-300 ms would be expected.

Table I.1: 99.9%-ile for DL latency

Network	Latency (ms)			
	DT	15 m	40 m	100 m
Operator 1	NA	290	NA	158
Operator 2	1168	62	70	1150

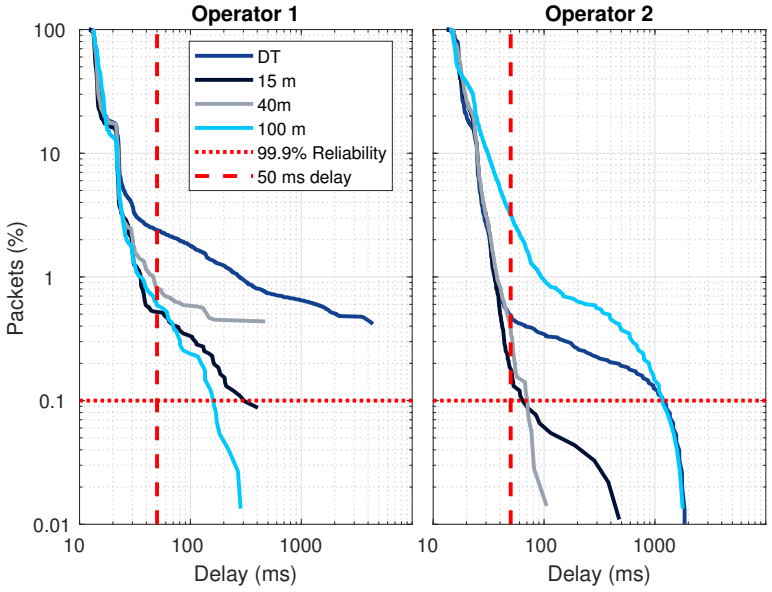

Fig. I.3: Complementary CDF for DL reliability results - Operators 1 and 2.

For Operator 2, the worst performance is observed at 100 m, where 3.2 % of packets are received with latency above 50 ms. In the other 3 cases, results ranged between 0.2 and 0.5%. Table I.1 shows that, for 15 and 40 meters flights, the latency's 99.9%-ile were close to the 50 ms target (60-70 ms). However For the results of the other two cases to be satisfactory the target latency should be above 1s.

The quality of the DL channel is important to ensure the radio link control information is properly received by the UAV. By design, the average UL delays in Long-Term Evolution (LTE) are expected to be higher than the DL values. This can be caused, for example, by a slower HARQ mechanism or a waiting time to receive scheduling grants coming from DL [15]. Fig. I.4 shows the CCDF for the latency measured in UL. It is possible to see that if a 50 ms latency is enforced, the number of packets missed will be between 1

Table I.2: 99.9%-ile for UL latency

Network	Latency (ms)			
	DT	15 m	40 m	100 m
Operator 1	NA	372	NA	NA
Operator 2	NA	79	68	734

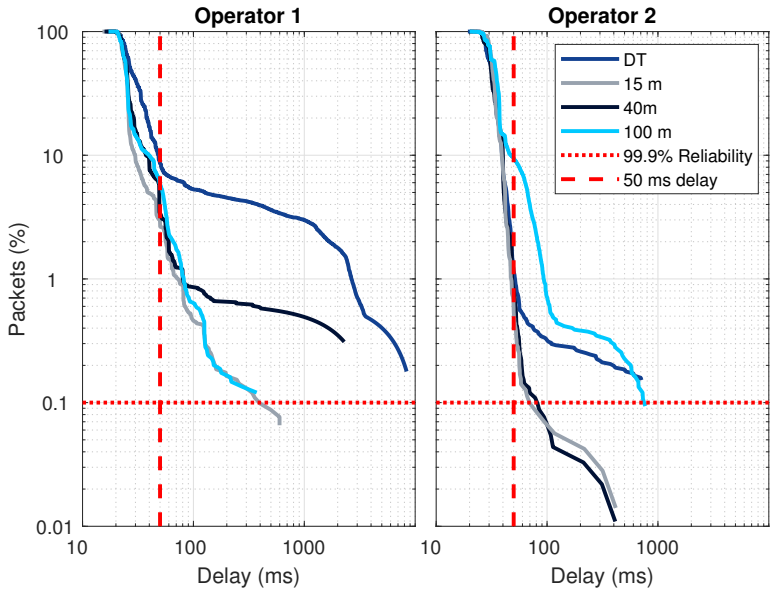

Fig. I.4: Complementary CDF for UL reliability results - Operators 1 and 2.

and 10 % in most cases.

In spite of the propagation and signal quality differences faced by flying UAVs [6], the results presented in Figs. I.3 and I.4 do not show significant relationship between packets latency and UAV flying heights. The causes for this will be discussed in Section VI.

In [10] the end-to-end round-trip latency is measured over a LTE-A network for drones flying at 50 m and 100 m. The results show that most samples are concentrated between 200 and 300 ms delay, which is above the values founds in our measurements, that is approximately 100 ms when combining UL and DL OWD. And also above reference values publicly available for LTE networks in many countries (between 40 and 60 ms) [16]. The differences could be potentially related to the test setup. The results presented in [10] are measured based on ping packages (32 bytes). If the interval between ping messages is high - typically above 200/300 ms - the user equipment may enter idle state, triggered by the discontinuous reception (DRX) settings presented in most LTE-A Networks. In such cases, the transmission of every new packet would depend on receiving a Physical Downlink Control Channel (PDCCH) during the next active time on DRX Cycle, increasing the average latency [15]. Another possible source of difference is the internal core network latency, depending on the network configuration and the routing of the ping packet.

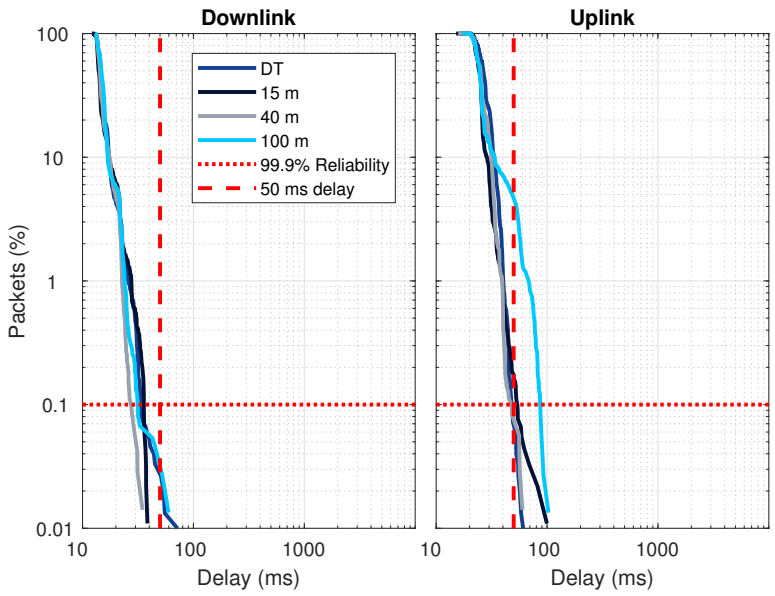

Fig. I.5: Hybrid Access Results for DL and UL.

V Dual Operator Hybrid Access Results

The single operator results show that achieving the requirements for the C2 link defined by 3GPP is difficult. The usage of interference management techniques to improve the reliability of UAV links has been previously examined [6,17]. Proposed solutions can be either based on the network side or in the UAV side.

In this paper, another solution is proposed to improve the reliability of the C2 link: a dual-operator link. This solution is of an easy implementation in the terminal side, and does not require changes in the mobile network. Moreover, it adds diversity against radio links failures or eventual network outages caused, for example, by problems in the core network or technical issues in some radio sites [12].

For the purposes of this paper, UL and DL packets were transmitted simultaneously through both operators. The results were evaluated by selecting the packet received within the smallest elapsed time as the one effectively used by the C2 application. The CCDF for the measured latency using this dual-operator hybrid access scheme is shown in Fig. I.5.

The DL results showed that the C2 requirements can be achieved for all the measurement scenarios. In the UL the 99.9% of reliability is achieved for

the DT and the 40 m height. At 15 m, the results showed 99.85% of reliability, which is acceptable when considering this is the end-to-end delay and not only the path between UAV and eNodeB. The worst performance is observed at 100 m, where the reliability achieved is around 95 %.

Table I.3: 99.9%-ile for hybrid access dual operator system

Network	Latency (ms)			
	DT	15 m	40 m	100 m
Downlink	34	36	27	31
Uplink	48	53	46	86

Table I.3 shows that there is a significant improvement when comparing with Tables I.1 and I.2, and the hybrid access solution shows great potential to reduce the latency associated to the cellular access of the C2 link. Even for the worst case scenario, UL at 100 m, it is possible to see a significant gain on the 99.9%-ile with values much closer of the target 50 ms. We present next some other considerations that could be associated with the dual-operator hybrid access system and the overall system performance.

VI Discussions

A. Link reliability versus height

As previously mentioned in Section IV, the height-dependent degradation of the radio connection is not completely transferred to the measured E2E latency because of LTE's adaptive Modulation and Coding Scheme (MCS). There is a target Block Error Rate (BLER) set on the network side, that aims at keep the average number of retransmissions approximately the same for different scenarios. Every time there is a degradation (or an improvement) in the radio connection, the MCS is adjusted favoring a more (less) robust first transmission, aiming at the target BLER.

On the other hand, a more robust transmission requires more radio resources used for the same amount of data conveyed. When the network is very loaded or the required amount of resources is very high, there may be insufficient resources to convey all data at once, thus the transmission of the packet can take several transmission intervals. However, current networks operate at 10-30% average load, and there are available capacity to support C2 traffic, whose data rate is much smaller than the typical LTE broadband application. Besides, the granularity of the LTE Transmission Time Interval (TTI), 1 ms, is much lower than the 50 ms of allowed latency. So, unless the drop in radio channel quality is so significant to cause a radio link failure or harms significantly the radio control channel, the results observed

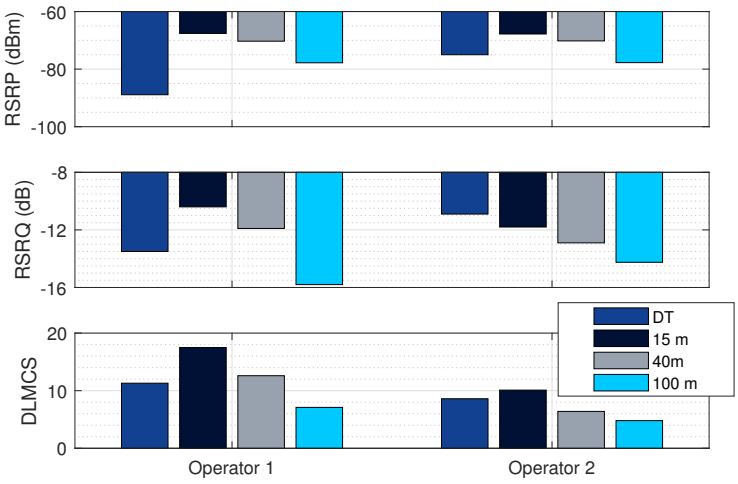

Fig. I.6: Bar plots with median RSRP, RSRQ and DL MCS measured by the test phones.

for a single operator are expected to be approximately the same at all UAV heights, because they are all set to the same target BLER.

This effect is demonstrated in the radio Key Performance Indicators (KPIs) reported by the phone, as observed in Fig. I.6. This figure shows the median RSRP and RSRQ measured in every case and DL MCS index. The median RSRP value improves at 15 m compared to the DT for both operators, as some of the surrounding obstacles in the radio path, such as buildings and trees, are removed in the path between eNodeB and the UAV. As the UAV moves up in height, there is a small degradation on the RSRP which is accounted for the downtilted pattern of the antennas in urban areas. For operator 1, the gains in the RSRP initially leads to a better RSRQ at 15 m, but then the high interference effect comes into play and there is a degradation in the RSRQ. For the conditions observed in operator 2, the gains in RSRP observed at 15 m are exceeded by the increase in interference and the RSRQ degrades at every step up in height.

The DL MCS in Fig. I.6 shows a correlation with the RSRQ trend, moving toward a more robust transmission when there is a degradation in the radio quality. The compensation on the DL MCS keeps the number of retransmissions approximately the same in most cases.

B. Peaks of High-Latency

LTE can perform several retransmissions of a packet within dozens of ms. This means that, the eventual retransmission of packets caused by the link BLER does not fully explain the high latency observed in the tail of the CCDF lines in Figs. I.3 and I.4. In some cases the connection can be lost or a radio link failure can take place, which can be caused by a sudden drop in the received signal, a coverage whole or peaks of load in the network.

Such cases of high latency can last for a few seconds, and compromise the latency of several consecutive packets, also impacting the overall reliability statistics. As a consequence, high-latency packets can come in burst and not only independently distributed from each other in time. In what concerns the hybrid access solutions proposed in this paper, it means that when such peaks of delays occur, the connection can rely on the other operator, until the connection is re-established on the first operator, which usually happens after a handover or a radio connection re-establishment.

This is exemplified in Fig. I.7, that shows a trace of the DT results for operator 1. Observe that in the area highlighted by the red circle, there is a period of more than 30 seconds of high latency (up to 1.5 second), where radio control mechanisms cannot properly recover the quality of the connection, specially on uplink. In this period, server and client sent 340 messages to each other with 78 DL messages (23 %) and 335 UL messages (96 %) exceeding 50 ms. The connection is restored after a handover is performed in the LTE network. Such long-lasting events can seriously compromise the 99.9 % reliability level expected for the system, as several packets are missed consecutively.

It is worthy mentioning also that there is also a possibility that some of the high-latency peaks may not be associated with the link between UAV and eNodeB, but to other parts of the end-to-end connection, such as the link between eNodeB and the core network, or the internet access. We believe that the internet connection of the Aalborg University server was not affected by high latency issues during these experiments, as this effect would be noticeable across both operators simultaneously.

C. Network Target BLER

In cellular networks, the target BLER is usually optimized to maximize average network spectral efficiency. If the target BLER is set too high, there would be several retransmissions. If too low, the unnecessary usage of very-robust MCS would consume several resources at once. For the mission critical C2 case however, a low latency performance is required. The latency can be further improved if the target BLER is set in a lower level compared to regular users. Considering the low data rate traffic of C2, and the current UAVs

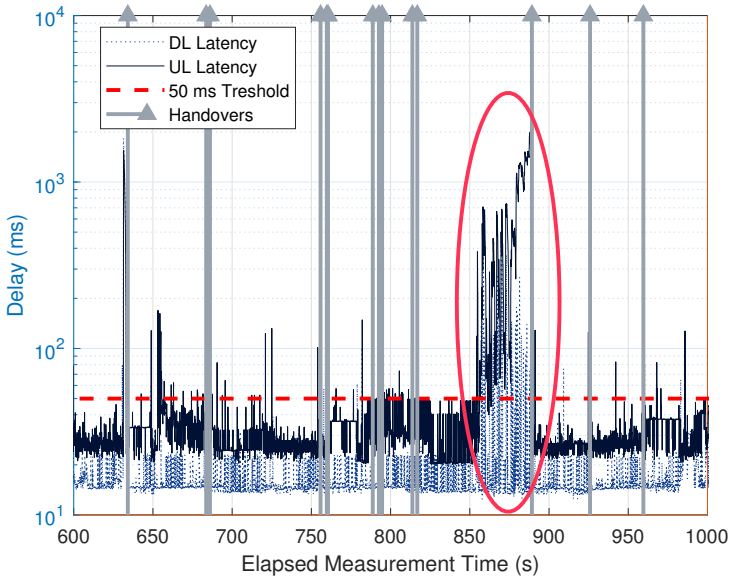

Fig. I.7: Trace of UL and DL delays and handover vents for Drive Test in Operator 1.

market size, the overall impact in resource consumption would be low.

Other advantages can be exploited by identifying the C2 links apart from the other regular data services. It opens the possibility of a semi-persistent allocation of resources, network slicing or other case-specific preventive features, such as the TTI bundling used for voice over LTE (VoLTE).

D. Relaxed Latency Constraints

In this paper the measurement results were compared with the 50 ms target latency proposed by the 3GPP. This strict requirement aims at the safety of the flight mission in any scenario. But for some scenarios, less strict requirements may be sufficient to guarantee it. It is reasonable to consider that the performance of the C2 can be more relaxed, depending on the category of the UAV, its application and the environment [18].

Although, relaxing the latency target to 75, 100 or 200 ms, would not suffice for achieving 99.9% reliability in the single operator test scenarios performed (see Tables I.1 and I.2). On the other hand, the hybrid access results would be even more robust, achieving reliability levels close to the order of 99.99% (see Fig. I.5).

E. Multi-Operator Hybrid Access

The dual-operator measurements performed in this paper showed that the achievable delay performance can get close to th 3GPP requirements for the C2 link. Measurements also showed that failures in the connection of one network can last for several seconds. In a multi-operator scenario, additional degrees of diversity are added, and the expectations are that the results will be even further improved.

F. Trade-Offs

The proposed hybrid access solution shows potential to significant improve the reliability of the C2 link, but some drawbacks must be considered in the designing phase. First of all, it requires the user to be active over two different connections, elevating the overall user power consumption. Moreover, the user-side application can be applied over different frequency layers of the same operator. From the operator's point of view, it would multiply the resource consumption required by each UAV inadvertently. As the number of UAVs scales up, this can increase the load in several frequency layers, causing undesired congestion of the resources.

It is then recommended, that the hybrid access solution must be deployed following some trigger criteria, preferentially with the involvement of the network centralized management, in order to avoid wast of user's power and network's resources.

VII Conclusions

This paper has analyzed the one-way end-to-end latency measured in LTE-A operating networks experienced by a flying UAV. The UAV traffic in the tests emulated the 3GPP requirements for C2 traffic. The dual-operator hybrid access system proposed in this paper shows potential to improve the latency and reliability to values close to the stringent 3GPP target performance levels, without requiring expensive changes or technological improvements on the network side. The hybrid solution overcomes the problem of losing several consecutive packets when radio link connectivity to one operator is highly degraded; which is by far the most important contributor in exceeding the latency target of 50ms. From discussion, the paper has argued that if the hybrid solution is complemented by technical solutions already available in current deployments, cellular networks can deliver reliable and robust C2 performance.

Acknowledgment

This research has received funding from the SESAR Joint Undertaking under the European Union's Horizon 2020 research and innovation programme, grant agreement No 763601. The research is conducted as part of the DroC2om project.

References

[1] EUROCONTROL, "Roadmap for the integration of civil Remotely-Piloted Aircraft Systems into the European Aviation System," 2013.

[2] FAA, "Integration of Civil Unmanned Aircraft Systems (UAS) in the National Airspace System (NAS) Roadmap," Tech. Rep., 2013.

[3] GSMA, "Using Mobile Networks to Coordinate Unmanned Aircraft Traffic," Tech. Rep., November 2018.

[4] 3GPP, "Enhanced LTE support for aerial vehicles," 3rd Generation Partnership Project (3GPP), Technical Specification (TS) 36.777, Jan. 2018, version 15.0.0.

[5] Y. Zeng, J. Lyu, and R. Zhang, "Cellular-Connected UAV: Potential, Challenges and Promising Technologies," *IEEE Wireless Communications*, pp. 1–8, 2018.

[6] H. C. Nguyen et al., "How to Ensure Reliable Connectivity for Aerial Vehicles Over Cellular Networks," *IEEE Access*, vol. 6, pp. 12 304–12 317, 2018.

[7] B. V. D. Bergh, A. Chiumento, and S. Pollin, "LTE in the sky: trading off propagation benefits with interference costs for aerial nodes," *IEEE Commun. Mag.*, vol. 54, no. 5, pp. 44–50, May 2016.

[8] M. M. Azari et al., "Coexistence of Terrestrial and Aerial Users in Cellular Networks," in *Proc. IEEE Glob. Commun. Conf. Workshops*, Singapore, Dec 2017, pp. 1–6.

[9] Qualcomm, "LTE Unmanned Aircraft Systems Trial Report," Qualcomm Technologies Inc., White Paper, May 2017.

[10] G. Yang, X. Lin, Y. Li, H. Cui, M. Xu, D. Wu, H. Rydén, and S. B. Redhwan, "A telecom perspective on the internet of drones: From lte-advanced to 5g," Submitted for publication. Available online in https://arxiv.org/, March 2018.

[11] B. Soret, P. Mogensen, K. I. Pedersen, and M. C. Aguayo-Torres, "Fundamental tradeoffs among reliability, latency and throughput in cellular networks," in *2014 IEEE Globecom Workshops (GC Wkshps)*, Dec 2014, pp. 1391–1396.

[12] M. Lauridsen, T. Kolding, G. Pocovi, and P. Mogensen, "Reducing handover outage for autonomous vehicles with lte hybrid access," in *2018 IEEE International Conference on Communications (ICC)*, May 2018, pp. 1–6.

[13] G. Pocovi, T. Kolding, M. Lauridsen, R. Mogensen, C. Markmller, and R. Jess-Williams, "Measurement framework for assessing reliable real-time capabilities of wireless networks," *IEEE Communications Magazine*, vol. 56, no. 12, pp. 156–163, December 2018.

[14] M. Lauridsen, L. C. Gimenez, I. Rodriguez, T. B. Sorensen, and P. Mogensen, "From LTE to 5G for Connected Mobility," *IEEE Communications Magazine*, vol. 55, no. 3, pp. 156–162, March 2017.

[15] G. Pocovi, I. Thibault, T. Kolding, M. Lauridsen, R. Canolli, N. Edwards, and D. Lister, "On the suitability of lte air interface for reliable low-latency applications," in *IEEE Wireless Communications and Networking Conference*, Accepted for Publication, April 2019.

[16] "Open Signal Market Analysis," Available Online in https://www.opensignal.com/market-analysis, 2019, accessed in Fev. 2019.

[17] B. Galkin, J. Kibilda, and L. A. D. Silva, "Coverage Analysis for Low-Altitude UAV Networks in Urban Environments," in *Proc. IEEE Glob. Commun. Conf.*, Singapore, Dec. 2017, pp. 1–6.

[18] D. Colin, "RPAS - Required C2 Performance (RLP) Concept," JARUS, Tech. Rep., May 2016.

Chapter 5 - Assignment of Dedicated Spectrum

The adavantages of reusing cellular network resources to provide Command and Control (C2) connectivity were laid out in Chapter 1. The subsequent chapters have demonstrated that the resource sharing imposes interference challenges, as terrestrial users and Unmanned Aerial Vehicles (UAVs) mutually interfere with each other. One alternative to improve the reliability of the C2 access is to employ dedicated frequency bands, protecting the link from interference caused by terrestrial users. The present chapter discuss the advantages and disadvantages of using dedicated spectrum or radio resources for C2 links, and forecast the bandwidth demand for C2 connectivity over the next 20 years.

5.1 Problem Description

There are performance challenges for the coexistence between terrestrial users and UAVs [1], specially under high traffic load conditions and when the UAVs are demanding very high reliability in their link (99.9 % for C2). The reliability of the C2 are very sensitive to increases in the network load, whereas broadband applications used for terrestrial users, combined with the high density of such users, can rapidly increase the load on the systems in certain periods of the day.

For similar reasons, the International Telecommunication Union (ITU) has envisioned the usage of a dedicated spectrum band for the C2 operation, stating it should be a band guarded from external sources of interference [2]. Such kind of solutions has the clear advantage of improving the performance of the C2, however it must be examined by its commercial potential – in terms of reducing costs – in order to evaluate the deployment feasibility.

Such solutions require a deployment on a licensed spectrum, as systems operating on unlicensed spectrum cannot guarantee a dedicated frequency use. This deployment can either be achieved by installing a new network planned for this specific use case or by reusing the operational infrastructure

available in other networks, such as those from cellular operators. Both with their own advantages and disadvantages.

5.1.1 Dedicated Network

The usage of dedicated network resources extrapolates the scope of the present work, which is focused on the usage of cellular technologies to provide C2 service. Notwithstanding, the following paragraphs discusses the advantages and disadvantages of such deployment.

Besides the absence of external (or caused by a different class of users) interference, the deployment of a dedicated infrastructure presents advantages in what regards the optimization of the network elements. The choice of base stations positions, transmit power and antennas tilt, for example, are elements that can be optimized to enhance the C2 reliability.

In some cases, small networks may offer an efficient solution for hotspots, industrial applications or ad-hoc demand. On the other hand, there are disadvantageous aspects that can make it unattractive from the commercial perspective for a large/regional network deployments, which is the main focus of the discussions presented in this chapter.

Site Density and Ubiquitous Coverage

In addition to the latency and throughput requirements, the availability of the connection is one important part of delivering a reliable service. The connection must be present in all phases of the flight, including operations of take-offs and landings. These two, in particular, impose significant challenges for the deployment of a new network, which can cause the required number of cells to soar.

The previous chapters have indicated favorable path loss conditions at cruise level heights, which suggests the coverage of one given cell is extended for several kilometers. This implies few cells are required to provide coverage for cruising UAVs in the absence of interference. The highest the flight level, the fewest base stations are required. This is exemplified by the case of Gogo, a company that provides internet connectivity for aircrafts on US. The number of cell sites deployed to cover whole US, including Alaska, and parts of Canada is approximately 260 [3] as of 2017.

However, to provide ubiquitous reliable service, including support for take-offs and landings operations, as well as for flights at very low level, the coverage at terrestrial level must be taken into account. The study presented in [4] assess the feasibility of a communication network to provide C2 service over a 800-mile (1290 km) long pipeline. The coverage evaluation shows that at heights around 1000 ft. (300 m), 100 % coverage can be achieved by optimization through an initial set of 57 *potential* cell site locations. At 100

ft. (30 m), only 83 % coverage can be achieved. By increasing the *potential* cell site locations to 149, it was possible to achieve only 91 % of coverage is achieved through 61 *effectively* deployed sites.

Because of the requirements of ubiquitous and reliable coverage also for the landing and take-off phases, a much more dense network will be required, increasing the deployment costs. For comparison with Gogo's numbers the number of macro base stations deployed over all the different cellular operators by the end of 2017 surpassed more than 220,000 for the whole US [5].

In addition to the physical installation, there are high expenses involved in providing backhaul access to all those cell sites, either by fiber, cables or microwave links. This connection, as part of the whole C2 system, must also be highly reliable. An example of the magnitude of such costs, for reference prices of 2013, is presented in [6]. The author has estimated the cost of a new Long-Term Evolution (LTE) macro site in approximately 120 thousand euros in the first year, where 38 % of the costs are associated with CAPEX, which includes expenses with masts, antennas, hardware, software, backhaul, etc.

The demand for C2 services typically relies on forecasts, because the drone-powered commercial applications are a very recent trend and therefore lack historical data. Moreover, current figures for the demand of beyond visual line-of-sight (BVLOS) flight services may be hard to estimate, as current legislation does not enable the full commercial potential of such services. Therefore the demand numbers are subject to several uncertainties [7].

In spite of this, it is reasonable to consider that the density of UAVs requiring C2 connectivity will grow over the years, but it will be relatively small in a first moment. Associated with the high costs aforementioned, it may be commercially unattractive.

Idle Capacity

Ubiquitous deployments are required from the C2 provider, in order to guarantee the *availability* of the link at any time and any place. On the other hand, some places will face higher demand, whereas isolated cell sites may be idle for long periods. Moreover, it is prudent to assume that, *on average*, medium-sized UAVs will spend more time on the ground than actually flying.

Hence, it is expected that the spectrum usage will be idle for long times or over large areas, as observed in cellular networks. The idle capacity represents an inefficient allocation of the usually expensive spectrum resources and of energy in the network sites.

Interoperability

The choice of technology made by each of these operators can jeopardize long range applications, depending on whether they cross region/country

boundaries. Flight missions that trespass areas served by different networks, for example by crossing countries borders, can be either become unfeasible or require a second modem, if these technologies are not provided with interoperability.

This requires a collaborative effort from the European Aviation Safety Agency (EASA) members and other air space authorities to guide the local decisions envisioning regional interoperability. This is one of the points addressed by the SESAR vision for the future of the airspace [8].

5.1.2 Dedicated Radio Resources in Cellular Networks

A similar interference "protection" can be achieved by reserving frequency bands – or alternatively time/frequency radio resources within the same band - in the cellular spectrum and reusing the operators' infrastructure, instead of implementing a new network. If the reservation is made on very large areas, based upon some planning or well defined dynamic triggers, this can be more easily managed than the current inter-cell interference coordination (ICIC) solutions.

The infrastructure reuse prevents the network to be fully optimized for the UAVs, as previously mentioned in this thesis. On the other hand, it provides solutions for many of the other challenges raised in Section 5.1.1.

Ready to Market Coverage

The readiness of the infrastructure presents one major advantage in favor of cellular networks. It reduces the waiting time and cuts significantly the Capital Expenditures (CAPEX) costs of implementing new sites, by reusing backhaul connection, core network, masts and towers.

Moreover, cellular networks already provide pervasive connectivity at terrestrial level [9]. The population covered by 3GPP cellular technologies was approximately 95% by 2017, where more than 60% are already covered by LTE networks [10]. Expectations are that by 2024, more than 90% of the population will be covered by LTE worldwide, while 40% will have access to 5G technologies [10]. For the remote areas, which have scarce access to cellular networks, connectivity at aerial heights may be provided by a few additional sites or in combination with hybrid solutions such as Non-Terrestrial Networks (NTN) networks [11], which is already being envisioned for future 3GPP releases [12].

The mobile network industry has also naturally evolved to uniformed practices and adoption of technologies that ensures worldwide interoperability, through collaboration groups like the GSM Association (GSMA), who represents more than 750 mobile operators. This also creates an stable demand for manufacturers of chipsets and devices, speeding up the readiness

of available products in the market.

Capacity Reallocation

Using dedicated spectrum in already operating cellular networks opens up possibilities for capacity reallocation, to avoid the waste of resources with idle capacity. The idea is to dynamically reallocate resources according to the UAVs demand. This would allow the network to cope with instantaneous increase in UAVs demand, while prevent resources to be reserved in areas/times where there are no flying UAVs.

However, the capacity reallocation strategies shall be widely designed and rapidly responsive such that the C2 can exploit resources protected from interference caused by other users or services almost at all times.

In Chapter 4, the analysis of management of radio resources provided by ICIC showed this mechanism, as it is implemented in current releases, it may be complex to manage. To alleviate this problem, the reservation of the resources can be made less complex, by more aggressive resource reservation policies. For example, the reservation of resources may be made for entire tracking areas at once.

In the next sections, the required bandwidth to provide C2 service is evaluated, according to the forecast for the next years. Then, some discussion is provided about strategies to perform the resource allocation for UAVs.

5.2 Paper Included

Paper J. Forecast of Bandwidth Demand for UAVs Served by Dedicated Cellular Spectrum

This paper uses the Federal Aviation Administration (FAA) forecast for number of commercial UAVs registered in the next years, to estimate the density of simultaneously airborne UAVs in different scenarios: from rural to very dense urban. Thereafter, simulations are performed using different inter site distances, to estimate the amount of UAVs that can be served by a certain bandwidth, reaching the target throughput (100 kbps) for at least 99.9% of the UAVs.

In the simulations, the interference is limited by the intrasystem interference caused by the other C2 links. The UAVs are deployed at 120 m, the current height limit, as this represents the most stringent interference scenario. The set of bandwidths evaluated was chosen from the current values specified for LTE: 1.4, 5, 10 and 20 MHz.

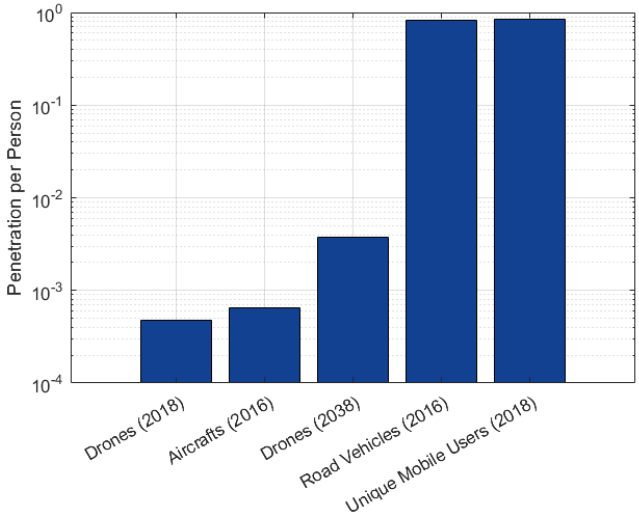

Fig. 5.1: Market penetration of drones today and in 2038 (peak projection), compared to aircrafts, road vehicles and unique mobile subscriptions.

5.3 Main Findings

5.3.1 Low geographical density of airborne UAVs

By april 2018, there were just above 150 thousand commercial UAVs registerd on the FAA database and the a total of up to 750 thousand units are projected in the market by 2022. Extrapolating their projections, presented in [7], using a Gompertz function [13], a total just above 1.2 million commercial UAV units are expected in the US by 2038.

Assuming the increase on the fleet will be proportional across all US counties, and an usage rate of 1 hour per work week, split in three fights of 20 minutes, the expected *peak* number of airborne UAVs in the market is below 1 UAV/km^2 in almost all cases, except for New York (2.5 UAV/km^2).

To give the idea of the penetration of drones per person, Fig. 5.1 shows the current and 2038 projections for commercial UAVs (see Paper J), in comparison with unique mobile subscribers [14], road vehicles and airplanes [15]. It is possible to see that the high projections show a number of commercial devices much lower than the number of road vehicles or mobile subscriptions, which explains the low density of airborne drones projected per area.

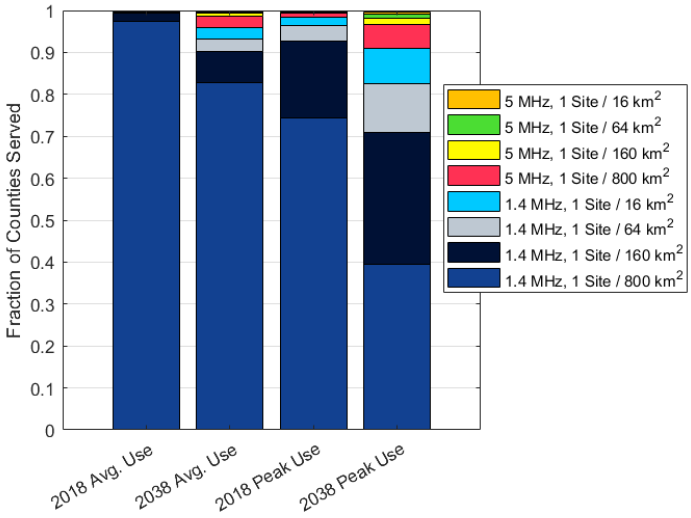

Fig. 5.2: Fraction of US counties served by different resources configuration according to projections in Paper J.

5.3.2 Bandwidth current requirements projected to 1.4 MHz

Section IV has discussed the spectrum requirements for the predicted amount of UAVs in the network. For the current number of units available in the market, only 1.4 MHz of spectrum are required for providing reliable services. Fig. 5.2 shows that, on average usage, almost all counties can be served with just 1.4 MHz, with more than 97% being served with only 1 site / 800 km^2. At peak usage, i.e. when the number of simultaneous UAVs peak, 92.8% of the US counties can be served with 1 site / 160 km^2 and up to 99.8% can be served using a higher site density.

For the scenarios that represent a density of active drones that cannot be satisfied with 1.4 MHz, enhanced solutions, such as those described in 4, can be used to increase the capacity of the system. Also, the network deployment can be further optimized to improve the results using user-specific settings. For example, antenna beamforming can be deployed or the choice of the site locations to be enabled for C2 service, among the different possible choices, may be optimized, also the resource allocation and load balancing to avoid one cell to run out of resources too early.

The 1.4 MHz is a relatively low bandwidth, corresponding to between 0.3 % and 0.5 % of the the spectrum already licensed for mobile systems of the fourth generation (4G), corresponding in many countries [16]. For reference, Fig. 5.3 shows the total spectrum already licensed for LTE in several

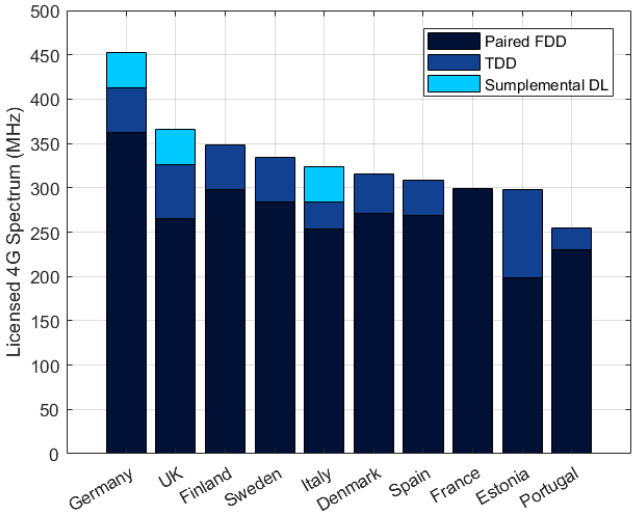

Fig. 5.3: Total bandwidth licensed at the time of writing for 4G systems in different European countries [16].

European countries – typically divided between 3 or 4 large operators.

5.3.3 Future bandwidth requirements projected between 1.4 to 5 MHz

Fig. 5.2 shows that for the scenarios represented by most US counties, 1.4 MHz can provide the service at peak usage, in more than 91 % of the cases. But at the most dense locations, 5 MHz would be necessary to guarantee the service. For approximately 9 % the scenarios the service required a 5 MHz bandwidth, and only in 0.4 % of the cases, more than 5 MHz would be required.

These results favor a more dynamic allocation of the resources, where the reserved bandwidth is adjusted with the network demand. The advantages are clear: allocating 5 MHz for all the scenarios would cause significant waste of resources in the majority of the locations, but it would still be insufficient at peak usage in the most dense areas. Cellular networks can more easily adapt to the circumstances than a network built on resources pre-reserved by local authorities for a specific service. Section 5.4 show how the dynamic allocation can be applied in the network.

It is worth noting that with the ongoing spectrum licensing processes active in many countries for 5G [17], the 5 MHz will correspond to a fraction even smaller to the total licensed spectrum for 4G and 5G mobile systems.

Currently, such a bandwidth corresponds to between 1 to 2% of the total licensed spectrum in many countries.

5.4 Discussion

The results presented in Paper J have demonstrated that a relatively narrow bandwidth is required to provide the C2 service, without any optimization on current standards. The results can be even further enhanced by technical solutions (see Chapter 4).

It is worth noting that these results were produced for UAVs flying at 120 meters, but it does not address the problems of taking off and landing operations at ground level. In order to guarantee reliability for such cases, the density of base stations shall be higher than shown in Fig. 5.2, as the signal may not be available at higher distances from the transmit base station at terrestrial level (as discussed in Chapter 2). Another option is to use the terrestrial network with high priority for those cases, until the UAVs can reach heights where there is coverage provided by the reserved resources.

The next subsections discusses the advantages of cellular networks, when comparing the different options for dedicated spectrum solutions. Insight about technical solutions that can be used to provide flexibility for the cellular deployment are also presented, aiming at profit from the available infrastructure while minimizing the costs associated with spectrum reservation.

5.4.1 Support for Take-Offs and Landing Operations

Cellular operators already provide coverage at terrestrial level, so their networks are already dense enough to provide seamless coverage. Moreover, the signal to interference plus noise ratio (SINR) and Dominant Interferer Ratio (DIR) close to ground is different from the airborne level's, and more likely to profit from techniques such Interference Rejection Combining (IRC), Coordinated Multipoint (CoMP) and ICIC, although the same tend to be ineffective at higher heights.

Yet, by reserving spectrum resources across all the network, the interference observed close to ground level tend to be significantly minimized.

5.4.2 Minimization of Spectrum Cost

Besides all the infrastructure related costs, there are also costs related to the frequency spectrum, which is an expensive component of the communication ecosystem, whose price tends to vary for different frequency bands. At the time of writing, several countries are in the process of auctioning and licensing frequency spectrum for 5G systems, with a few of them already concluded.

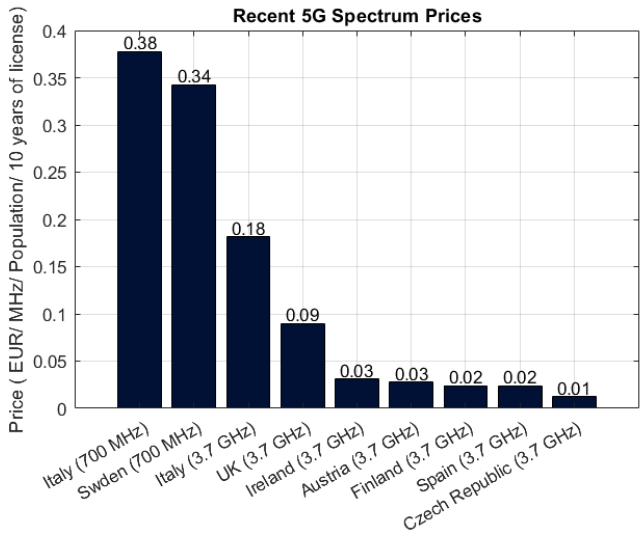

Fig. 5.4: Average price paid in 5G-related auctions for spectrum in 3.5 GHz bandwidth, according to [17].

The most recently finished spectrum auctions for the deployment of 5G systems resulted in prices around 0.01 to 0.38 EUR/MHz/Population/ 10 years of license, as shown in Fig. 5.4. It is worth noting that from the frequencies currently auctioned the 700 MHz has been the most expensive so far, which is closer to the frequency ranges evaluated in our research. This may be attributed to the scarcity of spectrum in this band. The 3.7 GHz frequency band was not assessed in this paper, but other studies have indicated that UAVs may benefit from the beamforming capability offered at this band [18].

Assuming a current density of 1 drone / 2000 people (Fig. 5.1), the costs escalate to 20 to 800 EUR/MHz/UAV/ 10 years of license, which can either be commercial unattractive or extend the return of investiment (ROI) period of the whole operation for several years. Over the years, the cost per unit will decrease as a consequence of the growth rate of the market.

The associated spectrum cost can be minimized by a dynamic allocation of the spectrum, that reserves only the bandwidth effectively required by the drone activity in a given area. This reduces the spectrum costs to the opportunity cost of allocating bandwidth exclusively for UAVs: it reduces the network capacity available for the other users in the whole reserved area. Section 5.4.3 discusses one method for performing the on-demand resource allocation.

5.4.3 Smart spectrum allocation

The wireless networks have evolved to provide several services with different requirements. These services present diverse constraints for the throughput, latency and power consumption, which demands high flexibility of the network, as those cannot be optimized at the same time [19]. The applications can also result in different traffic demands, varying from large number of users with small sized packets to users with broadband applications [20], while innovative cost-efficient business model are being discussed such as the multi-tenancy spectrum sharing [21].

These factors have pushed the wireless field to develop the concept of Wireless Network Virtualization (WNV), which consists in creating logical partitions of the network resources to create virtual decoupled networks [22]. These partioning enables the implementation of different settings and policies in the virtual instances of the networks. The differentiation of *Quality of Service* indicators can be used to assure different service requirements within each virtual network while alleviating the overall resource management complexity and tend to be one important component of 5G networks [23].

Regarding the UAV case, it is possible to use ad-hoc network slicing, it is possible to provide dedicated spectrum for these users, through the virtual network created, while enabling the resources to be shared with other network users in idle areas/times. Within the virtual network, the network settings, such as power control and mobility parameters, may be optimized for the UAV scenario.

This adaptive network virtualization for UAVs present some advantages compared to a pre-allocation of frequency resources, either offered by a dedicated network or by shared cellular operators infrastructure. One key point is that this setup provides a solution for event-driven high peaks in demand, which can happen locally exceeding the demand projections for a given time and area. Another advantage is providing better flexibility for cellular networks to steer the UAV traffic and its associated loss in network capacity to the less loaded bands, provided the required reliability and coverage can be maintained.

The network virtualization can be implemented following a principle similar to ICIC in the frequency domain. In other words, frequency resources will be reserved uniquely for providing C2 services. More aggressive policies can be used to make the management of the area less complex, once the idea is complete protection against external interference. As one example, the virtual network can be created in all sites on a set of X tracking areas surrounding the user, where X is defined by network design and depends on the size of the tracking areas.

References

[1] M. M. Azari et al., "Coexistence of Terrestrial and Aerial Users in Cellular Networks," in *Proc. IEEE Glob. Commun. Conf. Workshops*, Singapore, Dec 2017, pp. 1–6.

[2] "Characteristics of unmanned aircraft systems and spectrum requirements to support their safe operation in non-segregated airspace," ITU-R, Mobile, radiodetermination, amateur and related satellites services M.2171, 2009.

[3] Gogo, "Annual Report," SEC Annual Report, Feb. 2018.

[4] D. S. Ponchak, G. Church, E. Auld, and S. Henriksen, "A summary of two recent UAS command and control (C2) communications feasibility studies," in *2016 IEEE Aerospace Conference*, March 2016, pp. 1–11.

[5] CTIA, "State of Wireless 2018," Available Online in https://www.ctia.org/news/the-state-of-wireless-2018, Jul. 2018, accessed in Fev. 2019.

[6] C. Coletti, "Heterogeneous Deployment Analysis for Cost-Effective Mobile Network Evolution: - An LTE Operator Case Study," Ph.D. dissertation, Aalborg University, Sep. 2012.

[7] Federal Aviation Authority, "FAA Aerospace Forecast, Fiscal Years 2018-2038," Tech. Rep., March 2018.

[8] SESAR Joint Undertaking, "U-Space Blueprint brochure," Publications Office of the European Union, Luxembourg, 2017.

[9] GSA, "Evolution from LTE to 5G: Global Market Status," Available Online in https://gsacom.com/paper/evolution-lte-5g-2/, Jan. 2019, accessed in Fev. 2019.

[10] Ericsson, "Ericsson Mobility Report 2018," Available Online in https://www.ericsson.com/en/mobility-report, Nov. 2018, accessed in Fev. 2019.

[11] U. Turke, B. Hiller, D. Gotz, I. Z. Kovacs, J. Wigard, A. Eisenblatter, M. Clergeaud, and N. van Wambeke, "DroC2om - 763601 - Models for Combined Cellular-Satellite UAS Communications," SESAR Joint Undetaking, Deliverable 3.1, April 2018.

[12] 3GPP, "Solutions for NR to support non-terrestrial networks," 3rd Generation Partnership Project (3GPP), Technical Specification (TS) 38.821, 2019, version 0.4.0.

[13] I. Z. Kovacs, P. Mogensen, B. Christensen, and R. Jarvela, "Mobile broadband traffic forecast modeling for network evolution studies," in *2011 IEEE Vehicular Technology Conference (VTC Fall)*, Sept 2011, pp. 1–5.

[14] GSMA, "The Mobile Economy 2018," Available Online in https://www.gsmaintelligence.com/, 2018, accessed in Fev. 2019.

[15] "National Transportation Statistics," Available Online in https://www.bts.gov/topics/national-transportation-statistics, 2018, accessed in Fev. 2019.

[16] Spectrum Monitoring, "Frequencies," Available Online in https://www.spectrummonitoring.com/frequencies/, 2019, accessed in Mar. 2019.

[17] European 5G Observatory, "National 5G Spectrum Assignment," Available Online in http://5gobservatory.eu/5g-spectrum/national-5g-spectrum-assignment/, 2018, accessed in Fev. 2019.

[18] Y. Zeng, R. Zhang, and T. J. Lim, "Wireless communications with unmanned aerial vehicles: opportunities and challenges," *IEEE Communications Magazine*, vol. 54, no. 5, pp. 36–42, May 2016.

[19] B. Soret, P. Mogensen, K. I. Pedersen, and M. C. Aguayo-Torres, "Fundamental tradeoffs among reliability, latency and throughput in cellular networks," in *2014 IEEE Globecom Workshops (GC Wkshps)*, Dec 2014, pp. 1391–1396.

[20] L. C. Schmelz, C. Mannweiler, and A. Banchs, "Documentation of Requirements and KPIs and Definition of Suitable Evaluation Criterias," 5G PPP, Deliverable 6.1, September 2017.

[21] K. Samdanis, X. Costa-Perez, and V. Sciancalepore, "From network sharing to multi-tenancy: The 5G network slice broker," *IEEE Communications Magazine*, vol. 54, no. 7, pp. 32–39, July 2016.

[22] M. Richart, J. Baliosian, J. Serrat, and J. Gorricho, "Resource Slicing in Virtual Wireless Networks: A Survey," *IEEE Transactions on Network and Service Management*, vol. 13, no. 3, pp. 462–476, Sep. 2016.

[23] J. Erfanian and B. Daly, "5G white paper," NGMN Alliance, White Paper, Mar 2015.

Paper J

Forecasting Spectrum Demand for UAVs Served by Dedicated Allocation in Cellular Networks

R. Amorim, I. Z. Kovács, J. Wigard, T. B. Sørensen and P. Mogensen

The paper has been accepted for publication in
IEEE Wireless Communications and Networking Conference 2019.

© 2019 IEEE
The layout has been revised and reprinted with permission.

Abstract

In this paper, the usage of dedicated portions of cellular spectrum to provide the high-reliable Command and Control (C2) link for Unmanned Aerial Vehicles (UAVs) is evaluated. Simulations are performed using data settings of a real operating Long-Term Evolution (LTE) network in Denmark, in order to assess the reliability of the C2 link. Up to date databases of drone registrations and market projections are used to infer the drone densities and estimate the future traffic demand. Based on these estimations, network capacity results show that, deploying a sparse network with reservation of 1.4 MHz is sufficient for most cases according to current demands. In the next 20 years, the increase in demand can be followed by a continuous deployment of sites and an increase in the bandwidth up to 5 MHz. The paper also presents a discussion about which solutions can be used to further boost network capacity, and help to achieve high reliability even for the most stringent traffic demand cases.

I Introduction

The market for Unmanned Aerial Vehicle (UAV) applications is expanding rapidly, driven by advancements that make the technology more affordable to large audiences. By regulations, most of their applications shall guarantee direct visual line of sight (VLOS) — not to be confounded with radio line-of-sight (LOS) — between flight controller and UAV. In most cases, UAV and controller are connected over 802.11 or proprietary standards in unlicensed band. The lack of a long-distance reliable communication link for UAVs make authorities unwilling to allow beyond visual line-of-sight (BVLOS) flight ranges missions. In order to enable BVLOS ranges, in recent years, significant attention has been invested in creating a reliable Command and Control (C2) link between UAVs and flight controllers.

A feasibility study led by National Aeronautics and Space Administration (NASA) [1], argues that a nationwide Command and Control (C2) terrestrial network would entail prohibitive costs of operation and maintenance for the government. Additionally, the lack of an established demand for UAV traffic may impose risks for commercial entities interested in a Public-Private Partnership (PPP). The GSM Association (GSMA) presented cellular network as a potential solution to this problem in its official position released after a European Aviation Safety Agency (EASA)'s consultation [2]. In this document, three advantages of cellular networks are presented by GSMA: 1) a ready-to-market ubiquitous infrastructure; 2) 4^{th} Generation (4G) networks can already meet high-bandwidth and low latency requirements with good quality, which can enable not only the C2 link but innovative services through different payload applications; 3) operators have extensive experience and a long track-record in data privacy and security issues. The Third Generation

Partnership Project (3GPP) has made enhancements further improving cellular networks for UAV service in its work item to promote enhanced support for aerial vehicles [3].

On top of this, the Single European Sky ATM Research Programme (SESAR)[1] has launched a framework for UAVs flying at very low levels, with the goal of ensuring their safety in the airspace. Among the projects launched by SESAR, DroC2om is especially oriented to investigate and design a hybrid architecture that combines cellular and satellite networks to provide a reliable C2 link [2].

However, cellular networks are commonly designed for terrestrial users, whereas propagation studies have shown that UAVs are subjected to different radio conditions. In [4,5] authors show that airborne UAVs above rooftops are more likely to experience LOS and freespace propagation to the surrounding base stations. Therefore, the signals from the neighbor cells are stronger which can raise the interference level, as shown by the measurements in [6,7].

When legacy cellular users and UAVs are sharing the same network resources, the broadband traffic generated by the first group is a source of interference for the second group and it can harm the reliability of the C2 downlink (DL) link or affects the radio usage's efficiency [8,9]. In the uplink (UL), the signal transmitted by the UAVs will affect several neighboring base stations which will impact the legacy users [10], even though the LOS likelihood can reduce the required transmit power.

In this paper, the performance of UAVs in cellular networks is evaluated assuming a resource reservation approach, which aims at a middle ground solution between an expensive new dedicated network and the high interference resource sharing solution. In this approach, instead of licensing a large portion of the spectrum for C2 communications, operators can reserve a fraction of a carrier to the C2 link, while maintaining the remainder of the carrier available for legacy uses.

It is also discussed how this approach tends to be future proof, by adapting to the UAVs traffic demand as they increase over time, either by adjusting the density of deployed sites or the bandwidth reservation. For this exercise Federal Aviation Administration (FAA) projections for the US fleet, found in [11], is used as a reference number to project the UAV market size for the next 20 years.

The remainder of this paper is organized as follows: Section II presents traffic projections for airborne UAVs for the next 20 years. Sections III and IV present, respectively, the simulation scenario and the discussion of the results for the capacity of cellular networks to serve airborne UAVs. Further considerations on the assumptions and results are discussed in Section VI,

[1] https://www.sesarju.eu/

[2] https://www.droc2om.eu/

while the conclusions are presented in VI.

II UAV's Traffic Projection

This paper uses data from a real operating network in Aalborg, Denmark, to perform simulations and evaluate the reliability of the C2 link. Due to the scarcity of data in the number of UAV devices commercialized, it is generally difficult to estimate the UAV traffic demand. For this reason, the FAA has been chosen as a source, once it is one of the most complete databases that has been made publicly available. Based on their data, it is possible to roughly estimate the density of UAVs in use in the different US counties. These estimations cover a wide range of scenarios, from very dense areas such as Manhattan to rural areas in the countryside. By offering a multitude of scenarios, they provide a good generalization of the market size, and it is our understanding that the average figures for European scenarios should not differ much from these estimations, therefore, the scenario available for simulations fits the purpose of our evaluation. Section V-B discusses how the results should be weighed in according to discrepancies between the scenario in Aalborg and large metropolitan areas in US, such as Manhattan.

At the time of writing, there is no established demand for C2 links, as UAV's major applications are still limited to VLOS. Therefore, the assessment of estimations for spectrum requirements must be performed over forecasts.

In this paper, forecasts are based on FAA current numbers for the UAV market in the US. This is motivated on the grounds that FAA issues an early update on their forecasts and maintains a database that is publicly available with current drone registrations. The database, which contains the number of drones registered per US zip code[3], is used to estimate the density of registered drones. Henceforth, all mentions to this database refers to the class of non-hobbyist drones. The hobbyist drones, mostly used for leisure, are not considered part of the scope of the present work, because they are used much more infrequently, especially within the "busy hours" considered for the traffic prediction. Moreover, there is no indication that such class of drones will engage in BVLOS activities.

A. Today's Market

According to the FAA, there were right over 156 000 drones registered on US addresses as of April 2018. For reference, this corresponds to 1 drone for approximately 1300 personal cars. Regarding today's business models and assuming availability of C2 links, we estimate that each drone would be used

[3]Available online in: `https://www.faa.gov/foia/electronic_reading_room/`

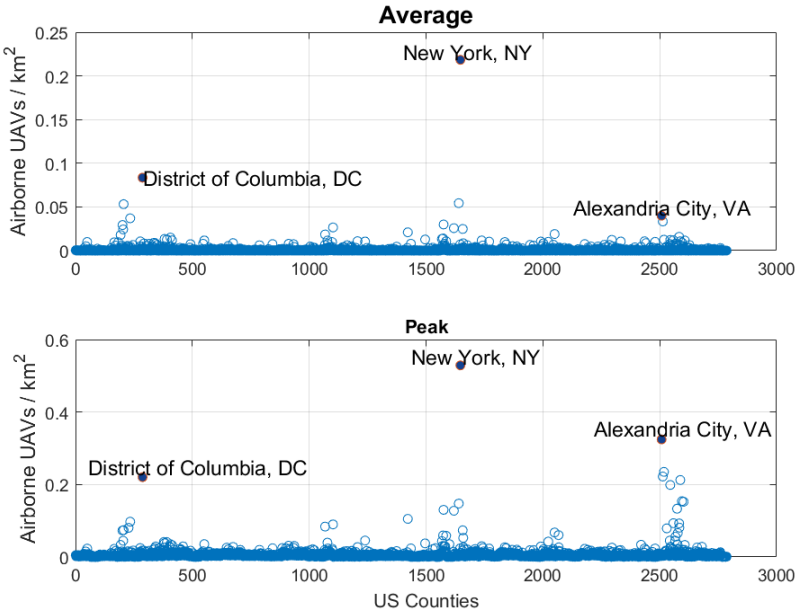

Fig. J.1: Densities of estimated simultaneous airborne UAVs (average and peak) per US County (april 2018).

on average 3 times per workweek (Monday to Friday, from 9 to 17 hs), with an average flight duration of 20 minutes.

Given such assumptions, and mapping the zip codes of drones registrations to US counties using the data from the Census Bureau[4], it is possible to determine what would be the UAV traffic demand today. Fig. J.1 shows the average and the peak values expected for the density of simultaneous airborne UAVs. Counties with less than 30 km^2 were filtered out of the analysis, as few UAVs could yield a misleading high density of UAVs, but in reality they would require just a few radio resources.

In New York county, the one with highest UAV density, there average density projected for airborne UAVs is 0.2 UAV / km^2, with peaks of 0.52 UAV / km^2. It is important to note that the numbers for average and peak densities are based on assumption of an independent and identical exponential distribution of the take-off times. It does not cover the case of an event where massive take-offs could be observed, for example, to support or assist a parade. Such events would require different planning and a specific solution.

[4]https://factfinder.census.gov

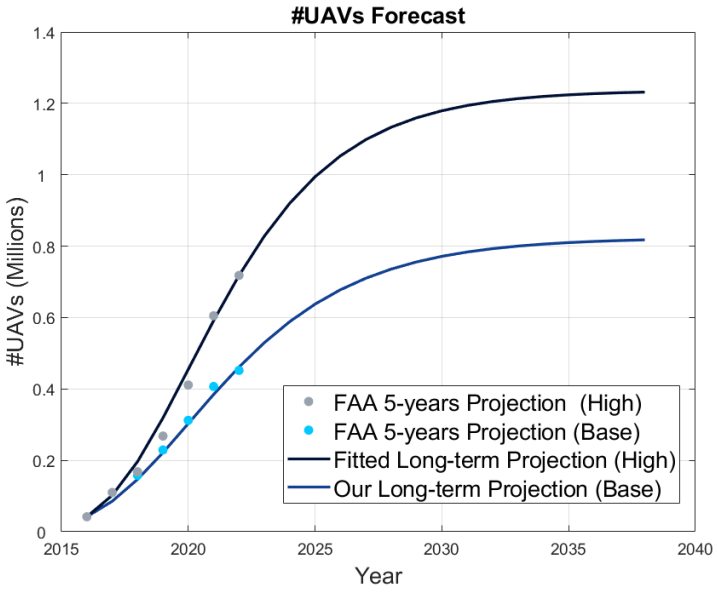

Fig. J.2: Projections for UAVs fleet size in the next 20 years, extrapolating FAA 5-years projection.

B. 20 years projections

The FAA in its recent forecast has released their expectations for the increase in the UAV's fleet for the next 5 years [11]. Because there are several uncertainties to be considered, such as fluctuations on economy and disruptive technological achievements, FAA provides two different projections: a "base" scenario, expected to be the most likely outcome, and the "high" projection, which embodies a high potential for UAVs given more sophisticated uses are identified and successfully deployed. They represent, respectively, 33 % and 46 % of cumulative year-on-year growth rates. These numbers were taken as reference and, by fitting them with a "S-shaped" Gompertz function, which has been proved a good model for mobile traffic projections [12], the projections are extrapolated for the next 20 years. Figure J.2 shows that, according to the long-term projections the fleet size is expected to increase from 5 to 7.5 times. In the high projection, the fleet exceeds 1.2 million UAVs around 2038. It is worth noting that these numbers represent a more agressive projection than the one provided by SESAR in November 2016, which projected 395 thousand commercial drones in the EU area for 2030.

Assuming that the increase of drones registered in each area is proportional to the national growing numbers, figure J.3 shows the CDF plots for the expected average and peak densities of drones in the air for the high growth

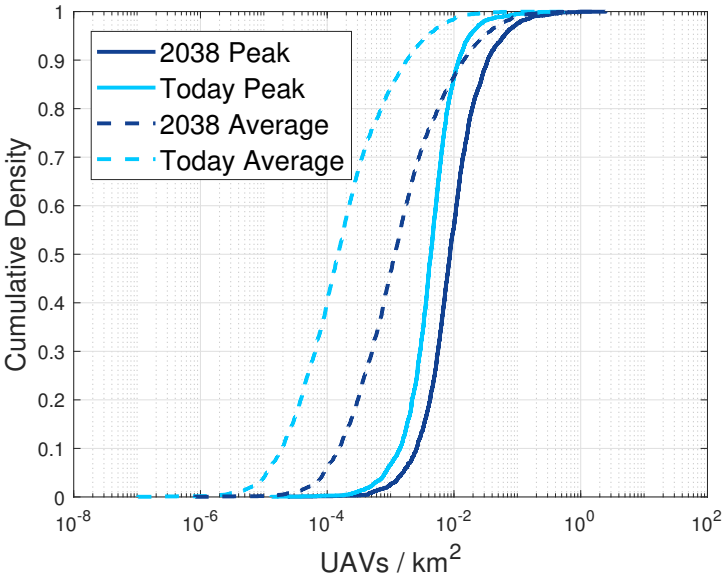

Fig. J.3: CDF plots for the average and peaks projected density of UAVs in the air for US Counties.

projection in 2038 in comparison with today's numbers. The peak density of drones, observed in New York County, is around 2.5 UAVs / km^2, while it is below 1 UAV / km^2 for the rest of the cases.

III Simulation Scenario

In order to evaluate the capacity of cellular technologies to provide connectivity for UAVs, system level simulations were performed, using a framework built to investigate user mobility with focus on the 3GPP LTE technology and that has been previously described in [9].

The scenario chosen for the simulations reproduces the settings of a real network deployment in 2018 in an area of 40 x 40 km centered in the city of Aalborg, Denmark's fourth largest city. The scenario choice was motivated by the fact that network data containing sites heights, locations and antenna patterns, was made available for a real LTE operator, which makes the results more realistic. Different site densities were simulated in order to investigate how a continuous deployment of sites can cope with the boost in connectivity demand from the UAV side. From the 100 sites available in the simulation area, two were enabled from the first simulation: one arbitrarily chosen in the

Table J.1: LTE Network Layout - Average Parameters

Parameter	Number of Sites			
	2	10	25	100
Site Height (m)	22.3	31.0	33.6	30.0
Downtilt (degrees)	6	4.6	4.6	7.2
Inter Site Distance (km)	25.0	10.6	6.3	1.9

Table J.2: Scenario Layout

Parameter	**Value**
Simulation area	40 x 40 km
Maximum number of sites	100
Number of sectors	3
Transmit power	49 dBm
Carrier frequency (MHz)	800 and 2500
MIMO configuration	2x2
Propagation Model	UAV Height Dependent Model [4]

center of the grid, and the other being the farthest from the first one. Then, continuously the next site enabled was the one that maximizes the inter site distance to the enabled set. Four different network sizes were evaluated: 2, 10, 25 and 100 sites, which correspond to site densities of 1 site for 800, 160, 64, and 16 km^2, respectively. For each case, four different LTE compatible bandwidths were evaluated: 1.4, 5, 10 and 20 MHz. Table J.1 shows the average parameters for the network data.

For these simulations, the C2 link between UAV and the network is modeled as a constant bit-rate traffic, with average throughput of 100 kbps and packet inter arrival time of 100 ms, in both, UL and DL directions. These values are based on 3GPP's requirements for UAVs' C2 traffic [3]. Informations about the network layout used in the campaign are described in Table J.2, whereas the open-loop power control mechanism used in uplink, whose parameters are listed in Table J.3, is implemented as described in [13]. Readers interested in more detailed simulation parameters can refer to [9]. It is worth noting that the transmitter antennas were not uptilted to provide coverage for the airborne UAVs. For the purpose of this paper it is assumed that the legacy cellular network infrastructure is used to minimize the installation costs, but a frequency band is reserved to the UAVs use case.

In our simulations, one UAV reaches outage if its throughput is below 100 kbps for a 50 ms window, which is the maximum transmission time of each C2 packet according to [3]. The reliability is defined as the number of UAVs that never reached outage divided by the total number of UAVs simu-

Table J.3: Uplink Power Control Parameters

Parameter	Value
Maximum Transmit Power	23 dBm
P0	-89 dBm per PRB
α	0.8

lated for the duration of 4000 C2 packets transmitted. UAVs were uniformly distributed in the simulation area at a constant height of 120 m, and their number gradually increased to elevate the system load until the C2 reliability fell below the 99.9 % [3]. The main goal of the simulations was to find the maximum capacity for each network deployment. The UAVs' height in the simulations was chosen to be compatible with the maximum allowed for flight in many countries as of the time of writing.

IV Results

No significant frequency dependent variations is expected between 800 and 2600 MHz for the height-dependent channel model [14]. Therefore the results obtained by simulating 800 and 2500 MHz bands were very similar. Fig. J.4 shows the maximum density of airborne UAVs achieved with a coverage reliability of 99.9 % for different bandwidths in the 800 MHz band.

Overall, simulations showed that due to the radio path clearance, the lack of signal is not a problem for flying UAVs even under very sparse networks. On the other hand, the good propagation conditions to several surrounding base stations causes a strong direct link interference, which is the main limiting factor for the system, as outlined in [9].

By loading up the network with more UAVs, the likelihood that two or more base stations are transmitting simultaneously in the same resources is increased, degrading the overall system signal to interference plus noise ratio (SINR). Therefore, the UAVs require more physical resources to transmit the same amount of data, and some users may get unserved if they are connected to a cell that runs out of radio resources. Increasing the bandwidth, not only provides more physical resources to the users, but it also decreases the likelihood of mutual interference, improving the overall SINR and therefore the spectrum efficiency. This last factor explains the nonlinear gains in system capacity provided by increases in the bandwidth. One example of such nonlinear gains are experienced when increasing the bandwidth from 1.4 MHz to 10 MHz for the most dense deployment case. This represents a 7 fold increase in the bandwidth, while the supported density increases from 0.0375 UAV / km^2 to 0.9375 UAV / km^2, a 25-fold increase.

On the UL, due to the power control mechanisms, the UAVs transmit po-

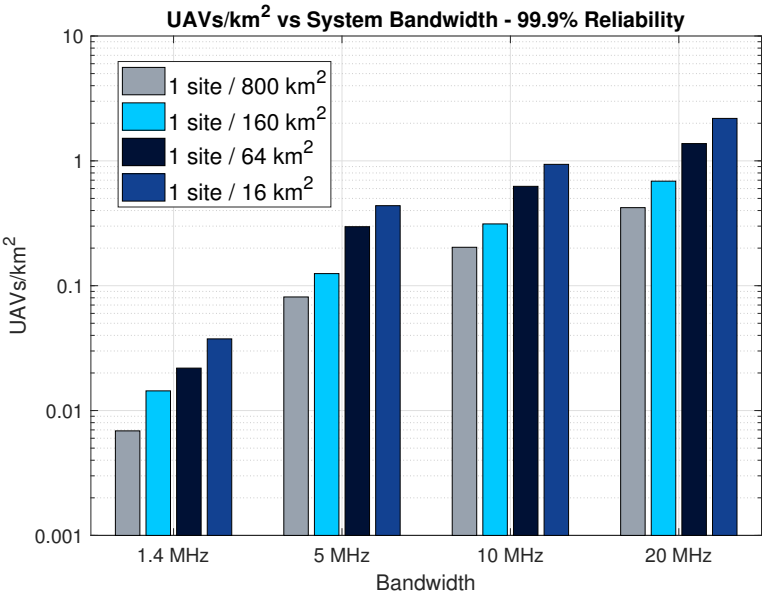

Fig. J.4: System capacity with 99.9 % of reliability per bandwidth and site density.

wer is, to a certain extent, proportional to their distances to the base stations. Therefore users close to the base stations transmit with less power, limiting the amount of interference radiated into the system. Because of this, the UL can handle more users before failing than the DL, which is the system's point of failure in the simulations. In all cases, the UL connection could be maintained above the 99.9 % reliability, when the DL failed to reach this requirement.

Although airborne UAVs cause interference to several base stations due to radio clearance [10], power control can be used to mitigate the overall interference increase observed on the base stations [9]. In other words, the UL power is kept at a level determined by the required SINR and the path losses, therefore there is no excess power radiated to the system. Whereas in DL users very close to the base station can experience a high SINR, beyond the point they can keep increasing the modulation and coding scheme for benefiting from it.

A. Current Spectral Requirements

By reserving 1.4 MHz of spectrum for C2 links, using a sparse setup with 1 site / 160 km^2, it is possible to offer coverage up to 0.014 UAV / km^2. Such service capacity would be capable of handling most of the scenarios under the assumptions of this paper. For reference, the peak density expected for

92.8 % of the US counties is below this capacity (fig. J.3).

Moreover, a gradual increase of the sites deployment can cope even with the most stringent assumptions for today's requirements. By increasing the site density to 1 site / 16 km^2, the system capacity increases to 0.038 UAV / km^2, which is above the peak demand projected for 99.8 % of US counties. The outliers, such as the one for New York county, may need a more optimized network or additional bandwidth. Section V discusses how the system efficiency can be improved, which could allow 1.4 MHz of bandwidth to provide enough capacity for this case.

In areas where site deployment and maintenance corresponds to a high cost, the number of required sites could be kept low by offering additional bandwidth. Such scenario would enable a gradual implementation of new sites, according to the increase of UAVs demand. For example, using a 5 MHz carrier, with just 1 site / 800 km^2, the system capacity observed in the simulations is 0.082 UAV / km^2, above the most dense network scenario simulated with 1.4 MHz. Increasing the dedicated bandwidth for UAVs relies on cost and availability of spectrum, especially considering that a 5 MHz spectrum would be underutilised given the current UAV densities.

B. Future Spectral Requirements

Results in fig. J.4 and J.3 suggest that the reservation of 1.4 MHz may not cope with the future demand in the most stringent scenarios. The projection shows that close to 9 % of the projected scenarios cannot be served with 1.4 MHz even for the most dense network simulated. However, with 5 MHz spectrum the peak demand projected by up to 99.6 % of the counties can be served. For the outliers, a higher bandwidth may be required or, alternatively, improvements on the spectrum efficiency. For instance, the demand projected for the New York County would require 20 MHz of spectrum. In denser areas, there is a high demand for radio connectivity from several types of services and applications, and for that reason, it can be impractical to allocate such high bandwidth for a specific service. Some of the aspects discussed in Section V can be further improved to mitigate the spectrum requirements for a dedicated frequency for C2 link.

V Discussion

In this section it is discussed which parameters can affect the results presented in Section IV. It is also presented features that can boost the network capacity and what are possible outcomes if there is a disruption in the density of airborne UAVs.

A. Dynamic Spectrum Allocation

In general, cellular networks do not use full capacity over a large area. In real deployments the network load is commonly around 10–30 % in the busy hours. But in some cases reserving resources for very large areas can affect negatively the overall network throughput. A modern strategy that are being envisioned to the future may be able to manage the spectrum allocation for UAVs, providing high reliability while being cost effective: dynamic spectrum allocation.

By dynamically reserving the spectrum in a large area, it is possible to protect the UAVs from undesired inter-cell interference. This can be achieved by monitoring the number of UAVs connected in an assigned area. Any time the interference reported by one of these devices increases significantly, the network can take two actions: increase the amount of resources reserved in the area, and/or expand the radius of the area where base stations are reserving these resources. This can prevent over-allocating resources, when the UAVs demand is very low, while providing reliable services regardless the fluctuations on demand.

B. System Improvements

In this paper, it is assumed that the transmitter antennae tilt and power was not optimized for the UAV use case. However, their optimization could lead to optimized SINR and therefore reduce the bandwidth/site density requirements. Moreover, the SINR could be further enhanced by interference management/suppression techniques. Techniques such as 3D beamforming, interference cancellation and directional transmission from the UAV side are expected to significantly improve the UAVs' SINR [9].

C. Dense Urban Scenarios

There is a caveat regarding the simulation for a very dense area like Manhattan. A more detailed model would be required to account for the tall buildings in this county. The presence of tall buildings can limit the LOS likelihood and therefore more interference insulation for the UAVs, reducing the amount of bandwidth required in comparison to the numbers presented in this paper.

D. Flight Take-off and Landing

It is important to note that, even though a very sparse network can provide connectivity for all airborne UAVs in a given area, it may face challenges in providing connectivity during the take-offs and landings phases. Cellular networks present one competitive advantage to solve this issue. They have

ubiquitous coverage and a hybrid solution could be designed to explore the legacy network setup. For example, UAVs could use the legacy network during flight start and termination, up to a certain height, until they are able to connect to the reserved C2 spectrum for airborne UAVs.

The UAV cruise height also is an important factor to be considered. In this paper, all UAVs were considered to be flying at 120 m. If some UAVs are flying at lower heights, they will observe and cause less interference in DL and UL respectively, therefore, the system capacity may be positively impacted.

E. Disruptive Solutions and 5G

Disruptive technologies and solutions can cause an unexpected boost in the number of UAV solutions. In the same manner, UAVs applications such as cargo delivery, may become a very important business once the BVLOS flight range is enabled for drones, and the average utilization ratio of the drone may go above the 3 take-offs per workweek.

If the average number of flights used in the projection increase by a factor of 15, from 3 per workweek to 9 per workday, the densest network scenario simulated could still provide connectivity for the demand projected by most scenarios. Some outliers, however, project a demand beyond the capacity observed in simulations. Advancements in the technology in the next 20 years can also provide a solution to these cases, without the need for additional bandwidth. For example, 5G technologies already provide some features that can improve the efficiency of the system, such as massive MIMO, 3D beamforming, on-demand power boost in the direct link and more advanced interference suppression techniques.

VI Conclusion and Future Works

This paper has discussed the usage of cellular networks to provide the C2 link for airborne UAVs in a dedicated portion of the spectrum. Both the infrastructure and the spectrum costs are expensive for a new network deployment. Depending on each specific case, the network design could start with a small bandwidth (such as 1.4 MHz) implemented in several sites, or with a larger bandwidth (5 MHz) implemented in fewer sites.

The paper also showed that a continuous deployment of resources, either by increasing the bandwidth reserved or the number of sites, can handle the increase in demand according to forecasts for the next 20 years, without the need to a very expensive implementation in the first moment.

Future work is being planned to investigate some of the challenges presented by having a sparse dedicated network, such as the initial and final

phases of the flight. Other works also will investigate how network parameters (antennae tilt and transmit power) can be optimized and interference management/suppression techniques implemented to boost UAVs SINR and therefore the system capacity.

Acknowledgment

This research has received funding from the SESAR Joint Undertaking under the European Union's Horizon 2020 research and innovation programme, grant agreement No 763601. The research is conducted as part of the DroC2om project. Authors would also like to acknowledge the contribution of Steffen Hansen and Daniel Kappers to the UAV flights.

References

[1] D. S. Ponchak, G. Church, E. Auld, and S. Henriksen, " A Summary of Two Recent UAS Command and Control (C2) Communications Feasibility Studies," in *2016 IEEE Aerospace Conference*, March 2016, pp. 1–11.

[2] GSMA, "GSMA Regulatory Position on Drones," Tech. Rep., August 2017.

[3] 3GPP, "Enhanced LTE support for aerial vehicles," 3rd Generation Partnership Project (3GPP), Technical Specification (TS) 36.777, Jan. 2018, version 15.0.0.

[4] R. Amorim et al., "Radio Channel Modeling for UAV Communication Over Cellular Networks," *IEEE Wireless Commun. Lett.*, vol. 6, no. 4, pp. 514–517, Aug. 2017.

[5] A. Al-Hourani and K. Gomez, "Modeling Cellular-to-UAV Path-Loss for Suburban Environments," *IEEE Wireless Commun. Lett.*, vol. 7, no. 1, pp. 82–85, Feb. 2018.

[6] B. V. D. Bergh, A. Chiumento, and S. Pollin, "LTE in the sky: trading off propagation benefits with interference costs for aerial nodes," *IEEE Commun. Mag.*, vol. 54, no. 5, pp. 44–50, May 2016.

[7] Qualcomm, "LTE Unmanned Aircraft Systems Trial Report," Qualcomm Technologies Inc., White Paper, May 2017.

[8] M. M. Azari et al., "Coexistence of Terrestrial and Aerial Users in Cellular Networks," in *Proc. IEEE Glob. Commun. Conf. Workshops*, Singapore, Dec 2017, pp. 1–6.

[9] H. C. Nguyen et al., "How to Ensure Reliable Connectivity for Aerial Vehicles Over Cellular Networks," *IEEE Access*, vol. 6, pp. 12 304–12 317, 2018.

[10] R. Amorim, H. Nguyen, J. Wigard, I. Z. Kovács, T. B. Sorensen, D. Z. Biro, M. Sørensen, and P. Mogensen, "Measured Uplink Interference Caused by Aerial Vehicles in LTE Cellular Networks," *IEEE Wireless Communications Letters*, pp. 1–1, 2018.

[11] Federal Aviation Authority, "FAA Aerospace Forecast, Fiscal Years 2018-2038," Tech. Rep., March 2018.

[12] I. Z. Kovacs, P. Mogensen, B. Christensen, and R. Jarvela, "Mobile broadband traffic forecast modeling for network evolution studies," in *2011 IEEE Vehicular Technology Conference (VTC Fall)*, Sept 2011, pp. 1–5.

[13] R. Mullner, C. F. Ball, K. Ivanov, J. Lienhart, and P. Hric, "Contrasting open-loop and closed-loop power control performance in utran lte uplink by ue trace analysis," in *2009 IEEE International Conference on Communications*, June 2009, pp. 1–6.

[14] R. Amorim, H. Nguyen, J. Wigard, I. Z. Kovács, T. B. Sorensen, and P. Mogensen, "LTE radio measurements above urban rooftops for aerial communications," in *2018 IEEE Wireless Communications and Networking Conference (WCNC)*, April 2018, pp. 1–6.

Chapter 6 - Identification of Airborne UEs

Some of the solutions presented in previous chapters discuss how the network-based solutions can benefit from distinguishing the terrestrial user equipment (UE) from airbone ones, enabling a different set of policies for each case. The present chapter shows the potential of autonomous detection of airborne users from the network side, and discusses how the detection of the different user classes can be performed within the network.

6.1 Problem Description

Throughout this work, advantages have been pointed out about the usage of public cellular networks to provide Command and Control (C2) service, such as the deployments cost and readiness to market. On the other hand, such networks are optimized for ground users and these poses interference challenges for the link reliability that have also been discussed in details in this work.

Because of these challenges, the implementation of case-specific technical solutions to enhance the link reliability are required. This means that the network can heavily benefit from upfront information of the airborne status of the user. The identification of airborne users may be performed in different ways, which are discussed in the next paragraphs that point some of their advantages and disadvantages. mission and beamforming.

6.1.1 UE Capabilities Information

During the initial registration process of the UE in the network, there is an exchange of messages between both, where the UE informs the network about their capabilities (Fig. 6.1). The UE responds a *UECapabilityEnquiry* message reporting all its capabilities coded within a *UECapabilityInformation* message [1].

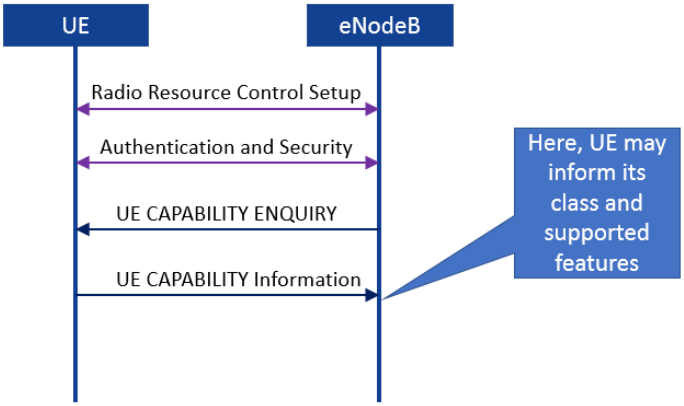

Fig. 6.1: Initial signalling exchange between UE and eNodeB. After initial setup, UE informs replies the capability enquiry with its capability information.

The capabilities include UE radio implementation details such as the UE category, bands supported, and their ability to support specific features, e.g. carrier aggregation, A4 reporting, long Discontinuous Reception (DRX) cycle, etc.

The *UECapabilityInformation* message can be used to inform the network that the UE modem is mounted on an aerial vehicle which requires high reliable C2 connectivity. Additionally, the UE may inform their capabilities in terms of Unmanned Aerial Vehicle (UAV)-specific performance enhancement techniques, that were aforementioned. This is an easy and smooth procedure, there are some caveats though, as this do not solve the problem completely.

The exchange of information takes place in the UE registration phase and it will identify the UE as one UAV. However, it does not inform when the UE connection request is not specifically related to C2 connectivity during flight missions. Assigning high priority for this UE will steer network resources in favor of it, in some cases this can be an unfair allocation of resources. For example, the user may be downloading new flight informations, loading new maps or downloading software/firmware updates, while still on the ground. Another example is the transmission of broadband uplink contents, such as media streaming, which does not need to be favored by the network. Moreover, to perform such operation, such identification content in the UE capability messages must be specified in the technological standards.

Table 6.1: QCI Definitions on 3GPP Standards [3] for Guaranteed Bit Rate Services

QCI	Resource Type	Priority Level	Packet Delay Budget	Packet Error Loss Rate	Example Services
1	Guaranteed Bit Rate	2	100 ms	10^{-2}	Conversational Voice
2		4	150 ms	10^{-3}	Conversational Video (Live Streaming)
3		3	50 ms	10^{-3}	Real Time Gaming, V2X messages etc.
4		5	300 ms	10^{-3}	Non Conversational Video (Buffered Streaming)
65		0.7	75 ms	10^{-3}	Mission Critical user plane Push To Talk voice
66		2	100 ms	10^{-3}	Non-Mission-Critical user plane Push To Talk voice
67		1.5	100 ms	10^{-3}	Mission Critical Video user plane
75		2.5	50 ms	10^{-3}	V2X (vehicle-to-everything) messages

6.1.2 QoS-based Setup

In modern cellular networks, the Quality of Service (QoS) classes are used to identify and address the minimum requirements necessary to satisfactory deliver the QoS for Protocol Data Unit (PDU) sessions. For complying with the requirements, the network may adapt its allocation policies, prioritizing certain services and tuning their performance enhancement features.

The concept has been widely discussed for Third Generation Partnership Project (3GPP) technologies. In 4G Long-Term Evolution (LTE) and LTE-Advanced (LTE-A) networks, the QoS Class Identifier (QCI) is used as a way to differentiate the different type of services according to their priority, maximum acceptable delay and packet error loss [2]. Table 6.1 shows the current definitions for guaranteed bit rate services presented in 3GPP standards [3]. It is worth noting that QCI 3 and 75 already defines a bearer with current requirements that resembles those set for the C2, for delay and reliability, however they are preceded by other services, such as conversational voice, in terms of priority. Given it is a critical link which is related to the service of the flight applications it could have a high priority in the scheduling of physical resources. On the other hand, video streaming from UAVs does not require high priority and should be preceded by the C2.

Currently, though, LTE operators seldom set many QCI values to be used with different services in practice. Most services are managed by a "best-

effort" policy and non guaranteed bit rates (QCI 6 to 9), whereas Voice over LTE (VoLTE) is set over QCI 1. For the UAV case, the operator would be required to set a QCI value for the C2 link, for example QCI 75, set for vehicular services and that the service can be identified in its setup phase.

Network Virtualization

In 5G, the QoS definitions follow a similar principle but has evolved into a flow-based QoS, where the packets are classified and marked with a QoS Flow Identity (QFI). The classification may concern the source/destination address, the type of traffic or others [2]. This provides more flexibility allowing, for example, that the traffic between controller and UAV are prioritized according to a QFI following a special user subscription.

Because of this flexibility in 5G, this solution sounds more practical in future applications, enabling a more manageable use of network virtualization. For example, this can be used to create a virtual network for users connected to the Unmanned Aircraft System Traffic Management (UTM), based on the source/destination of the IP packets. The virtual network created exclusively for UAVs can implement settings and policies that enhance the performance of the C2 link, while protecting it from interference originated from the load caused by other users in the network.

C2 Identification in 3GPP's standards

In 2019, in the final months of the present research, the 3GPP's has opened a study item for the specification group at the stage 2 for enhancements envisioned for UAVs applications, regarding its release 17. In the initial discussions, the identification of the C2 QoS in the 3GPP architecture is paramount for a successful integration of the UTM services to the Radio Access Network (RAN) [4].

The document cites, among the list of potential new requirements, that, for example:

The 5G system shall provide a mechanism to allow UTM to provision traffic parameters e.g. traffic flows, traffic types, of C2 communication associated to the same or different application, and request differentiated QoS accordingly.

— 3GPP, TR 22.829, March 2019 [4].

The identification of the UAV height and the heights separation are also being discussed, envisioning the enhancement of the QoS policies. This can be achieved, for example, based on the interconnection with the UTM.

6.1.3 Autonomous Identification of airborne UAVs

The aforementioned methods are simple and effective, but require some level of standardization in the technologies. As another possible drawback they

are not able to identify airborne modems that are being used for broadband services instead of C2 connection. For example, it can be either a camera associated with its own cellular subscription, or a regular terrestrial modem is experimentally placed by a user onboard of a flying UAV. In such cases, knowing the airborne status of the user can provide benefits from the perspective of the resource management policies used by the network.

There is another way of performing the identification of the airborne status is by means of autonomous identification which can be performed in different ways:

- altitude sensors coupled to the modem;
- radio measurements based decision;
- machine learning;
- or ideally a combination of the aforementioned methods for mitigating the chances of wrongful detection.

The decision based on radio measurements evaluate some of the radio reports collected and/or transmitted by the phones trying to characterize the environment either as terrestrial or aerial. for example, this can be done by comparing the expected distribution of the interfering cells in the power domain at terrestrial level to the current profile observed by the UAV.

In some cases, though, it may be difficult for the network engineer to establish the threshold intervals and which measurements are actually significant for detecting the airborne nature of the user. For these, machine learning classification algorithms can be trained with the measurement data and provide a decision-making tool for differing airborne and terrestrial users.

Examples of autonomous identification of airborne users are experimented and analyzed in this chapter. The results mentioned hereafter are not exhaustive and provide just an indication of the potential of such applications. It is the author's understanding that a whole dedicated thesis could be produced to cover all the aspects related to autonomous identification, and the extensive collection of data to test the proof of concept in several scenarios.

6.2 Papers Included

Paper K. Machine-Learning Identification of Airborne UAV-UEs Based on LTE Radio Measurements

This paper utilizes three different machine-learning techniques to perform the identification of the airborne users in the network. The input features are

constrained to standard LTE measurements, such that the solution emulates a tool that could be deployed at application level, without requiring any modification in the firmware or hardware of the legacy UEs.

The dataset is compound by measurements collected over LTE networks in a rural location at five different heights: 1.5, 10, 25, 50 and 100 m. The paper addresses the implications of false positives and false negatives and how they can impact the perceived performance of this classification algorithms. Regarding these aspects, a discussion is followed about the accuracy of the algorithms, and how the designer can fine tune the algorithms to privilege either their sensibility or the sensitivity, according to the problem specifications.

Paper L. Method for Detection of Airborne UEs Based on LTE Radio Measurements

The paper presents an algorithm that classifies UEs into either aerial or terrestrial, based on LTE radio measurements. The idea behind the algorithm is to apply a detection function that can be conversed into LTE Events, i.e., that can be objectively measured by the UE and reported back to the network following certain pre-conditions.

In the paper, the detection function is optimized locally for different measurements in a rural scenario over two different live operators. The optimization is used to increase the detection rate, while minimizing the false alarms observed in the classification phase. The set of data samples are collected over terrestrial heights and four different airborne heights (15, 30, 60, 120 m).

6.3 Main Findings

6.3.1 Promising potential for radio identification of airborne users

Both papers have demonstrated a promising potential for identifying airborne users based on the radio measurements. The summary for the specificity, the capability of avoiding false positives in identification of airborne devices, and sensibility, the capability of avoiding false negatives, are shown in Fig. 6.2.

Across the different measured scenarios and detection algorithms used, the results for the correct detection probability were kept above 95% in most cases, demonstrating the usage of radio measurements present potential to be used for identifying airborne devices.

6.3.2 Solutions must be optimized locally

It is worth noting that the performance difference observed in the different scenarios are related to the specificities of each case. In Scenario 1 the set of measurements are collected through 4 different routes that sample a range of 3.5 km by a cellular phone connected to a single operator. In Paper K these measurements are presented to machine learning algorithms as it seems linear separation cannot be used with such high accuracy. The reason behind that is that linear separation is more easy to treat mathematically when two (or three) features are used for the classification of the samples, as it is easier to visualize and derive a line (or plane) separating the classes than a hyperplane in a multidimensional space. Fig. K.1 shows that, in scenario 1, the separation based on a few features do not perform so well.

On the other hand, in Scenario 2, presented in Paper L, a measurement scanner is used for sampling two different operators in a different measurement location. This set of measurements responded very well to the linear separation, indicating just a few features, namely the serving cell Received Signal Strength Indicator (RSSI) and serving and first neighbor cells Reference Signal Received Power (RSRP), can be used to linear separate the samples.

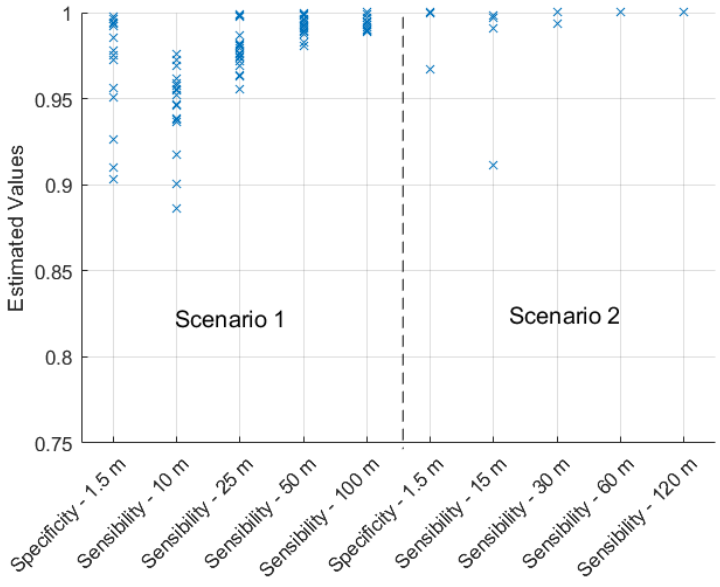

Fig. 6.2: Summary of Sensibility and Specificity results measured in Papers K (Scenario 1) and L (Scenario 2)

.

A drawback, though, is that the usage of RSSI in the detection algorithm would require a significant higher data collection for real world applications, as this feature is intrinsically related to the instantaneous load observed in the network.

Moreover, in Paper L, the cross-validation of the separation lines obtained for each case have showed that the classification performance degrades when the separation line is applied over different locations/operators (see Table L.6).

Therefore, although there is promising potential for developing identification methods for airborne devices based on radio measurements, those must be optimized locally, regarding the network settings and deployment, as well as the usual load conditions observed.

6.3.3 Results improve with height increase

The results in Fig. 6.2 indicate that at lower heights, for example below 25 m, the detection of airborne devices is less accurate, while it improves considerably as the UE moves up. At 100 m, the detection algorithms can accurately identify the radio characteristics of the measured scenario, which tends to be fundamentally different from those observed at ground level.

Also, because of the uniqueness of the scenario, at higher heights the number of features required to be mapped for a more precise detection of the airborne devices in the network is also reduced, as depicted in Fig. K.1

6.4 Discussion

The results provided in this Chapter indicate that there is a potential for identification of airborne users based on radio measurements. But there is a drawback associated with the fact that the algorithm may require a large dataset collected locally to be correctly optimized.

These algorithms can be used in combination with other methods, such the ones provided in Section 6.1. Additionally, other solutions may also be used, such as cellular positioning algorithms [5] or exchange of information with the UTM.

Is is recommended that amidst these options and eventually other novel ones, the identification of airborne devices shall be considered in the next phases of cellular technology standards, as this information opens up several possibilities for performance enhancement on the network side. As an example, the next subsections provide a non exhaustive list of ways the network can benefit from the airborne status of the UAV.

References

[1] 3GPP, “Radio Resource Control (RRC); Protocol specification ,” 3rd Generation Partnership Project (3GPP), Technical Specification (TS) 36.331, Dec. 2018, version 15.4.0.

[2] Airbus, “Quality of Service in 4G/5G networks,” Airbus, White Paper, Apr. 2017.

[3] 3GPP, “ Policy and charging control architecture ,” 3GPP, Tech. Rep. TS 23.203 V15.14.0, Jan. 2019.

[4] ——, “ Technical Specification Group Services and System Aspects; Study on Enhancement for Unmanned Aerial Vehicles; Stage 1 ,” 3GPP, Release 17 TS 22.829 V1.0.0, Mar. 2019.

[5] J. Medbo, I. Siomina, A. Kangas, and J. Furuskog, “Propagation channel impact on LTE positioning accuracy: A study based on real measurements of observed time difference of arrival,” in *2009 IEEE 20th International Symposium on Personal, Indoor and Mobile Radio Communications*, Sep. 2009, pp. 2213–2217.

Paper K

Machine-Learning Identification of Airborne UAV-UEs Based on LTE Radio Measurements

Rafhael Amorim, Jeroen Wigard, Huan Nguyen, Istvan Z. Kovacs and Preben Mogensen

The paper has been published in the
IEEE Globecom Workshops 2017.

© 2017 IEEE
The layout has been revised and reprinted with permission.

Abstract

The overall cellular network performance can be optimized for both ground and aerial users, if different treatment is given for the two user classes. Airborne UAVs experience different radio conditions that terrestrial users due to clearance in the radio path, which leads to strong desired signal reception, but at the same time increases the interference. Based on this, one can for instance use different interference coordination techniques for aerial users as for terrestrial user and/or use specific mobility settings for each class. This paper compares three different classification algorithms, which use standard LTE measurements from the UE as input, for detecting the presence of airborne users in the network. The algorithms are evaluated based on measurements done with mobile phones attached under a flying drone and on a car. Results are discussed showing the advantages and drawbacks for each option regarding different use cases, and the compromise between specificity and sensibility. For the collected data results show reliability close to 99% in most cases and also discuss how waiting for the final decision can even improve this accuracy to values close to 100%.

I Introduction

A swarm of small and medium sized Unmanned Aerial Vehicles (UAVs) is expected to take on the airspace in the next few years. A PwC report has estimated a potential market value of drone powered solutions at $127 billion [1].

From cellular networks perspective, it represents an emerging source of new subscribers: they might provide the flight control link between operators and UAVs and/or data payload links, which can be used for different services such as surveillance footage and search and rescue missions, telemetry from monitoring applications, relaying data for ground users in areas affected by disasters and others. Looking at this potential, at the time of writing, the 3rd Generation Partnership Project (3GPP) is holding standardization activities within a study item on enhanced support for aerial vehicles [2].

Cellular networks are designed and optimized to provide coverage for ground users. But field measurements have shown that the propagation environment observed by UAVs differ from that experienced by ground users [3,4]. A height-dependent propagation model was presented in [4], where measurements show the radio path losses tend to approximate free space losses as the UAV moves to heights above 60m. At heights around 100m, radio line of sight ranges can extend to tens of kilometers due to radio path clearance. As a consequence, interference levels for UAVs are expected to be very high, compromising the reliability of the radio link [5]. It can also lead to inefficient use of radio resources or even to harmful level of interference added to

the network, requiring much more complex interference mitigation solutions. For instance, coordination schemes for aerial users are expected to involve a very high number of sites over a larger area, when compared to the solutions deployed for terrestrial users [6]. On top of that, handover parameters might also be optimized to better exploit the radio propagation characteristics.

Applying solutions optimized for UAVs to all users in the network is not desirable though, as the number of ground users in the network vastly outnumber the number of expected flying UAVs. However, if the network is able to identify the different classes of User Equipments (UEs), it can apply different settings for UAVs and ground users. There are two ways of performing such identification: direct reporting or aerial users discovery. The first could be achieved through the design of special modems that have the capability of self-reporting or through interconnection between the network and airspace management solutions. It is our understanding that one cannot rely solely on this, because legacy equipment (cameras, sensors, phones, etc.), that are not capable of reporting their ground/aerial status, can be attached by a regular user to the UAV. The second identification method - network discovery of aerial users - is the focus of the present work. Aiming at backward compatibility, it is assumed throughout this paper that this task must be performed by base stations that do not have access to any information other than the standard LTE radio measurements regularly exchanged between networks and (UEs).

In this paper, the suitability of three different machine learnings (ML) techniques (Support Vector Machines (SVM), Multi-Layer Perceptron (MLP) and Bayesian Estimators) to address this problem is investigated. The focus is not comparing these methods in details, as this has been extensively addressed in previous works [7]. The main goal in the present work is to address the feasibility of airborne users detection and to discuss which method presents the best approach for the different use cases. Currently drawing significant attention of the research community, deep learning techniques were left out of this paper, due to the relatively small number of features and samples available from the measurements, which compromises its performance gains compared to the other ML techniques, despite requiring more computational complexity.

The remainder of this paper is organized as follows. Section II briefly describes the algorithms used throughout the paper. Section III and IV present, respectively, the setup used for collecting the data samples used in this paper and the metrics adopted to evaluate the classification algorithms. They are followed by the results discussion in V. At last, Section VI wraps-up the paper with the conclusion and discussion of the findings.

II Review on Classification Algorithms

Throughout this section, there are brief descriptions, regarding the space constraints of this paper, of each method, altogether with source references that can provide more detailed explanation. The radio measurements to be presented in Section III are split in two datasets: training and testing. The training dataset is used in the ML "learning" phase, while the testing is used to emulate how accurate the algorithm would perform when tested against unknown samples (training phase).

The ML algorithm most suitable for each use case depends on several metrics: accuracy, convergence speed of training phase, complexity of testing phase, required information and others, which are briefly presented here for each algorithm.

A. Support Vector Machines

Proposed in [8] SVM is a machine-learning algorithm commonly used for many classification problems. It constructs a surface (hyperplane) that separate the two classes. If a linear hyperplane is not enough to separate the classes, a “Kernel trick” [9] can be applied to create nonlinear classifiers into high-dimension space. The support vectors are the training samples that lie nearest to the max-margin hyperplane built between the two classes.

During the training phase, if the samples cannot be completely separated, a penalty is considered for misclassifications (samples lying in the wrong side of the boundary). The magnitude of penalties scores can differ from the different classes, and this property will be later used in this paper.

SVM generalization capacity does not require a very large number of samples, nor similar size training sets for both classes and also have the advantage of a converging convex optimization problems with no local minima [10]. On the other hand, SVMs present high computational complexity on training and test phase, that increases quadratically with the number of training samples and support vectors [10]; they cannot also learn online with new examples, i.e., during the operation phase of the algorithm it cannot learn changes in the patterns of classes inputs. As cellular networks are very dynamic, i.e., are subject to new base stations deployments, optimization changes and others, scenarios can change considerably over time, but if the ML solution cannot learn online, a new ML solution - and therefore a new training phase - is required.

B. Multi-Layer Perceptron (MLP)

A multilayer perceptron [11] is a feedforward neural network composed of multiple layers (input, one or more hidden and an output layer) of nodes.

Each node, also called neuron, has one activation function that converts its weighted inputs into an output. The information is then feedforwarded to the next layer. The neurons are fully connected, which means each node in one layer is interconnected to all nodes of the next layer. There is no connection between neurons in the same layer.

In the input layer, the number of neurons is equal to the number of features in the data, and each feature is connected to a different neuron. After the calculation of the activation function is performed in the input layer, the information is forwarded to the first hidden layer. The process is carried subsequently, until the output layer receives the information from the outer hidden layer. Usually, each output neuron represents a class, and the neuron with the highest activation function represents the "winner" class.

The MLP is initiated with weights and biases randomly assigned. During the training process, the samples are presented to the MLP in a random order, and after each example, the error between the expected output and actual output for that example is calculated, and backpropagated through the network to adjust the weights and biases. The process continues iteratively for several epochs (one epoch corresponds to the MLP being presented to all examples available in the training set). Throughout this paper, MLP were built with a single 20-neurons sized hidden layer, and 3000 epochs of training.

If MLP can avoid local minima in the training phase, it usually shows high accuracy in the classification process when compared to other ML algorithms. It also has a low-complexity test phase and fast decision process. However, due to its learning process, MLP depends heavily on the training set size and distribution. It is higly subjected to overfitting (specialization on one small region of the subspace) [12]. For example, the generalization capacity can also be compromised if the training set of one of the classes heavily outnumber the other. Its training phase also is significantly complex and very slow. Despite these drawbacks, this training method allows online training, which is a significant advantage for the dynamic environment of cellular networks.

C. Bayesian Classifier

The Bayesian classifier [13] applies the Bayes' theorem over the data distribution to classify its samples. The sample is attributed to the class that maximizes the a posteriori probability $P(C_k|\mathbf{x})$ of a given vector of features, $\mathbf{x}$, belonging to a class C_k. Using the Bayesian theorem:

$$\arg\max_k \left(P(C_k|\mathbf{x})\right) = \arg\max_k \left(\frac{P(C_k)P(\mathbf{x}|C_k)}{P(\mathbf{x})}\right) \tag{K.1}$$

As the probability of the evidence $\mathbf{x}$, $P(\mathbf{x})$, is independent of the class being assessed, it suffices to look for the class k that maximizes the product $P(C_k)P(\mathbf{x}|C_k)$, where $P(C_k)$ represent the a priori probability of the class C_k,

e.g., in a uniform distribution, all classes have $P(C_k) = 1/k$ for all classes. The likelihood $P(\mathbf{x}|C_k)$ is estimated assuming it follows a multivariate Gaussian distribution, whose mean and covariance estimators are obtained from the training data.

Once a given distribution is assumed, the parametric approach of the bayesian classifier create results that can be interpretable by network engineers and help in the selection of optimum parameters for each case. It also has low cost training and classification phases. It also generalizes well with few training samples, but it generally tends to offer lower accuracy than the other two methods and the parameters cannot be updated online. However, the ouput of the bayesian estimators can be weighted by changing the a priori estimation of probabilities, which can give some space for later refinements, as will be discussed later in this paper. Also, the classification output depends on far less parameters, and those can be conveyed to the users so they can perform the identification of their own status and avoid excessive radio report exchange loading the air interface.

III Measurements Campaign

To collect data from airborne and terrestrial UEs for our classification, a measurement campaign was conducted in a rural location at Northern Denmark. The surrounding area is relatively-flat, with terrain profile variation from 15 to 35 meters, with small hills up to 80 meters of altitude. The measurements were performed by QualiPoc[1] Android smart phones, attached to the 800 MHz LTE carrier of a live Danish operator. The reports saved by the phone include metrics as defined by technology standards [14], such as RSRP (Reference Signal Received Power) and RSSI (Received Signal Strength Indicator) for the serving cell. Additionally, RSRP measurements are also included in the reports. The actual number of neighbor cells reported depends on how many cells can be rightfully decoded by the phone. The signal-to-noise ratio (SINR) threshold values observed for this detection in the measurements is around -20 dB

The airborne data was collected by attaching the measurement device underneath a commercial UAV. The Danish regulation for UAVs requires the pilot to keep the drone in constant visual line-of-sight (VLOS). To comply with this rules, the UAV is flown in 4 different rectangular routes, each with the long edge ranging from 0.45 to 0.75 km. The four routes form a line of 3.5 km length, and the distance between routes is around 300m. The height dimension was sampled at 4 different levels: 10m, 25m, 50m and 100m, measured from ground level at the take-off point. This sampling allows an inves-

[1]More information about the Qualipoc software in https://www.rohdeschwarz.com/us/brochure-datasheet/qualipoc_android/

tigation of at what heights the algorithms starts to produce reliable detection results. The ground data was collected by performing a drive-test with the phone in the roads surrounding the areas of the selected routes.

IV Evaluation Metrics

The task of the identification algorithm is to identify the airborne users. Classification algorithms will analyze the radio measurements and triggers a "positive" if the user should be flagged as airborne or a "negative" if the user is not classified as being airborne. The performance evaluation on the algorithm relies on comparing the classification with the real status of the user (see Table K.1).

Table K.1: Classification Outputs

Real-World User Status	Classification Label	
	Non-Airbone	Airborne
Ground UE	True Negative (TN)	False Positive (FP)
Airborne UE	False Negative(FN)	True Positive (TP)

If a real airborne UE triggers a positive, this output is a True Positive (TP), if not this is a False Negative (FN). The sensibility, *Sens*, of the algorithm measures how good it is in identifying airborne users:

$$Sens = \frac{TP}{TP + FN}. \tag{K.2}$$

The higher the sensibility, the fewer the number of airborne users undetected by the algorithm. Setting a very low-identification threshold for airborne users tend to increase the sensibility, as most of the samples will be classified as airborne. However, the clear majority of users in the network are ground users, and if the network uses this classification to apply different settings to users identified as airborne, it is important to minimize the number of users penalized. The specificity, *Spec*, measures how good the algorithm can recognize ground UEs, avoiding false positives outputs (FP) and hitting true negatives (TN):

$$Spec = \frac{TN}{TN + FP}. \tag{K.3}$$

There is a trade-off between *Spec* and *Sens* and the evaluation algorithm must consider that. In this case, as the number of ground users is much higher, it is important to keep *Spec*, as close as possible of 100%, to avoid the false-positive [15].

V Results

Table K.2 shows the number of data samples collected from the measurement campaign described in Section III, divided in two datasets: Ground samples and Airborne samples. It also shows the percentage of reports according to the distribution of number of detected cells, N.

It is important to acknowledge that due to the nature of the experiment the number of ground samples available are outnumbered by the airborne ones, which is not expected if these algorithms are applied in most networks, as ground samples are easier and cheaper to collect. The impact of the distribution of the data samples will be assessed in this paper.

All measurements are mixed in a single set, and 10% of the samples, randomly selected, are assigned as training dataset. The remainder of the samples, called testing dataset, is presented to each algorithm to be assigned to a class: airborne (Positive) or non-airborne (Negative) and *Sens* and *Spec* are calculated. Unless stated otherwise, the a priori distribution between the two classes is considered uniform, although this is a simplification of the problem, it serves as a starting point for the evaluation of the classification algorithms.

Table K.2: Dataset Breakdown

Trial	**Ground Samples**	**Airborne Samples**			
		10m	**25m**	**50m**	**100m**
# of Samples	1535	1727	1463	1328	1404
$N = 0$ **(%)**	3.3	9.9	15.2	8.4	4.0
$N = 1$ **(%)**	7.1	2.0	1.3	1.2	1.9
$N = 2$ **(%)**	15.1	3.7	2.8	2.8	4.0
$N = 3$ **(%)**	22.6	14.1	7.4	5.3	8.0
$N = 4$ **(%)**	18.2	10.8	11.4	10.5	7.9
$N \geq 5$ **(%)**	33.8	59.6	61.9	71.9	74.2

Previous results have showed that RSRP of serving and neighbor cells tend to get closer to each other in the power domain as the UE moves up ([6]). Table K.2 also shows that the number of neighbors increases with height. In this paper the ML algorithms are tested using samples with M features are compound by: RSSI, the serving cell RSRP, and RSRP of $M - 2$ neighboring cells.

A. Dependency on Number of Features

The first important point is about the suitability of ML detection methods of airborne users based on radio measurements. In Fig. K.1 it is showed the

results obtained by the algorithms for inputs with 3, 5 and 7 features. Results show that it is possible to achieve values of *Sens* and *Spec* above 98% for most configurations. It is possible to see that the higher the number of meaningful samples, the better the algorithm perfomance. This is expected as the higher dimensionality helps the algorithms to define the edges of each class (airborne or ground). With 7 features, i.e., with information on the RSRP of 5 neighbors, all three algorithms show sensibility above 99.8% for all heights equal or above 25m. UAVs are expected to fly at heights between 60-120m, but this result shows that an early detection is possible and settings can be tunned in the network before the UAV starts to create significant interference impact in the network.

On the other hand, increasing the number of features also leads to a longer decision time. In Table K.2 it is possible to see that only 33.8% of ground samples have 7 features available. All the other 66% of samples had to be discarded from training and testing phase. In real scenarios, these defective samples would not be useful, and therefore longer waiting times would follow: the network has to wait until one measurement report with all features available is received. In denser and loaded scenarios this can become a problem if the number of detected cells is capped by degraded SINR. The investigation in the next subsections were performed by using the 5-features space.

In Fig. K.1 one can also see that the MLP was outperformed in *Spec* by the other two algorithms in all cases, while produced better results for *Sens*. Due to the nature of the training phase, the network tends to specialize more in the regions of the subspace with more dense distribution of examples. As the number of airborne samples collected is higher than the number of ground samples (See Table K.2), this network is specializing in detect airborne UEs. For real deployments, an uneven distribution of the samples between the classes is expected, as currently is much easier and cheaper for cellular networks collect radio measurements from ground positions than from airbone positions. This can cause some problems of generalization for this solution. In the next subsection we show how the performance can be improved by changing the distribution of collected datasets.

B. Training Set

In this subsection, the training set uses a weighted distribution in order to obtain a more uniform distribution of samples between the two training datasets. The weighted distribution considers that ground samples are four times more likely to be drawn than any other sample from the other heights, which compensates the fact ground samples are approximately one fourth of the total number of airborne's (Table K.2).

Fig. K.2 shows the results obtained by using this weighted distribution

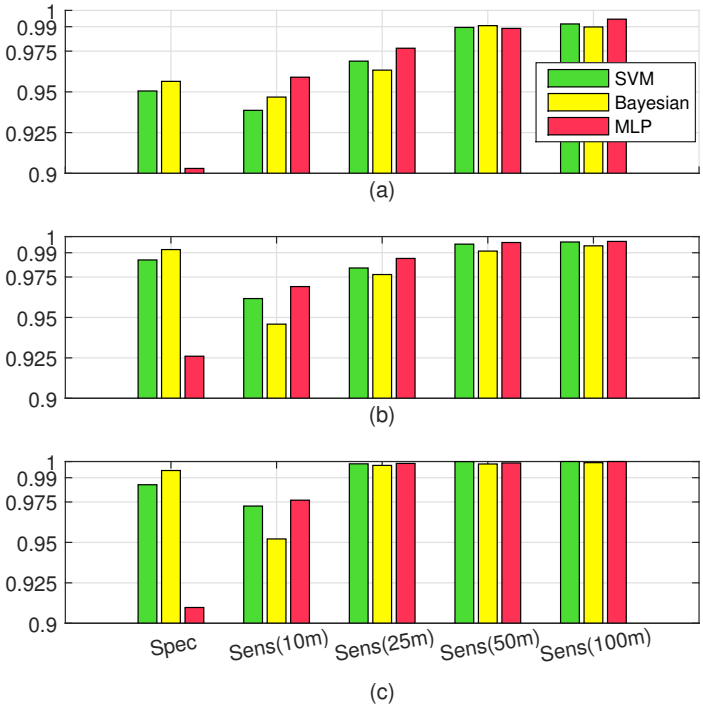

Fig. K.1: Baseline result using samples with M-features. (a) M=3, (b) M=5, (c) M=7

improves significantly the performance of *Spec* for MLP (from 93% to 97.5%). On the other hand, it has reduced slgihtly its *Sens* response: from 99.5% and 99.7% at 50 and 100m, to 99.2% and 99.4%, being slightly outperformed by the SVM for these two heights. It is interesting to note that the other two algorithms did not present considerably change in their results, indicating, as expected, that they are not very sensitive to variations in the dataset distributions.

Depends on the dataset available network planner might lean to different solutions. If the examples are uneven balanced Bayesian or SVM estimators show better generalization capacity. However, if the intention is focusing on one of the metrics, MLP can be chosen and the collection of samples for the training set designed to achieve a good compromise between generalization and specialization.

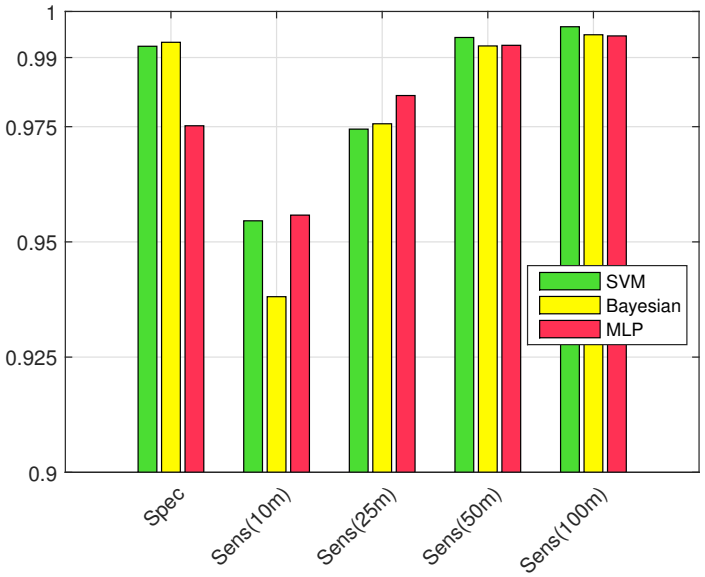

Fig. K.2: Classification output using 5-features space, with ground samples as likely to be selected to the training set then airborne samples.

C. A priori probability

In the previous section, it was showed that MLP can specialize more in one class than in the other, regarding how samples are presented in the training phase. Generally, it is considered a drawback, but it can be used in favor of the network, if it is assumed that the correct detection of one class has to be more reliable than the other. For instance, ground users currently outnumber airborne users by far, it can be used to avoid the false-positive paradox. For the other two solutions, there are also options for tuning results in favor of one of the classes. It can be achieved by assigning different a priori probabilities, $P(C_k)$, to the airborne and non-airborne classes for the Bayesian estimator, redefining the boundaries between the classes. These a priori probabilities, can also be used to construct an uneven cost function for misclassification during SVM training phase.

To illustrate this, the classifier algorithm was evaluated using the same parameters of those in Fig. K.2, with modifications in the a priori probability for non-airborne and airborne classes priorly assumed uniformly distributed, i.e., 0.5 for each class. After modification, probabilities were respectively set to 0.75 and 0.25 for ground class and airborne class (case 1) and to 0.9 and 0.1 (case 2).

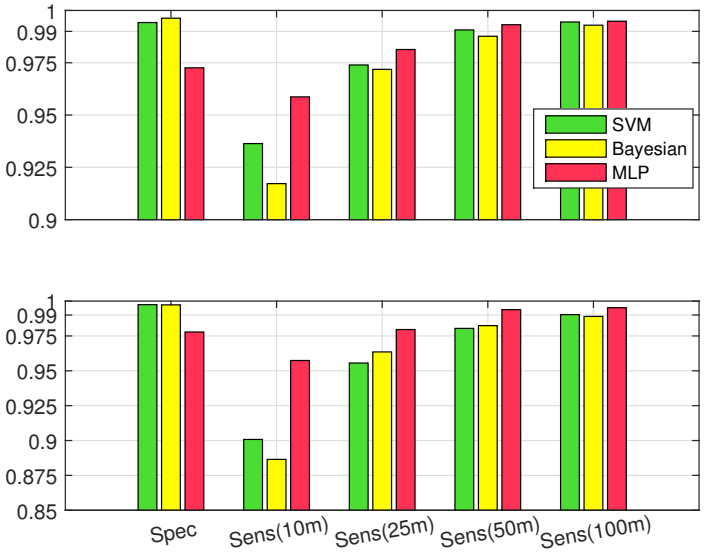

Fig. K.3: On top: classification using uneven a priori probabilities for airborne and non-airborne classes (top: 0.25 and 0.75; bottom: 0.1 and 0.9)

Results, in Fig. K.3, show that it is possible to obtain improvements in specificity with such modifications in the a priori probabilities. *Spec* goes from 99.2% (SVM) and 99.3%(Bayesian) to 99.4% and 99.6% in case 1 and 99.7% (both algorithms) in case 2. But, as expected this gains in *Spec* comes with a compromise of *Sens* (going down from 99.7% and 99.4% to 99% at 100m). The advantage of the Bayesian system is that these a priori probabilities are used later on the estimation phase and are not part of the tuning of the parameters in the training phase. It gives space for artificial tunning on classes boundaries later, if scenario changes or if network focus is shifted towards one class or other. For SVM, such changes would require the setup of a new set of support vectors, increasing significantly the cost and time of such changes.

With learning parameters properly set, the MLP can still learn online with the new examples, and automatically adjust to changes on the environment, without the need to manually set such changes or recalculate the entire classifier system.

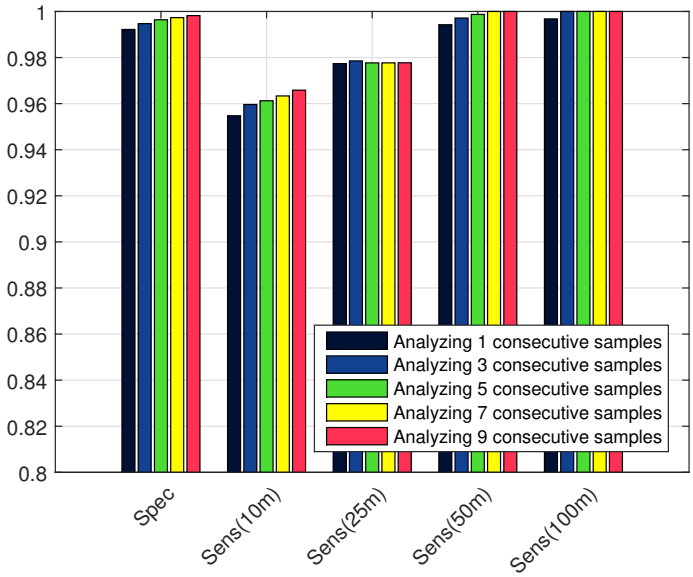

Fig. K.4: Classification by temporal decision of consecutive samples using the SVM classifier.

D. Majority Decision over temporal samples

Another way to improve the accuracy of the decision, is to gather information from consecutive temporal samples, before deciding if a user should be classified as airborne or not. A decision scheme was created where the algorithm evaluates X consecutive samples in the testing set, and then assigns the user class based on the majority of "votes". The SVM was chosen as an example, the other algorithms were left out in regard to the space constraints of this paper although the results can be extended for them, as they presented similar pattern.

Results are showed in Fig. K.4. It is possible to observe that although the reference value for specificity was already high for 1 sample case (99.2%), a few basis points were gained by the extra information gained by the additional samples (up to 99.8% with 9 samples). While *Spec* was kept very high, higher gains were obtained in sensibility levels, improving the accuracy of the decision. By waiting 9 consecutive samples it was possible to achieve 100% at 100m, 100% at 50m and 97.7% at 25m and 96.6% at 10m.

VI Conclusion

Throughout this paper we investigated how different supervised learning algorithms can be used to identify airborne users in the network based solely on LTE radio measurements. The study indicated that the identification could be performed using a relatively small number of training samples. This is an important point of this feature, regarding the data collection and training should be done locally at the base stations. Further research is also indicated, in order to check if the results found in this paper can generalize for different networks density, terrains and cell locations.

The Bayesian estimator, which is rather simple, is capable of providing reasonable separation of the data, and can be tuned by changing the a priori probability of the data. This method seems to be more insensitive to the distribution or size of the training set, as it only needs to infer its statistical mean and variance. Compared to it, the SVM estimator provided also good results, in general with lower specificity and higher sensibility.

The MLP showed high dependency with the training set distribution, and in most cases, was outperformed by the other two algorithms, which is in line with other studies in literature. However, we decided to show it here, as it still can perform the task and show promising results, and have an advantage compared to the other two methods: online training. The MLP can be trained on the fly, without the need of storing all the previous examples learned in its memory. This feature can save storage costs on the base station side.

The results of the classification algorithm also can be improved by a longer waiting decision time. Increasing the number of features, for example, can improve significantly the performance of the classification algorithms, achieving up to 99% of sensitivity and specificity, although leading to higher waiting time until the complete information is available. Also, waiting for consecutive measurement samples can lead to significantly better results. In our example waiting for 9 consecutive samples containing the information of the first neighbor led to specificity and sensitivity for higher flight levels above 99%.

In this paper, we focused the tuning algorithm to optimize the specificity and reduce the false positive paradox, however, the optimization could be performed in the other direction (optimizing sensibility) if the costs of an airborne user misclassification is considered higher for the network. Another algorithms can be tested, as LTE radio measurements show high potential of airborne users identification. Unsupervised learning techniques might be evaluated, as they provide a cheaper solution and independency of previous data collection and labeling. This can considerably reduce costs, especially for airborne users report samples. Deep learning strategies might also be investigated, provided the number of samples available is much higher than

those used in this paper. In more complex scenarios and with larger number of samples collected in different times of the day, the performance found for these measurements can be degraded, but other information can be applied to improve these classifiers, such as time alignment information, 3D localization algorithms based on cellular signals - also combined with physical path loss models - and information of the IDs of the physical cells detected by the phone.

References

[1] M. Mazur and et all, "Clarity from above. pwc global report on the commercial applications of drone technology," PwC, Tech. Rep., May 2016.

[2] "Enhanced LTE support for aerial vehicles," 3GPP, Tech. Rep. TS 36.777 V0.1.0, August 2017.

[3] B. V. D. Bergh, A. Chiumento, and S. Pollin, "Lte in the sky: trading off propagation benefits with interference costs for aerial nodes," *IEEE Communications Magazine*, vol. 54, no. 5, pp. 44–50, May 2016.

[4] R. Amorim, H. Nguyen, P. Mogensen, I. Kovacs, J. Wigard, and T. Sorensen, "Radio channel modelling for uav communication over cellular networks," *IEEE Wireless Communications Letters*, vol. PP, no. 99, pp. 1–1, 2017.

[5] H. Nguyen, R. Amorim, J. Wigard, I. Kovacs, and P. Mogensen, *Using LTE Networks for UAV Command and Control Link: A Rural-Area Coverage Analysis*. IEEE Vehicular Technology Society, 5 2017.

[6] I. Kovacs, R. Amorim, H. Nguyen, J. Wigard, and P. Mogensen, *Interference analysis for UAV connectivity over LTE using aerial radio measurements*. IEEE Vehicular Technology Society, 5 2017.

[7] R. Caruana and A. Niculescu-Mizil, "An empirical comparison of supervised learning algorithms," in *Proceedings of the 23rd International Conference on Machine Learning*, ser. ICML '06. New York, NY, USA: ACM, 2006, pp. 161–168. [Online]. Available: http://doi.acm.org/10.1145/1143844.1143865

[8] C. Cortes. and V. Vapnik, ""support vector networks"," *Machine Learning*, vol. 20, no. 3, pp. 273–297, September 1995.

[9] V. V. B.E. Boser, I. Guyon, "A training algorithm for optimal margin classifiers," in *"Fifth Annual Workshop of Computational Learning Theory"*. ACM, 1992, pp. 144–152.

[10] L. Bottou and C. jen Lin, "Support vector machine solvers," 2006.

[11] J. F. T.Hastie, R. Tibshirani, *"The Elements of Statistical Learning: Data Mining, Inference, and Prediction"*. New York, NY: Springer, 2009.

[12] S. Lawrence and C. L. Giles, "Overfitting and neural networks: conjugate gradient and backpropagation," in *Proceedings of the IEEE-INNS-ENNS International Joint Conference on Neural Networks. IJCNN 2000. Neural Computing: New Challenges and Perspectives for the New Millennium*, vol. 1, 2000, pp. 114–119 vol.1.

[13] E. Alpaydın, *"Introduction to Machine Learning"*, 2nd ed. The MIT Press, 2010.

[14] " Evolved Universal Terrestrial Radio Access (E-UTRA); Physical Layer Measurements," 3GPP, Tech. Rep. TS 36.214 V8.7.0, September 2009.

[15] M. Rheinfurth and L. Howell, *"Probability and Statistics in Aerospace Engineering"*. Nasa, March 1998.

Paper L

Method for Detection of Airborne UEs Based on LTE Radio Measurements

J. Wigard, R. Amorim, Huan C. Nguyen, I. Z. Kovács, P. Mogensen

The paper has been submitted to
IEEE International Symposium on Personal, Indoor and Mobile Radio Communications (PIMRC) 2017.

© 2017 IEEE
The layout has been revised and reprinted with permission.

Abstract

Unmanned Aerial Vehicles (UAVs) are expected to be connected through cellular networks. As the radio characteristics are different for airborne UEs compared to terrestrial UEs, it is beneficial to identify whether a UE is airborne (on a UAV) or on the ground, such that interference and mobility management can be optimized for UAVs separately from terrestrial UEs. In this paper, we present a classification algorithm using existing LTE UE radio measurements to identify whether a UE is airborne or terrestrial. The method is verified with LTE measurements made in a rural area at different heights, including terrestrial measurements and it is shown that the method in 3 out of the 4 different measurement cases can detect a UE to be airborne with 99% likelihood, while the fourth case still can classify a UE correctly in 95% of the cases. The right classification can further be improved by taking multiple consecutive samples into account before making a classification decision.

I Introduction

In recent years, small and medium sized Unmanned Aerial Vehicles (UAVs) have become an emerging commercial success. With decreasing price tags and evolving solutions, their market numbers are expected to observe a significant growth in the next years. A recent report from PwC estimates the potential market value of drone powered solutions at $127 billion [1].

As many UAVs are expected to take into the air in the near future, regulatory actions have been triggered by authorities around the globe to ensure safe operations and harmonious integration of these devices in the shared airspace. Currently, typical UAVs are limited to ranges within the visual-line-of-sight of their respective controllers [2–4]. To unleash the allowed ranges to wider distances, and therefore maximizing the commercial potential of UAVs, technical solutions requirements have been discussed by airspace regulators. One of these key solutions regards the existence of a reliable communication-and-control link between controller and UAV in all phases of the flight. Cellular networks arise as potential candidates to provide this link, due to their ubiquitous coverage and ready-to-market operating infrastructure and therefore 3GPP has recently started a study on enhanced support for aerial vehicles [5].

Moreover, besides the control link, some UAVs applications might demand payload data. For instance, a UAV used in a search and rescue could use the cellular network to transmit real-time footage from the area being inspected, as well as other information coming from its sensors. It can also act as a relay for people on the ground, in areas affected by disasters [6].

Recent studies have shown that airborne UAVs connected to cellular networks experience pathloss which is height dependent and presents losses

close to that observed by regular pedestrian users at low heights and moves to free space propagation as UAV heights increases [7]. At higher heights, e.g. 100 m, the radio line of sight can be extended to tens of kilometers due to the absence of obstructions in the radio path, and the radio propagation approximates free space conditions. Consequently, the radio environment for pedestrian and aerial users tends to differ significantly. Cellular networks today are optimized for the performance of pedestrian users, which from the point of view of a UAV sharing the same network resources, may represent underachieved reliability of the control link, inefficient use of the radio resources or even harmful level of interference added to the network. Some examples of configuration aspects which can be changed to enhance UAV connectivity are mobility parameters and setup of interference management algorithms. However, as the number of UAVs is expected to be much smaller than the number of terrestrial users, this optimization requires to be done per class of user equipment (UE), i.e. potentially separate settings need to be used for aerial UEs and terrestrial UEs. Therefore, the network requires the capability of distinguishing aerial and pedestrian users, as is also expressed in the 3GPP study [5].

In the future, UAV control modems might have the capability of reporting their status and height to the base stations. However, the network ability to detect the airborne radio modems cannot rely solely on this. Legacy equipment, such as cameras, sensors or others can be attached to the UAV by its owner for different purposes and these devices do not have the capability of reporting their ground/aerial status. This paper proposes a method to distinguish aerial and terrestrial users in the network based on standard LTE radio measurements. The advantage of this method is that no additional exchange of information between base stations and UEs is needed, as these measurements are included in the radio reports commonly exchanged between UEs and the network. Besides describing the method, we also provide an evaluation of the method using LTE radio measurements collected using UAVs in real LTE networks [7].

The remainder of this paper is organized as follows. Section III describes the measurements used in this study. Section II provides the discussion about what are the key performance indicators in such detection algorithm and the metrics that will be used to evaluate their performance. Section IV presents the identification method for airborne users, followed by the results of the verification in Section V. The discussion about the results is outlined in Section VI, and at last, Section VII provides the conclusions of this work.

Table L.1: Measurement Case Overview

	Operator 1	Operator 2
Measurement Location 1	Case 1	Case 2
Measurement Location 2	Case 3	Case 4

II Data Collection Measurements

The method proposed in this study was based on a measurement campaign performed in a rural location in the middle of Denmark. The surrounding area is relatively flat, with terrain profile varying mostly between 40 and 120 meters above sea level. The measurements were conducted in two different live operating LTE networks in the 800 MHz band, with base station heights ranging from 19m to 50m, and electrical antenna down-tilt angles between 0°and 9°. The measurements were performed using a portable radio network scanner (R&S TSMA [8], attached underneath a commercial UAV [7]). The scanner is capable of reporting radio frequency measurements from up to 32 cells. The reports include the reference signal received power (RSRP) and received signal quality indicator (RSRQ) of each detected cell. The UAV carrying the scanner was set to fly over circular paths of 500 m diameter, in two locations set 7 km apart from each other. Each route was repeated 4 times, in different heights: 15, 30, 60 and 120 m. For effects of comparison, a drive-test was performed with the same scanner, to collect information at ground level. The scanner measured the cells of two different LTE networks, leading to four different cases as shown in Table L.1. More details on the measurement setup can be found in [7].

III Classification Algorithm Requirements and Evaluation Metrics

The idea behind the detection algorithm is to apply a binary classification test to each UE in the network. After the test is performed the UE is labeled as AC (airborne class) or TC (terrestrial class). For evaluating the performance of the classification algorithm is important to compare the outcome with the real-world status of the UE. The terminology adopted throughout this paper uses AU (airborne UE) and TU (terrestrial UE) for defining the real status of each UE.

Each AC labeling by the classification algorithm may either be a True Airborne (TA) or a False Airborne (FA). In the same manner, TC labeling can be True Terrestrial (TT) and False Terrestrial (FT). Table L.2 presents the definition of TA, TT, FT, and FA based on the classification of a user compared

Table L.2: Classification Outputs

Real-world User Status	Classification Label	
	TC	AC
TU	True Terrestrial (TT)	False Airborne (FA)
AU	False Terrestrial (FT)	True Airborne (TA)

with its real-world status.

There are different metrics to evaluate a classification algorithm, based on the definitions of Table L.2, and they differ on the performance criteria being assessed. For the sake of this paper, there are two metrics that should be evaluated combined: sensitivity and specificity. The sensitivity, *Sens*, measures the number of airborne users correctly identified as such:

$$Sens = \frac{TA}{TA + FT} \tag{L.1}$$

A high sensitivity rate indicates a high percentage of the airborne UAVs might benefit from network adaptivity. However, a high is not enough to produce a good classification algorithm. For example, a dummy classification algorithm that says all users are airborne UAVs, will result in *Sens*=100%. However, all terrestrial users will also be identified as such, and will be subject to parameters optimized for aerial users. For avoid this effect, the specificity, *Spec*, should be evaluated altogether with the *Sens*. Specificity measures the number of terrestrial users identified as such:

$$Spec = \frac{TT}{TT + FA} \tag{L.2}$$

In other words, a specificity rate of 90% means that one in every ten terrestrial users will be treated by the network as an aerial node. It is worth mentioning that in cellular networks, the number of terrestrial users is expected to vastly outnumber the expected number of airborne devices. Because of this the specificity should be more important when developing the classification system, to avoid that the radio optimization for a few UAVs comes at a cost of misclassification of a high number of terrestrial users.

The classification system must also provide a quick classification process: the longer the delay to detect the UE status, the smaller are the benefits the network can exploit from the classification. Moreover, the algorithm must be able to adjust to different local network deployment conditions, as the radio environment are subject to local characteristics: inter-site distance, building heights and density and terrain profiles.

IV Proposed Methodology for Airborne UE detection

Different methods can be used to determine whether a UE is airborne or not. One can think of methods using the location of the observed cells in the measurement reports. This, however, suffers from the fact that a standard LTE UE will report up to 8 neighbors, where an airborne UE will potentially see many more cells [7]. Another method is to use information from external sensors and global navigation satellite systems (GNSS) systems. However, this information is not directly visible for the cellular radio access networks. We have chosen a method using the RSRP and RSRQ measurements of the serving cell and the neighboring cells. RSRP and RSRQ are key measures of signal level and quality for LTE network, specified by 3GPP [9]. Each UE measures the RSRP for its neighbor cells and serving cell, and Received Signal Strength Indicator (RSSI). The RSSI measures the average total received power observed only in OFDM symbols containing reference symbols for antenna port 0 and includes the power from co-channel serving and non-serving cells, adjacent channel interference and thermal noise. The RSRP is received power of one resource element, measured per detected cell, while the RSRQ is defined as $N * RSRP/RSSI$, where N is the number of resource blocks across the RSSI measurement [9].

We have observed in [7] that the interference level a UE experiences increases when moving up in height. At the same time, it is known that the RSSI for terrestrial users depends a lot on the location in the cell. We use these two properties and show in Figures L.1 to L.4 the RSSI vs the difference between the RSRP of the serving cell (RSRP SC) and the strongest neighbor cell (RSRP 1NB), referred to as ΔRSRP for the four different cases (see Table L.1 for the case description). The term ΔRSRP is a representation of the location in the cell, i.e. how close to the cell center is the UE located. The Figures show the results based on the measurements described in Section III.

From the Figures, we can make the following observations:

- The RSSI is in general higher for airborne UEs compared to terrestrial UEs and the average RSSI increases with height.
- For terrestrial UEs there is a linear relation between the difference between the RSRP of the serving cell and the strongest neighbor and the RSSI. The larger the difference, i.e. the farther away from the cell border, the stronger the RSSI. Reason for this is that the UE is so close to the serving cell that most of the wideband power is coming from there.
- The points belonging to the terrestrial UEs are not overlapping much with the points belonging to airborne UEs. The overlap is worst for case 4.

Based on these results we make the assumption that the points belonging to airborne UEs can be separated from the points belonging to terrestrial UEs by a separation line:

$$\alpha.(\Delta RSRP) + \beta.RSSI + \phi = 0 \tag{L.3}$$

Next, we determine the factors α, β and ϕ . We consider the 4 cases separately and derive first the best combination of the factors for each case based on the full data set in each case, which minimizes the cost function K:

$$K = \sum_i k(i) \tag{L.4}$$

where $k(1)$ is 1 for sample i if it is on the wrong side of the decision line, shown in equation L.3, and 0 if it is on the correct side. Setting β to 1 and evaluating all combinations of α and ϕ we obtain the optimal combinations, which are shown in Table L.3.

As can be seen, the parameters are rather close for the different cases, but not completely identical. This points into the direction of having to train the algorithm with a certain dataset for optimal performance. This approach will be verified in the next section.

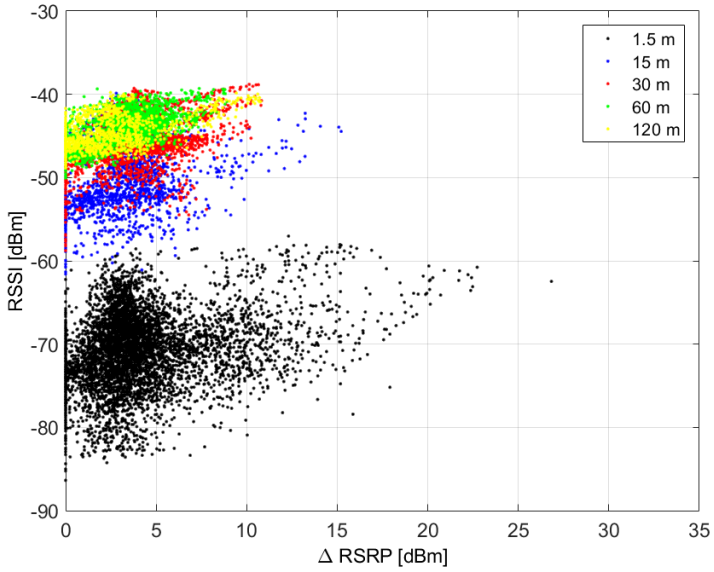

Fig. L.1: RSSI vs ΔRSRP for different heights (case 1).

Table L.3: Optimal Factors for the Different Cases

	Case 1	Case 2	Case 3	Case 4
α	0.3	0.4	0.4	0.8
ϕ (dBm)	-60	-60	-58	-58

V Algorithm Verification

In this section the performance of the algorithm described in the previous section is verified. Verification of the algorithm is done by using a subset of data as training set to determine the factors of equation L.3 and then test the outcome on a different subset of data. Two different verification tests are done: 1) the data of each of the four cases is split into two parts, where the data for each height is split equally, and half is used as training set and half is used to test the outcome. 2) similar to the first test, but now the training data and verification data come from the different cases.

The outcome is measured by looking at the *Sens* and *Spec* metrics as defined in section II. Table L.4 shows the outcome of the first test, where the training data and the verification data is selected randomly from the data available per case. The amount of data in each case corresponds to about

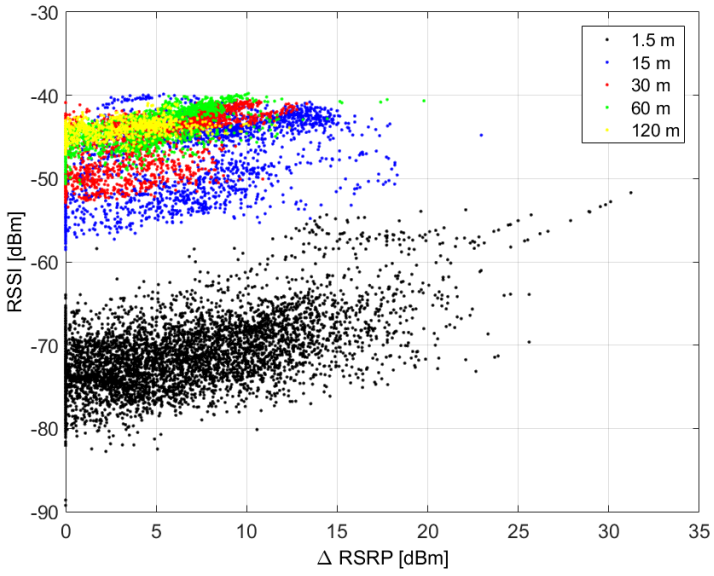

Fig. L.2: RSSI vs ΔRSRP for different heights (case 2).

Table L.4: *Sens* and *Spec* for the case where the data per case is split and half of the data is used as training set

	Case 1	Case 2	Case 3	Case 4
Sens	0.9992	0.9994	0.9974	0.97150.3
Spec (dBm)	0.9997	1	1	0.9668

13000 samples, corresponding to 25 minutes of measuring with a measurement reporting frequency of 9 Hz, so the training and verification data subset both correspond to about 6500 samples. It can be seen that for the first 3 cases the results are very good, as both *Sens* and *Spec* are above 99%. The results are worse for case 4 for both *Sens* and *Spec*. Reason for this can be seen when carefully looking at Figure L.4: the points belonging to terrestrial users are overlapping quite a lot of the points belonging to 15 m, which makes it hard to differentiate between them.

Figure L.5 shows more details per UE height, as it depicts the fraction of correct decisions per height. Again it can be seen that case 4 is worst, but is also can be seen that for all cases airborne UEs at heights 60 or 120 m are always recognized as such. The cases where an airborne UE is not recognized as such are typically at the lowest flying height of 15 m, as the characteristics

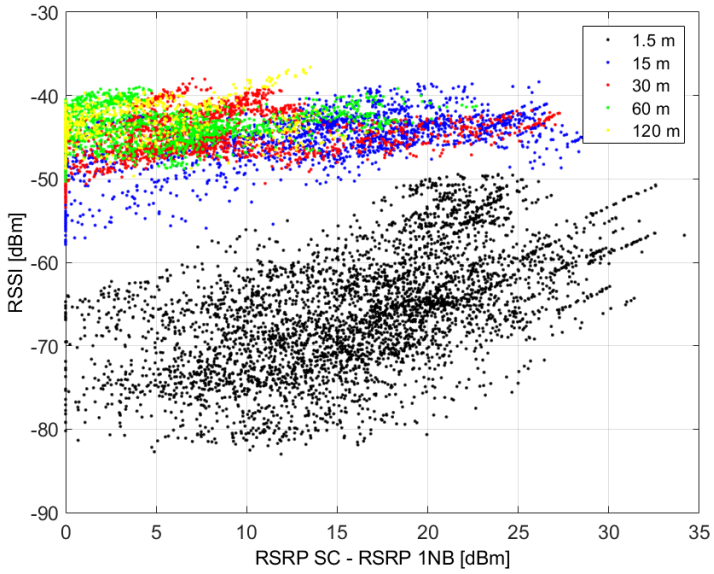

Fig. L.3: RSSI vs ΔRSRP for different heights (case 3).

of a low flying UE are not that different from the characteristics of a terrestrial UE.

The results of *Sens* and *Spec* can be improved by not just looking at a

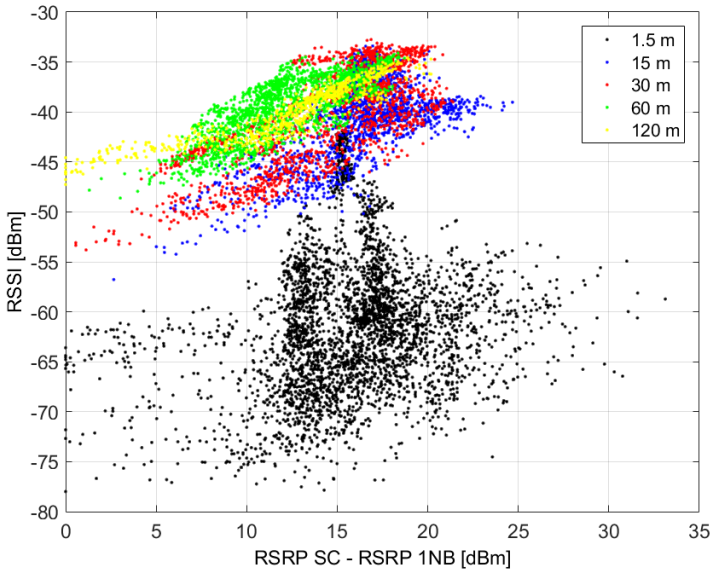

Fig. L.4: RSSI vs ΔRSRP for different heights (case 4).

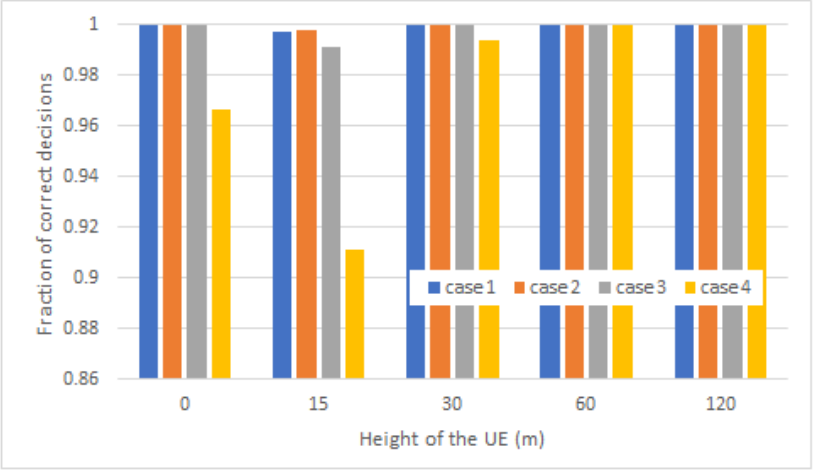

Fig. L.5: Fraction of correct decision vs UE height for the different cases.

Table L.5: *Sens* and *Spec* for the case where the data per case is split and half of the data is used as training set

N	*Sens*	*Spec*	Indecisive
1	0.9715	0.9668	0
2	0.9996	0.9985	0.05
4	1	1	0.1
8	1	1	0.2

single sample, but taking several consecutive samples, N,into account. This is illustrated for case 4 in Table L.5, where we only classify a UE as aerial or terrestrial if all N samples point in one direction. The values for N equal to 1 are identical to the values in Table L.4ready when taking 2 consecutive samples into account both *Sens* and *Spec* are very close to 1. It can also be seen that the amount of indecisive decisions grows fast for increasing N, as we assume that both samples must point in one direction.

In the above results, half of the available data was used as training data subset. In Figure L.6 we show the results when a smaller percentage of the data is used as training dataset for case 1 and 4. The training data sub set is always selected randomly from the full data set and for the verification data subset always 50% of the available data is used, also selected randomly. It can be seen that for case 1 results are still very good with both *Spec* and *Sens* being above 99% when only 5% of the data set is used as trainings set, corresponding to about 650 samples. The results for case 4 show a different behavior: while *Spec* is decreasing when the training data subset gets smaller, *Sens* stays stable or even increases. Reason is there are many points corresponding to the terrestrial users overlapping with the 15 m users, as shown in Figure L.4. Now with a smaller trainings subset there is a likelihood of not detecting many of those points, leading to a lower detection line (ϕ decreases). This increases *Sens* but decreases *Spec*. The majority of wrong detections for aerial UEs are made at low flying heights (primary at 15 m) for all cases.

The outcome of the second test, where we always use 50% of the available data as training subset and 50% as verification data subset, but use different cases for the training and verification data set, can be seen in Table L.6. When case 4 is not involved results are very good: both *Spec* and *Sens* are in all but one case above 99%. When case 4 is involved results degrade. Reason is the data, as shown in Figure L.4. Closer inspection of the details of the case 4 measurements reflect a difference from the other measurement cases: the case 4 measurements are done very close to the serving cell and the network is rather sparse, i.e. the neighboring cells are far away. This leads to the RSRP of the serving cell and the RSSI being very correlated and ΔRSRP being rather

Table L.6: *Sens* (top number) and *Spec* (bottom number) for different training sets (50% of samples) and verifcation sets (50% of samples)

		Verification Set			
		Case 1	Case 2	Case 3	Case 4
Training Set	Case 1	0.9992 0.9997	0.9972 0.9997	1 0.9614	1 0.8815
	Case 2	0.9977 1	0.9994 1	1 0.9993	1 0.8821
	Case 3	0.9918 1	0.9963 1	0.9974 1	1 0.9223
	Case 4	0.99 1	0.9573 1	0.8515 1	0.9715 0.9668

large. This behavior is very similar for aerial and terrestrial users, which makes it harder, in this case, to differentiate and classify them correctly. It is for further study to improve the classification for this kind of cases.

VI Discussion

The results in the previous section show good performance if case 4 is not involved. At the same time it is shown that not much data is needed as training subset. In reality training data subsets can be based on measurement

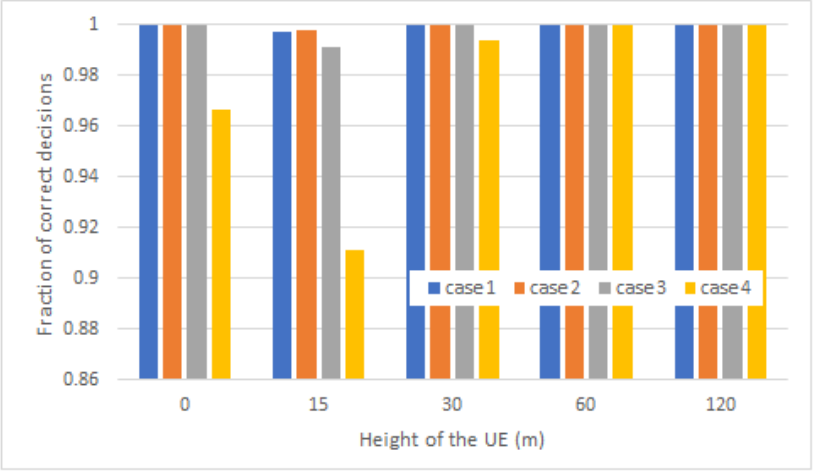

Fig. L.6: *Sens* and *Spec* for case 1 and 4 vs the length of the trainings data set (as % of the full data set).

reports, including both RSRP and RSRQ from the serving and neighboring cells from UEs, either through the normal measurement report triggers or through having UEs report periodically their measurements for some period of time, when the load in the network allows to do so. For the training of the classification algorithm it is needed to know whether a UE is airborne or not in order to train the algorithm. This can be solved by either using test UEs collecting data and for which the status is known or through correlating the measurements with the presence of a control link to a UAV control. The latter requires the network is aware of this, but this is currently one of the topics of discussion in 3GPP [9].

VII Conclusions

Unmanned Aerial Vehicles (UAVs) are expected to be connected through cellular networks for their control link. As the radio characteristics in the air are different from the ground, it is beneficial to identify whether a UE is airborne (on a UAV) or terrestrial, such that interference and mobility management can be optimized for UAVs separately from terrestrial UEs. We presented a classification method using existing LTE UE based radio measurements, which can identify whether a UE is airborne or terrestrial. The method uses LTE measurements made and it is shown when tested on a dataset from aerial measurements that in most cases it can classify a UE correctly as flying or terrestrial in 99% of the cases by looking at a single sample. For the cases where the classification performs worse, it can easily be improved by taking multiple consecutive samples into account.

References

[1] M. Mazur and et all, "Clarity from above. pwc global report on the commercial applications of drone technology," PwC, Tech. Rep., May 2016.

[2] EUROCONTROL, "Roadmap for the integration of civil Remotely-Piloted Aircraft Systems into the European Aviation System," 2013.

[3] FAA, "Integration of civil unmanned aircraft systems (uas) in the national airspace system (nas) roadmap," Tech. Rep., 2013.

[4] , "Global Drone Regulations Database," https://droneregulations.info/, available March 30, 2017.

[5] 3GPP TSG RAN WG1, "RP-170779 - Study on enhanced Support for Aerial Vehicles, note = March 6-9, 2017, howpublished = Dubrovnik, Croatia,."

[6] M. Erdelj and E. Natalizio, "Uav-assisted disaster management: Applications and open issues," in *2016 International Conference on Computing, Networking and Communications (ICNC)*, Feb 2016, pp. 1–5.

[7] R. Amorim et al., "Radio Channel Modeling for UAV Communication Over Cellular Networks," *IEEE Wireless Commun. Lett.*, vol. 6, no. 4, pp. 514–517, Aug. 2017.

[8] Rohde & Schwarz, Mobile Network Testing, "R&S TSMA Autonomous Mobile network Scanner," june 2016.

[9] 3GPP, " Evolved Universal Terrestrial Radio Access (E-UTRA); Physical Layer Measurements," 3GPP, Tech. Rep. TS 36.214 V8.7.0, Sep. 2009.

Chapter 7 - Conclusion

In the previous chapters, this thesis has evaluated the usage of cellular networks, more specifically Long-Term Evolution (LTE) networks, on their suitability in providing reliable Command and Control (C2) connectivity for Unmanned Aerial Vehicles (UAVs). In the present chapter, the research is wrapped up by a summary of the observations and their respective implications. It also presents recommendations regarding the deployment of this service and suggestions for future works.

7.1 Summary of Observations

There are several options to provide connectivity services for UAVs, such as reusing the cellular spectrum and infrastructural resources, Non-Terrestrial Networks (NTN) and new dedicated networks. Although cellular networks are not the only option available for providing C2 services, they present several advantages that can benefit a fast and less expensive deployment. Therefore, their usage to this end shall be regarded as one main candidate solution.

There are several different aspects to be observed about technologies or networks candidacies to provide this kind of services. Each of them shall be evaluated in order to decide their suitability for the application. Examples of such aspects include:

- radio connection reliability;
- the security of the link;
- the secrecy on the users identification;
- interconnection with related services, such as the Unmanned Aircraft System Traffic Management (UTM); and others.

The research presented here covers the radio connectivity part of this evaluation and has aimed at assessing current state-of-the-art performance as well as propose modifications to address challenges specific to this use case.

The requirements used as baseline for the link performance evaluation, described in Chapter 1, are those defined by the Third Generation Partnership Project (3GPP) in their related study-item.

Chapter 2 has established the necessity of reassessing the performance of LTE networks in the light of different propagation models. Although, LTE networks have been thoroughly assessed in the state-of-the-art literature for many years, because of the different propagation effects observed by UAVs in the air the performance results could deviate from the norm.

Field measurements collected by airborne devices have demonstrated the propagation losses observed by an airborne UAV approximates free space losses, indicating a high probability of line-of-sight (LOS) that extends for several tens of kilometers at higher heights. Because of this, the power radiated by a base station can be received above certain levels at farther distances, which means a lower density of sites would be required to provide coverage for airborne UAV. However, the density of sites in cellular networks are designed by the coverage and capacity estimations based on terrestrial users distribution and demand. As a consequence, the interference power levels increase compared to typical values at terrestrial heights, once there is no buildings or other elements to attenuate the power radiated by neighbor cells.

Two main findings are extracted from the assessment of the received power distribution for serving and neighbor cells: 1) neighbor cells are much closer to the serving cell and to each other in the power domain; 2) there are a higher number of significant sources of interferences. The outcome of this two factors is that there is no clear dominant interfering cell, which minimizes the potential signal to interference plus noise ratio (SINR) gains of well-known techniques such as Coordinated Multipoint (CoMP) and interference cancellation (IC). This is specially important, at it is also observed a degradation on the downlink (DL) SINR with increase in height, as the increase in the interference power can supersede the gains in serving cell received power depending on network traffic load and site density.

In the uplink (UL), the interference caused by the UAVs tends to be observed at a higher level at the network base stations, when compared with similar transmissions performed by a terrestrial users. However, the effect caused by the C2 is assumed of minor importance for the scope of this thesis, first because the density of UAVs is expected to be much smaller than regular terrestrial user equipments (UEs), but also because the low-throughput traffic required for this service does not tend to consume significant radio resources.

Chapter 4 concentrated on the performance evaluation of the C2 link over LTE networks, in special, in terms of the specifications proposed by 3GPP. This assessment was performed both by simulations and by field measurements.

The simulations have indicated that when subjected to middle or heavy network load conditions, airborne UAVs tend to experience outage above the

0.1% limit established for the 3GPP. The main failure reason observed in such circumstances in the simulations was the disruption of the LTE Physical Downlink Control Channel (PDCCH) reception, which causes a radio link failure. In order to revert this performance degradation, some interference management/suppression techniques have been evaluated.

The analysis of inter-cell interference coordination (ICIC) and IC techniques indicate slim performance improvements, unless several - up to 10 or more - interfering cells are canceled or coordinated with the main serving cell. The reason behind these results is the absence of a clear dominant interfering source. Because of this, this work concludes, the usage of both ICIC and IC techniques should not be considered an important feature for deployments of C2 links, specially in the absence of other improvements. If any other technique to be proposed indicates to be capable of modifying the distribution of the neighboring cells in the power domain, the gain provided by such interference management features could be reassessed.

The simulations have demonstrated that the usage of directional antennas in the UE may be beneficial, as it has the capability of boosting the received power from the dominant cell while it reduces the power received from several sources that lie outside the main beam's direction. This was asserted in this investigation by means of the simulation of a fixed grid of beams. Among all solutions evaluated in this thesis, this one has been observed with the largest performance enhancements among all single operator solutions.

In what regards, solutions for the UL connection, a UAV specific Power Control (PC) is proposed. The reduction on the noise generated by C2 links is assumed to not be significant, as the proportion of C2 users in the network is much smaller than other typical cellular network users and it requires lower traffic, occupying few radio resources.

In addition to the simulation results, field measurements have assessed the latency experienced by UAVs C2 traffic over cellular networks. The average network load in the operating network is not as high as the values evaluated in the simulations. The results indicate that degradations of the quality of the DL transmissions tends to affect also UL latency, as the whole management and configuration of the radio connection are performed through the DL.

Overall, the measurements indicate that most part of the time the 50 ms maximum latency can be achieved through a regular LTE-Advanced (LTE-A) connection not optimized for C2 or aerial UEs. However, there are still packets in the tail of latency's cumulative distribution whose latency is above the 50 ms threshold. The number of such packets exceeds the 0.1 % admissible failure rate for the C2 link. One of the main problems perceived in the measurements campaign were radio link failures and re-establishments caused by poor connection. These yielded a high number of failures in a short amount of time, for example, 335 out of 340 (98.5 %) packets received with

latency above the thresholds in one of such cases.

The tests have indicated that the usage of a hybrid access with dual LTE connectivity has significant potential to improve the C2 performance. This technique, which duplicates the packets over two different network connections, provides diversity to the transmission and increases significantly the reliability of the C2 link.

After the thorough examination on the system performance with shared network infrastructure between UAVs and other cellular users, the usage of a dedicated bandwidth for the UAVs has been examined in Chapter 5. Based on current market projections, the demand for C2 connectivity has been estimated for the next 20 years.

Because of the low throughput required by C2 links and the infrequent deployment of such devices in a low number of simultaneous missions per km^2, the estimated bandwidth required for providing the service is rather low. In most of the scenarios projected, 1.4 MHz of bandwidth is enough to fulfill the system requirements for today's numbers. In most cases, the site density required is way lower than commonly seen in public cellular networks (as low as 1 site $/800\ km^2$). For the future projections, while 1.4 MHz can perform well in most scenarios, in the most dense areas, where a higher density of UAV missions is expected, up to 5 MHz are demanded. In very stringent locations, such as New York, the demand can go above such numbers during peak demand.

It is important to notice that the bandwidth requirements may get lowered by technical improvements. Compared with LTE-A, 5G New Radio (NR) promises improved spectral efficiency based on a more flexible and optimized physical layer. In special for this application, beamforming can improve substantially the SINR observed by the system users, while more advanced Modulation and Coding Scheme (MCS) can reduce the network congestion by minimizing the number of used resources. Despite this, one important aspect to be observed is that it may be economically unattractive to use dedicated spectrum and infrastructure to provide C2 service, due to low utilization of spectrum and smaller penetration of users, considering the spectrum license average prices and infrastructure implementation.

At last in the thesis, Chapter 6 has discussed the importance of detecting UAV users in the network and an enabler to differentiate the C2 service from the others. Such capability would open several possibilities for spectrum and interference management, and also enable priority assignment for the C2 over best-effort service allocations. The chapter has also discussed the potential to perform the detection of airborne devices based on regularly collected radio measurements. Although the evaluation is still incipient it provides insightful results about the potential to perform such operations.

7.2 Assessment of the Research Questions

In this section we repeat the research questions posed in Chapter 1, and assess them in the light of the results presented throughout this thesis. The following list brings the research questions (Q) and their respective answers (A).

Q1 What is a good path loss model for describing the radio attenuation observed between the cellular base stations and flying devices at heights up to 120 m?

A1 The field measurement results in this thesis have demonstrated that as the UAV takes-off and move away from the ground level, the path loss coefficient decreases. At higher heights, for example above 50 meters, the propagation approximates the free space model, extended for at least 10-20 kilometers, due to increased likelihood of LOS.

Q2 How this potentially height dependent path loss model impacts the network interference levels?

A2 In the DL, it tends to lead to increase the interference levels experienced by the UAV in comparison to user on ground level. Depending on the network load and site density, it can cause a high degradation of the SINR, which can compromise the reliability of the C2. In the UL, it causes the UAV to cause more interference in the neighboring cells, and also at larger number of victim cells, due to the low attenuation in the signal radiated by the UAV. However, unless the density of UAVs increases significantly or they use a service with higher payload than the C2, this effect tends to have minor impact in other users due to the low utilization of radio resources by UAVs.

Q3 Can cellular networks cope with the requirements for C2 links over a LTE network?

A3 The traffic load experienced by network operators is a challenge for achieving the requirements for C2 as specified by 3GPP. The 99.9 % of reliability within a maximum latency of 50 ms is a stringent requirement. Measurement campaigns and simulations have indicated that, that with no changes in the PHY or MAC layer, LTE networks tend to fail to achieve such high reliability, in special under high load conditions. However, enhancements in LTE's link can be used to overcome this limitation and approximates the reliability to the desired levels, such as:

- Quality of Service (QoS) differentiation between C2 and broadband applications, with different allocation and radio management policies, as higher priority allocation and more robust MCS usage;

- deployment of case-specific strategies for interference management and/or suppression, in special those discussed in Q4-A4;
- technical improvements on the air-interface, such as those to be introduced in the next generation of 3GPP technologies, the 5^{th} Generation (5G) NR, that will represent an evolution of the 4^{th} Generation (4G) LTE.

Q4 Which techniques can best enhance C2 performance?

A4 The most promising gains observed in all our measurements and simulations were perceived for the UAVs using a directional antenna transmission and reception at the UAV and the usage of network diversity. The directional antenna array in our study was simulated by a fixed grid of beams implemented on the UAV, in which the beam selection was based on an algorithm of RSRQ maximization. It is reasonable to assume that the usage of adaptive beamforming can also present a good option for future deployments. The network diversity was emulated in our study by means of a hybrid access scheme with two different operators. Another option regarding future deployments is the implementation of "multi-carrier" diversity within the same operator.

Q5 What are the costs and benefits in a dedicated resource allocation policy associated to the C2?

A5 Using a band of spectrum fully designated for C2 services is very effective in protecting the link from interference originated by other types of users and services and can increase the number of UAVs served with high reliability in a given area. However, it tends to be very cost inefficient, as the penetration of the UAVs market is very low compared to other types of users, specially considering the average spectrum costs. A good compromise is to use network virtualization with a dynamic spectrum allocation. This solution allows the cellular network to share the operational costs between UAVs and other subscribers, while being responsive to the UAVs demand, avoiding waste of reserved spectrum.

7.3 Recommendations

The C2 service is one of the mission critical services that requires data connectivity. Regarding the usage of cellular networks to provide such kind of services, some action is required to achieve the reliability of the link in comparison with other less critical services. This is specially important under stringent circumstances, such as high network traffic load and site density. The results in this thesis corroborate these assumptions. The performance

is within the requirements most part of the time, but it requires enhancements for the most severe cases. It seems to be, in special, highly sensitive to variations in the network load.

This Section provides recommendations on the way forward for developing solutions for the C2 link connected over cellular networks based upon the findings of the present research. The recommendations are divided in two groups: network based and UAV based implementations.

7.3.1 Network-based Implementations

Solutions crafted for the network side can either take place via technological standards evolution or by implementation/design. In common, both type of solutions require knowledge about the UAV and the C2 link as *sui generis* entities apart from the other users in the network. So it is paramount recommended to drive efforts in developing solutions for UAV detection and their C2 link traffic.

UAV's Traffic steering

The results indicate airborne UAVs are very sensitive to increases in the network load. One way of mitigating this effect is by steering the C2 link primarily to less congested frequency bands. The usage of load balancing features is a well-known feature of 3GPP technologies.

Looking forward for 5G NR deployments, it also seems potentially advantageous to make the higher frequency layers the preferred options for supporting the C2 requests. This clears up the lower frequency layers to support terrestrial users, which observe higher propagation losses and are less likely to experience LOS, while steer the C2 to frequencies more suited to beamforming and that can benefit from the high LOS likelihood.

Carrier Aggregation and Dual Connectivity Solutions

In combination with the traffic steering, carrier aggregation is one solution that can readily provide online flexibility to sudden changes in the traffic conditions in the network. This can be done by configuring multiple carriers for the UAV connection, and activating those that are in the less loaded frequencies.

Additionally, the inter-site carrier aggregation can provide robustness and diversity against failures in the radio link channel, if implemented aiming at a solution similar to the hybrid access setup presented in Chapter 4. The results suggest great performance enhancement is achievable through creating link diversity.

Dual connectivity solutions may also create opportunities for the C2 to benefit from the link diversity. Although these require more investigations as the results presented in this thesis cannot be straightforward extrapolated for this technique.

Beamforming

One of the main conclusions of this thesis about the connectivity for drones is that the link is not isolated from other interfering sources by obstacles in the radio path, such as buildings or terrain elevation. It follows then that using very directional and narrow beams on the base stations can be highly beneficial for the UAV use case, first because it focus the transmitted power in the direction of the receiving UAV, but more importantly, the power radiated by neighboring cells can stay confined within the main beam direction, reducing the overall interference power radiated toward the UAVs.

7.3.2 Robust Scheduling Policies

The scheduling policies adopted by the network can help to enhance the link performance. In that sense, it is important that the network can properly identify the C2 related Channel Quality Indicator (CQI), to properly address the service requirements.

This can be done, for example, by using more robust MCS since the first transmission, minimizing the probability of error on the wireless channel; setting up a semi-persistent scheduler, diminishing the necessity of keep continuously scheduling grants and other control information on the PDCCH or implementing specific features designed to enhance the reliability. Example of such features are the TTI bundling or the proactive HARQ retransmissions.

7.3.3 UAV-based Implementations

The implementation on the UAVs side have the advantage of being transparent to the network, therefore requiring less or no standardization effort or technical improvements. But, as indicated by the results collected through this thesis, they also present great potential to enhance the network performance.

Dual/Multi Hybrid Access

The dual connectivity setup evaluated in Chapter 4 has demonstrated significant improvements on the overall reliability of the C2 link. This solution is fairly simple to be implemented at the application level and can be considered one viable option. The drawback is the increase in billing charges, as more mobile subscriptions will be required, for duplicating the link by

a hybrid access solution. On the other hand, in some countries this increase may be not so significant, particularly given the critically of the C2. Moreover the number of connections may be increased by as much network operators are available locally and/or as much as required to reach desired reliability levels.

Directional Antenna Patterns

The implementation of directional antenna system on the UAV side has demonstrated great potential to improve the reliability of the system. Likewise the beamforming, this solution aims at focusing the energy on the direction that maximizes the received power, which has the side benefit of minimizing the energy received from other directions.

The implementation of such solutions may be performed either by a grid of fixed beams, which do not require explicit information from the network side, or by developing beamforming implementations for the user-end. This last alternative require some specifications on the standards and is a topic expected to be presented in 3GPP release 17 for 5G NR

7.4 Final Remarks and Suggestions of Future Works

The usage of cellular networks, besides the commercial and economical appeal, has demonstrated potential to provide the C2 connectivity. However, it requires more dedicated solutions, aiming at improve the system performance at very high reliable standards, which, to a great extent, does not differ from other critical services envisioned to run through cellular networks. Cellular networks may adapt to different service requirements on a on-demand basis. This is one of the main reasons why it is the evidence-based opinion of the author that the differentiation of the C2 services apart from the others is a key enabler for the service provision.

An additional possibility is that regulations and technological specifications may also enforce more advanced technical solutions on the user-end side for C2 compliant modems, denying access for UAV-UEs that does not present a set of minimal mandatory capabilities.

Partially, the PHY improvements present in the 3GPP 5G NR technology already addres some of the inefficiencies that could be explored to improve the C2 link performance. It is then expected that it advances the reliability levels beyond the values presented in this research.

7.4.1 More Relaxed Requirements

The reliability results presented throughout this thesis were measured considering the set of requirements for the C2 traffic proposed by 3GPP, i.e., 99.9 %

Table 7.1: Proposed requirements for C2 traffic in [1]

Traffic Type	Throughput (Mbps)	Latency (ms)
Command and Control	0.001	VLOS: TBD BVLOS:TBD
Telemetry	0.012 (without video)	1000
Real-time	0.06 (without video)	100
Video Streaming	4 (720p video) 9 (1080p video) 30 (4k video)	100
Situation Aware Report	1	10-100

of reliability for a 60-100 kbps throughput payload, with a maximum packet latency of 50 ms. However, recent discussions have presented more relaxed latency values, in special for some UAVs applications, and this can render *reachable* reliability for current networks, even considering no modifications or very few enhancements, as discussed in Chapter 4 and Paper I.

SESAR has recently proposed the total delay to be as high as 3 seconds (down to 1 second close to airports). For such values, it is possible that the 99.9 % reliability is reachable for current network deployments, as depicted in Paper I latency distribution results.

In the latest months of this research, in the beginning of 2019, 3GPP has opened a study item to propose specification for network architecture regarding the UAV's connectivity services. In this document the C2 traffic is split in several categories, with different latency constraints [1]. The most recent version of the document at the time of writing, released in March 2019, the proposed requirements in this document are those presented in Table 7.1.

From this table, it is possible to derive a few conclusions. First, the command and control traffic is defined by a very low payload, which represents just 1 % of the 100 kbps used as reference in this thesis and because of this – considering an equal latency requirement (50 ms) – the achievable reliability tends to increase. However, in those situations when the loss of reliability is caused by a radio link failure due to SINR degradation, a small throughput does not help to improve the reliability. Therefore, the gain in reliability is limited, when compared to the values presented in this thesis.

The Telemetry, however, is expected to observe a significant increase in the reliability, as the latency constraint has been significantly relaxed. The results indicate that the 1 second of latency – for a 12 kbps traffic - probably can be served with current network deployments without any traffic differentiation. Some improvement (compared to the values presented in this thesis) is also expected for the real-time traffic which has a required throughput of 60 kbps within 100 ms, a latency twice as high as the reference value used throughout

the thesis.

The video streaming and the situation aware report represent the most challenging demands, as they require a very high throughput in a rather low latency. Albeit they are not expected to be used for all scenarios, applications or UAV classes, it is important to be aware of these challenges when designing a C2 link solution that is connected to the UTM, regarding safety reasons.

For the most challenging two cases, it is important that some of the recommendations aforementioned should be deployed, in order to enhance the connectivity performance between UAV and RAN. Moreover, it is important to notice that the 3GPP is likely to consider such solutions to be available in future versions of its standards, i.e. from release 17 onwards. This represents that several enhancements are expected to be developed such that these requirements are reachable within the next couple of years, which may include some of the recommendations provided in this thesis.

7.4.2 Future Works

Some open the points discussed throughout this thesis can be further advanced by future works. One example, is the usage of the grid of beams in the UAV side, which requires investigation on the handover mechanisms, since it is important to assess how the directivity of the radio link can impact the detection of neighbor target cells. Another point that could be assessed more directly concerns the usage of beamforming applications for UAVs.

One important aspect that can further investigated is the bandwidth demand for C2 services that could be evaluated under different scenarios deployments, since the network settings used in the simulations was not optimized for the UAV coverage. Additionally, the implementation of performance enhancement features over dedicated spectrum can also be object of study. Another key aspect of the dedicated spectrum coverage is the link availability at ground level for taking-off and landing procedures, which was not covered by the simulations presented in this research.

References

[1] 3GPP, " Technical Specification Group Services and System Aspects; Study on Enhancement for Unmanned Aerial Vehicles; Stage 1 ," 3GPP, Release 17 TS 22.829 V1.0.0, Mar. 2019.

ISSN (online): 2446-1628
ISBN (online): 978-87-7210-420-1

AALBORG UNIVERSITY PRESS